

DTIC FILE COPY

UNCLASSIFIED

~~RB 169 224~~

①

REPORT
HSA 20



DEPARTMENT OF SUPPLY
AUSTRALIAN DEFENCE SCIENTIFIC SERVICE

WEAPONS RESEARCH ESTABLISHMENT

SALISBURY, SOUTH AUSTRALIA

REPORT HSA 20

*at 2-AD-74785
at 3-764881
at 4-4006869*

DTIC
ELECTE
JUN 18 1990
S D

AD-A955 921

RESULTS AND CONCLUSIONS OF THE JOINT R.A.E./W.R.E.
RESEARCH PROGRAMME ON THE FLIGHT DYNAMICS AND
BALLISTIC CONSISTENCY OF FREELY FALLING MISSILES
PART I BOMBS STABILISED BY FIXED CRUCIFORM FINS

FEB 14 1966

C.W. RHODES and J.H.W. SHANNON

Code 61

DISTRIBUTION STATEMENT A
Approved for public release
Distribution Unlimited



CLEARINGHOUSE
FOR SCIENTIFIC AND
TECHNICAL INFORMATION
4.02 1.00/35 BA
ADHIVE COPY
PROCESSED COPY

90 06 15 102

COPY No.

NOVEMBER 1965

UNCLASSIFIED

UNCLASSIFIED

DEPARTMENT OF SUPPLY
AUSTRALIAN DEFENCE SCIENTIFIC SERVICE
WEAPONS RESEARCH ESTABLISHMENT

REPORT HSA 20

RESULTS AND CONCLUSIONS OF THE JOINT R.A.E./W.R.E. RESEARCH
PROGRAMME ON THE FLIGHT DYNAMICS AND BALLISTIC CONSISTENCY
OF FREELY FALLING MISSILES

PART I. BOMBS STABILISED BY FIXED CRUCIFORM FINS

C.W. Rhodes* and J.H.W. Shannon**

S U M M A R Y

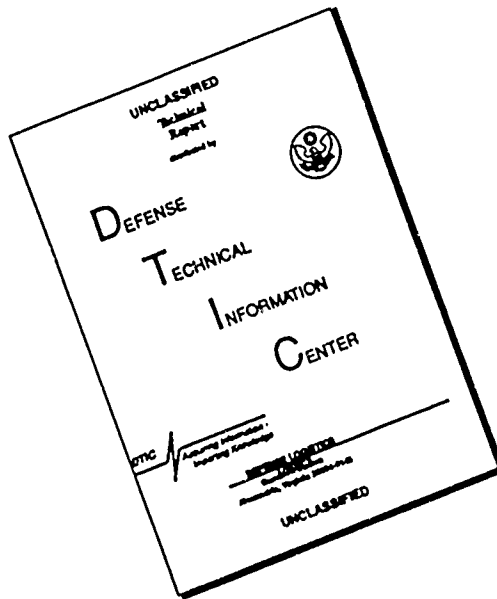
A general investigation of the stability problems of freely falling missiles has been made. This report presents results of a joint R.A.E./W.R.E. research programme which was initiated in 1960 and incorporated a series of free flight trials of full scale instrumented test vehicles, wind tunnel tests carried out over a wide range of Reynolds numbers and mathematical model studies using a fast digital computer. Correlations between predicted motions of the vehicle and behaviour actually observed in the trials confirmed both the formulation of the mathematical model and the validity of wind tunnel measurements. The results have provided considerable insight into problems associated with the release disturbance and stability requirements needed for good ballistic consistency. Finally, suggestions are made for the aerodynamic design of fin stabilised bombs.

This report is being issued simultaneously by the Weapons Research Establishment and by the Royal Aircraft Establishment, Farnborough, Hants, U.K. The R.A.E. reference is R.A.E. Tech. Report TR65200.

- * (Weapons Department R.A.E.)
- ** (Aerodynamics Division W.R.E.)

POSTAL ADDRESS: The Director, Weapons Research Establishment,
Box 1424H, G.P.O., Adelaide, South Australia.

DISCLAIMER NOTICE



THIS DOCUMENT IS BEST QUALITY AVAILABLE. THE COPY FURNISHED TO DTIC CONTAINED A SIGNIFICANT NUMBER OF PAGES WHICH DO NOT REPRODUCE LEGIBLY.

TABLE OF CONTENTS

	Page No.
1. INTRODUCTION	1 - 2
2. ORIGIN OF R.A.E./W.R.E. EXPERIMENTS IN BOMB BALLISTICS	2 - 3
3. DEVELOPMENT OF FLIGHT DYNAMIC THEORY	3 - 4
4. UNITED KINGDOM/AUSTRALIAN JOINT PROJECT FOR FULL SCALE INSTRUMENTED BOMB TRIALS	5 - 6
5. EXPERIMENTAL METHOD	6 - 7
6. WIND TUNNEL TESTS AND RESULTS	7 - 18
6.1 Test conditions and presentation of data	8 - 12
6.1.1 Model scales and Reynolds numbers	8 - 9
6.1.2 Coefficient definitions, systems of axes, etc.	9 - 10
6.1.3 Transition fixing	10
6.1.4 Test ranges of incidence angle, roll attitude, Mach number etc.	10 - 12
6.2 Static measurements of normal force and restoring moment on the low drag shapes	12 - 14
6.3 Static measurements of normal force and restoring moment on the bluff M557B shape	14 - 15
6.4 Static measurements of induced side force, side moment and rolling moment for the M557A and M557B shapes	15 - 16
6.5 Pitch and roll damping measurements on the M823 low drag shape	16 - 18
7. FREE FLIGHT TRIALS AND RESULTS	18 - 31
7.1 The test vehicles	18 - 19
7.2 Instrumentation	19 - 21
7.2.1 Ground based measurements of trajectory	20
7.2.2 Test vehicle instrumentation	20 - 21
7.2.3 Aircraft instrumentation	21
7.2.4 Meteorological data	21
7.3 Results of instrumented ballistic trials	22 - 23
7.3.1 Streamlined body M557A shape	23 - 27
7.3.2 Bluff body M557B shape	27

	Page No.
7.4 Results of transient response trials	28
7.4.1 Data analysis	28 - 30
7.4.2 Comparisons with wind tunnel data	30 - 31
8. COMPUTER STUDIES AND RESULTS	31 - 37
8.1 Response to the release disturbance	32 - 34
8.2 Dynamic behaviour at low incidence	34 - 37
8.2.1 Effect of static instability near zero yaw with no fin-body misalignment	35 - 36
8.2.2 Effect of fin-body misalignment	36 - 37
9. CONCLUSIONS AND RECOMMENDATIONS	38
9.1 Flight dynamics and ballistic consistency	38 - 39
9.2 New concept for ballistic trials	39 - 40
9.3 Aerodynamic aspects of bomb design practice	40 - 41
9.4 Bomb design procedure	41 - 43
9.5 Further research	43 - 44
REFERENCES	45 - 50

LIST OF TABLES

1. PHYSICAL PROPERTIES OF INSTRUMENTED BOMB TEST VEHICLES INCLUDING RELEASE CONDITIONS AND IMPACT DEVIATIONS FROM PARTICLE TRAJECTORIES	51
2. ESTIMATED IMPACT DEVIATIONS DUE TO LOW INCIDENCE INSTABILITY (RELEASE 25000 FT, VELOCITY 509 FT/S, NO DISTURBANCE, C.G. AT 51.7%)	52
3. ESTIMATED IMPACT DEVIATIONS DUE TO 0.5° FIN-BODY MISALIGNMENT (RELEASE 45000 FT, VELOCITY 578 FT/S, NO DISTURBANCE, C.G. AT 51.7%)	53

LIST OF FIGURES

1. ORIGINAL SHAPE FOR THE LOW DRAG SHAPE RESEARCH VEHICLE (M557A)
2. BLUFF NOSED RESEARCH VEHICLE SHAPE (M557B)
3. MODIFICATION TO ORIGINAL LOW DRAG SHAPE (M557A) TO PRODUCE THE M823 SHAPE

4. VARIATION OF NORMAL FORCE WITH ANGLE OF INCIDENCE, ROLL ATTITUDE AND MACH NUMBER FOR THE M557A LOW DRAG SHAPE
5. CHANGES IN NORMAL FORCE CHARACTERISTICS WITH CHANGE FROM M557A TO M823 BODY SHAPE
6. (a) VARIATION OF RESTORING MOMENT WITH ANGLE OF INCIDENCE, ROLL ATTITUDE AND MACH NUMBER FOR THE M557A LOW DRAG SHAPE
(b) EFFECT OF THE DESIGN OF THE SUPPORTING STING BALANCE ON RESTORING MOMENT FOR THE M557A LOW DRAG SHAPE
7. FLOW VISUALISATION EXPERIMENTS ON THE LOW DRAG M557A SHAPE
8. FLOW VISUALISATION EXPERIMENTS ON THE LOW DRAG M557A SHAPE
9. CHANGES IN LOW MACH NUMBER RESTORING MOMENT CHARACTERISTICS WITH CHANGE FROM M557A TO M823 BODY SHAPE
10. CHANGES IN RESTORING MOMENT CHARACTERISTICS WITH CHANGE FROM M557A TO M823 SHAPE. LOW INCIDENCE REGION AT ENLARGED SCALES
11. VARIATION OF NORMAL FORCE WITH ANGLE OF INCIDENCE, ROLL ATTITUDE AND MACH NUMBER FOR THE M557B BLUFF BODY SHAPE
12. VARIATION OF RESTORING MOMENT WITH ANGLE OF INCIDENCE, ROLL ATTITUDE AND MACH NUMBER FOR THE M557B BLUFF BODY SHAPE
13. VARIATION OF INDUCED SIDE FORCE WITH ROLL ATTITUDE FOR THE M557A LOW DRAG SHAPE
14. VARIATION OF PEAK INDUCED SIDE FORCE WITH ANGLE OF INCIDENCE FOR THE M557A LOW DRAG SHAPE ($\phi = 22\frac{1}{2}^{\circ}$)
15. VARIATION OF PEAK INDUCED SIDE FORCE WITH ANGLE OF INCIDENCE FOR THE M557B BLUFF BODY SHAPE ($\phi = 22\frac{1}{2}^{\circ}$)
16. VARIATION OF INDUCED SIDE MOMENT WITH ROLL ATTITUDE FOR THE M557A LOW DRAG AND M557B BLUFF BODY SHAPES
17. VARIATION OF PEAK INDUCED SIDE MOMENT WITH ANGLE OF INCIDENCE FOR THE M557A LOW DRAG AND M557B BLUFF BODY SHAPES ($\phi = 22\frac{1}{2}^{\circ}$)
18. VARIATION OF INDUCED ROLLING MOMENT WITH ROLL ATTITUDE FOR THE M557A LOW DRAG SHAPE
19. VARIATION OF PEAK INDUCED ROLLING MOMENT WITH ANGLE OF INCIDENCE FOR THE M557A LOW DRAG SHAPE ($\phi = 22\frac{1}{2}^{\circ}$)
20. VARIATION OF INDUCED ROLLING MOMENT WITH ROLL ATTITUDE FOR THE M557B BLUFF BODY SHAPE
21. VARIATION OF PEAK INDUCED ROLLING MOMENT WITH ANGLE OF INCIDENCE FOR THE M557B BLUFF BODY SHAPE ($\phi = 22\frac{1}{2}^{\circ}$)

22. (a and b) VARIATION OF PITCH DAMPING WITH INCIDENCE, ROLL AND MACH NUMBER FOR THE M823 LOW DRAG SHAPE. TESTS IN THE A.R.A. WIND TUNNEL
- (c) SUBSONIC VARIATION OF PITCH DAMPING WITH INCIDENCE AND ROLL FOR THE M823 LOW DRAG SHAPE. TESTS IN THE R.A.E. 8 FT S.S. WIND TUNNEL
23. VARIATION OF PITCH DAMPING WITH MACH NUMBER FOR THE M823 LOW DRAG SHAPE ($\phi = 0$)
24. VARIATION OF ROLL DAMPING WITH MACH NUMBER
25. VARIATION OF ROLL DAMPING WITH INCIDENCE ANGLE AT LOW MACH NUMBER ($M = 0.5$)
26. GENERAL ASSEMBLY OF THE M557A TEST VEHICLE
27. GENERAL ASSEMBLY OF THE M557B TEST VEHICLE
28. GENERAL ASSEMBLY OF THE M557A TEST VEHICLE FITTED WITH LATERAL PULSE ROCKETS
29. CANBERRA CAMERA INSTALLATION
30. MEASURED VARIATION OF DRAG COEFFICIENT WITH MACH NUMBER FOR THE M557A AND M557B BODY SHAPES
31. TYPICAL PARTICLE TRAJECTORIES OF THE M557A AND M557B BODY SHAPES (LEVEL RELEASES FROM 25000 FT AND 45000 FT ALTITUDE)
32. TIME HISTORIES OF MACH NUMBER AND DYNAMIC PRESSURE FOR PARTICLE TRAJECTORIES OF THE M557A AND M557B BODY SHAPES (LEVEL RELEASES FROM 25000 FT AND 45000 FT ALTITUDE)
33. ROLL HISTORIES OF ROUND NUMBERS 701, 702, 709, 716, 717, 718 AND 736
34. ROLL HISTORIES OF ROUND NUMBERS 708, 709, 714 AND 715
35. ROLL HISTORIES OF ROUND NUMBERS 724, 725, 726 AND 732
36. ROLL HISTORY OF ROUND NUMBER 72
37. ROLL HISTORIES OF ROUND NUMBERS 703, 706, 707 AND 713
38. ROLL HISTORIES OF ROUND NUMBERS 722 AND 723
39. ROLL HISTORIES OF ROUND NUMBERS 719, 720 AND 721
40. ROLL HISTORIES OF ROUND NUMBERS 704, 727 AND 728
41. ROLL HISTORIES OF ROUND NUMBERS 751, 752 AND 753
42. COMPARISON OF FREE FLIGHT AND WIND TUNNEL MEASUREMENTS: VARIATION OF NORMAL FORCE WITH INCIDENCE ϕ , ROLL ATTITUDE ψ AND MACH NUMBER M FOR THE M557A BODY

43. COMPARISON OF FREE FLIGHT AND WIND TUNNEL MEASUREMENTS: VARIATION OF NORMAL FORCE WITH INCIDENCE θ , ROLL ATTITUDE ϕ AND MACH NUMBER M FOR M823 BODY
44. COMPARISON OF FREE FLIGHT AND WIND TUNNEL MEASUREMENTS: VARIATION OF RESTORING MOMENT WITH INCIDENCE θ , ROLL ATTITUDE ϕ AND MACH NUMBER M FOR THE M557A BODY
45. COMPARISON OF FREE FLIGHT AND WIND TUNNEL MEASUREMENTS: VARIATION OF RESTORING MOMENT WITH INCIDENCE θ , ROLL ATTITUDE ϕ AND MACH NUMBER M FOR THE M823 BODY
46. COMPARISON OF WIND TUNNEL AND FREE FLIGHT MEASUREMENTS: CHANGE IN RESTORING MOMENT WITH CHANGE OF BODY SHAPE AT LOW INCIDENCE FOR VARIOUS MACH NUMBERS ($\phi = 0$)
47. COMPARISON OF FREE FLIGHT AND WIND TUNNEL MEASUREMENTS: VARIATION OF INDUCED SIDE FORCE ($\theta = 10^\circ$) AND SIDE MOMENT ($\theta = 10^\circ$) WITH MACH NUMBER
48. COMPARISON OF FREE FLIGHT AND WIND TUNNEL MEASUREMENTS: VARIATION OF PITCH DAMPING WITH MACH NUMBER
49. COMPARISON OF FREE FLIGHT AND WIND TUNNEL MEASUREMENTS: INDUCED ROLLING MOMENT AT $\phi = 22\frac{1}{2}^\circ$, $M = 0.5$ (M557A BODY)
50. RELEASE DISTURBANCE FOR THE M557A BODY SHAPE: COMPARISON OF MEASURED AND PREDICTED FIRST PEAK AMPLITUDES
51. BOUNDARIES OF DYNAMIC BEHAVIOUR DURING RESPONSE TO RELEASE DISTURBANCE AS FUNCTIONS OF C.G. POSITION AND FIN CANT (M557A BODY SHAPE $\phi_0 = 45^\circ$)
52. (a) TYPICAL COMPUTED RESPONSE TO RELEASE DISTURBANCE: M557A BODY SHAPE WITH C.G. AT 51.7%, $\eta = 0.17^\circ$ AND $\phi_0 = 45^\circ$
 (b) TYPICAL COMPUTED RESPONSE TO RELEASE DISTURBANCE: M557A BODY SHAPE WITH C.G. AT 51.7%, $\eta = 0.44^\circ$ AND $\phi_0 = 45^\circ$
 (c) TYPICAL COMPUTED RESPONSE TO RELEASE DISTURBANCE: M557A BODY SHAPE WITH C.G. AT 51.7%, $\eta = 1.41^\circ$ AND $\phi_0 = 45^\circ$
 (d) TYPICAL COMPUTED RESPONSE TO RELEASE DISTURBANCE: M557A BODY SHAPE WITH C.G. AT 55.5%, $\eta = 2.0^\circ$ AND $\phi_0 = 45^\circ$
53. (a) WING TIP CAMERA RECORD OF M557A BOMB: CLEAN RELEASE
 (b) WING TIP CAMERA RECORD OF M557A BOMB: TOPPLE AT RELEASE
 (c) WING TIP CAMERA RECORD OF M557B BOMB: CLEAN RELEASE
54. COMPARISON OF MEASURED AND PREDICTED ROLL RATES FOR ROUND NUMBER 726
55. COMPARISON OF MEASURED AND PREDICTED RESPONSE OF ROUND NUMBER 726 TO RELEASE DISTURBANCE (PREDICTION BASED ON MEASURED ROLL RATE)
56. FLOW VISUALISATION OF VORTICES SHED FROM THE M823 BODY SHAPE

57. (a) COMPARISON OF MEASURED AND PREDICTED ROLL RATE HISTORIES FOR ROUND NUMBER 716 ($\eta = 0.17^\circ$)
- (b) COMPARISON OF MEASURED AND PREDICTED ROLL RATE HISTORIES FOR ROUND NUMBER 709 ($\eta = 0.44^\circ$)
- (c) COMPARISON OF MEASURED AND PREDICTED ROLL RATE HISTORIES FOR ROUND NUMBER 708 ($\eta = 1.41^\circ$)

Accession For	
NTIS CRA&I	<input checked="" type="checkbox"/>
DTIC TAB	<input type="checkbox"/>
Unannounced	<input type="checkbox"/>
Justification	
By <u>AD-A704785</u>	
Distribution /	
Availability Codes	
Dist	Avail and/or Special
A-1	CMY 23

UNANNOUNCED



1. INTRODUCTION

The rapid advances in aircraft performance since World War II have placed increasingly stringent requirements upon the design of bombs. Under modern conditions of height and speed at release, bombs frequently experience prolonged periods of fall in the transonic speed range for which there has been little data available until recent years. Consequently, the preparation of ballistic tables often continued on the basis of assumed or inadequate experimental data for the variation of drag with Mach number, and the influence of dynamic behaviour upon a bomb's trajectory has nearly always been assessed by the indirect method of end-point ballistic trials. Under these circumstances such trials gave ballistic indices which varied appreciably with release conditions and with the trajectory parameters (time of fall, trail distance, air range, etc.) used to derive it. Interpolation and extrapolation from the ballistic tables was seriously hampered and large increases in end-point bomb ballistic programmes were necessary to ensure reliability.

It was with such difficulties in mind that, late in 1960, the joint R.A.E./W.R. research programme on instrumented bombs was formulated. At that time much information had already been obtained on the zero yaw drag of bombs at subsonic and transonic speeds. Ground launched model tests were one of the experimental techniques used extensively in acquiring these data and examination of the flight dynamics of freely rolling bombs by closely controlled trials with full scale instrumented bombs formed a logical extension of the aerodynamic work previously carried out by both R.A.E. and W.R.E. In addition, it was considered that new knowledge gained from the bomb research programme would be of general interest in the missile field and immediately useful in the development of unguided rocket test vehicles.

Events which led to the proposal for a joint United Kingdom/Australian research programme and the factors considered in its ultimate formulation are outlined in Sections 2, 3 and 4. In these sections it is shown how understanding of the basic theory of flight dynamics depended very heavily upon the extensive American contributions in this field. At an early stage in the R.A.E./W.R.E. experimental programme direct contact was made with corresponding U.S. research establishments for exchange of ideas and experience. In this connection representatives from R.A.E. and W.R.E. have since visited America on two occasions (in April 1963 and April 1964) to take part in technical discussions with representatives from the Naval Ordnance Laboratories, White Oak; Naval Weapons Laboratories, Dahlgren; Ballistic Research Laboratories, Aberdeen; National Aeronautics and Space Administration, Langley Field; Air Proving Ground Centre, Eglin Air Force Base; and Naval Ordnance Test Station, China Lake. These visits stimulated considerable American interest in the United Kingdom/Australian contribution to the study of missile dynamics with the result that there has been a very free exchange of data, ideas and experiences, and the original experimental programme was substantially modified to include new techniques and novel stabilising devices.

Following the tripartite discussions of 1963 the scope of the research program was extended with three main objectives :-

- (i) to provide a more rigorous check on the validity of current stability theories by making correlations between the full scale research vehicle observed behaviour and that predicted from its mathematical model using the most complete sets of wind tunnel and free flight data obtainable; and

- (ii) to investigate theoretically and experimentally ideas and techniques which appear to provide solutions to some of the stability problems and to offer the possibility of weapons with greater tactical flexibility; and
- (iii) to develop where necessary, new experimental methods for obtaining aerodynamic data.

These objectives were based on the conviction that if the validity of the theory and the mathematical model could be firmly established, then only wind tunnel and digital computer facilities would be necessary to predict the effectiveness of any particular missile configuration. After the second series of tripartite discussions (in April 1964) it was decided that wind tunnel facilities at the Naval Ordnance Laboratory, White Oak, would be used to augment the aerodynamic data previously obtained in Australia by the Aeronautical Research Laboratories and in England by the Aircraft Research Association Ltd. and the Royal Aircraft Establishment, Bedford. The American wind tunnel experiments were planned to use the basic body shape of the R.A.E./W.R.E. bomb research test vehicle in conjunction with the following stabilising devices :

- (1) Fixed cruciform tail
- (2) Spinning cruciform tail
- (3) Fixed split skirt
- (4) Spinning split skirt
- (5) Spinning monoplane tail.

This work included measurements of Magnus forces and moments in addition to measurements similar to those being made in England, thereby giving particularly valuable support to the research programme since neither England nor Australia had suitable Magnus test rig facilities.

Free flight experiments have so far been performed only with the fixed cruciform tail configuration and the purpose of this report is to present the results obtained from a total of 33 trials using this type of stabilising device. A second report, covering the use of split skirts and spinning tails will be published subsequently.

2. ORIGIN OF R.A.E./W.R.E. EXPERIMENTS IN BOMB BALLISTICS

Australian participation in the study of bomb ballistics stemmed from a programme of research and development initiated at the Royal Aircraft Establishment, Farnborough, U.K. in 1949(1,2). Up to that time Armament Department, R.A.E., had used the design criteria earlier established by Capper(3,4,5,6) which ensured that bombs would have an acceptably low dispersion, but these empirical rules based on trials at relatively low altitudes were being shown to be inadequate when applied to bombs released by modern high altitude aircraft. There was then, as there is now, a considerable interest in the reduction of tail sizes needed to improve bomb-bay storage efficiency and to lessen the effects of vibration, buffeting and release disturbance(7). Thus the problem of correlating bomb stability with dispersion(8) became highly significant and the research programme outlined by Richards(1) was

intended to determine the possibility of establishing closer limits on bomb d parameter values necessary for good ballistic consistency. This programme, comprised a total of approximately 240 end-point trials conducted at the Woom Range in the period 1951 to 1955, did not succeed in establishing minimum stability criteria since in general the bombs tested were too stable and little variation in dispersion was found.

Results of these end-point ballistic trials showed that direct measurement dispersion and the variation of ballistic index was not a sufficiently sensitive method of optimising bomb stability criteria unless separate measurements were made to isolate the causes of such variation. One of the most urgent requirements for accurate drag data, particularly in the transonic speed range, and the technique of using freely flying models launched from the ground by rocket boost-motors a proven method well suited to the study of aerodynamic drag. In England between 1950 and 1951, Dudley and Lawrence (9) conducted the first experiments of this kind on bombs. These experiments were performed to show the effects of five variations of nose shape on the drag of a basic bomb-body. Later, toward the end of 1951, the Weapons Research Establishment began a programme of drag and stability tests proposed as an extension of Dudley and Lawrence's work with the object of providing additional data applicable to service bombs, while Greenwood (10, 11) of R.A.E. carried out similar free flight experiments in England. The W.R.E. programme totalling 28 test vehicles, was based on a series of six body shapes (12) chosen systematically to give a good representation of nose shape and fineness ratio for bombs then in use. Information obtained from the model experiments was applied with moderate success to the prediction of full scale bomb performance (13), but the lack of incidence data prevented a detailed analysis of flight dynamic behaviour. The presence of nonlinear aerodynamic cross-coupling forces and moments and the limited scope of the results was consequently limited.

Many instances of abnormal behaviour were observed in the ground launched tests when lateral pulse rockets were used to initiate transient responses. Although useful data could not be extracted from such trials, modern developments in the flight dynamic theory for symmetric missiles gave a strong background of information making it possible to understand and appreciate the significance of the abnormalities. The implications of this theory substantially influenced the decision to conduct full scale trials with instrumented bombs, and its development is therefore briefly outlined in the following section.

3. DEVELOPMENT OF FLIGHT DYNAMIC THEORY

Prediction of missile motion under the influence of large angles of attack remained one of the most challenging problems in exterior ballistics and only in recent years has the theory of nonlinear mechanics been fruitfully applied to the analysis of this problem. In the past, the classical "linearised" theory of yawing motion (14 to 19) was thought to be valid up to about ten degrees in angle of yaw. Apparently this limit was decided from consideration of the geometric approximations used, and a comparison of the errors caused by these approximations with the precision of the most advanced contemporary experimental techniques. About the year 1948, wind tunnel measurements in both England and America of the static properties (lift, drag and pitching moment) for a wide variety of projectiles had largely eliminated the most obvious cause of erratic behaviour, namely, that of static stability. However, the occurrence of short ranges and large dispersion for mortar shells, bombs and rockets still occurred and could not be explained

the basis of linear theory and the available data, and hence no corrective action could be taken to prevent rogue behaviour.

The failure of linear theory to account for large dispersion and sporadic shorts experienced by freely rolling projectiles led to a diversity of suggestions for the mechanism of dispersion. Important contributions to this study were made by such people as Nicolaides(20, 21), Murphy(22,23,24), Maple(25), Synge(25) and Zarodny(26, 27,28), resulting in the prediction of novel conditions of dynamic instability.

Briefly, the response of a finned symmetric missile to disturbances at launch or during steady flight is characterised by an initial transient oscillation which under the influence of spin invariably degenerates to an almost pure circular pitching and yawing motion. Stable modes of this circular motion (which are termed "limit cycles" (23)) may occur in steady rolling flight conditions, and may persist indefinitely with quite large constant amplitude or may gradually decay. Low incidence motions of this type are frequently experienced by mortar shells having well streamlined shapes. The larger yawing motions, however, are sustained by amplitude dependent aerodynamic nonlinearities and most particularly by the nonlinear Magnus couple. The occurrence and nature of "limit cycles" in particular cases stems primarily from the magnitude of the initial disturbance and the subsequent growth of roll rate.

In addition to these sustained, constant amplitude motions, three types of flight instability have been isolated for freely rolling finned ballistic missiles and identified as (20, 21) :-

- (1) roll-yaw resonance instability
- (2) catastrophic yaw, and
- (3) nonlinear Magnus instability.

Of these the first is predicted by linear theory which demonstrates that the presence of small configurational asymmetries together with rolling velocity can result in instability due to resonance between rolling and pitching motions. Numerical integrations indicate that the rapidity of passage through the resonant region is a significant factor affecting the temporary magnification of the small trimmed angles in pitch and yaw caused by slight configurational asymmetries. The other two forms of instability are characteristic of nonlinear behaviour. Catastrophic yaw is exhibited by missiles having low roll rates (of the order of the natural yawing frequency) and is caused by periodic yaw-induced rolling moments and side moments associated with flight at large angles of attack. Magnus instability occurs at higher roll rates (greater than the natural yawing frequency) and the destabilising Magnus moments which produce excessive yawing amplitudes are strongly dependent on both spin rate and yawing amplitude.

In general, cruciform finned aircraft bombs are much more susceptible to resonance and catastrophic yaw phenomena associated with low roll rates caused by small errors in fin alignment than to Magnus instability. The latter form of instability is likely to occur at somewhat higher roll rates, as may be produced by deliberate fin cant. Such considerations formed the basis of technical discussions when the research programme was being planned.

4. UNITED KINGDOM/AUSTRALIAN JOINT PROJECT FOR FULL SCALE INSTRUMENTED BOMB TRIALS

As outlined in Section 2, Australian interest in missile flight dynamics stems from experimental investigations of the drag and stability characteristics for a number of aircraft bomb shapes undertaken at Weapons Research Establishment between about 1955 to 1959. In analysing the results of ground launched model tests, full scale instrumented bomb trials and end-point ballistic trials, evidence was accumulated which indicated that roll-yaw cross coupling effects had a strong influence upon flight behaviour. This evidence was well supported by the modern developments of the flight dynamic theory previously described, thereby emphasizing the need to acquire reliable and comprehensive aerodynamic data by conducting experiments specifically aimed at detailed assessments of flight performance. It is apparent from references 29, 30 and 31 that American bomb designers were experiencing similar problems.

During the latter half of 1960, Armament Department, R.A.E., proposed a program of bomb ballistic trials(7) to be carried out in conjunction with wind tunnel tests. This experimental programme was planned to establish the minimum aerodynamic stability of bombs consistent with low dispersion and was originally intended to be linked with trials of a weapon to meet a current British Operational Requirement. It was considered that the Operational Requirement could be met by having a centre section comprising the bomb itself to which a streamlined or bluff nose could be fitted, for either external or internal carriage, and a series of tails added to suit the various tactical requirements. Some of these proposed weapon shapes seemed quite suitable for simultaneous use as instrumented vehicles for stability research work.

Following an exchange of technical views between R.A.E. and W.R.E., representatives from the U.K. Ministry of Aviation and Armament Department, R.A.E., visited Weapons Research Establishment during November 1960 to formulate a joint United Kingdom/Australian programme of trials. As a result of discussions then held it was agreed that an adequate determination of the factors which contribute to dispersion for given type of bomb would require as a minimum :-

- (1) accurate knowledge of the bomb's static and dynamic derivatives over an appreciable range of yawing angles and for speeds including the transonic regime;
- (2) the use of a computing facility capable of solving the nonlinear equation of motion with high precision, and
- (3) a programme of full scale ballistic trials, properly instrumented, to provide a check of the mathematical model predictions and to assess the effects of release disturbance.

The philosophy adopted was to use the instrumented bomb trials to determine minimum design requirements for adequate ballistic consistency and when these were established to carry out a limited number of end-point ballistic trials to measure the dispersion figure for selected borderline cases.

A streamlined and a bluff body shape were chosen for study and it was proposed that comprehensive tests would be made first using only the streamlined body. Results so obtained were then to be taken as a basis for planning the bluff body trials. The original trials programme was divided into the following three phases :-

- PART 1 : 12 to 15 instrumented bombs dropped from a Canberra aircraft flying at 500 mile/h and 45000 ft altitude. This release condition, however, was to be subject to wind tunnel tests showing no large changes in the aerodynamic derivatives over the Mach number range involved. The effects of variation of fin cant angle and static margin were to be investigated on the low drag shape with fixed cruciform fins set at zero cant plus three fin cant angles and for a range of three static margins obtained by shifting the bomb's centre of gravity. Using the results obtained from each trial, the order of drops would be chosen to give a maximum of information and to avoid tests which previous results showed were no longer useful.
- PART 2 : Further instrumented bombs, bringing the total to a maximum of 30, dropped from a Canberra Aircraft under various conditions to check missile behaviour during loft bombing, to investigate Reynolds number effects and to verify the performance of the bluff body shape. During these trials low range linear and angular Donner accelerometers were to be used to obtain accurate drag and stability data. Records from these instruments and other lateral accelerometers and Contrave trajectory information were then expected to give all the information necessary for determining aiming data for the weapons with the same shapes.
- PART 3 : Up to 20 uninstrumented bombs dropped from a Canberra aircraft to determine a typical dispersion figure and obtain any additional ballistic data that might be found necessary.

It was agreed that the manufacture of the bomb bodies should be carried out in Australia under the control of Weapons Research Establishment since it was necessary to ensure that the design would satisfy the instrumentation requirements for trials at Woomera.

The first trial was performed in December 1961 and since then Parts 1 and 2 of the research programme have been completed. The third part of the programme has been withheld because by early in 1963 the instrumented bomb trials had provided sufficient data to establish a suitable method of conducting proving trials and this method (Section 9.2) has been demonstrated with two other newly designed British service bombs (32,33). These proving trials replaced the originally planned part 3, and the remaining bomb test vehicles have now been set aside for future tests on split skirt and spinning tail stabilising devices.

5. EXPERIMENTAL METHOD

The experimental method for studying the aerodynamic behaviour of bombs has been developed to meet the following basic requirements :-

- (1) Obtain data on the aerodynamic forces and moments covering the expected range of flight conditions.
- (2) Use such aerodynamic data to predict missile response and ballistic performance under representative flight conditions.
- (3) Check the validity of predicted responses by comparing them with direct observations of dynamic behaviour in full scale free flight trials.

The first of these requirements was fulfilled by wind tunnel tests carried out at the Aeronautical Research Laboratories, Melbourne, at the Royal Aircraft Establishment, Bedford, and by the Aircraft Research Association, which is also Bedford. A full account of these tests is given in Section 6.

To meet the second requirement, aerodynamic data obtained from the wind tunnel tests were programmed on the IBM 7090 computer at W.R.E. enabling numerical solutions of the equations of motion to be obtained. These solutions provided basis for correlations between the observed full scale trials results and the corresponding predicted performances, though these correlations were not in themselves sufficient to satisfy completely the third requirement of the experiment method because any differences could be attributed to either errors in the predicted performances or possible inaccuracy of the wind tunnel data. For this reason the instrumented bomb trials were augmented by a limited number of "transient response" experiments in which selected bombs were disturbed during otherwise steady flight by means of lateral pulse rockets or "bonkers". Aerodynamic data obtained from analysis of the resulting oscillations were then available for direct comparison with the wind tunnel measurements.

Although this method gives comparisons of the overall aerodynamic force and moment system as determined by model and full scale experiments, it does not permit correlations of the local flow conditions unless additional measurements of surface pressure are made. Since such measurements were not of immediate interest in the bomb research work, no full scale tests of this kind have been conducted.

6. WIND TUNNEL TESTS AND RESULTS

The first wind tunnel tests of the two original body shapes (M557A and M557B figures 1 and 2) were five-component static force and moment measurements carried out at the Aeronautical Research Laboratories in Melbourne. In these tests the Reynolds numbers were an order less than those appropriate to full scale conditions (a 1/9th scale model was used in a 21 in. x 32 in. working section) and some of the early results showed rather more scatter than would normally be expected by A.R.L. This was caused by the use of an existing sting balance which was not sufficiently sensitive for the small forces and moments in the low incidence range. Nevertheless, it was adequate to reveal a markedly nonlinear pitching moment variation for the M557A body at small pitch angles. Because some doubt was cast upon the effectiveness of transition fixing at such low Reynolds numbers a two component sting balance was subsequently constructed specifically with high sensitivity to normal force and pitching moment. Using this balance, measurements were repeated with greater accuracy and in more detail for the low incidence range and it was demonstrated that roughness bands on the fins caused nonlinear behaviour at low incidence to be virtually independent of Reynolds number within the test range (34). In view of these results it was concluded that extrapolation to higher Reynolds numbers could well be based on the data obtained with fin roughness bands present.

Since the A.R.L. data had a limited test range, the measurements were extended in Britain to cover much higher Reynolds numbers and a wider range of Mach number in the 10ft x 8ft Transonic Wind Tunnel of the Aircraft Research Association, Bedford. These results essentially confirmed the nonlinearity in force and moment shown by the measurements made in Melbourne, and the static wind tunnel data given here are all taken from the A.R.A. (Bedford) results. Measurements were also in two further series of tests at A.R.A. and in one series of tests at P.A.E. (Bedford) of the damping in pitch and roll on the low drag shape using the R.A.

oscillatory derivative measuring rig and method described in reference 35. For these tests it was necessary to modify the model tail cone slightly to accommodate the damping balance and the modified low drag shape M823 (figure 3) was the result. During the damping tests, measurements of static normal force and pitching moment were also obtained so that comparative data are available showing the effects of the change in the low drag outline from the M557A and M823 shapes.

6.1 Test conditions and presentation of data

6.1.1 Model scales and Reynolds numbers

The static force and moment tests on the M557A low drag and M557B bluff body shapes in the Aircraft Research Association wind tunnel were made with quarter scale models of the full size research vehicles shown in figures 1 and 2. Most tests were made with a stagnation pressure of 0.8 atmosphere, though a few were carried out with stagnation pressures of 1.0 and 1.2 atmospheres. Under these conditions Reynolds number increases with Mach number and values of Reynolds number for representative Mach numbers are tabulated below. Maximum body diameter is used as characteristic length.

Reynolds' Numbers x 10⁻⁶

Stagnation Pressure \ Mach number	0.50	0.75	1.00	1.25
	0.8 atmosphere	0.94	1.21	1.33
1.0 atmosphere	1.17	1.56	1.72	1.80
1.2 atmosphere	1.48	1.84	2.07	2.15

The pitch and roll damping tests, and the accompanying static force and moment measurements on the M823 low drag shape were made using a half scale model at 1.0 atmosphere stagnation pressure. The corresponding Reynolds numbers based on body diameter were :-

Mach number	0.50	0.75	1.00	1.25
R.N. x 10 ⁻⁶	2.34	3.12	3.42	3.60

For comparison, the Reynolds numbers (multiplied by 10⁻⁶) for the full scale vehicle trials are given for the two extremes of height.

Mach number	0.50	0.75	1.00	1.25
At sea level	5.64	8.50	11.2	14.2
At 45 000 ft	1.20	1.80	2.38	2.99

The wind tunnel Reynolds numbers were high and the changes in the during testing produced no significant effect; even with the quarter scale model the wind tunnel Reynolds numbers overlapped the full scale Reynolds number range a little and the Reynolds numbers of the test the half scale M823 shape were equal to those for full scale experiments between 30 000 and 40 000 ft (depending on Mach number). Since many of the most important vehicle motions investigated in the full scale trials place at the higher altitudes soon after release from the aircraft, the wind tunnel tests Reynolds numbers can be considered as almost full

6.1.2 Coefficient definitions, systems of axes, etc.

All coefficients are based on the maximum body cross section area and the maximum body diameter (d) as reference area and length. The values of S and d for the full scale vehicle are 1.918 ft² and 1.562 ft for all three shapes tested.

The moment reference point is at 0.50 of the body length for the low drag shapes (72.0 in. aft of the nose) and at 0.365 of the body length for the bluff body shape (38.0 in. aft of the nose).

Two sets of right-handed rectangular Cartesian axes are used. One set of body-fixed axes centred at the moment reference point. X, Y and N are the force components along these axes and l, m, n, the moments about the reference point. At zero roll ($\phi = 0$), Y is positive out to starboard, N is positive vertically upwards, n is positive nose to starboard, m is positive moment about the reference point upwards and l is positive for starboard side down. Since the wind tunnel balance was fixed in the body, the five components of static force and moment which were measured were obtained in body-fixed axes. Their coefficients are defined as :-

$$C_Y = \frac{Y}{\frac{1}{2} \rho V^2 S}$$

$$C_N = \frac{N}{\frac{1}{2} \rho V^2 S}$$

$$C_n = \frac{n}{\frac{1}{2} \rho V^2 S d}$$

$$C_m = \frac{m}{\frac{1}{2} \rho V^2 S d}$$

$$C_l = \frac{l}{\frac{1}{2} \rho V^2 S d}$$

The wind tunnel results were recomputed in terms of non-rolling body axes OX'Y'Z' ("Incidence plane axes") which are centred at the moment reference point and pitch with the body but do not roll with it. Hence for the wind tunnel results OX'Z' is always the vertical plane and is always the plane of the angle of incidence of the model. In this case the roll angle ϕ gives the attitude of the fins to the plane of incidence.

and $\phi = 0$ is defined as one pair of fins in the incidence plane. For the pitch damping tests the model oscillation was in the plane of incidence. X' , Y' , N' are the components of force along $OX'Y'Z'$ and l' , m' and n' are the moments about them. All the wind tunnel results are presented in terms of these non-rolling body axes since they make much clearer the pattern of changes in the forces and moments acting with change of attitude - restoring moment (m') and normal force (N') are always in the plane of the incidence while Y' and n' are the side forces and moments induced in the plane at right angles.

Y' is positive to starboard and N' is positive upwards in the vertical plane. With these definitions :-

$$C_{Y'} = C_N \sin \phi + C_Y \cos \phi$$

$$C_{N'} = C_N \cos \phi - C_Y \sin \phi$$

$$C_{m'} = C_m \cos \phi - C_n \sin \phi$$

$$C_{n'} = C_m \sin \phi + C_n \cos \phi$$

$$C_{l'} = C_l$$

6.1.3 Transition fixing

In all the A.R.A. wind tunnel tests on the quarter scale model of the low drag M557A shape, transition was fixed on the body by a roughness band 2 in. aft of the nose (model scale) which was $\frac{1}{2}$ in. wide and 0.004 in. to 0.005 in. high. No attempt was made to fix transition on the fins as it was believed that it was unnecessary at these Reynolds numbers with this sharp leading edge section. With the larger (half scale) size M823 low drag shape transition was again fixed on the body at the same relative position using a roughness band approximately 0.010 in. high and transition left free on the fins. With the bluff M557B shape, transition was left free on both body and fins since it seemed certain that transition would always take place at the front corner of the body.

6.1.4 Test ranges of incidence angle, roll attitude, Mach number, etc.

Only a representative sample of the wind tunnel data is reproduced in this report. Full results are tabulated in references 36 to 40. The full range of tests made at A.R.A. and R.A.E. Bedford is summarised below, with the exception of some repetitions checking incidence hysteresis effects on restoring moment, and incidence and Mach number hysteresis effects on drag.

Static force and moment measurements on the M557A low drag shape

(a) 0.8 atmosphere stagnation pressure

$$\theta = -2^\circ \text{ to } +20^\circ \text{ for } \phi = 0^\circ, 22\frac{1}{2}^\circ \text{ and } 45^\circ$$

$$\phi = 0 \text{ to } 45^\circ \text{ for } \theta = 15^\circ, 17^\circ \text{ and } 20^\circ$$

UNCLASSIFIED

These were repeated for each Mach number of $M = 0.5, 0.65, 0.75, 0.85, 0.90, 0.95, 1.00, 1.05, 1.25$.

(b) 1.2 atmosphere stagnation pressure

Limited Reynolds number check at $M = 0.85, 0.95, 1.05$

$\theta = -2^\circ$ to $+10^\circ$ for $\varphi = 0$ only

(c) 0.8 and 1.2 atmosphere stagnation pressure measurements with improved design of sting support

$\theta = -2^\circ$ to $+8.5^\circ$ for $\varphi = 0$ only at $M = 0.65, 0.85, 0.95, 1.00, 1.05, 1.10, 1.15, 1.25$.

(d) Flow visualisation experiments on the low drag shape. Tests in the range $\theta = 0$ to 9° at $M = 0.95$ and 1.25 .

(e) Low drag shape fitted with the bluff body fins

$\theta = -2^\circ$ to $+10^\circ$ for $\varphi = 0$ only at $M = 0.75, 0.85, 0.95, 1.05, 1.2$

Static force and moment measurements on the M823 low drag shape

$\varphi = 0,$ $\left\{ \begin{array}{l} \theta = -2^\circ \text{ to } +17^\circ \text{ at } M = 0.5 \\ \theta = -2.5^\circ \text{ to } +21^\circ \text{ at } M = 0.7 \text{ and } 0.8 \\ \theta = -2^\circ \text{ to } +7^\circ \text{ at } M = 0.75, 0.95, 1.00, 1.05, 1.30. \end{array} \right.$

$\varphi = 22\frac{1}{2}^\circ,$ $\left\{ \begin{array}{l} \theta = -0.5^\circ \text{ to } +21^\circ \text{ at } M = 0.7 \\ \theta = -2^\circ \text{ to } +8^\circ \text{ at } M = 1.0 \end{array} \right.$

$\varphi = 45^\circ,$ $\left\{ \begin{array}{l} \theta = -0.5^\circ \text{ to } +21^\circ \text{ at } M = 0.7 \\ \theta = -2^\circ \text{ to } +8^\circ \text{ at } M = 0.5 \text{ and } 1.0 \end{array} \right.$

Static force and moment measurements on the M557B bluff body shape

$\theta = -2^\circ$ to $+20^\circ$ for $\varphi = 0, 22\frac{1}{2}^\circ$ and 45°

$\varphi = 0$ to 45° for $\theta = 15^\circ, 17^\circ$ and 20°

These were repeated for each Mach number of $M = 0.5, 0.65, 0.75, 0.85, 0.90, 0.95, 1.00, 1.05, 1.25$.

Pitch damping measurements on the M823 low drag shape

$\varphi = 0,$ $\left\{ \begin{array}{l} \theta = -2^\circ \text{ to } +17^\circ \text{ at } M = 0.5 \\ \theta = -2.5^\circ \text{ to } +21^\circ \text{ at } M = 0.7 \text{ and } 0.8 \\ \theta = -2^\circ \text{ to } +7^\circ \text{ at } M = 0.75, 0.95, 1.00, 1.05, 1.30 \end{array} \right.$

UNCLASSIFIED

$$\varphi = 22\frac{1}{2}^{\circ}, \quad \begin{cases} \theta = -0.5^{\circ} \text{ to } +21^{\circ} \text{ at } M = 0.7 \\ \theta = -2^{\circ} \text{ to } +8^{\circ} \text{ at } M = 1.0 \end{cases}$$

$$\varphi = 45^{\circ}, \quad \begin{cases} \theta = -0.5^{\circ} \text{ to } +21^{\circ} \text{ at } M = 0.7 \\ \theta = -2^{\circ} \text{ to } +8^{\circ} \text{ at } M = 0.5 \text{ and } 1.0 \end{cases}$$

Roll damping measurements on the M823 low drag shape

$\theta = 0$ tests at $\varphi = 0$ and 45° at $M = 0.5, 0.75, 0.90, 0.95, 1.0, 1.05, 1.15, 1.30$

Limited incidence range tests ($\theta = -6^{\circ}$ to $+10^{\circ}$) at $M = 0.50$
for $\varphi = 0, 22\frac{1}{2}^{\circ}$ and 45° .

6.2 Static measurements of normal force and restoring moment on the low drag shapes

The wind tunnel tests made in the A.R.A. transonic wind tunnel were first planned as a straightforward series of measurements to extend the small scale measurements made in the A.R.L. wind tunnel which had shown restoring moment nonlinearities thought at that time to be an effect of the transition fixing at the small scale of the A.R.L. tunnel tests. The first A.R.A. wind tunnel measurements at the larger scale repeated the nonlinear restoring moment curves, confirmed the A.R.L. results and showed that another explanation would have to be sought. The subsequent additions and modifications during the investigations are responsible for the rather rambling additions to the original systematic test programme.

The variation of the normal force acting on the original M557A low drag shape with angle of incidence, roll attitude and Mach number is shown in figure 4. There is little to comment on in the results, though the variation of normal force with incidence for Mach numbers of 1.05 and below is more than usually nonlinear for angles below 10° . This nonlinearity is associated with the much more strongly marked nonlinearity in the restoring moment curves and is almost entirely eliminated by the relatively small change in the tail cone shape which converts the M557A shape to the M823 shape, (figures 5(a) and (b)). For the M823 shape the normal force curves are smooth and much more nearly straight.

The variation in the restoring moment acting on the M557A shape with angle of incidence, roll attitude and Mach number is shown in figure 6(a). The most important feature is undoubtedly the low incidence nonlinearities for Mach numbers up to $M = 1.05$ and much effort was put into explaining and verifying these. When the high Reynolds number tests in the A.R.A. wind tunnel had shown that the nonlinearities were not due to the effects of the transition fixing devices at very small scale, it was thought that they might be due to the design of the M557A fins with their very low aspect ratio and sharp leading edges. Measurement of restoring moments on the bluff M557B shape had not shown the same systematic nonlinearities as with M557A, even though the bluff body moments were irregular at Mach numbers near 1.0 (figure 12) and so a limited test at a few Mach numbers was carried out with the M557B fins mounted on the low drag M557A body. This showed that though subsonically these fins had given a reasonably linear restoring moment curve when on the bluff body,

there was still the same type of marked nonlinearity in restoring moment for low drag body with these fins fitted. Suspicion now centred on the low drag body shape and oil flow experiments were carried out to trace the cause. Some of the oil flow pictures are reproduced in figures 7 and 8*. First there was a run through the Mach number range between $M = 0.95$ and $M = 1.25$ at $\theta = 3^\circ$, and then a set at $\theta = 3^\circ, 6^\circ$ and 9° at $M = 0.95$. At $\theta = 3^\circ, M = 0.95$, there is a triangle at the root of the fin on its upper surface where the flow looks so sluggish as to suggest a complete local separation (figure 7): presumably the increasing convergence of the tail (which is not a true cone but is radiused, figure 1) reaches a limit where the flow can no longer remain attached to the body in the region of the adverse pressure gradient on the top of the fin. In the positive pressure region under the fin the flow can remain attached and the separation region is not there (figure 7(d)). With increasing incidence at $M = 0.95$ the triangle on the upper fin surface where the flow is dominated by the body interference grows in extent, but a more important point is that whereas the flow in this triangle is very sluggish at 3° incidence the fin surface in it seems to be thoroughly scrubbed at 9° by a high velocity air stream, as if there is a vortex (due to body cross-flow?) lying across the fin upper surface at this higher incidence. The enlarged picture of the fin (figure 8) shows that there is certainly not a separation from the fin surface at 9° incidence and the supposition regarding the separation being prevented by a cross-flow body vortex lying across the fin surface is supported by the flow markings on the body which indicate the areas where the vortex springs from the body down on to the fin root. (Indicated by A on figures 8(a) and (b)). Another point from the oil flow experiments which shows how the body influences at these Mach numbers (M less than 1.05) reduces fin effectiveness at low incidence and so contributes to the low incidence nonlinearities in the restoring moment is that at the higher incidences (say $\theta = 9^\circ$ or more) the oil lines on the body show that there is some body upwash in addition to the incidence (figure 8), whereas at $\theta = 3^\circ$ the flow lines suggest a negative incidence in the region of the fins. Hence the local body downwash is decreasing the fin lift at low incidence and increasing it at high - this in itself would contribute the right sense to the nonlinearities in restoring moment.

Summarising, at subsonic and transonic Mach numbers (below about $M = 1.05$) there is a restoring moment nonlinearity because at the very rear of the body the tail cone is too convergent for the flow to remain attached above the fin and there is a separation in the fin root triangle which reduces fin efficiency. At higher incidences a body cross-flow vortex prevents this separation and the fin recovers its full effectiveness. Supersonically, at Mach numbers above $M = 1.05$, the flow is able to remain attached to the body at low incidences and the appearance of body cross-flow vortices lying across the fin surface at the higher incidences no longer make a sudden difference to fin effectiveness.

These conclusions caused some concern over possible sting-support interference effects. The sting balance used was one already in existence and had been used for another purpose and was not ideal. The sting diameter was fairly large relative to the body base diameter and diverged very slightly aft of the model. It was felt that the slight sting divergence immediately aft of the model might accentuate the after body separation and a few further tests were carried out with an improved sting design. The improved sting was parallel for more than six body base diameters downstream of the model. Apart from results at low

* These photographs are reproduced by kind permission of the Aircraft Research Association Bedford.

incidence and transonic speeds little difference was found with the improved sting design and these tests effectively dispelled all doubts about any important sting interference effects on the wind tunnel results. The restoring moment measurements for the M557A body with both sting balances are given in figure 6(b); this shows results throughout the Mach number range for the lower incidences where any possible differences would occur. In the subsonic and transonic Mach number region (up to a Mach number just below 1.05) the difference between the two sets of curves is very small, the slightly divergent sting design causing a small increase in the upper fin surface separated flow region and so very slightly increasing the low incidence restoring moment non-linearity (cf. restoring moment curves on figure 6(b) for $M = 0.85$ to $M = 1.00$). The only other difference with the new sting was that the low incidence flow separation ceased (and hence the marked nonlinearity in the restoring moment vanished) at just below $M = 1.05$ instead of just above - cf. the $M = 1.05$ and 1.25 curves on figure 6(b). However, it will be shown later (see Section 8.2) that the trajectory of a bomb may be critically affected by the extent of the unstable region near zero incidence.

When this explanation of the restoring moment nonlinearities of the M557A shape had been established, it was predicted that it would be possible to eliminate them easily by reducing slightly the convergence of the rearmost part of the body. Since these separations were entirely low incidence effects (θ less than 7°), it was argued that the small modification to eliminate them would have virtually no effect on the aerodynamics at high incidence (θ greater than 7°). Soon afterwards a new model was made for the pitch and roll damping tests (see paragraph 6.5) and by coincidence it was found necessary to make this small change to the body shape to accommodate the oscillatory derivative balance and support. The M823 low drag body shape resulted (figure 7). The predictions regarding the aerodynamics were completely justified. Figure 9 shows examples of how the low incidence nonlinearity in restoring moment was eliminated with virtually no effect on the high incidence values, and figure 10 shows enlarged the detail of the changes produced at low incidence with almost complete elimination of the restoring moment nonlinearity at all Mach numbers.

The other feature of the restoring moment results to be noted is the large variation in restoring moment with roll attitude at incidences above about 10° (figure 6(a)). It is obvious that for any satisfactory prediction of a missile's behaviour during oscillatory motions which include angles of incidence of 10° or more it is essential to have a reliable knowledge of the variation of restoring moment with roll attitude as well as with incidence.

6.3 Static measurements of normal force and restoring moment on the bluff M557B shape

The variation of normal force and restoring moment acting on the M557B shape with incidence, roll attitude and Mach number is shown in figures 11 and 12. The systematic nonlinearities in restoring moment found at subsonic speeds with the low drag M557A shape were not present with this bluff body. The curves of both normal force and restoring moment are reasonably smooth for Mach numbers up to about 0.95, though the curves of restoring moment in particular are very irregular in the transonic region. ($M = 1.00$ to 1.05). These irregularities with the bluff body did not affect the full scale trials in any way since the drag/weight ratio of the bluff store was high enough to keep its full scale free-flight Mach number subsonic at all times.

The pattern of restoring moments and normal forces acting on this bluff body is in accord with what has been found previously with bluff nosed bodies (e.g.

references 11, 41, 42 and 43). Subsonically, the flow separates from the top of the body leaving an open bubble with the after-body submerged in a wake which is already completely separated; under these circumstances the convergence of the rear tail cone cannot cause the local separations on the fin upper surf at low incidence which caused the nonlinearities with the M557A body. At some Mach number near unity, the flow around the body changes; the flow still separates from the body nose but re-attaches soon afterwards leaving only a small closed separation bubble at the nose and the flow is attached over the rest of the body. Between $M = 1.0$ and about $M = 1.10$ the flow re-attachment is not firmly established and a complete separation or, in some instances, partial separation on one side of the body can be caused by a one or two degrees change in incidence. This together with the passage of shock wave down the tail cone over the fins is the cause of the rapid fluctuations in restoring moment with incidence for θ below 10° shown at $M = 1.0$ and $M = 1.1$ in figure 12. At higher Mach numbers the flow reattachment always occurs and the restoring moment and normal force curves are again more linear.

6.4 Static measurements of induced side force, side moment and rolling moment for the M557A and M557B shapes

The side forces and moments (i.e. those in the plane perpendicular to the plane of incidence) and the rolling moments induced on a symmetric vehicle at the asymmetric attitudes produced by combinations of incidence and roll angle are only of a significant size at large incidences - say above about 10° . Consequently, the low incidence aerodynamic differences between the M823 and M557A low drag shapes discussed in Section 6.2 will not apply to these induced forces and moments, and it is firmly believed that the small differences in configuration between the two low drag shapes will not lead to any noticeable difference in their high incidence aerodynamics. Hence the data on induced forces and moments given here for the M557A shape will also apply to the M823 shape.

The variation of the induced side forces with incidence, roll attitude and Mach number for the low drag shape is shown in figures 13 and 14. At fixed incidence, the variation with roll angle approximates to but does not exactly reproduce the sinusoidal form which has usually been assumed in theoretical studies such as those of this report and of, for example (20). These induced side forces (and the induced side moments and rolling moments discussed below) are mainly the result of the interaction between the fins and the high incidence body vortices discussed in Section 8.1. With this explanation, the variation of the induced forces and moments depends on the position of the fins relative to the cores of the body vortices, and the displacement of the peak values to roll angles less than the $\phi = 22\frac{1}{2}^\circ$ given by the $\sin \phi$ approximation is real and not due to experimental error in the wind tunnel measurement. The peak induced side force, closely represented in figure 14 by the value $C = 22\frac{1}{2}^\circ$, increases rapidly with incidence between $\theta = 10^\circ$ and $\theta = 20^\circ$ for Mach numbers but by $\theta = 20^\circ$ it shows signs of levelling off. The induced forces for the bluff body are much smaller than the corresponding ones for the low drag body and apparently less regular, though this may be a reflection of their very small size and the inability of the balance system to measure them accurately in the presence of the very much larger normal forces and restoring moments. The variation of the peak induced side force ($C = 22\frac{1}{2}^\circ$) is shown in figure 15, but the variation with roll attitude is not shown because experimental scatter on the small values tends to mask any systematic change.

The variation of the induced side moment with incidence, roll attitude and Mach number is shown in figures 16 and 17 for both the low drag and bluff shapes. Once again the values are very much larger for the low drag than for the bluff body, though in this instance the bluff body values are large enough to show trends fairly clearly. The variation with roll attitude at constant incidence is approximately but not exactly sinusoidal for both bodies (figure 16). As with the side forces the peak moments (figure 17) rise rapidly with incidence above 10° , but the moments rise much more rapidly for the low drag shape and the rise shows no sign of stopping until about 20° incidence; with the bluff shape the peak values tend to level out by about $\theta = 15^\circ$.

Induced rolling moment variations with incidence, roll attitude and Mach number for the low drag M557A shape are shown in figures 18 and 19. Once again there is the approximately sinusoidal variation with roll attitude of the induced rolling moment at the higher incidences, but the variation of the peak induced rolling moment ($\phi = 22\frac{1}{2}^\circ$) with incidence shows some differences from the corresponding variation of the induced side forces and side moments. Between $\theta = 0$ and about $\theta = 13^\circ$ there is a slight but definite negative C_{l1} , but at about $\theta = 13^\circ$ or 14° , there is a very rapid rise in C_{l1} to large positive values for all Mach numbers from $M = 0.75$ upwards (for $M = 0.5$ the pattern is the same but the rolling moments are all considerably less than those at the higher Mach numbers). The induced rolling moments are very large, by $\theta = 20^\circ$ they exceed the rolling moments corresponding to 2° of cant on all four fins. There is no certain knowledge as to whether this peak induced rolling moment increases still further as θ continues to increase above 20° - the evidence on this point from other bomb shapes is contradictory. The U.S. measurements on a very similar configuration, the EX-10 low drag bomb shape, suggest that the rise may halt between $\theta = 20^\circ$ and $\theta = 25^\circ$ (31, 34) while British measurements on similar weapon shapes suggest that the induced rolling moments may continue to rise up to $\theta = 30^\circ$, though the increase in C_{l1} above $\theta = 20^\circ$ will not be so rapid (45, 46). The point is important because of the significance of the induced rolling moments when the possibility of roll lock-in is being considered.

The rolling moments induced on the M557B bluff body shape by the asymmetric attitudes at high incidence are shown in figures 20 and 21. These rolling moments are very much smaller than those for the low drag shape and their increase with incidence resembles much more closely the behaviour of the induced side forces and side moments at all Mach numbers. There is no suggestion of a negative C_{l1} at low incidence, the rise of peak induced rolling moment starts at a lower incidence ($\theta = 10^\circ$), and is more gradual than for the low drag body.

6.5 Pitch and roll damping measurements on the M823 low drag shape

The variation of pitch damping with incidence, roll attitude and Mach number for the M823 low drag shape is shown in figures 22(a) to (c) and 23. Many of these measurements are for incidences from 0 to 6° and in this incidence range the fin root separation effects on the M557A low drag shape led to large differences in static restoring moment and smaller but still significant differences in static normal force between the M557A and M823 shapes (figures 5 and 10). It would hardly be surprising therefore if differences also occurred at low incidence between the damping in pitch for the two low drag shapes and this should be remembered when, of necessity, the pitch damping results for the M823 shape are also applied to the M557A shape. The order of difference between the pitch damping for the two shapes is more likely to be

similar to the smaller differences between their normal forces than to the larger differences between their restoring moments; the restoring moments are comparatively small differences between the larger body destabilising moments and fin stabilising moments and they can be disproportionately affected by a few percent reduction in fin efficiency, while with both normal force and pitch damping the contributions due to body and fins are of the same sign and are additive.

At all Mach numbers some increase in pitch damping with incidence was found for the low incidence range ($\theta = 0$ to 6°) with greater increases for the high Mach numbers (figures 22(a) to (c)). For the subsonic cases investigated in greater detail ($M = 0.7$ and 0.8) the rise in damping with incidence was shown to continue up to at least $\theta = 16^\circ$ to 20° .

Roll attitude was found to have little effect on pitch damping up to about 16° of incidence (figures 22(a) and (c)), though the damping was always slightly less for the asymmetric attitude ($\varphi = 22\frac{1}{2}^\circ$) than for the two symmetric cases. The more detailed subsonic investigation of effects of roll attitude and incidence however did show up an interesting and possibly important effect at the higher incidences. Above about $\theta = 16^\circ$, the pitch damping curve diverged quite sharply (figure 22(c)), with the damping curve for the asymmetric attitude $\varphi = 22\frac{1}{2}^\circ$ (and by symmetry for $\varphi = 67\frac{1}{2}^\circ$ also) falling rapidly; tunnel limitations which restricted the maximum incidence to about $\theta = 21^\circ$ made it impossible to see whether the damping continued to drop to very low values (or even to change sign). This change in damping occurs at the same roll attitude and over the same incidence range as that in which the induced rolling moments side forces and side moments suddenly become important. - it is likely to be another indication of a change taking place in the basic flow pattern over the fins.

Throughout the incidence range tested there was a large increase in pitch damping with Mach number transonically and in the low supersonic region ($M = 0.95$ to $M = 1.30$, figure 23).

Experimental measurements of pitch damping for comparison are not common and the only ones known on a very similar shape are those on the U.S. EX-10 drag shape (3', 47'). Allowing for configuration differences, these are quantitatively rather similar at $\theta = 0$, $\varphi = 0$, but there are differences in the effect of roll attitude and incidence. While the M823 tests showed little effect of roll attitude, the EX-10 tests showed almost a doubling in damping coefficients in going from $\varphi = 0$ to $\varphi = 45^\circ$. No logical explanation can be forward for this big roll attitude effect with the EX-10 shape and it is believed that the M823 results are more likely to be correct.

Another difference between the M823 results and the U.S. EX-10 results was in the effect of incidence over the M823 test range. The M823 results show much more effect of incidence but in this case the difference is understandable the M823 results were obtained using the forced oscillation technique of reference 35 and the amplitude of the forced oscillation was small (only $\pm 1^\circ$) while the EX-10 results were obtained from the free decay of much larger oscillations. The method used in the EX-10 case would tend to average the damping over the incidence range and so mask the incidence effects, and it is likely that in this respect the M823 results are more precise. The large transonic and supersonic increase in damping with Mach number is in agreement with the EX-10 results.

The variation of roll damping with incidence, roll attitude and Mach number is shown in figures 24 and 25. These results were subject to the support vibration troubles referred to earlier and with the accuracy obtainable no

effect of roll attitude was detected. There was a slight but definite increase of roll damping with Mach number, and a very definite increase with incidence. Once again the only closely comparable shape for which there are roll damping results available is the EX-10 shape. As before different techniques prevented comparisons of all the effects - the EX-10 results(48) came from tests with a continually spinning model which averaged out roll attitude effects while the M823 results came from a small forced oscillation technique. Allowing for configuration differences, the results compare closely for magnitude and effect of Mach number at zero incidence. No comparison of roll attitude effect was possible and none is available for effect of incidence.

7. FREE FLIGHT TRIALS AND RESULTS

As mentioned in Section 5, full scale instrumented bomb trials were conducted to obtain free flight data on the trajectory and dynamic behaviour of the research store. For this purpose, the research stores were fitted with a spin sensor, accelerometers, and a telemetry sender to measure the effects of release disturbance and subsequent flight behaviour. Information telemetered from the research stores gave a measure of roll rate and of the amplitude, frequency and damping of oscillations caused by external disturbances throughout the period of fall from release to impact. In addition, wing tip and bomb bay cameras were installed on the "bombing" aircraft to record the pitching and yawing attitudes actually reached by each store in response to the release disturbance. Finally, trajectories were obtained by means of Contrave kine-theodolites, enabling the determination of missile position and speed. The true air speed and Mach number were then found from a knowledge of the appropriate meteorological data.

The trials programme included systematic variations in c.g. position and fin cant on both bluff body and streamlined configurations of the same basic shape. At the outset of the research programme, initial small scale wind tunnel tests conducted at A.R.L. showed an unexpected nonlinearity in the static restoring moment near zero yaw (see Section 6) and because of this "transient response" experiments were planned to make direct measurements of force and moment in free flight, using lateral pulse rockets to generate artificial disturbances.

A description of the transient response trials is given separately in Section 7.4.

7.1 The test vehicles

External dimensions of the research stores are given in figures 1 and 2. The stores were manufactured in the W.R.E. workshops and the method of construction adopted is shown in figures 26, 27 and 28. Basically, the streamlined M557A body (figure 26) comprised six cast aluminium alloy sections, four of which were flanged and fitted with studs to facilitate assembly of the overall centre body. The tail cone was attached by means of a single tie-rod anchored to a subsidiary conical casting which was held within the adjacent section. To maintain a "clean" external surface, the body sections were bolted together by studs placed below the skin line, making it necessary to assemble the store progressively from the aft end with a threaded nose cone giving final closure of the vehicle. Ready access to the telemetry sender was obtained by installing it as far forward as possible.

The body sections were cast in a "free flowing" aluminium alloy, permitting a nominal wall thickness of 0.375 in. with a smooth outer skin held to a contour tolerance of $\pm 1/32$ in. as cast. Thus the need for external machining was

limited to local blending at the five junctions of the body sections and the total weight of the complete streamlined body was kept down to about 400 lb. This left considerable freedom for the disposition of ballast needed to vary the c.g. position and moment of inertia within the specified all up weight of 860 lb. Circular ballast weights of 25 lb each were bolted at the body junction to give the desired overall inertial properties. Body alignment was maintained by ensuring that the flanged ends of the cast sections were machined square to their individual axes of symmetry.

Because the experiments demanded control of fin cant to within $\pm 0.1^\circ$ precision, plastic fins were designed with the required cant angle set on an integrally moulded stock to ensure repeatability of the fin geometry. The fins were located in parallel sided slots, accurately machine' in the tail casting giving a range of cant angles from zero up to 3° . Each fin was firmly wedged in position at its root leading and trailing edges and the complete tail assembly was subjected to systematic measurements of the individual cant and chordwise camber and spanwise twist. Telemetry aeriels were formed by metal plating a section of the leading edges on one pair of diametrically opposite fins.

Figure 27 illustrates the construction of the bluff M557B body which was similar to the streamlined configuration with the exception that the nose cone and forward section were replaced by a flat disc, and smaller fins were fitted. Without ballast, the bluff body structure weighed approximately 340 lb, and with the streamlined body, its all up weight was specified at 860 lb. The physical properties and release conditions for each of the research stores are listed in table 1.

For transient response experiments four lateral pulse rockets ("bonkers") were fitted in the body section ahead of the tail cone as shown in figure 28. Each bonker unit comprised a group of three 3.5 in "Bazooka" rocket motors fired simultaneously to give a combined total impulse of 180 lb sec with a burning time of approximately 25 msec. Lower impulses of 120 lb sec or 60 lb sec could also be obtained by simply reducing the number of Bazooka motors fired. A fuse clock and commutator were used to initiate the bonkers at predetermined times after release from the aircraft.

During the wind tunnel tests at A.R.A., it was found that the nonlinearity in static restoring moment near zero yaw could be substantially reduced by a small change in the tail cone shape. (Section 6.2). Full scale bodies were modified to the M823 shape shown in figure 3 and full scale transient response experiments were also performed with these to confirm the wind tunnel data.

7.2 Instrumentation

Measurements which were required during the free flight trials may be divided conveniently into four main groups, namely :-

- (1) Ground based measurements of trajectory.
- (2) Measurements made by instruments carried in the test vehicles.
- (3) Observation of the release disturbance from aircraft cameras.
- (4) Meteorological measurements.

The methods used to obtain these measurements are outlined below together with an assessment of the accuracy achieved under the operating conditions at the Woomera Range.

7.2.1 Ground based measurement of trajectory

Ground speed and trajectory of the bomb test vehicles were determined by means of Contreves kinetheodolites. These instruments had a measured total error of 15sec of arc (1 S.D.) and normally, four were used per trial, each operating at 20 frames/s, from which average errors of ± 5 ft in position and ± 2 ft/s in ground speed were obtained over the entire trajectory after appropriate smoothing of individual readings. It should be noted that most of the error in the kinetheodolite measurements was due to bias which did not affect the determination of velocity (49).

In conjunction with the kinetheodolites, three 35mm Vinten high speed cameras were used to provide a high resolution, slow motion photographic record of the test vehicles' dynamic behaviour throughout the fall.

7.2.2 Test vehicle instrumentation

In the test vehicles, accelerations and incidence were measured by variable inductance transducers used in conjunction with a twenty-four channel 465Kc/s sub-miniature telemetry system. There were normally twenty-three information channels and one synchronising channel, time multiplexed by means of a mechanical rotating switch giving a sampling rate of 80 per second per channel. For the purpose of determining the accuracy of data transmission, the telemetry system was considered to include that equipment between the input to the multiplexer in the airborne sender (that is, excluding the transducers) and the data output from the demodulation and demultiplexing equipment on replay of a copy of a primary magnetic tape record. In these terms the maximum r.m.s. error in data transmission was $\frac{3}{4}\%$ of full scale deflection which compounded with the individual transducer errors to give the overall accuracy of the raw data. This overall accuracy was found to lie within $1\frac{1}{2}\%$ and 2% of full scale deflection or within about 1% of full scale deflection if mathematical smoothing techniques were applied.

For the measurement of lateral forces and moments, six accelerometers were used, one pair with a range of $\pm 2g$ placed ahead of the vehicle's c.g. and two pairs with ranges of $\pm 3g$ and $\pm 5g$ placed aft of the c.g. Each pair of accelerometers was mounted with their sensitive axes perpendicular to each other and to the vehicle's axis of symmetry, and lying in planes parallel with those of the stabilising fins. These transducers were manufactured to an R.A.E. specification, and their performance approximated a second order linear system with the damping factor set at 0.7 of critical. The natural frequencies of the instruments were about 100c/s, 120c/s and 160c/s for the ranges of $\pm 2g$, $\pm 3g$ and $\pm 5g$ respectively.

In the case of incidence measurements, a differential pressure incidence meter was developed and calibrated at A.R.L. (50). This incorporated a hemispherical-head probe fitted with differential pressure transducers to measure the components of incidence in two planes at right angles. Subsequent to the tests described in reference 50, static calibrations of a full scale probe indicated that incidence could be measured to within $\pm 1^\circ$. However, it has not yet been possible to devise a satisfactory method of measuring the dynamic response of this instrument and reference 51 has been used to estimate phase lags associated with the tube lengths leading from the surface tapping points to the pressure transducers. The installation required a tube length of 18in. which gave estimated phase lags of 2° at sea level rising to 10° at an altitude

of 45000 ft, for an oscillation frequency of 5 c/s. At a frequency of 1 c/s the corresponding phase lags were reduced to 0.4° and 2° .

The primary means of measuring roll-rate was to use photo-electric cells placed behind narrow slits to observe the variation in light intensity as the vehicle rolled. Two slits in the body surface were located at an angular displacement of 90° and the output of the cells transmitted by the telemetry link. Roll-rate was also obtained from the telemetry system by using plane polarised aerials. The telemetry receiving station operated on signals in the 430 to 490 Mc/s band and a rotating dipole, mounted in a tracking parabolic aerial, received the telemetry signals radiated by the test vehicle throughout its fall so that the amplitude of the received signal was a maximum when the axis of the rotating dipole was parallel with the plane of polarisation of the radiated signal, and a minimum when the dipole was perpendicular to the plane. A coded disc which rotated with the dipole produced a series of marker pulses at a constant angular relationship to the position of the receiving dipole. The amplitude modulated signal was demodulated and after filtering out the high frequency component of the telemetry signal was recorded on film together with the marker pulses and a suitable time sequence. Roll data was then obtained by comparing the relationship between the amplitude minima of the roll signal and the marker pulses.

7.2.3 Aircraft instrumentation

A photographic record of the test vehicle's response to the release disturbance was obtained by four cameras installed in the "bombing" aircraft. Details of the camera location and their fields of view are shown in figure 23. Two wing tip and two bomb-bay cameras were used to give timed records of the combined pitching and yawing motions during the first $1\frac{1}{2}$ sec of fall. These cameras were modified 35mm G.W.1 instruments operating at about 28 frames/s and with timing provided on the edge of film by means of neon lamps. The two wing tip and one of the bomb-bay cameras had 1 in. focal length lenses giving approximately 30° field of view, while the second bomb-bay camera had a 10 in. focal length lens with only 5° field of view. However, this latter instrument proved to have too narrow a field for anything other than very "clean" releases.

Instant of release from the aircraft was recorded by a radio signal initiated through the operation of a micro-switch attached to the bomb slip.

7.2.4 Meteorological data

Ground level measurements of barometric pressure, ambient temperature and wind velocity were recorded continuously at the Range meteorological station. At altitude, hourly measurements of pressure and temperature were made by means of radiosonde, while the wind velocity was determined by the balloon-tracking method. Data for a given trial were obtained by interpolation, with the result that atmospheric pressure was measured to an accuracy of $\pm 1\frac{1}{2}$ mb, temperature within $\pm 1\frac{1}{2}^\circ$ C, and wind velocity within ± 10 ft/s. By combining local wind velocity with the vehicle velocity determined by the kinetheodolites, the true air speed was obtained, and in turn the Mach number computed from the ambient air temperature. The Mach number was determined within ± 0.012 and true air speed within ± 12 ft/s.

7.3 Results of instrumented ballistic trials

The free flight research programme comprised a total of thirty-three test vehicles with trials conducted in the period from December 1961 to December 1964. Each test vehicle was released singly from the same station in the bomb-bay and details of the various store configurations, release conditions and impact deviations are listed in table 1. Only a limited number of bluff M57B bodies were tested because this configuration suffered only a small release disturbance, and since all the induced forces and moments were small (figures 15, 16, 17, 20 and 21) its flight behaviour was not influenced by adverse roll-yaw interactions. It should be noticed also that round numbers 729 and 731, in group H of table 1, did not contribute to the research programme other than to prove a parachute recovery system required in the development of a special technique for measuring vehicle attitude by optical means.

Throughout the trials programme all of the required data were obtained from both the airborne and ground instrumentation with the exception of round number 702. On this trial the kinetheodolites did not record the release conditions. The only other failure occurred with round number 754 which had to be jettisoned because of a faulty bomb-slip.

To assess the overall ballistic performance of individual test vehicles, the observed impact conditions were compared with those predicted on the IBM 7090 computer using the measured release conditions and meteorological data together with a measured drag function for the bomb. For simplicity, particle trajectories were computed initially assuming that the bomb moved in a non-rotating field with a constant gravitational attraction everywhere perpendicular to a plane; corrections for the earth's rotation, the variation of gravity with height and the variable direction of gravity, were estimated on the basis of reference 52 and subtracted from the observed impact data to give the impact deviations in range, line and time of fall listed in table 1. These corrections were calculated for vacuum conditions because such an approximation was found to give results with sufficient accuracy. Furthermore, the variation of drag coefficient with Mach number was established from the observed trajectories of selected trials by a method of double differentiating the missile position - time data. For this a multistation solution of the trajectory was computed from a minimum of three kinetheodolites. The position coordinates were smoothed on the IBM 7090 computer by fitting a third order curve over successive groups of 21 points using a moving arc technique. Smoothed values of velocity components, trajectory slope and acceleration were obtained at the centre point of each group. True air speed and Mach number were then computed from the trajectory and the meteorological data for each time interval of 0.2sec. Finally, the following expression for the drag coefficient was tabulated against Mach number at 1 sec intervals.

$$C_D = \frac{2m}{A} \left(\frac{f - g \cos \theta}{\rho V^2} \right)$$

where

- C_D is the drag coefficient
- V is the true airspeed
- g is the acceleration due to gravity
- f is the missile acceleration
- m is the missile mass
- θ is the slope of the trajectory
- ρ is the air density

Variations of drag coefficient with Mach number obtained by this method shown in figures 30(a) and (b) for the M557A and M557B shapes respectively. In addition, typical particle trajectories for both the streamlined and blunt body configurations are shown in figure 31 and the corresponding time history of Mach number and dynamic pressure are given in figure 32 for release conditions representative of the actual flight trials.

7.3.1 Streamlined body M557A shape

Referring first to table 1, for the streamlined body, Groups A, C, E and G list those stores which were scheduled for release from 45000 ft at $M = 0.7$ and which had c.g. positions specified respectively to be at 52, 54, 57, 47.5 and 50 percent of the body length from the nose. The stores of Group B were released from a lower nominal altitude of 25000 ft at $M = 0.5$, with the c.g. at 52% from the nose. Finally, Group F includes three loft bombing trials and Group H two parachute recovery trials.

In the following paragraphs a brief description of the flight behavior is given for bombs within each group. Comparisons with theoretical studies are made in Section 8.

Group A :- 45000 ft $M = 0.7$, intended c.g. position 52%.

With the c.g. at a nominal 52% body-length the overall ballistic performance was generally satisfactory for fin cants ranging from zero to 1° , as shown by round numbers 701, 702, 716, 717, 718, 709 and 714. For these configurations the release disturbance remained almost planar with a first peak amplitude in pitch of approximately 20° .

Of the two stores with nominally zero fin cant, number 701 had standard sharp leading edge fins and number 702 had rounded leading fins. This fin modification was made in an early attempt to reduce nonlinearity in static restoring moment at low incidence. However, comparisons of the lateral acceleration records obtained during the test of these two stores, it was evident that the minor fin change had no appreciable effect and the low incidence nonlinearity in restoring moment was subsequently shown to result from a body interference effect (Section 6.2). Roll rates exhibited by rounds 701 and 702 (figures 33(a) and (b)) did not exceed about 0.9 c/s. Since the ratio of roll rate to natural yawing frequency remained below 0.5 throughout the test, adverse roll-yaw interactions were avoided.

With an average fin cant of 0.17° , round 716 released cleanly and passed through resonance at about 18 sec after release and again at 22 sec. A low amplitude oscillation of less than 5° was detected between 15 and 25 sec, and the deviation at impact was somewhat higher (15 mils in range) than that experienced with rounds 717, 718, 709 and 714.

Rounds 717, 718, 709 and 714 had average fin cants of 0.31° , 0.41° , 0.44° and 0.91° respectively. Each exhibited a normal response to release disturbance with peak pitch amplitudes of about 20° and initial yawing amplitudes increasing slightly with fin cant from approximately 7° to 10° . For round 717 resonance was passed through 10 sec after release and for rounds 718, 709 and 714 somewhat earlier. In each case the roll rate increased quite steadily but showed some influence of induced rolling moments particularly during response to the release disturbance as shown in figures 33(a), 33(b), 34(a) and 34(b). The ballistic performance of rounds 717 and 714 was good, with deviation

impact not exceeding 3 mils. However, rounds 718 and 709 gave total deviations of approximately 10 mils. This variation in performance for fin cants between 0.31° and 0.91° can only be attributed to the effects of the release disturbance because none of these particular rounds showed any significant yawing motions later in flight.

Round 708 with a fin cant of 1.41° performed a large amplitude (30° maximum) circular yawing motion at release which was characteristic of roll lock-in(21) and which persisted from about 3 sec to 6 sec after release. Recovery from this motion was abrupt and roll break-out is thought to have been caused by stalling of the fins at high incidence. This explanation is supported by the wind tunnel results (figure 6(a)) which indicate a rapid loss of fin lift at incidences greater than about 20° for angles of attack in planes other than those of the fins. Thus, as the fins approach the stalled condition the circular yawing frequency suddenly decreases and no longer equals the roll rate so that the state of roll lock-in is broken; the sense of the destabilising side moments then rapidly changes and a complete recovery to low incidence is accomplished. The ballistic performance of round 708 was not good having a deviation at impact in excess of 35 mils.

Round 715 with 2.8° fin cant gave a response to the release disturbance very similar to that experienced with round 708 but with a slightly greater yawing amplitude. The greater fin cant forced the bomb through resonance without lock-in and after recovering from the release disturbance no further large yawing motions were observed, and the deviation at impact was approximately 15 mils.

The trial for round 736 was scheduled in the closing phase of the fixed cruciform fin research programme with the main purpose of demonstrating the ballistic performance of the straight tapered tail cone (M823 body). This store gave a clean release with 20° peak amplitude in pitch. There were no indications of adverse roll yaw interaction throughout the trajectory and the deviation at impact was 10 mils.

It should be noted that where comments have been made concerning mid-flight roll-yaw resonance of stores in Group A after recovery from the release disturbance, the magnitude of the yawing motion was generally found to be little greater than 5° . The resonant condition was detected by comparing the natural yawing frequency of the store as given by the telemetered acceleration data with the measured roll rate.

Group B :- 25000 ft, $M = 0.5$, intended c.g. position 52%.

Rounds 724, 725, 726 and 732 had nominal c.g. position at 52% from the nose and fin cants of 0.12° , 0.90° , 0.46° and 0.40° respectively. This group of trials was planned to demonstrate the effect of the small region of static instability near zero incidence which the wind tunnel measurements had shown at subsonic speeds. The release conditions were changed to 25000 ft at $M = 0.5$ for these trials so that the period of subsonic flight would occur under conditions of greater dynamic pressure than with higher altitude releases, thereby enhancing the attitude sensitivity of the missile-borne accelerometers and yawmeter. Response to the release disturbance for each of the four stores was respectively similar to that experienced by the stores in Group A with corresponding fin cants, the E.A.S. at release being about the same. Records obtained from the lateral accelerometers and direct incidence measurements revealed details of low incidence behaviour over the later part of the trajectories

which had previously been obscured in the higher altitude releases. Thus with 0.12° fin cant, round 724 exhibited a condition of roll lock-in with a yawing amplitude of approximately 2° which was sustained at speeds up to $M = 0.95$, when the motion ceased abruptly. Round 725, its higher roll rate (see figure 35) was observed to spin at a steady incidence of about 1° , and this motion also decayed at $M = 0.95$.

During response to the release disturbance, round 726 showed an abnormally high roll acceleration, as may be seen from figure 35. This test vehicle was the first to be fitted with a yaw meter and although the instrument gave useful evidence of the incidence history, lack of accurate roll acceleration data made it impossible to analyse fully this unusual behaviour. Between 2 and 3 sec after release, a brief periodic roll lock-in occurred and during this time the vehicle swung rapidly through a 25° circular yawing motion. Shortly thereafter the roll rate decayed back to the value expected from the fin cant alone and the yawing amplitude began to decrease; at 12 sec after release recovery from the disturbance was complete. Later in the trajectory a low amplitude nutational oscillation of about 3° amplitude developed and, as previously with rounds 724 and 725, this motion died away when $M = 0.95$ was reached. In an attempt to gain further information on the unexpected behaviour of round 726, round 732 was fitted with an angular accelerometer and released under as nearly identical conditions as possible. On this occasion at between 0.5 and 0.8 sec after release, the store experienced large rolling moments in a sense opposed to the fin cant and also contrary to that expected from yaw induced effects. These moments were apparently associated with particular asymmetric attitudes experienced during the release disturbance and resulted in a roll rate of $1/3$ c/s against the fin cant. After 0.8 sec, the measured rolling moments changed sign and came into reasonable agreement with the wind tunnel data; when recovery from the release disturbance had been accomplished the dynamic behaviour of round 732 was similar to that of round 726.

Group C :- 45000 ft, $M = 0.7$, intended c.g. position 54%.

Round 712 with c.g. at 54.2% from the nose and an average fin cant of -0.03° toppled at release but recovered from the resulting large amplitude circular yawing motion within about 0.5 sec in much the same way as did round 708. The maximum roll rate was about 1 c/s just before impact and showed marked evidence of roll lock-in during the release disturbance (see figure 36). This round had a deviation at impact slightly in excess of 100 mils, entirely due to the behaviour at release.

Group D :- 45000 ft, $M = 0.7$, intended c.g. position 57%.

With the c.g. at 57% from the nose, the static margin is approximately 0.5 calibre less than with the c.g. at 52% and the consequent loss of static stability increases the nonlinearity in the restoring moment. For this c.g. position the sudden growth of yaw at release which is associated with roll lock-in was apparent for each of the fin cant's namely -0.13° , 0.50° , 1.44° and 2.90° on round numbers 703, 706, 707 and 713 respectively. The behaviour at release became progressively more violent with increase of fin cant, as is demonstrated by the erratic growth of roll rate shown in figure 37. Round 703 recovered from the yawing motion within a few seconds after release but had a deviation

about 70 mils at impact. Rounds 706, 707 and 713 all toppled at release and experienced large amplitude oscillations for most of the remaining flight giving impact deviations greater than 200 mils in each case. Over the latter half of the trajectories of rounds 707 and 713 a slowly decaying nutational motion was observed; the amplitude of this slowly decreased from 40° to about 10° at impact. These were the rounds with large cant angles and high spin rates, and Magnus effects are believed to be responsible for the motions.

Group E :- 45000 ft, $M = 0.7$, intended c.g. position 47%.

Rounds 722 and 723 were planned to demonstrate repeatability for stores with a favourably chosen combination of fin cant and c.g. position. Both rounds gave clean releases with a first peak amplitude of about 20° and subsequent flight histories quite free from adverse roll-yaw interactions. In each instance the maximum roll rate was approximately 0.8c/s at 50 sec from release (see figure 38) and the impact deviation did not exceed 6.5 mils.

Group F :- Loft manoeuvre

Rounds 719, 720 and 721 were released with c.g. at 51.7% from the nose and fin cants of 0.11° , 0.97° and 0.11° respectively. Round 721 was uninstrumented. In the loft manoeuvre the aircraft performed a simple pull-up from 1000 ft to the release height of about 5500 ft. At release the normal acceleration was approximately 2g and flight path elevations from the horizontal were 62° , 67° and 63° respectively. In each case the peak amplitude of the release disturbance did not exceed 11° in pitch and 5° in yaw and no abnormal behaviour was observed throughout all three trajectories. The roll rate of round 719 was almost negligible, and for round 720 it closely followed the predicted history giving observed values of 0.8c/s at apogee rising to 2.5c/s at impact (see figure 39). All three rounds negotiated the highly curved portion of the trajectory around apogee without any large oscillations.

Group G :- Transient response trials

In these trials the store was disturbed on several separate occasions by lateral pulse rockets and the response to the disturbances was carefully analysed. Of the three transient response trials, that for round 704 was conducted early in the research programme with the purpose of obtaining preliminary free flight data on normal force and restoring moment coefficients at transonic speeds for comparison with the wind tunnel results. At the time of this trial no suitable instrument was available to measure angle of attack so that analysis of the bonker responses was limited to an "equivalent linear" treatment of the recorded lateral accelerations. With such a simplified analysis it was necessary to assume that the aerodynamic force and moments were axially symmetric, thereby restricting the range of incidences which could be examined usefully. (Wind tunnel tests had already shown that aerodynamic cross-coupling effects became appreciable at incidences greater than about 10°). Although only low incidence data were obtained from round 704, the results showed quite good agreement with the A.R.A. wind tunnel measurements. Rounds 727 and 728 were both fitted with differential pressure yaw meters making it possible to perform quite detailed analyses of the nonlinear aerodynamic forces and moments as outlined later in Section 7.4. Each

vehicle had four bonkers timed to operate at 10, 20, 27 and 36 sec. after release from the aircraft, at which times the Mach number was approximately 0.74, 0.91, 1.06 and 1.17 respectively. To compensate for effects of changing dynamic pressure, the size of the bonker units changed; the total impulse of the first bonker was 60lb sec, the second and third were 120lb sec, and the fourth was 180lb sec. In this maximum amplitude of each disturbance was kept below about 16° . These stores were carefully selected with the lowest possible fin area to avoid roll-yaw interactions at high incidence, and to keep the free response requirements within the capabilities of the transducers by minimizing roll-rates. From figure 40 it may be seen that the rolls were affected by the bonker impulses which clearly generated quite transient rolling moments.

Round 728 had a straight tapered tail cone (M823 shape) and the test of this store included the first test of a break-up and parachute being developed to recover an airborne nose camera. This camera was used in future experiments to obtain accurate attitude data by photographing lights on the ground.

Detailed analysis of the results is discussed in Section 7.4.

Group H :- Parachute recovery trials.

In conjunction with round 728, rounds 729 and 731 were planned to develop the recovery system and aiming technique for the nose camera experiment mentioned above. Results obtained in future trials using this technique will be published separately later.

7.3.2 Bluff body M5573 shape

Rounds 751, 752 and 753 of Group I were released from nominally 45000 ft altitude at $M = C.7$. With c.g. positions at 36.6 and 38 percent of the body length from the nose, rounds 751 and 753 each had a static margin of approximately one calibre for Mach numbers less than 0.85. Both of these stores had small release disturbances and their first peak amplitudes in pitch were no greater than 5° . The roll of round 751 built up erratically to a maximum of 0.3c/s (see figure 40) and between 30 and 40 seconds after release an oscillation of about 0.3c/s amplitude occurred though the remainder of the flight showed no further abnormal motions. During the period of the oscillations the average Mach number was 0.95, and at this speed there is an abrupt loss of stability near zero yaw as shown by the wind tunnel data in figure 40. It is believed that this accounts for the observed flight behavior of round 751. In the case of round 753, the maximum Mach number was 1.17 and the flight of this store was quite uneventful with the roll rate increasing steadily to 2.5c/s at impact.

For round 752 (c.g. at 45% from the nose) the release disturbance was again small, the maximum Mach number did not exceed 0.93 and the subsequent flight was quite free from yawing oscillations.

As would be expected from such flight performances, the impact deviations for the three bluff body stores indicated good ballistic consistency. Because the bluff body stores suffered only small release disturbances and since none of their yaw induced forces and moments were large, their flight behaviour was uneventful and insufficiently irregular to justify further instrumented trials. In addition the body vibrations caused by the separated flow from the bluff nose resulted in very noisy accelerometer records.

7.4 Results of transient response trials

Analysis of short-period oscillations provided a very useful means of determining the aerodynamic forces and moments. In the transient response trials, the method adopted was to study the free oscillations of a bomb disturbed from its steady flight condition by a bonker fired laterally from a position aft of the bomb's centre of gravity.

Because wind tunnel tests had shown the existence of marked aerodynamic nonlinearity, direct measurements of incidence were necessary to ensure that in the free flight experiments nonlinearities would be defined with adequate accuracy. For this purpose the differential pressure incidence meter mentioned in Section 7.2.2 was used to measure the magnitude and direction of the total incidence vector. Unfortunately, the instrument's dynamic response limited useful test conditions to oscillation frequencies below about 10c/s so that it was not possible to make a direct analysis of Magnus effects since these only become of measurable size at high roll rates. In order to achieve the accuracy required in attitude measurement to investigate nonlinearities in the normal forces and static restoring moments, roll rates had to be limited to about 1 c/s.

7.4.1 Data analysis

The test vehicle instrumentation measured linear acceleration, angle of attack and roll rate. These measurements, in conjunction with trajectory data obtained from the ground based instruments, then gave sufficient information to determine complete time histories of the total aerodynamic forces and moments acting on the test vehicle. A detailed account of the methods which were used in analysing the flight data may be found in reference 53 and the following statement is intended merely to outline the principles involved.

Each test vehicle was fitted with at least 5 accelerometers; one of these measured the axial force component acting along the X axis and the others were arranged in pairs at the front and rear to measure accelerations parallel with the Y and Z body axes. (For definition of body axis system see Section 6.1.2, and for accelerometer installations see figures 26 to 28). With some test vehicles, extra accelerometers of different sensitivities were added for special measurements. To prevent overloading the accelerometers at high roll rates, they were deliberately installed to be insensitive to spin about the X-axis. With this arrangement, it was possible to determine the components of linear acceleration at the vehicle c.g. together with the terms $(qr \pm \dot{p})$, $(pq + \dot{r})$ and $(pr - \dot{q})$ which arose from the rotational velocities and accelerations. Using the additional knowledge of the observed roll rate p and true air velocity components u , v and w obtained from trajectory and incidence data, the rigid body equations of motion were applied to obtain separate measurements of the angular velocities q and r . Finally, expressions for the total force and total moment coefficients were defined as :

$$C_y = \frac{m a_y}{\frac{1}{2} \rho V^2 S} \quad ; \quad C_z = \frac{m a_z}{\frac{1}{2} \rho V^2 S}$$

$$C_m = [B (\dot{q} - pr) + A pr] / (\frac{1}{2} \rho V^2 S d)$$

$$\text{and } C_n = [B (\dot{r} + pq) - A pq] / (\frac{1}{2} \rho V^2 S d)$$

where C_y and C_z are the total force coefficients in directions OY respectively.

C_m and C_n are the total moment coefficients about the Y and Z axes respectively

a_y and a_z are linear accelerations at the vehicle's c.g. in directions OY and OZ respectively

m is the vehicle mass

A is the vehicle's principal moment of inertia about the X-axis

B is the vehicle's principal moment of inertia about the Y and Z axes

S is the maximum body cross section area

d is the maximum body diameter

p , q and r are components of angular velocity about the X, Y and Z axes respectively

u , v and w are components of true air speed in the X, Y and Z directions respectively

V is the true air speed

ρ is the ambient air density and

dot notation indicates differentiation with respect to time.

To interpret the data on total force and moment coefficients it is necessary to correlate them in time with the corresponding historical incidence and Mach number. For this, analyses were performed over selected intervals of time during which the Mach number could be considered constant. In general such intervals did not exceed two seconds and the resulting change in Mach number remained less than 0.02. Subsequent data analysis used to determine the static and dynamic components of the overall force and moment system was based upon the formulation of Synge(25) in which the implications of aerodynamic symmetry are used to give expressions for the various coefficients in series form. Polynomials in the angle of attack θ and roll orientation angle ϕ were fitted to the force and moment coefficient data by the method of least squares.

In general it was found that the measurements of aerodynamic force and moments could best be represented in the following manner :-

(a) Static restoring moment and normal force defined by similar expressions of the form :

$$a\theta + b\theta^3 + c\theta^5 + (d\phi^2 + e\theta^2) \cos 4\phi$$

(b) Static side moment and side force defined by similar expressions of the form :

$$(d\theta + f\theta^3) \sin 4\phi$$

(c) Pitch damping moment defined by the expression :

$$(\xi + h\theta^2) (q + i r)$$

where the coefficients a, b, c etc. depend upon Mach number and spin rate only.

Throughout the analysis, the IBM 7090 computer was used wherever practicable to ensure the best accuracy in reducing the data. The overall accuracy of the technique varied with the dynamic pressure. Normal force and moment coefficients were measured with a possible error of about 4% of their values at an incidence of 20° under the flight conditions at 45 000 ft altitude, and at 20 000 ft this error was approximately halved. Because of their relatively small magnitude, the side force and side moment coefficients were determined with a correspondingly reduced accuracy and in the best circumstances there were possible errors of up to 15%; in the case of pitch damping the results could only be classed as qualitative.

7.4.2 Comparisons with wind tunnel data

Comparisons between free flight and wind tunnel measurements of the variation in normal force with incidence, roll attitude and Mach number are shown for the M557A body in figure 42 and for the M823 body in figure 43. Corresponding comparisons of the variation in restoring moment are also given in figures 44 and 45.

The correlation between free flight and wind tunnel data on normal force and restoring moment is in general very good. The only apparent discrepancy which needs explanation is in the degree of restoring moment nonlinearity which occurs with the M557A body at low angles of attack at transonic speeds. Nearly all the wind tunnel data shown in figures 42 and 44 for this body were obtained using a sting balance support which was shown to have a low incidence interference effect on the moment measurements at transonic speeds ("original sting data"), and repeat measurements later with an improved sting support ("modified sting") substantially reduced this low incidence interference (wind tunnel results discussed in detail in Section 6.2). The correlation between free flight results and these later wind tunnel measurements of restoring moment was much better and is shown in figure 46.

In the case of the M823 body with its larger base diameter and straight tapered tail cone, the problem of sting interference did not arise and from figures 43, 45 and 46 it may be seen that very good agreement was obtained over the full range of measurements. In fact, with the exception of data on the M557A body near sonic speed at incidences below about 6°, the difference between wind tunnel and free flight measurements of normal force and restoring moment are nowhere greater than would be expected from instrumentation uncertainty alone.

Because in free flight the side force and side moment measurements could have errors of up to about 15%, figure 47 gives comparisons of these force and moment coefficients at one incidence only, namely 10°. The results are typical of data obtained for incidences up to 15°, and the free flight results for the two bodies confirm that the slight differences in body shape have little effect at the higher angles of attack. Although the experimental accuracy of the free flight measurements is not as good as for the normal force and restoring moment, overall

agreement with the wind tunnel data is obtained.

So far as pitch damping is concerned, it was not possible to determine any incidence dependence from the free flight trials and little can be said of the comparisons shown in figure 48 other than that a qualitative agreement is exhibited.

Data on induced rolling moments were obtained from only one test vehicle in the free flight programme, round 732, which was fitted with an angular accelerometer as described in Section 7.3.1. For incidence angles less than 17° a polynomial of the form $(A\theta^4 + B\theta^6) \sin 4\phi$ was fitted to the telemetered data in conjunction with simple linear expressions for the effects of roll damping and fin cant. Although the accuracy of this analysis was seriously degraded by a high level of noise in the raw flight data, the comparison with wind tunnel measurements given in figure 49 indicates a good degree of correlation.

8. COMPUTER STUDIES AND RESULTS

During the early stages of the research programme, when wind tunnel data first became available, it was not known to what extent the induced rolling moments, side forces and moments would contribute to the overall flight dynamic behaviour of the bomb test vehicles. Consequently, the basic equations of motion were originally formulated for solution on the IBM 7090 computer at W.R.E. (54, 55) with the purpose of isolating the dominant effects of aerodynamic cross-coupling. Six degree of freedom solutions were obtained for a cruciform finned configuration assuming rigid body dynamics, and the aerodynamic force and moment system was deliberately simplified by considering that, with the exception of the induced components, it contained only linear functions of the total angle of attack. In addition, Mach number dependence was neglected apart from its effect upon zero lift drag. Such simplification was expected to give a better understanding of the influence of the cross-coupling terms during a bomb's response to a release disturbance and during roll-yaw resonance.

Results of these initial studies showed qualitative agreement with dynamic behaviour observed in the full scale flight trials and succeeded in demonstrating the basic mechanisms of roll lock-in and catastrophic yaw. However, subsequent analyses (56) using the best available aerodynamic data have since indicated that nonlinearity in the static restoring moment can substantially modify the dynamic behaviour. In this more recent work, formulation of the mathematical model is based on the method of Cohen and Werner (57) who have used the unimodular quaternion to define angular coordinates rather than the commonly chosen Eulerian angles. As explained in reference 57, use of the quaternion avoids the singularity which occurs in Eulerian expressions near the vertical, where large truncation errors may be introduced by the integration process.

A summary of the results obtained from Goodale's studies is given in the following sections where flight dynamic effects are described for both high and low incidence behaviour of the streamlined body. In the absence of appropriate wind tunnel data it has not yet been possible to include Magnus forces and moments so that the analyses have been limited to flight conditions for which such terms are negligible. However, further studies will be made if Magnus data become available. Finally, it should be mentioned that throughout his work Goodale assumed the side forces and moments and induced rolling moments to vary sinusoidally with roll orientation of the total incidence vector instead of reproducing exact

the approximately sinusoidal shapes shown in figures 13, 16 and 18. The maximum amplitudes were of course matched in each case.

8.1 Response to the release disturbance

During the flight trials the initial release disturbance was a nose up pitching motion with a first peak amplitude of about 20° . This motion was caused by the air-flow in the Canberra bomb-bay; the type of airflow in the Canberra bomb-bay is well known(58) and in the computer studies it was simulated mathematically by assuming that prior to release the bomb was subject to an upwash at the nose and downwash at the tail. The upwash and downwash were taken to be of equal magnitude and to decrease linearly with distance fallen by the bomb so that at a depth of two calibres below the bomb-slip, the flow had completely straightened. The flow angles assumed were chosen to give pitch responses similar to those observed in the trials and it was found the measured variation in first peak amplitude with change in static margin could be quite adequately reproduced by using an initial upwash and downwash angle of 8° . All of the trial releases were made with fins at 45° to the vertical and figure 50 compares the theoretically determined first peak amplitudes of the responses with the observed values for c.g. positions between 47 and 57% of the body length from the nose.

The theoretical curve of figure 50 is based upon average properties of 173 slugft^2 for the bomb's transverse moment of inertia, 5.9 slugft^2 for inertia in roll and a weight of 855lb, in conjunction with aerodynamic restoring moment data for incidences up to 40° obtained from the U.S. Naval Ordnance Laboratory. Experimental values are identified by the appropriate round numbers. It is interesting to note the extremely rapid increase in first peak amplitude as the c.g. is moved progressively rearward. Ultimately a condition is reached at c.g. positions near 57% where the forward centre of pressure movement during the first upward swing of the bomb nose leads to a complete loss of static stability so that the bomb topples. Restoring moment data presented in figure 6(a) clearly indicate that this toppling effect will be most pronounced for angles of attack in planes at 45° to the fins where stalling occurs at about 20° . In addition to correlating the first peak amplitude, it was necessary that the simulated release disturbance should provide a representative mechanism for the growth of induced aerodynamic forces and moments with incidence. This requirement has also been satisfied by applying the concept of varying upwash and downwash in the bomb-bay.

A series of mathematical model studies was carried out to examine the flight dynamic behaviour during response to the release disturbance and to determine what combinations of fin cant and c.g. position would be likely to initiate catastrophic yaw. These studies included both the M557A and M823 bodies and, as would be expected for large amplitude motions, there was no detectable difference in general performance of the two configurations.

Releases in planes with fins at 0° , $22\frac{1}{2}^\circ$ and 45° to the vertical were considered in conjunction with fin cants of C, $\frac{1}{4}$, $\frac{1}{2}$, 1, 2 and 3 degrees for c.g. positions ranging from 45 to 62% of the body length from the nose.

For the case of releases with fins initially at 45° to the plane of disturbance, figure 51 illustrates the theoretical boundaries of dynamic behaviour which were established by computer calculations with many different combinations of fin cant and c.g. position. Configurations tested in the free flight trials programme are identified by the round numbers and with only three exceptions the predicted patterns of behaviour agreed quite closely with those observed. Thus,

each of rounds 703, 706, 707 and 713 with c.g. positions further aft than those that toppled due to static instability at high incidence; whereas all of the rounds with c.g. at between 50 and 52% simply exhibited a tendency to increasing pitch during the first pitch oscillations but in every case these rounds recover before the motion developed into catastrophic yaw. Typical responses computed to show the effect of increasing fin cant are given in figures 52(a), (b) and (c). Free flight rounds 708 and 715 are also examples of this - although they recovered from the release disturbance (as described in Section 7.3.1) yawing motion induced by an initial period of roll lock-in caused their ballistic accuracy to be unsatisfactory. Figure 52(d) is a typical computer response showing a divergent motion for a configuration in the region of catastrophic yaw. Finally, for c.g. positions forward of 49% the first peak amplitude was less than 16° so that the response remained virtually free of cross-coupling effects and this condition was well demonstrated by rounds 720 and 723 - figures 53 are sample wing tip camera records of the observed release disturbances.

For a given static margin canted fin designs appear to be more prone to instability at release than those with straight fins. The mechanism of this instability is as follows. On release the disturbance given to the bomb is in a plane passing through zero incidence; this plane is usually vertical (i.e. the pitch plane) or very near to it. If the fins are canted the bomb immediately begins to roll out of a symmetrical attitude relative to the pitch plane and soon has an attitude causing an induced side moment as well as the direct restoring moment, and the bomb yaws as well as pitches. Because of the symmetry of the bomb, the frequency of this yaw oscillation will be the same as the pitch but the two components will be out of phase and the disturbance will no longer be planar. By the time the bomb has reached its first maximum pitch after release it can have enough yaw and rolling velocity for roll lock-in to occur. The corresponding bomb with nominally straight fins will usually start to roll very much more slowly if at all (though a bomb released from an asymmetrical position such as under a swept wing can receive some rolling moment), it will be acted upon by much smaller induced side forces and hence its pitching tends to remain uniplanar and be more likely damp out before the bomb receives any significant yaw.

The three rounds which gave unexpected results were numbers 712, 726 and 732. Of these rounds 712 was predicted to give a first peak amplitude of about 23° but it toppled. This is not surprising because with the very low static margin which the round had only small changes in the disturbing impulses are needed to topple or push it to the predicted 23° of pitch. Consequently, it was not considered worthwhile to carry out further trials at c.g. positions near 54% and only later did the computer studies produce the results on which figure 51 is based. The figure shows that unfortunately there was no free flight round in the region of catastrophic yaw.

In the case of rounds 726 and 732, these exhibited abnormal rolling behaviour at high incidence during the first few seconds of fall which could not be explained on the basis of the available induced rolling moment data (Sections 7.3.1 and 7.4.2). The measured and predicted roll rates for round 726 are compared in figure 54. Because this vehicle was not fitted with an accelerometer, direct analysis of the rolling moments was not possible and attempts were made to reproduce the observed rolling and yawing motions with a computer using the A.R.A. wind tunnel data and free flight measured roll rate as input. In this way it was possible to produce a simulated yawing motion with the effects of rolling moments arbitrarily introduced to match those

actually experienced. A comparison of the resulting predicted motion with the measured flight response is given in figure 55 which indicates a very high degree of correlation. From this analysis it was inferred that the major difference between wind tunnel and full scale observations occurred in the results for induced rolling moments and that otherwise the agreement appeared to be very good. Results for round 732 generally confirm those of round 726 in that agreement between wind tunnel and free flight data for the induced rolling moments could only be obtained at incidences below about 17° .

Although it has not yet been possible to obtain a full understanding of the rolling behaviour at large angles of attack it is known that vortices shed from the bomb body can induce strong rolling moments if they pass in close proximity to the stabilising fins (59, 60). A series of small scale smoke tunnel tests (61) was therefore carried out at W.R.E. to provide some knowledge of the position and nature of such vortices for the M82J body. In general, these tests confirmed the existence of a symmetric vortex pair as would be inferred from the cyclic variation of the induced rolling moments shown in figure 18. However, a condition of flow asymmetry set in abruptly when the incidence exceeded about 45° , giving rise to a wake pattern somewhat resembling a Karman vortex street. The sequence of photographs in figure 56 clearly indicates the wake behaviour. Vortex flows of this kind are subject to scale effect, and it has been estimated that the flow change which was observed at 45° incidence in the smoke tunnel tests would be expected to occur at about 25° incidence under full scale conditions at 25000 ft altitude and $M = 0.5$. This type of flow change could well account for the abnormal rolling behaviour of rounds 726 and 732, and although such evidence is by no means conclusive, it is considered sufficient to justify further flow investigations up to the maximum Reynolds' numbers.

Summarising the examination of response to the release disturbance, it is evident that rearward movement of the bomb's c.g. enhances the susceptibility to catastrophic yaw. As the static margin decreases, the maximum angles of attack after release from the aircraft increase and at these greater angles of incidence the induced side and rolling moments rapidly increase in relative importance. Hence catastrophic yaw is most likely to be initiated by disturbances occurring in planes at 45° to the fins where the static restoring moment for cruciform configurations is lowest and falls off most rapidly with increasing incidence. Furthermore, for practical values of fin cant (up to about 2°) the dangers of catastrophic yaw are again increased as greater fin cants are applied. However, it should be emphasized that the studies outlined above refer to release disturbances which caused responses of approximately 20° initial amplitude. If these disturbances had been smaller, the region of catastrophic yaw shown in figure 51 would be correspondingly reduced.

8.2 Dynamic behaviour at low incidences

When the existence of a small region of static instability near zero yaw at high subsonic and transonic Mach numbers had been confirmed by both wind tunnel and free flight measurements on the M557A body, it was feared that this characteristic might well degrade the bomb's ballistic consistency, because under such conditions an appreciable trimmed incidence could be achieved during flight, even in the absence of small configurational asymmetries. Furthermore, the magnitude of trimmed incidence would be very sensitive to the bomb's c.g. position. Release conditions for the stores listed in group B of table 1 were therefore changed to 25000 ft at $M = 0.5$ so that the effects of aerodynamic non-linearity at low incidence could be examined more closely; these release conditions gave higher dynamic pressures during the critical part of the

trajectories. In conjunction with these trials a series of trajectories computed to investigate theoretically how the impact deviation would be with and without the presence of configurational asymmetry. Only one c. position was considered, namely 51.7% from the nose, and the influence of various fin cants was examined using the A.R.A. wind tunnel (modified at data as input. The results of this investigation are presented below. It should be noted that all trajectories are based upon conditions of zero disturbance at release.

8.2.1 Effect of static instability near zero yaw with no fin-body misalign

Flight dynamic behaviour of a symmetric bomb was computed for fin cant angles of 0° , $1/10^\circ$, $1/4^\circ$, $1/2^\circ$ and 1° . Configurations with fin cants of zero and 0.1° locked in with a trimmed incidence vector of approximately 3° lay in a plane close to that containing one pair of fins. Consequently the effects of induced rolling moments were almost negligible and the frequency of the resultant lunar motion approached the roll rate as determined by fin cant alone. For fin cants of $1/4^\circ$, $1/2^\circ$ and 1° the bomb again trimmed at an angle of approximately 3° and rolled at a rate determined by the fin cant but in these cases the bomb did not lock in.

Computed impact deviations from the particle trajectory are given in table 2. As would be expected, a large deviation occurred under the condition of lock-in if the fin cant was identically zero and the roll rate exceedingly low. With even very small fin cants of $1/10^\circ$ or however, the biasing affect of lock-in was largely eliminated by the but steady roll rate (0.2c/s for $1/10^\circ$ cant) and the resultant deviation was considerably reduced. In the case of fin cants ranging from $1/4^\circ$ to 1° further large deviations were obtained and in all cases impact occurred at a range in excess of the particle trajectory, and to the left.

From these investigations it is apparent that the flight behaviour at low incidence falls into two categories determined by the magnitude of the fin cant. For fin cants below a critical value (approximately 0.1°) it is possible for the corresponding roll exciting torques to be balanced by small induced rolling moments which are generated at angles of attack less than about 5° (see figure 19). Furthermore, with the existence of static instability near zero yaw, incidences are developed which, though small, are sufficient to cause roll lock-in, particularly if there is a fin-body misalignment to establish a preferred plane of trimmed incidence. Under these conditions the fixed orientation of the trimmed incidence vector is governed by the balance of rolling moments and the bomb barrel roll rate determined by the fin cant, consequently, the biasing effect of lock-in is averaged out and the resulting ballistic dispersion is small. For fin cants above the critical value of about 0.1° , the induced rolling moments at angles of attack less than 5° can no longer match those of the fin cant and so cannot cause roll lock-in, and because the trimmed incidence vector which results from the small region of static instability has no preferred plane in the missile body, its roll orientation is determined by the balance between the static restoring moment and the pitch damping moment due to curvature of the flight path. As a result the bomb spins at a yaw of repose which is effectively increased by an amount equal to the trimmed incidence, and the lift force so generated causes the missile to "kite" or "float" above the particle trajectory. At the same time, gyroscopic effects cause the trajectory to veer to the left.

the right or left according to the direction of spin.

Although the computer studies clearly confirmed that static instability near zero yaw could seriously degrade the ballistic performance of a bomb with cant angles from $\frac{1}{2}^{\circ}$ to 1° , the deviations predicted to arise from this cause were considerably greater than would be inferred from the trials results. The reason for this discrepancy was largely revealed by data obtained from round numbers 724, 725, 726 and 732 (see Section 7.3.1). These stores exhibited dynamic behaviour at low incidence very closely resembling that predicted for a symmetric bomb, but their trimmed incidence was smaller than the value predicted on the basis of the A.R.A. tunnel data and it abruptly vanished for speeds greater than $M = 0.90$. This behaviour was consistent with the free flight measurements of restoring moment presented in figure 46 which indicate that the region of static instability near zero incidence is somewhat smaller than that shown by the wind tunnel data and it vanishes earlier, at $M = 0.90$. Since the bomb was flying at these Mach numbers for much of the time, in the trajectory predictions the increase in range caused by "float" was substantially over-estimated.

Figures 57 (a), (b) and (c) show the quality of agreement obtained between the measured and predicted roll rates for round numbers 716, 709 and 708 respectively, with the predictions based upon a fin-body misalignment of 0.32° . These vehicles had fin cants of 0.17° , 0.44° and 1.41° and during response to the release disturbance their roll histories were clearly very sensitive to initial conditions which could not be reproduced identically on the computer. In the case of rounds 716 and 709 effects of fin camber were also indicated by a sudden loss of roll acceleration when transonic speeds were first reached a little after 20 sec from release. Since fin camber was generally quite small such effects were not included in the mathematical model studies, otherwise the rolling behaviour at low incidence was adequately simulated. The sudden loss of roll rate between 12 and 15sec after release predicted for round 716 (see figure 57(a)) was caused by a transient condition of roll lock-in at low incidence. Such an occurrence is critically dependent upon the extent of static instability near zero incidence and predictions of this particular motion require extremely accurate aerodynamic data. Clearly this behaviour was not experienced in the flight of round 716.

8.2.2 Effect of fin-body misalignment

The effect of side moment and induced rolling moment upon the magnitude and orientation of the trim vector in rolling flight was examined by Chadwick(55) for an idealised case in which the normal force and static restoring moment were assumed to be linear functions of the angle of attack. It was shown that sustained resonance could occur even under the non-steady conditions prevailing during the fall of a bomb. In particular the destabilising influence of the side moment was highlighted in its association with the direction of the trim vector in rolling flight. It was further demonstrated that the roll rate, and hence the plane of the trim vector in rolling flight, was significantly influenced by induced rolling moments, giving rise to such effects as roll speed-up, roll lock-in and roll break-out, all of which have been observed in actual flight trials. This orientation of the rolling trim vector appeared to be a dominant factor in determining the dynamic stability of a bomb's yawing motion.

Against this background of information a broader assessment of the effect of missile asymmetry upon dynamic behaviour and impact deviation was undertaken with trajectory computations arbitrarily based on misalignment of $\frac{1}{2}^\circ$ between the fin and body axes oriented in planes at 0° , 24.5° and $67\frac{1}{2}^\circ$ successively from a fin. A single release condition of 45000 ft at a speed of 678 ft/s was studied for configurations with fin cants of 0° , $\frac{1}{4}^\circ$, $\frac{3}{8}^\circ$, $\frac{1}{2}^\circ$ and 1° at each orientation of the misalignment. Results of the assessment including brief descriptions of the dynamic behaviour predicted in each trajectory are given in table 3 which clearly shows deviations generally much greater than those observed in the flight trials with c.g. at 51.7% from the nose.

It is interesting to note that with a fin-body misalignment of $\frac{1}{2}^\circ$ a trimmed incidence vector immediately had a preferred plane in the bomb and the floating effect which was exhibited by the symmetric bomb occurred. Fin cants of 1° gave trajectories with the smallest deviation and in all other instances the deviations were excessive and showed a tendency to be greatest for fin cants between $\frac{3}{8}^\circ$ and $\frac{1}{2}^\circ$ when the misalignment was in the plane of a fin. For the research test vehicle measured fin-body misalignment averaged approximately 0.02° . Trajectory computations repeated with this value indicated that the dynamic behaviour reverted to that of a symmetric missile as described in the previous section.

From the results contained in tables 2 and 3, which were computed under the condition of zero release disturbance, at first sight it appears in terms of ballistic performance there is little to choose between a symmetric missile and one which has a substantial misalignment between the fin and body axes. In general, the former configuration tends to overshoot to about the same extent that the latter falls short; the magnitude of impact deviations being influenced almost equally by the effects of float in one case and resonance in the other. However, equality is largely coincidental and is critically dependent upon the degree of aerodynamic nonlinearity near zero yaw and the data of tables 2 and 3 are only relevant to a bomb having a small region of static stability at low incidence. Had this region and the static trim incidence been eliminated by an appropriate change in c.g. position, the tendency to float exhibited by the symmetric missile would no longer occur and its ballistic performance would be markedly improved, but the same would not be true for the bomb with tail misalignment. In this case the effects of resonance are not removed because the misalignment provides an alternative way of sustaining a trimmed incidence and although the ballistic performance may be improved it will not match that of the symmetric bomb. At subsonic speeds the M557A configuration happens to have a centre of pressure position at zero incidence close to 50% from the nose so that the region of static instability for small angles of attack is very sensitive to movements in c.g. about the 50% station. Inability to define this aerodynamic nonlinearity with sufficient accuracy has been a limiting factor in the prediction of ballistic dispersion.

9. CONCLUSIONS AND RECOMMENDATIONS

Before drawing specific conclusions from the results of the research programme, it is important to emphasize how the use of modern high speed digital computing facilities significantly influenced the conduct and analysis of the aerodynamic experiments. Thus, it has been demonstrated that with quite modest airborne instrumentation and the aid of a digital computer, it was feasible to apply curve fitting techniques to very large quantities of flight data, making it possible to obtain detailed information on the aerodynamic force and moment system of a test vehicle. The results of such full scale analyses were then available for direct comparison with wind tunnel measurements. Furthermore, by programming the rigid body equations of motion on a digital computer and using wind tunnel data as input, missile behaviour could be predicted over simulated trajectories for subsequent correlation with the observed flight trial performances. In this way an additional check was imposed upon the underlying theory of flight dynamics.

Although it was not possible to obtain completely equivalent motion histories of flight behaviour in every case, the predicted motions showed good qualitative agreement with reality. This difficulty stemmed from the complicating effects of aerodynamic nonlinearity and incomplete knowledge of true initial conditions in the disturbed flow field around the aircraft. Instances of anomalous behaviour were observed only at large angles of attack for which it was shown that the wind tunnel data did not always properly represent full scale flight conditions or when too great a simplification of wind tunnel data was made. Consequently, within the limits of experimental accuracy and scope of the research programme no reason was found to doubt the validity of the basic theory of quasi-steady aerodynamics. One of the main objectives of the research programme has therefore been achieved, namely, to establish validity of the mathematical model and so demonstrate that the effectiveness of any particular missile configuration may be adequately predicted using only wind tunnel and digital computer facilities.

9.1 Flight dynamics and ballistic consistency

Results obtained from the flight trials, and confirmed my mathematical model studies, have clearly indicated that the dynamic behaviour of a streamlined fin stabilised bomb falls into two basic classes. The first of these is associated with flight at large angles of attack where separated flow phenomena have a dominating influence, and the second class refers to flight at small angles of attack when the bomb may be subject to such adverse effects as roll-yaw resonance and centre of pressure movement with small incidence changes.

In the case of bluff body shapes, at subsonic speeds flow separation takes place at the nose leaving the afterbody submerged in a completely separated wake, so that the influence of body vortices is substantially reduced and there is relatively little centre of pressure movement with incidence. Since the drag-weight ratio of the bluff body stores limited trials of this shape to subsonic flight conditions the resulting dynamic behaviour was quite uneventful. Consequently the following remarks are concerned more particularly with behaviour of the streamlined configuration. In general, large amplitude yawing motions were found to be either initiated directly by external disturbances which occurred during the release phase or indirectly by the onset of some undesirable dynamic condition such as resonance or Magnus instability. Where motions of the former kind were concerned it was necessary to show how to determine whether the bomb would recover from the disturbance, and for the second type of motion criteria were required covering low incidence behaviour to ensure that large yawing amplitudes would not be developed.

At high angles of attack nonlinear variation of the restoring moment incidence may cause complete loss of static stability for a bomb which otherwise behaves quite satisfactorily. This problem is associated with fin stalling which can lead to toppling at release if the disturbance imposed on the aircraft is excessive or if the bomb has too little static margin at the angle of incidence. For cruciform fin configurations the tendency to topple is greatest for angles of attack in planes at 45° to the fins where the restoring moment is at a minimum. A further source of trouble stems from the rapid growth of induced rolling moment with angle of attack. This moment is of particular significance during response to the release disturbance because it is capable of balancing the bomb's rolling motion so that the roll rate is constant at the nutation frequency leading to catastrophic yaw. Hence, for practicable design the problem of bomb stability cannot be entirely separated from the problem of its disturbance on release from an aircraft and to ensure the stability of weapons it may be essential rather than desirable to be able to control this disturbance to some extent. The significance of the effect of pitch amplitude upon the stability of a bomb during its response to the release disturbance has only been fully realised within the last year or two. Previously, dispersion caused by the release disturbance had been attributed to the inconsistency of the disturbance itself. This fact highlights the need for a better knowledge of the way that rolling moments induced by combined pitch and roll increase at high angles of attack since the more rapidly they increase the more necessary it is to limit release disturbance.

Once a bomb has recovered from the release disturbance the ballistic performance over the subsequent trajectory is determined by its ability to continue flying at or near zero incidence. During this phase of flight the main problems are to avoid roll-yaw resonance which occurs when the roll rate approaches the same value as the natural pitching frequency, and to avoid roll rates high enough to cause Magnus instability. In the resonant condition a small trim angle resulting from configurational or mass asymmetry is amplified to a considerable angle of attack, thereby increasing the bomb's susceptibility to roll lock-in and catastrophic yaw. Another problem in flight at small angles of attack is caused by nonlinear variations in the restoring moment which can create a small region of static instability at zero yaw. A bomb with this characteristic flies at a trimmed incidence determined by the degree of aerodynamic nonlinearity, even in the absence of small configurational asymmetries, and furthermore, the magnitude of the trimmed incidence is sensitive to the bomb's c.g. position. If deliberate fin cant is applied to generate roll rates greater than the natural pitching frequency the ballistic consistency may be seriously degraded.

9.2 New concept for ballistic trials

Since it has been shown that the stability problem is associated separately with flight conditions at either high or low angles of attack, the requirements for a bomb to have good ballistic consistency and acceptably small dispersion may be summarised in the following general terms :-

- (a) The release disturbance should be kept within reasonable limits.
- (b) The bomb should have enough static stability to recover quickly from the release disturbance.
- (c) The bomb should remain free from adverse roll-yaw interaction during its fall.
- (d) The roll rates should not be high enough to cause Magnus instability.

Once these conditions are satisfied the assessment of any new bomb design may be based primarily on determining the susceptibility to roll-yaw interaction which is now considered to be directly responsible for "rogue" behaviour in otherwise good bombs. It is maintained that considerable improvements can be made on the old method of end point ballistic trials in which dispersion is determined statistically from a relatively large number of trials, and rogue bombs identified as those deviating significantly from the mean. Thus if roll histories are measured, the additional information provides a more sensitive indication of ballistic performance because it can not only be seen whether a bomb has locked-in at the nutation frequency but also it can be determined how closely a resonant condition was approached or how quickly it was traversed. With a smaller number of bombs therefore, a better estimate can be obtained of the likelihood of badly behaved bombs occurring in further samples. Although it may be difficult to interpret resonant conditions in cases where aerodynamic nonlinearity causes the natural pitching frequency of a bomb to be amplitude dependent, in general, if roll-yaw interaction is severe enough to produce a significant deviation at impact then it will inevitably show an anomaly in the corresponding roll history.

The new concept for ballistic trials outlined above has been tested successfully by linking the 28lb practice bomb (32) and 1000 lb N.I. bomb (33) ballistic trials with the R.A.E./W.R.E. research programme. In these trials it was shown that aircraft bomb-bay and wing-tip cameras gave an adequate coverage of the bomb's response to the release disturbance and that for bombs of the 1000 lb size it was quite easy to obtain roll histories simply by painting patterns on the bomb and analysing ground based cine camera records. Because it was too small for optical tracking in daylight the 28lb practice bomb was fitted with a bright light visible through only 180° of its circumference and the trials conducted at night.

9.3 Aerodynamic aspects of bomb design practice

The ultimate aim in designing a bomb is to devise a configuration which is capable of maintaining adequate ballistic consistency over the range of flight conditions determined by its operational requirement; this implies that the weapon should recover quickly from the release disturbance and remain free from adverse roll-yaw interaction during its fall.

Factors which must be considered in avoiding instability during response to the release disturbance involve three mutually interacting terms, namely static stability, fin cant and size of the initial external disturbance. Figure 50 shows typical effects of static stability upon the first peak amplitude of a bomb's response to a specific release disturbance. Here it may be seen that severity of the response increases steadily as the static stability is reduced until a condition is reached at which the fins stall and the bomb topples. Thus the choice of static margin must be linked with considerations of the expected release disturbance unless the requirements for aircraft release characteristics are such that a limit can be assumed on the magnitude of this disturbance angle. The additional effects of fin cant upon dynamic behaviour of a bomb during the release phase are indicated by the stability boundaries shown in figure 51 for the low drag bomb body released from the Canberra bomb-bay. A significant fact illustrated by this figure is that there is a forwardmost c.g. position beyond which the amplitude of the disturbance angle is too small to cause roll lock-in and catastrophic yaw because the induced rolling moment is not significant up to such angles of attack. For a low drag configuration this critical angle of attack is apparently about 20°, and if

response to the release disturbance could be kept below this value the of dynamic instability for a bomb would be greatly reduced. When fin applied the danger of catastrophic yaw at release is seriously enhanced angles of attack greater than about 20° (Section 8.1) and it would require cant angles in excess of 3° to preclude all possibility of roll lock-in. Under such conditions spin rates generated later in flight would inevitably introduce problems associated with Magnus instability. Consequently, limitation can be placed upon the magnitude of the release disturbance, adverse roll-yaw interaction during this phase can best be minimized by maintaining the fin cant below about $\frac{1}{2}^\circ$, and nominally zero cant would be optimum.

During its fall the roll history of a bomb is largely determined by effective mean cant angle of its fins. Whether these are deliberately to spin the bomb quickly through resonance with relatively little transverse disturbance or whether the fins are nominally straight to keep the roll below the pitch frequency; manufacturing tolerances on the fins will be important and fin designs cannot be decided upon without knowledge of what manufacturing standards are feasible for the type of weapon. Bad fins reduce the roll rate of a canted design and cause it to pass too slowly through resonance or they can give an unintentional roll rate to a straight fin and accelerate it slowly up to the dangerous resonance region. In either case stability trials of full scale production weapons are only meaningful if it is taken of the likely random variation of effective fin cant angles due to manufacturing asymmetries. It is difficult to devise inspection routines which will give measurements which can be interpreted in terms of equivalent fin cant angles to the accuracy needed with any confidence. Therefore a full scale check on stability is to have much meaning it must include a number of bomb trials to assess the variation in roll rate due to these errors in fin cant on at least a limited statistical basis.

9.4 Bomb design procedure

On the basis of the results of the stability research programme suggestions can now be made for bomb design procedure. Ideally, before making any decision regarding the external shape of a weapon experimental measurements would be made of all possible aerodynamic derivatives for the suggested design alternative. Full six-degrees-of-freedom computations would be made of the bomb's motion following all possible disturbances, and these results would then be checked against full scale trials. This would take many months or even years and in many cases decisions have to be taken on a much simpler basis to be confirmed as far as possible afterwards by a more thorough investigation. For example, in many cases limitations for internal and external carriage on several aircraft are to lead to several alternative weapon design schemes for each of which an estimate of c.g. limitations and fin sizes are needed. The different alternatives may give alternative limits on length, body diameter and span, there may be the choice between bluff short layouts for internal carriage only or lean layouts taking more space but also suitable for external carriage, then alternative warheads, there may be effects of store size on aircraft design speed and range to be considered, and so on. Detailed investigation of conceivable motion for each alternative configuration is not possible on the time-scale, and wind tunnel testing of even one or two layouts may be long in model making and testing. The need in preliminary project estimates is for fairly quick simple methods, which may not be absolutely accurate but which can be relied upon to provide an adequate basis for design so that

minor modifications are subsequently required when thorough investigations have confirmed the preliminary studies.

As a first step it is suggested that the choice of tail size be based upon static stability which can be estimated fairly simply and reliably. Dynamic stability derivatives in a particular case are neither so easily or reliably estimated. Though there is no general theoretical relationship between the static and dynamic derivatives of bombs, the basic similarity between almost all bomb designs ensures that in practice they are not unrelated. Nearly all bombs are heavy bodies with their c.g. at 35% to 45% of the total body length stabilised by fins at the end of comparatively long moment arms, the fins producing about 70% to 80% of the total lift. Most of both the static restoring moment and the pitch damping come from the tail and increasing one also increases the other. If bombs are divided into two groups (low drag and bluff) on the basis of whether or not the airflow separates completely from the bomb nose there is fair correlation in each group between static stability and pitch damping, and static stability alone can be used as a first rough guide to stability. Computations undertaken in the R.A.E./W.R.E. research programme and past experience suggests that the minimum static margin to avoid any instability at release is likely to be about 12% to 15% of body length as body fineness ratio changes from about 8:1 to 6:1. For example, in one set of over 90 complete motions computed for the low drag research vehicle with static margins of 0.5 and 0.75 calibres and fin cants up to 1.75° , the release disturbance degenerated into complete instability in 23 cases; out of 90 more computed motions with 1 calibre static margin, only one case of instability was found. In addition, the estimated pitch frequency corresponding to the chosen static margin must be checked for roll resonance down critical specimen trajectories. With an experimental or estimated spanwise lift distribution for the fin, roll acceleration and limiting roll rates can be estimated and histories of roll rate and pitch frequency down the trajectories should be compared. Experience suggests that after making allowance for all effects such as possible fin cant variations due to manufacturing asymmetries, variations in pitch frequency due to Mach number etc., the roll rate should never be allowed to stay within 25% of the pitch frequency. In addition, after estimating from past results the maximum rolling moment due to combined pitch and roll attitude and also the likely pitch frequencies and damping, it should be shown that with (say) a 20° limit on initial maximum pitch the rolling moments due to possible fin cants plus those which could be induced by combined pitch and roll cannot force the roll rate up to a value near the pitch frequency within the time taken for the initial disturbance to damp down to not more than 10° of pitch.

It is thought that these investigations are enough for a reliable first guide to adequate stability. It must be emphasised however that they are limited and do not pretend to cope with any unexpected nonlinearities - for example, with any loss of fin effectiveness due to flow separations on the bomb tail cone, with large changes in pitch damping in the transonic region, etc. The investigations for the selected configuration need backing up as soon as possible by experimental checking of the aerodynamic derivatives and by full computation of the weapon's response to any likely disturbance.

A final and possibly much later stage would be some full scale checking of the wind tunnel and computational results. Under normal circumstances these full scale stability trials would also be used for drag and dispersion measurements for aiming data and this might affect detailed trials specifications. The stability information that would be sought from these trials would be confirmation that the roll rates of production weapons stayed below the expected

limits or built up in the expected way (because of the difficulty in it for manufacturing asymmetries to define the equivalent fin cant angles to the required accuracy), and confirmation that some typical large di. damped out as predicted. It is not suggested that very extensive full stability trials are desirable - there are so many possible release di. in terms of combinations of initial pitching, yawing and rolling motion could be forced on the weapon that full scale trials can at best only recovery from a small proportion. The most rational approach is to use a computer to investigate all the permutations of possible initial motion; rely on full scale trials only as a check on the accuracy of a few self predictions.

9.5 Further research

Although the joint R.A.E./W.R.E. research programme has been closely related to bombs the results obtained have a considerable bearing upon other aerodynamically stabilised missiles such as mortar shells and un rockets. Furthermore, much interest has been stimulated by the good tions achieved between the results of wind tunnel tests carried out un varying conditions in different countries, and between wind tunnel and scale free flight measurements of aerodynamic coefficients.

So far as fixed cruciform fin stabilisation is concerned significant discrepancies between wind tunnel and full scale measurements were observed only for rolling behaviour of the streamlined bomb at large angles of and low spin rates. This flight condition was found to be greatly induced by vortices shed from the bomb body which induced strong rolling moment they passed in close proximity to the stabilising fins. Preliminary visualisation studies showed the existence of a critical angle of attack which the separated vortical flow about the bomb body suddenly became . It is to be expected that such changes in flow characteristics would be accompanied by large and sudden changes in rolling moment as were observed some of the flight trials. Because these flows are sensitive to scale it is extremely difficult to make accurate predictions from wind tunnel. obtained under these conditions and further full scale measurements are required. For this purpose it is proposed to construct a five-component strain-gauge balance for in-flight measurement of the aerodynamic force moments on complete cruciform tail units on some of the remaining vehicles. It is also suggested that wind tunnel flow visualisation studies be extended to the highest possible Reynolds' numbers.

Theoretical investigations of both split skirt and free spinning tail stabilising devices are currently being made at W.R.E. with the object of providing background information for the ultimate conduct of free flight tests. The U.S. wind tunnel tests have already shown that split skirt configurations almost completely eliminate the cross-coupling effects of yaw-induced rolling moments, and this design appears to be effective as a stabiliser for conventional ballistic bomb, or a retarded bomb, or possibly a guided bomb (by differential opening of the stabilisers). The advantages of split skirt stabilisers over the simpler fixed cruciform fins are in offering the possibility of greater tactical flexibility within a single weapon design, and in being very compact, low drag shape when the skirts are closed for carriage.

Free spinning tails offer the advantages of a reduction in Magnus effect and give a high roll acceleration at release without developing excessive rates in later flight. They may also permit the use of a monoplane configuration with only two fins instead of a cruciform tail, giving obvious advantages in aircraft installation.

UNCLASSIFIED

Report HSA 20

Recently, three free flight experiments on free spinning tails were successfully conducted using the M823 body shape and a further six instrumented bomb test vehicles have been set aside for tests of the split skirt and spinning monoplane tail designs. In supporting the free flight work, considerable effort has been devoted to the improvement of transducer calibrating techniques; an airborne camera and lens system has also been developed to increase the accuracy of missile attitude measurements. Results of this additional work will be published later.

UNCLASSIFIED

UNCLASSIFIED

REFERENCES

No.	Author	Title
1	Richards, G.J.	"A Bomb Ballistic Trial Programme in Australia - Part I." RAE Tech.Note Arm. 409. February 194
2	Ross, A.C.	"Bomb Ballistic Trial Programme in Australia - Part II." RAE Tech. Note Arm. 410. February 194
3	Capper, J.F.	"Note No.1 on the Theory of Bomb Stability." RAE Arm. Dept. Note Arm 1942.
4	Capper, J.F.	"Note No.2 on the Theory of Bomb Stability." RAE Arm. Dept. Note Arm 1943.
5	Bomb Ballistics Group, Armament Dept., RAE	"Low Altitude Technique for Measureme Stability Factors of Bombs." RAE Tech. Note Arm. 349. April 1946.
6	Bomb Ballistics Group, Armament Dept., RAE	"The Stability and Consistency of Var Bombs." RAE Tech. Note Arm. 331. June 1945.
7	Rhodes, C.W.	"The Establishment of the Minimum Aerodynamic Stability of Bombs Consis with Low Dispersion." RAE Tech. Memo. Arm. 1793. June 196C
8	Richards, G.J.	"The Problem of Correlation of Bomb Stability with Dispersion." RAE Tech. Memo. Arm. 1123. August 19
9	Dudley, R., and Lawrence, T.	"Measurement of the Drag of Bombs at Transonic Speeds by the Ground-launch Rocket-boosted Model Technique." RAE Tech. Note Aero. 2150. March 195
10	Greenwood, G.H.	"Drag Measurements of the 1000lb MC 2 Using the Free Flight Model Technique RAE Tech. Note Aero. 2471. November 1
11	Greenwood, G.H.	"Free Flight Measurements of Transoni Zero Lift Drag on a Family of Blunt N Bodi's of Revolution." RAE Tech. Not Aero. 2603. February 1959.

UNCLASSIFIED

No.	Author	Title
12	Shannon, J.H.W.	"Drag and Stability Measurements of Six Bomb Shapes from Ground Launched Model Tests." WRE Report HSA 14. September 1960.
13	Shannon, J.H.W.	"The Prediction of Bomb Performance from Ground Launched Model Tests." WRE Report HSA 13. August 1960.
14	Fowler, R.H., Gallop, E.G., Lock, C.N.H., and Richmond, H.W.	"The Aerodynamics of a Spinning Shell." Phil. Trans. Roy. Soc. London 1920.
15	Fowler, R.H., and Lock, C.N.H.	"The Aerodynamics of a Spinning Shell - Part II." Phil. Trans. Roy. Soc. London 1921.
16	Kent, R.H.	"An Elementary Treatment of the Motion of a Spinning Projectile about its Centre of Gravity." BRL Report No.95, 1937; and revision with McShane, E.J. BRL Report No.459, 1944.
17	Kelly, J.L., and McShane, E.J.	"On the Motion of a Projectile with Small or Slowly Changing Yaw." BRL Report No.446, 1944.
18	Phillips, W.H.	"Effect of Steady Rolling on Longitudinal and Directional Stability." NACA TN 1627. June 1948.
19	Nielsen, K.L., and Synge, J.L.	"On the Motion of a Spinning Shell." Quart. App. Math. Vol. IV No.3 October 1946.
20	Nicolaidis, J.D.	"On the Free Flight Motion of Missiles having Slight Configurational Asymmetries." BRL Report No.858. June 1953.
21	Nicolaidis, J.D.	"Two Non-Linear Problems in the Flight Dynamics of Modern Ballistic Missiles." IAS Report No.59-17.
22	Murphy, C.H.	"The Measurement of Non-Linear Forces and Moments by Means of Free Flight Tests." BRL Report No.974. February, 1956.
23	Murphy, C.H.	"Prediction of the Motion of Missiles Acted on by Non-Linear Forces and Moments." BRL Report No.995. October 1956.

UNCLASSIFIED

No.	Author	Title
24	Murphy, C.H.	"Limit Cycles for Non-Spinning Statically Stable Symmetric Missiles." BRL Report No.1071. March 1959.
25	Maple, C.G., and Synge, J.L.	"Aerodynamic Symmetry of Projectiles." Quart. App. Math. Vol. VI, No. 4, January
26	Zaroodny, S.J.	"On the Mechanics of Dispersion and Short Ranges of Mortar Fire." BRL Report No.668. April 1949.
27	Zaroodny, S.J., and Mott, R.S.	"Dynamic Measurements on the 81 M.M. Shell in N.B.S. Wind Tunnel." BRL Report No.882. October 1953.
28	Zaroodny, S.J., and Bomberger, N.E.	"Spiral Yawing Motions of 81 M.M. M.56 She A Study in Non-Linear Theory." BRL Memo Report No.682. May 1953.
29	Long, J.E.	"Free-Flight Investigation of the Stability and Drag of the EX-10 General Purpose Bomb NAVORD Report 2916. July 1953.
30	Piper, W.D.	"Static Stability Characteristics of the Low Drag Bomb with Different Fin Configurations NAVORD Report 4503. January 1958.
31	Piper, W.D., and DeMeritte, F.J.	"Summary of the NOL Investigations to Determine the Aerodynamic Characteristics of the No Drag Bomb." NAVORD Report 5679. February 1960.
32	Dudley, R.E.	"Measurement of the Ballistic Performance of the 28lb Practice Bomb No.1 Mark I when Released from High Altitude." WRE Tech. Note HSA to be published
33	Gilder, Mrs. J.	"Ballistic Trials of the 1000lb Mark I Bomb RAE Tech. Report to be published.
34	Secomb, D.A.	"Transonic Wind Tunnel Measurements of the Effect of Roughness Bands on a Bomb with Edged Fins." Australian Aeronautical Research Laboratories, ARL A.213. May 1953.
35	Thompson, J.S., and Fail, R.A.	"Oscillatory Derivative Measurements on a Bomb Mounted Wind Tunnel Model." RAE Report Aero. 2668. July 1962.

UNCLASSIFIED

No.	Author	Title
36	-	"Results of Tests on a Streamlined and a Bluff Research Store over the Mach number Range 0.50 to 1.25." (RAE Models M557A and M557B). A.R.A. Wind Tunnels Test Report S44. May 1963.
37	-	"Aircraft Research Association Preliminary Test Report on Model M7." (RAE Model M823). August 1963.
38	-	"Unpublished Wind Tunnel Data Communicated by R.A. Fail, RAE Bedford. 21.10.63."
39	-	"Unpublished Wind Tunnel Data Communicated by R.A. Fail, RAE Bedford. 20.12.63."
40	-	"Unpublished Wind Tunnel Data Communicated by J.S. Thompson, RAE Bedford. 24.9.64."
41	Stanbrook, A.	"Experimental Pressure Distribution on a Bluff-Nosed Cylinder at Subsonic and Transonic Speeds." RAE Tech. Note Aero. 2876. March 1963.
42	Carter, E.C.	"Results of Some Pressure Measurements made on a Bluff Nosed Cylindrical Body at Transonic Mach numbers." ARA Model Test Note S19/1. March 1962.
43	Göthert, B.	"High Speed Tests on Bodies of Revolution and a Comparison with Dropping Tests." L.G.L. 156 pp. 89-108. Translated as M.O.S. Volkenrode Reports and Translations No.367. (ARC 11399) February 1947.
44	Rhodes, C.W.	"Stability Problems of Wingless Field Missiles." RAE Tech. Note No.WE60. April 1964.
45	Fellows, Mrs. K.A.	"Some Results of Force and Pressure Plotting Tests on a Symmetrical Store." (ARA Model S46). Aircraft Research Association Model Test Note S46/2.
46	Fellows, Mrs. K.A.	"Some Results of Force Measurements on a Long Store with Fins and Asymmetric Strakes at Transonic Speeds." (ARA Model S46/3). Aircraft Research Association Model Test Note S46/3.
47	Shantz, I., and Groves, R.T.	"Subsonic Damping Moment Measurements for the EX-10 Bomb, EX-30 Projectiles and 6 inch Test Vehicle." NAVORD Report 4025. April 1958.

No.	Author	Title
48	Long, J.E.	"Roll Coefficients for the Low Drag Bomb (EX.10 in the Transonic Velocity Region ($0.65 < M < 1.31$)). NAVORD Report 4389. November 1956.
49	Harkin, B.	"Contrave Locational Error Contours, Range E, Woomera." Part I June 1960, Part II January 19 WRE Tech. Note SAD 59.
50	Secomb, D.A.	"Transonic Wind Tunnel Measurements of the Performance of a Hemispherical-Head Incidence Meter. ARL Note Aero. 223. August 1963.
51	Iberall, A.S.	"Attenuation of Oscillatory Pressures in Instrument Lines." U.S. Department of Commerce National Bureau of Standards, Research Paper RP 2115. Vol.45. July 1950.
52	Frame, J.W.	"The Effect of the Form and Rotation of Earth on Bomb Trajectories." RAE Tech. Note Arm 471. April 1951.
53	Brown, D.P.	"Free Flight Measurements of Aerodynamic Forces and Moments on a Streamlined Bomb with Cruciform Fins." WRE Tech. Note (to be published).
54	Chadwick, W.R.	"A Programme for the Numerical Analysis of the Dynamic Behaviour and Dispersion Characteristics of Bombs with Low Static Stability." WRE Tech. Note SAD 83. October 1961.
55	Chadwick, W.R.	"The Flight Dynamics of a Bomb with Cruciform Tail: Note on the Effect of Nonlinear Yaw-Induced Rolling Moments and Side Moments." WRE Tech. Note SAD 102. September 1962.
56	Goodale, P.L.	"A Theoretical Study of the Flight Dynamics and Ballistic Consistency of a Streamlined Bomb with Cruciform Fins and Low Static Stability." WRE Tech. Note (to be published).
57	Cohen, C.J., and Werner, D.	"A Formulation of the Equations of Motion of a Four-Finned Missile." NAVORD Report 5133. September 1956.
58	Rhodes, C.W.	"Bomb Bay Buffeting on Weapon Vibration in Open Bomb Bays." RAE Tech. Note Arm 709. December 1961.

No.	Author	Title
59	Mello, J.F., and Sivier, K.R.	"Supersonic Induced Rolling Moment Characteristics of Cruciform Wing-Body Configurations at High Angles of Attack." McDonnell Aircraft Corporation. Report 5642. January 1958.
60	Spar, J.R.	"Contributions of the Wing Panels to the Forces and Moments of Supersonic Wing Body Combinations at Combined Angles." NACA Tech Note 4146. January 1958.
61	Thomson, K.D.	"On the Flow Over a Bomb Shape at Large Angles of Incidences." WRE Tech. Memo. HSA 137. April 1965.

DISTRIBUTION

	Copy No.
External	
In United Kingdom	
Senior Representative, Department of Supply, Australia House, London	1
Royal Aircraft Establishment:	
Aerodynamics Department	2 - 3
Weapons Department	4 - 7
Space Department	8 - 9
Bedford	10
West Freugh	11
Library	12
Ministry of Aviation:	
D.A. Arm (Attention ADA Arm 2)	13 - 16
D.A. Navy	17
A.D./G.W.(A)	18
G.W.(A)5	19
Technical Information Library Services	20 - 25
Secretary, Ordnance Board	26
Air Ministry: OR4(a)	27
Science 2	28
CPS B+	29
In U.S.A.	
Defence Research and Development Attache Washington	30 - 31
Project Officer, Annex 35 M.W.D.D.E.A., Eglin Air Force Base Florida	32 - 56
for distribution to:	
Dr. W. Kemper	N.W.L.
Mr. C. Wingo	N.W.L.
Mr. P. Daniels	N.W.L.
Library	N.W.L.
Dr. W.R. Haseltine	N.O.T.S.
Dr. P. Rodgers	N.O.T.S.
Library	N.O.T.S.
Mr. S. Hastings	N.O.L.
Mr. F. Regan	N.O.L.
Library	N.O.L.
Mr. L.C. MacAllister	B.R.L.
Mr. S. Zarodny	B.R.L.
Library	B.R.L.
Dr. J.D. Nicolaidis	
Mr. C. Martin	Eglin Air Force Base
Mr. F. Burgess	Eglin Air Force Base
Library	Eglin Air Force Base
Mr. S. Baker	B.U.W.E.P.S.
Library	B.U.W.E.P.S.
Spares	6

UNCLASSIFIED

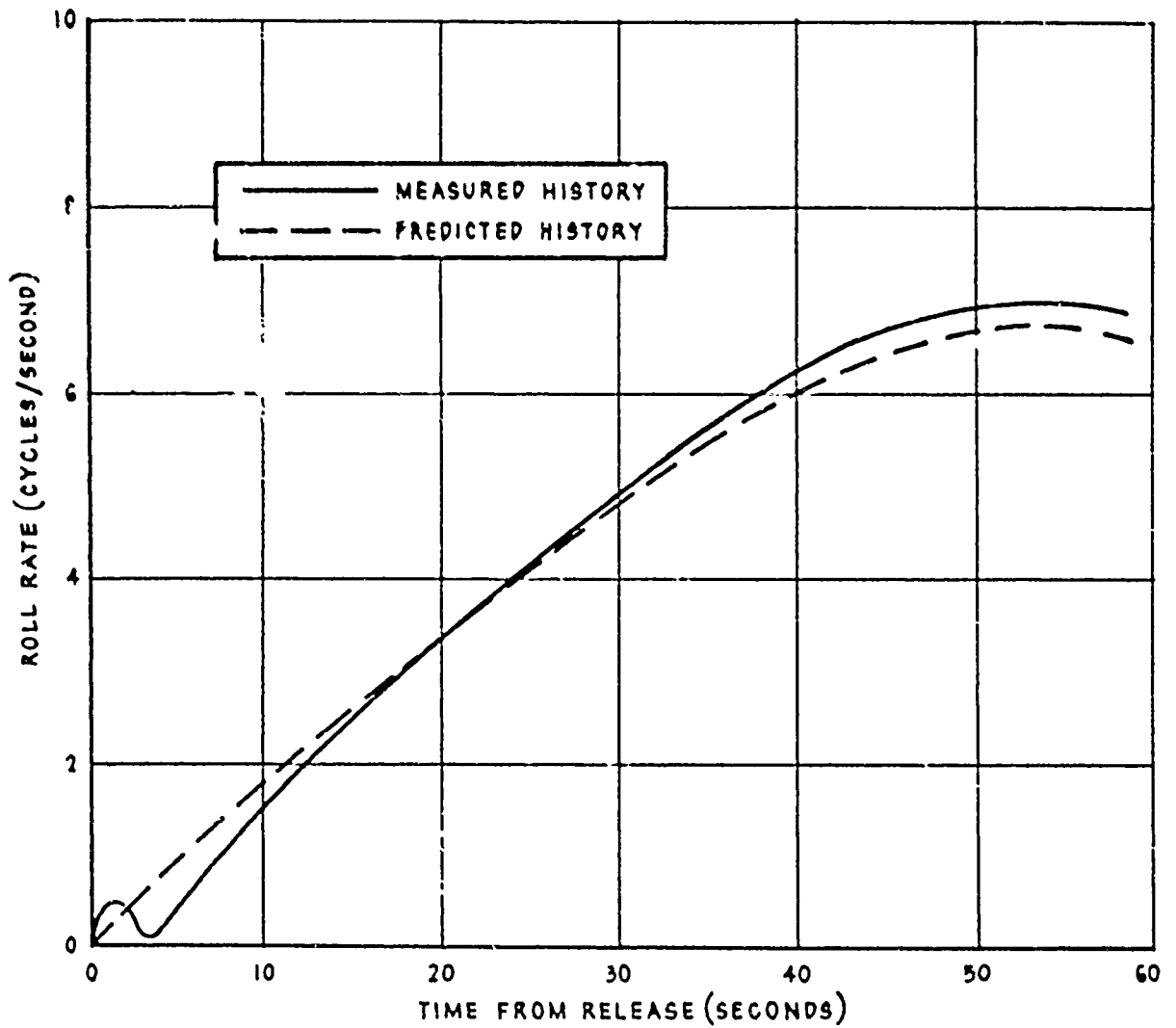


FIGURE 57(c). COMPARISON OF MEASURED AND PREDICTED ROLL RATE HISTORIES FOR ROUND NUMBER 708 ($\eta = 1.41^\circ$)

UNCLASSIFIED

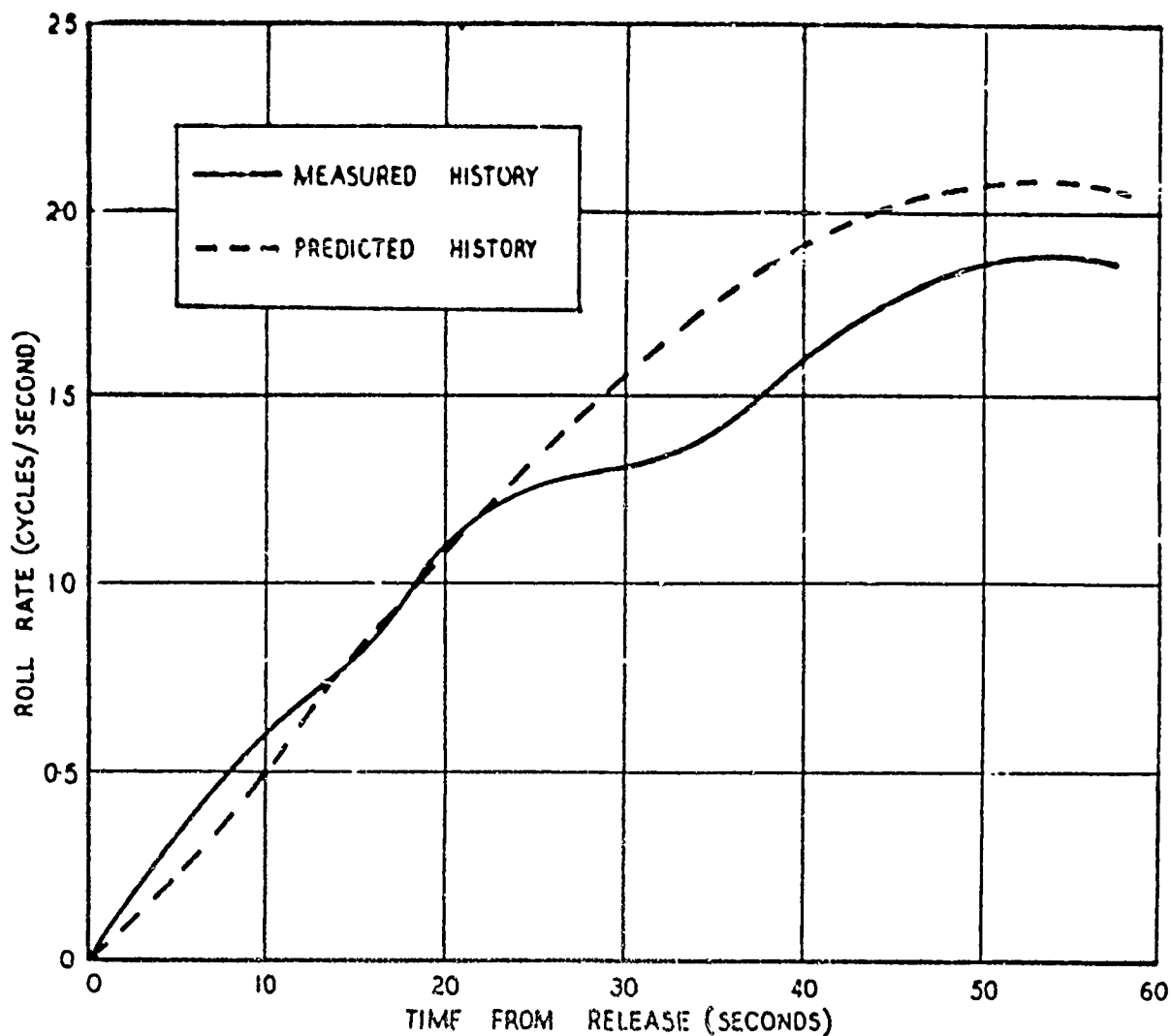


FIGURE 57(b). COMPARISON OF MEASURED AND PREDICTED ROLL RATE HISTORIES FOR ROUND NUMBER 709 ($\eta = 0.44^\circ$)

Figure 57(a)

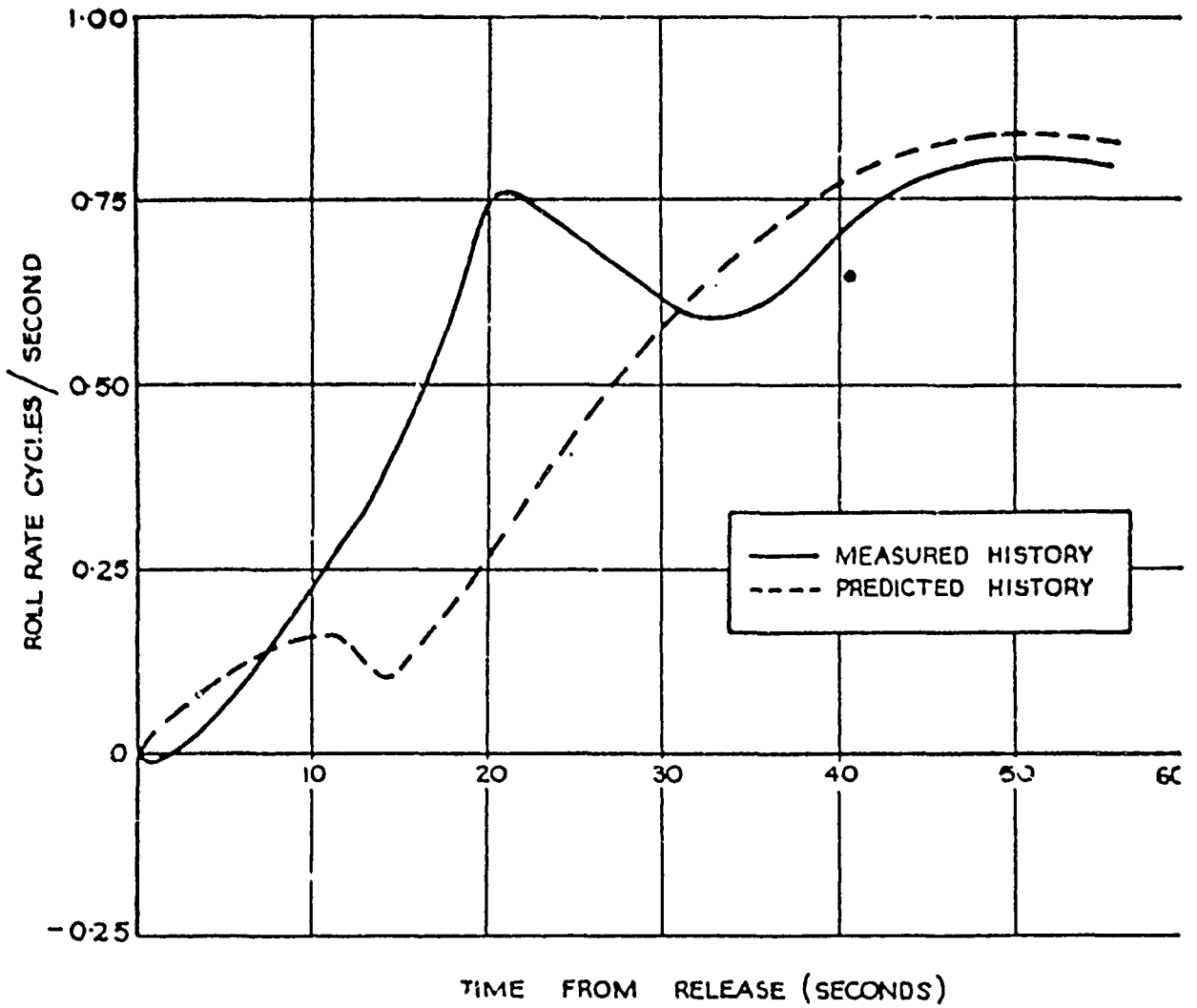
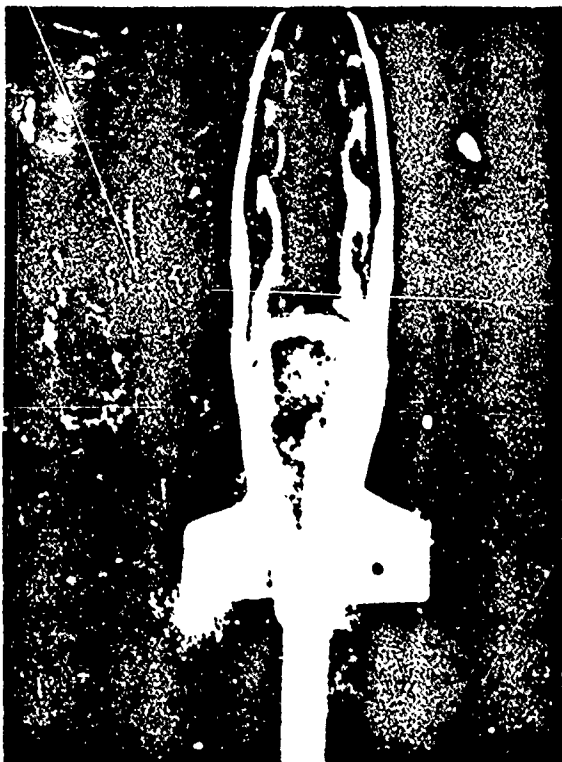


FIGURE 57(a). COMPARISON OF MEASURED AND PREDICTED ROLL RATE HISTORIES FOR ROUND NUMBER 716 ($\eta = 0.17^\circ$)

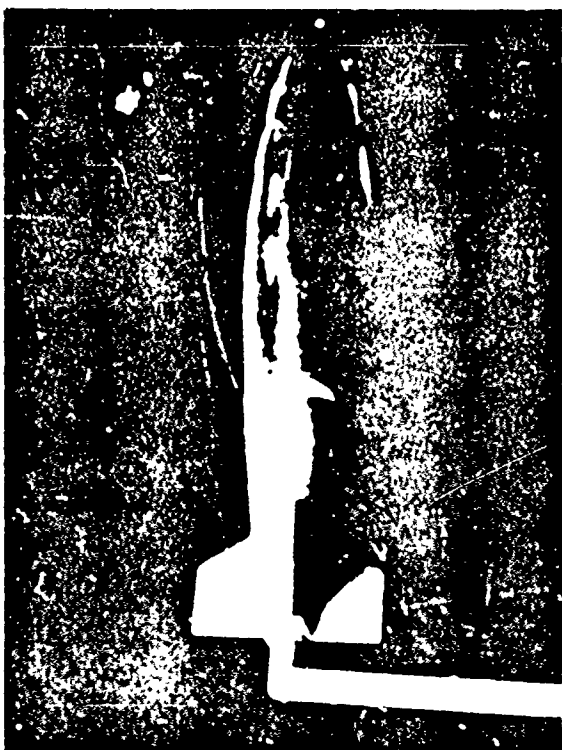
UNCLASSIFIED



35 deg. INCIDENCE



40 deg. INCIDENCE

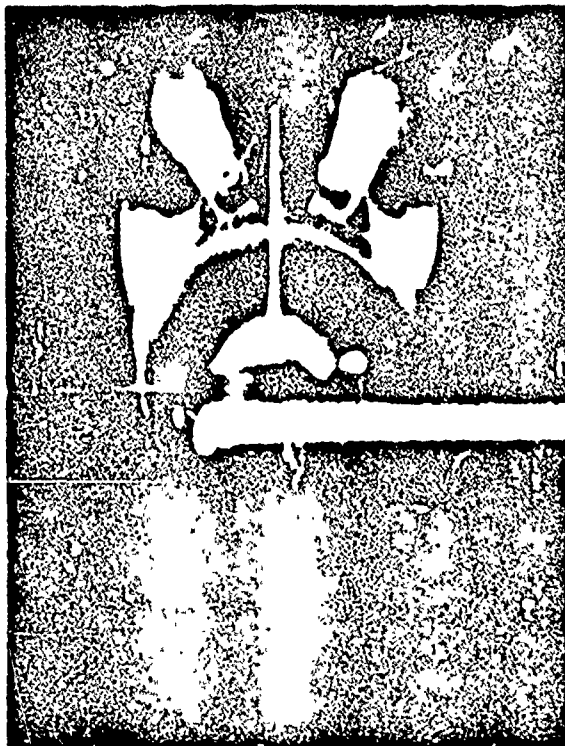


45 deg. INCIDENCE

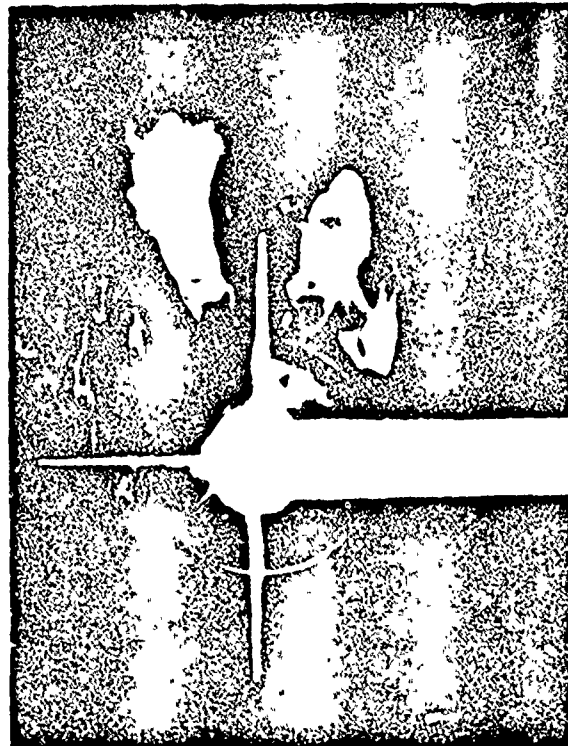


50 deg. INCIDENCE

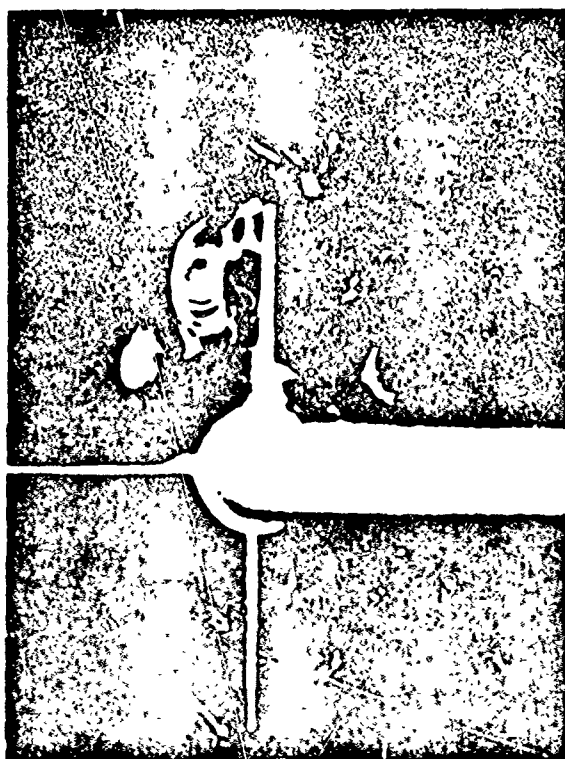
FIGURE 56 (CONT.) FLOW VISUALIZATION OF VORTICES SHED FROM THE M923 BODY SHAPE



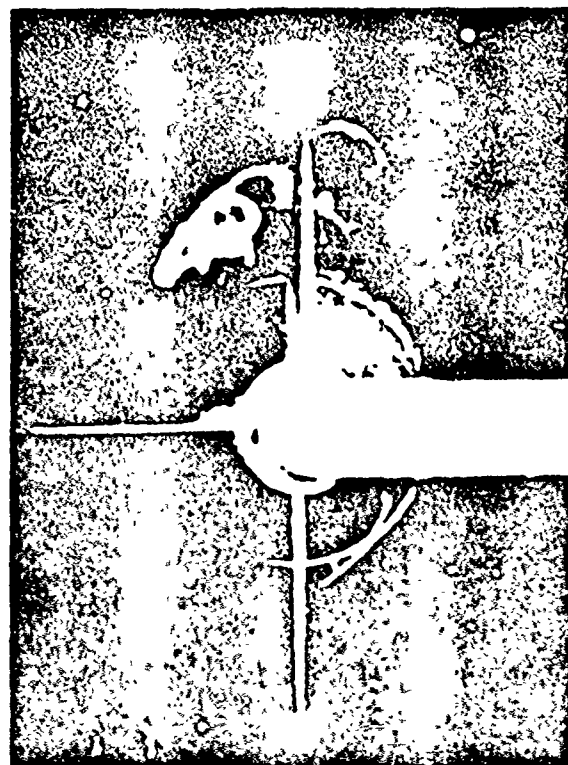
35 deg. INCIDENCE



40 deg. INCIDENCE



45 deg. INCIDENCE



50 deg. INCIDENCE

FIGURE 56. FLOW VISUALIZATION OF VORTICES SHED FROM THE M823 BODY SHAPE

UNCLASSIFIED

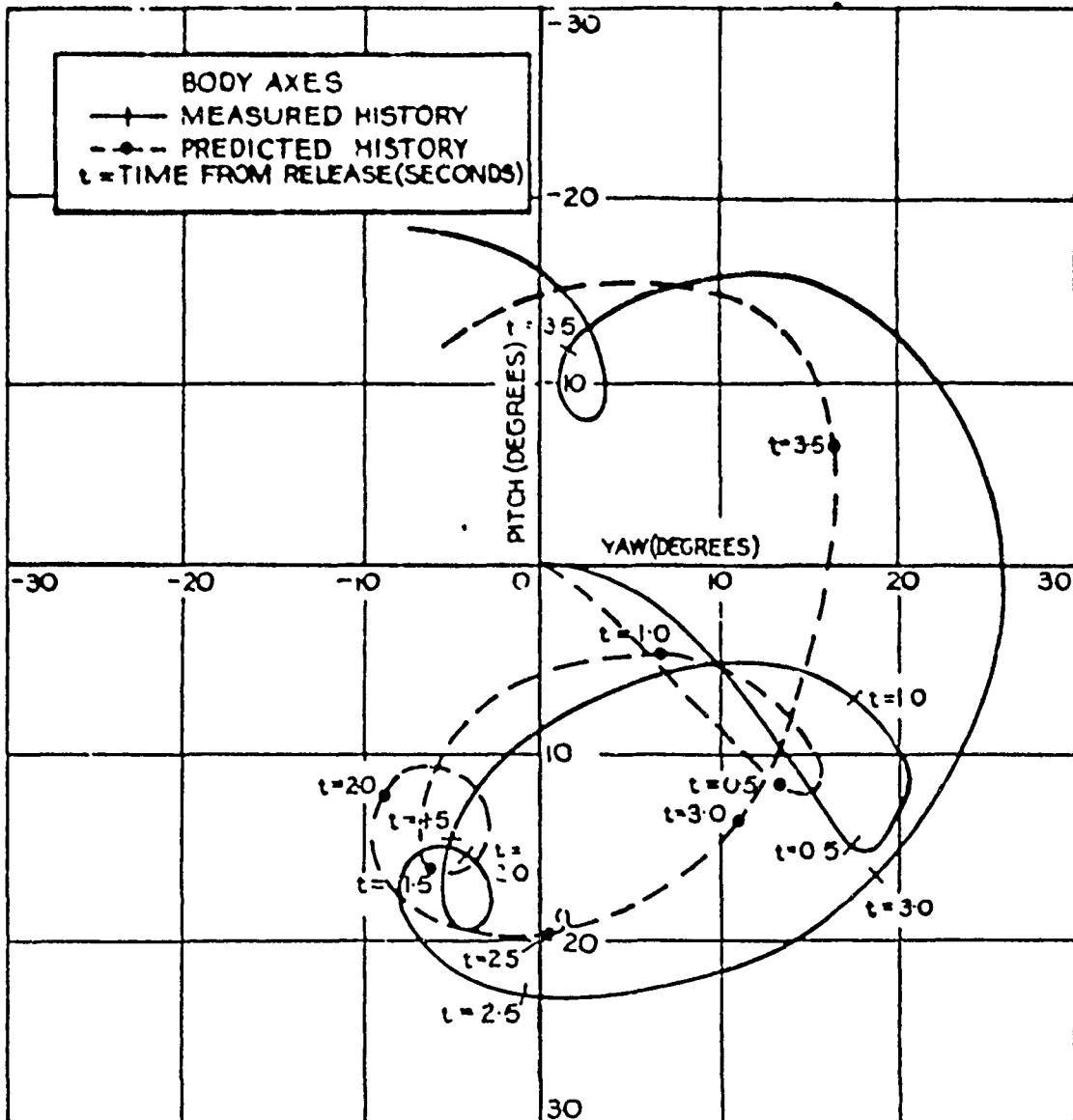


FIGURE 55. COMPARISON OF MEASURED AND PREDICTED RESPONSE OF ROUND NUMBER 726 TO RELEASE DISTURBANCE (PREDICTION BASED ON MEASURED ROLL RATE)

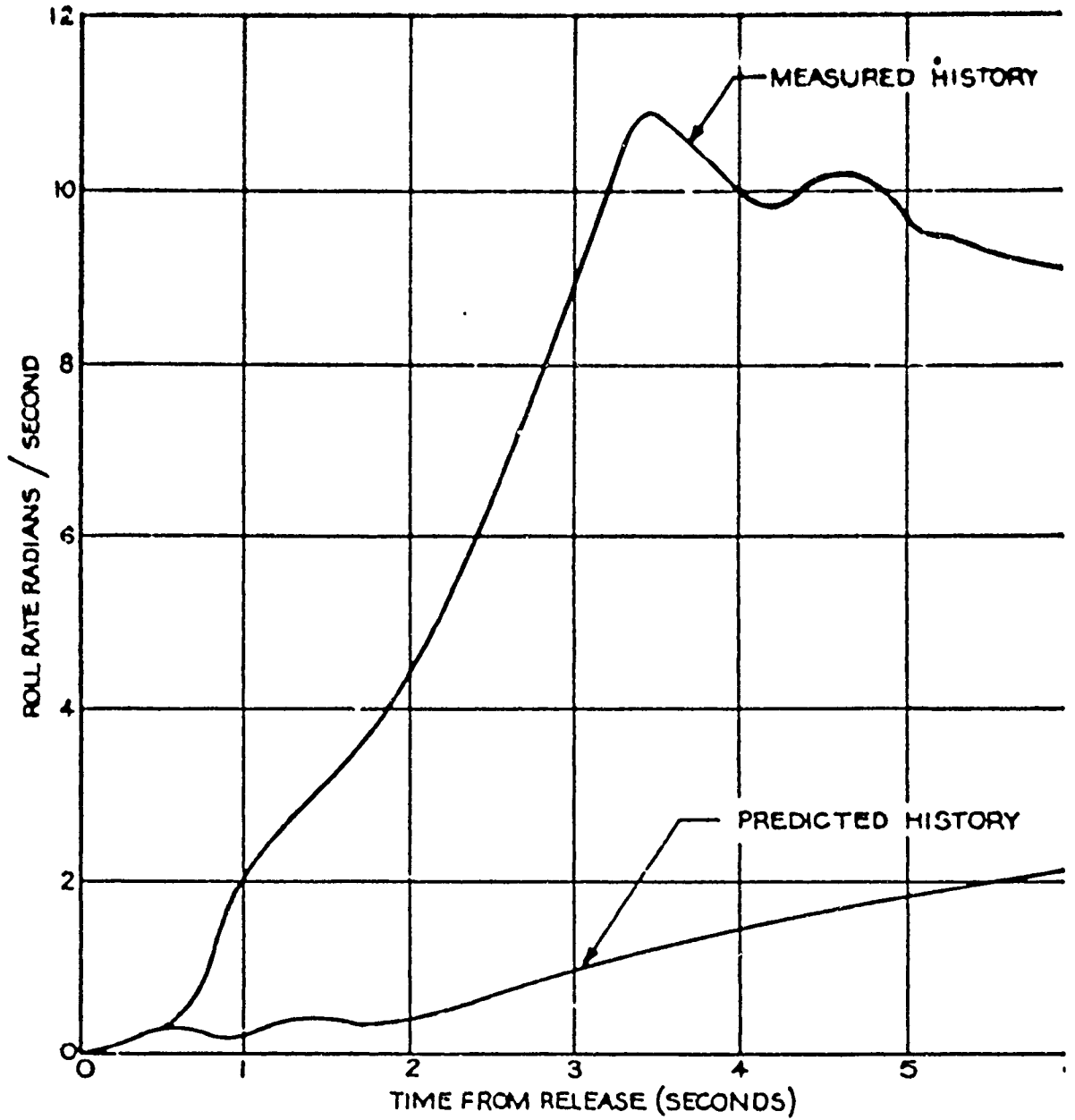


FIGURE 54. COMPARISON OF MEASURED AND PREDICTED ROLL RATES FOR ROUND NUMBER 726

UNCLASSIFIED

TABLE 1
PHYSICAL PROPERTIES OF IMPACTED BOW TIE VEHICLES INCLUDING RELEASE CONDITIONS
AND IMPACT DETAIL FOR PARTICLE TRAJECTORY

GROUP NO.	BOND NO.	BODY SHAPE	SCALE OF QUANTITY (% of body length from nose)	NORMAL FIN CAPT (deg)	AVERAGE FIN CAPT (deg)	AVERAGE FIN CAPT RECALCULATED (deg)	ALL 77 FIN CAPT (deg)	TRANSVERSE DISTANCE FROM NOSE (in)	POLAR ANGLE OF FIN (deg)	RELEASE VELOCITY (ft/sec)	IMPACT DETAIL FOR PARTICLE TRAJECTORY				REMARKS	
											FIN CAPT (deg)	FIN CAPT (deg)	FIN CAPT (deg)	FIN CAPT (deg)		
A	701	B557A	51.6	0	0.05	-	94	173.4	6.6	0.75	100	3	31.5	8	0.76	No release conditions. Electrode-plates started late.
	702	B557B	41.9	0	-0.01	-	86	175.9	5.6	0.75	100	3	31.5	8	0.76	
B	716	B557A	51.7	0.2	0.17	-0.001	85	167.9	6.9	0.75	100	5	24.8	5	0.06	Top meter fitted
	717	B557A	51.7	0.3	0.31	-0.004	85	167.2	6.5	0.75	100	5	24.8	5	0.06	
	718	B557A	51.7	0.4	0.41	-0.004	85	167.2	6.4	0.75	100	5	24.8	5	0.06	
	719	B557A	51.7	0.5	0.51	-0.004	85	167.2	6.4	0.75	100	5	24.8	5	0.06	
	720	B557A	51.7	1.0	0.99	0.004	85	167.0	6.3	0.75	100	5	24.8	5	0.06	
	721	B557A	51.7	1.5	1.41	0	85	166.1	6.2	0.75	100	5	24.8	5	0.06	
C	724	B557A	51.7	0.1	0.12	0.002	87	168.1	6.4	0.75	100	5	24.8	5	0.06	Top meter fitted
	725	B557A	51.6	1.0	0.99	0	85	167.0	6.2	0.75	100	5	24.8	5	0.06	
	726	B557A	51.7	0.5	0.46	-0.010	84	167.8	6.3	0.75	100	5	24.8	5	0.06	
D	732	B557A	51.2	0.5	0.40	0.015	87	167.5	6.4	0.75	100	5	24.8	5	0.06	Top meter fitted
	733	B557A	51.2	0.5	0.40	0.015	87	167.5	6.4	0.75	100	5	24.8	5	0.06	
E	742	B557A	51.2	0.1	-0.03	0.008	86	168.1	6.6	0.75	100	5	24.8	5	0.06	Top meter fitted
	743	B557A	51.2	0.1	-0.03	0.008	86	168.1	6.6	0.75	100	5	24.8	5	0.06	
F	749	B557A	51.7	0.1	0.11	0.002	87	167.9	6.5	0.75	100	5	24.8	5	0.06	Top meter fitted
	750	B557A	51.7	1.0	0.97	0.009	85	167.0	6.3	0.75	100	5	24.8	5	0.06	
G	756	B557A	51.7	0.1	0.11	0.001	85	168.0	6.4	0.75	100	5	24.8	5	0.06	Top meter fitted
	757	B557A	51.7	0.1	0.11	0.001	85	168.0	6.4	0.75	100	5	24.8	5	0.06	
H	764	B557A	51.9	0	-0.25	0.006	85	173.7	6.7	0.75	100	5	24.8	5	0.06	Top meter fitted
	765	B557A	51.9	0	0.00	0.005	85	173.7	6.7	0.75	100	5	24.8	5	0.06	
I	779	B557A	49.8	0	-	-	83	175.3	8.2	0.75	100	5	24.8	5	0.06	Top meter fitted
	780	B557A	49.7	0	-	-	83	175.3	8.2	0.75	100	5	24.8	5	0.06	
J	791	B557B	51.6	0.1	0.10	0	84	167.5	6.6	0.75	100	5	24.8	5	0.06	Top meter fitted
	792	B557B	51.6	0.1	0.10	0	84	167.5	6.6	0.75	100	5	24.8	5	0.06	
K	801	B557B	51.7	1.0	0.09	-0.001	84	167.5	6.7	0.75	100	5	24.8	5	0.06	Top meter fitted
	802	B557B	51.7	1.0	0.09	-0.001	84	167.5	6.7	0.75	100	5	24.8	5	0.06	

Note - All based on release height.

TABLE 2

ESTIMATED IMPACT DEVIATIONS DUE TO LOW INCIDENCE INSTABILITY
 (RELEASE 25 000 FT, VELOCITY 509 FT 'S, NO DISTURBLANCE, C.G. AT 51.7%)

FIN CANT (DEGREES)	DEVIATION (MILS)				REMARKS
	RANGE S-Short O-Over		LINE R-Right L-Left		
0	64.5	0	24.8	L	"lock-in" at approximately 3° incidence, roll period approximately 30-40 seconds per cycle.
0.1	2.9	0	4.3	L	"lock-in" at approximately 3° incidence, roll period approximately 5 seconds per cycle.
0.25	62.6	0	25.2	L	rolled freely at rate dictated by fin cant; approximately 3° trim incidence.
0.50	58.8	0	49.8	L	As above.
1.00	47.0	0	62.5	L	As above.

Note; mils based on release height

TABLE 3

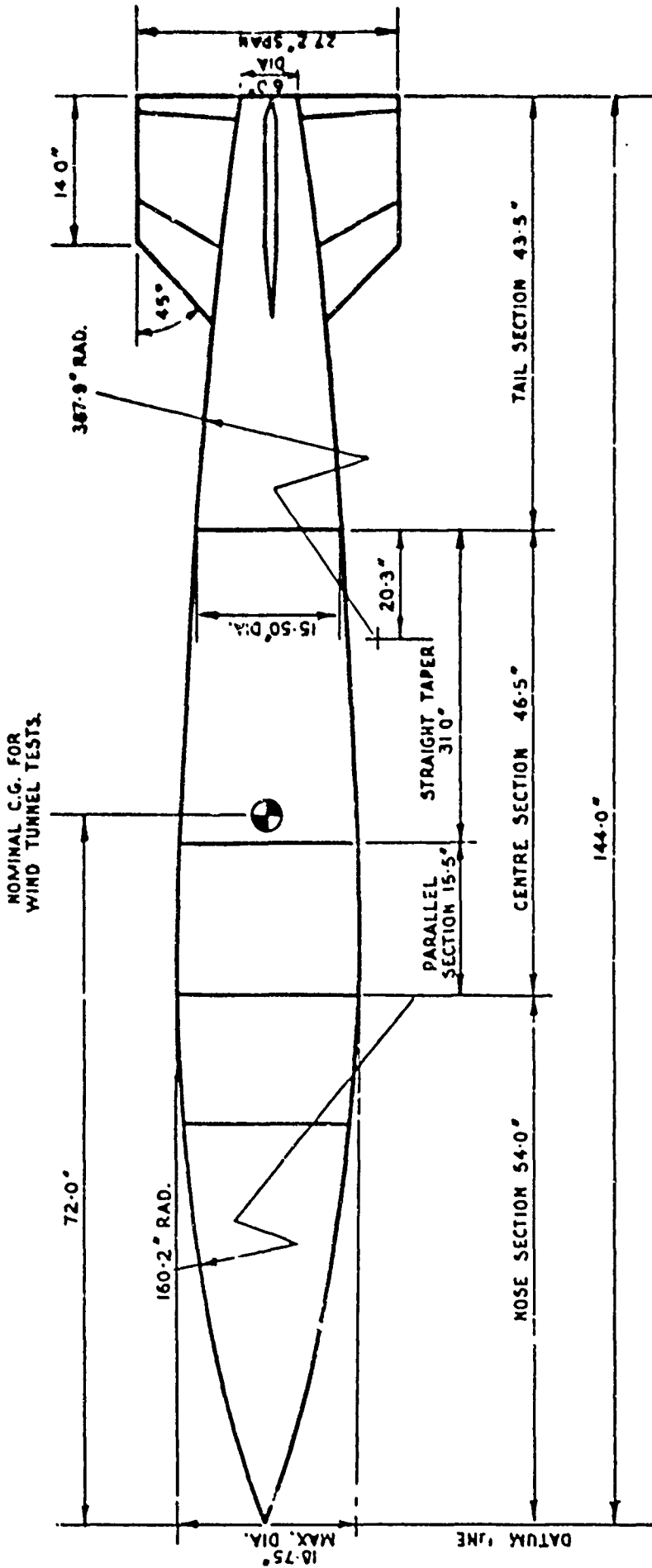
ESTIMATED IMPACT DEVIATIONS DUE TO 0.5° FIN BODY MISALIGNMENT
 (RELEASE 45000 FT VELOCITY 678 FT/S NO DISTURBANCE, G.G. AT 51.7%)

PLANE OF MISALIGNMENT	FIN CANT (DEGREES)	DEVIATION (FEET)		TOTAL DEVIATION (Mils)	REMARKS
		RANGE S=Short O=Over	LINE R=Right L=Left		
0°	0	2686 O	1480 L	68	Lock-in barrel roll approximately 30 sec period.
	0.25	90 S	202 L	5	Lock-in barrel roll below resonance, stable side moment.
	0.375	6121 S	541 R	136	Destabilising side moment - subsequent lock-in to natural frequency at large incidence. Incidence did not grow catastrophically.
	0.50	7132 S	401 L	158	
	1.00	70 O	290 L	7	Passed through resonance at about 3 sec.
22½°	0	1491 S	423 R	33	Initial trim leading to roll lock-in and destabilising side moment. Recovered at about 20 sec.
	0.25	878 S	329 L	21	Incidence vector unsteady initially at low incidence, lock-in at about 25 sec. $\psi = 267^\circ$, $\theta = 7^\circ$.
	0.375	4210 S	79 L	94	Unsteady large incidence behaviour up to 25 sec subsequent lock-in as above $\theta = 6.7^\circ$, $\psi = 269^\circ$.
	0.50	445 S	150 L	10	Passed through resonance at about 8 sec.
	1.00	54 S	45 R	2	Passed through resonance at about 3 sec.
45°	0	1719 S	323 R	39	Lock-in $\theta = 8^\circ$ $\psi = 186^\circ$ roll anti-clockwise.
	0.25	1944 S	805 L	47	Destabilising side moment caused incidence growth about 10 sec; subsequent lock-in $\theta = 6^\circ$, $\psi = 268^\circ$.
	0.375	1152 S	329 R	27	Destabilising side moment caused large incidence about 7 sec, recovery and lock-in at 30 sec $\theta = 3.4^\circ$ $\psi = 0^\circ$.
	0.50	430 S	126 L	10	Destabilising side moment caused large incidence prior to passage through resonance at about 8 sec. Lock-in at about 35 sec $\theta = 2.5^\circ$ $\psi = 0^\circ$.

TABLE 3 (Continued)

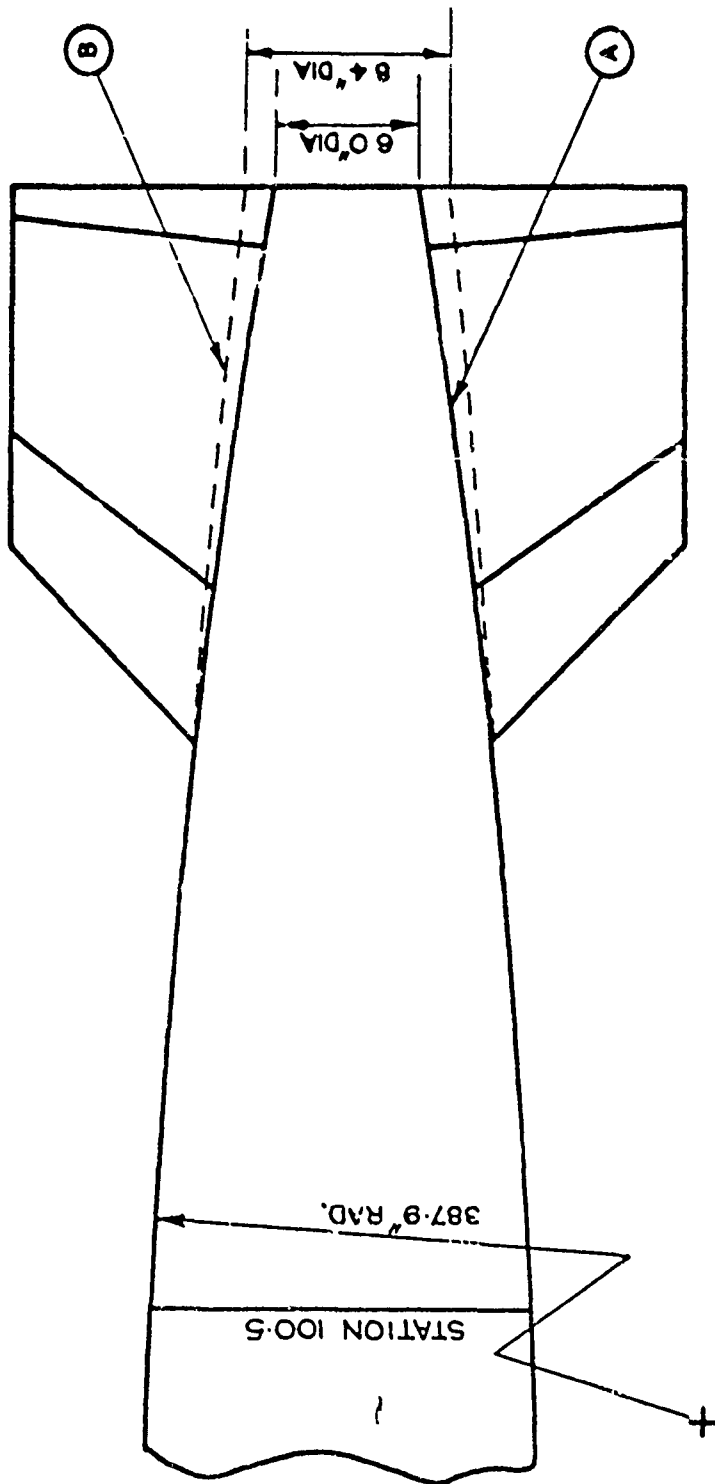
PLANE OF MISALIGNMENT	FIN CANT (DEGREES)	DEVIATION (FEET)		TOTAL DEVIATION (Mils)	REMARKS
		RANGE S=Short O=Over	LINE R=Right L=Left		
45°	1.00	155 O	161 L	5	Passed rapidly through resonance at about 4 sec. Low incidence (0.1°) lock-in well above resonance from about 35 sec.
67½°	0	1489 S	424 L	33	Destabilising side moment caused large incidence growth at about 18 sec subsequent recovery and low incidence lock-in at $\phi = 260^\circ$.
	0.25	476 S	161 L	11	Lock-in at $\phi = 270^\circ$ for entire trajectory.
	0.375	7196 S	648 L	160	Lock-in at large incidence $\phi = 315^\circ$ from about 10 sec.
	0.50	356 S	69 L	8	Passed through resonance at about 8 sec.
	1.00	16 S	96 L	2	Passed through resonance at about 1½ sec.

NOTE: Mils based on release height.



- NOTES:
1. Full scale test vehicle c.g. is variable about the point shown here.
 2. Full scale vehicle weight is 840lb and moment of inertia in pitch is 5500 lbft² for all c.g. positions.
 3. Full scale fin cant angles adjustable between 0 and 30°. All wind tunnel tests carried out with zero cant.
 4. Fin section is an extended double wedge. Max. thickness (t/c) = 3%. Paralleol section between 30% and 90% chord.

FIGURE 1. ORIGINAL SHAPE FOR THE LOW DRAG SHAPE RESEARCH VEHICLE (M557A)



(a) Original body shape. 387.9 in. radius taken right through to the 6.0 in. dia. base

(b) M.823 shape. Straight tangent from the 8.4 in. dia. base to the 387.9 in. radius

FIGURE 3. MODIFICATION TO ORIGINAL LOW DRAG SHAPE (M557A) TO PRODUCE THE M823 SHAPE

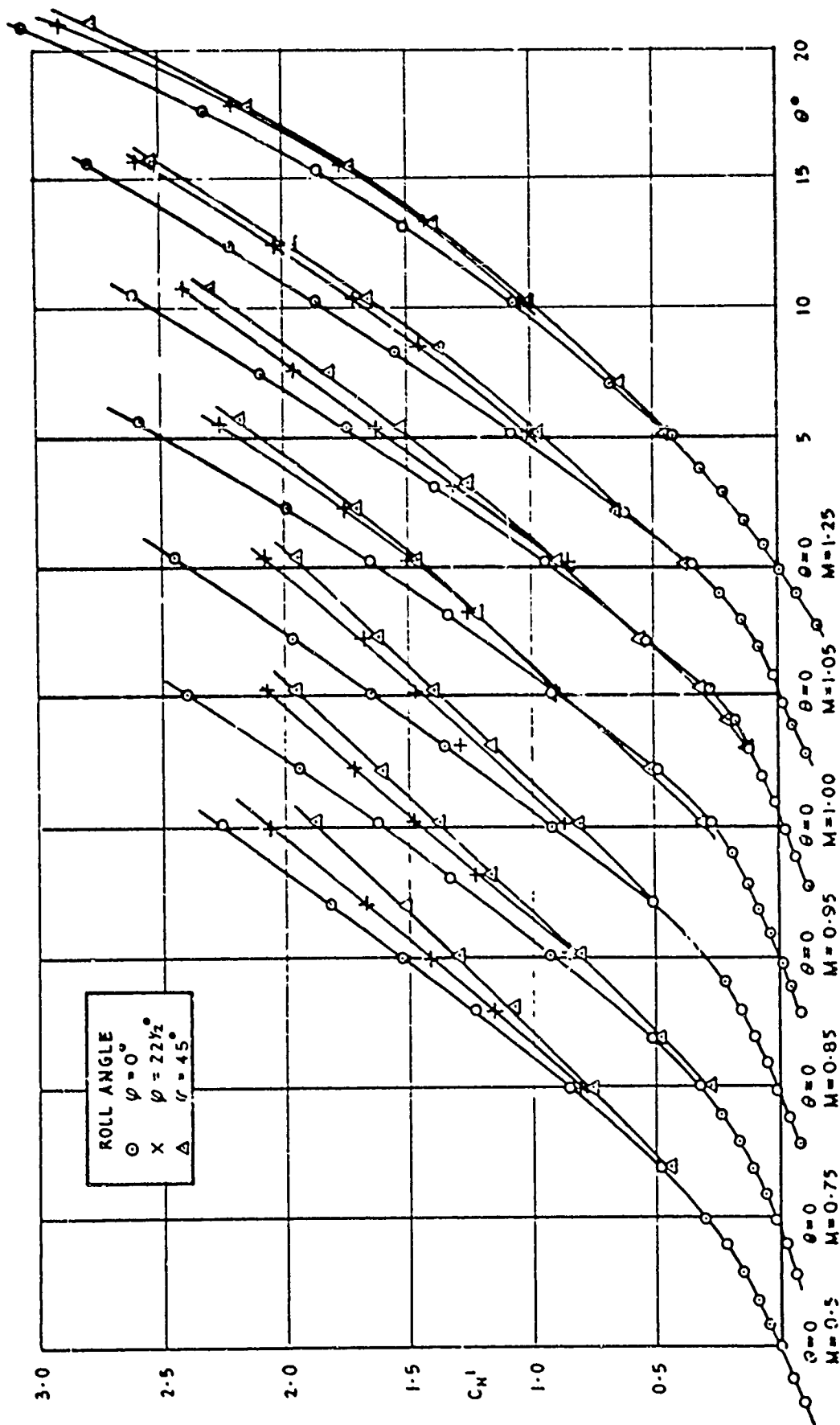
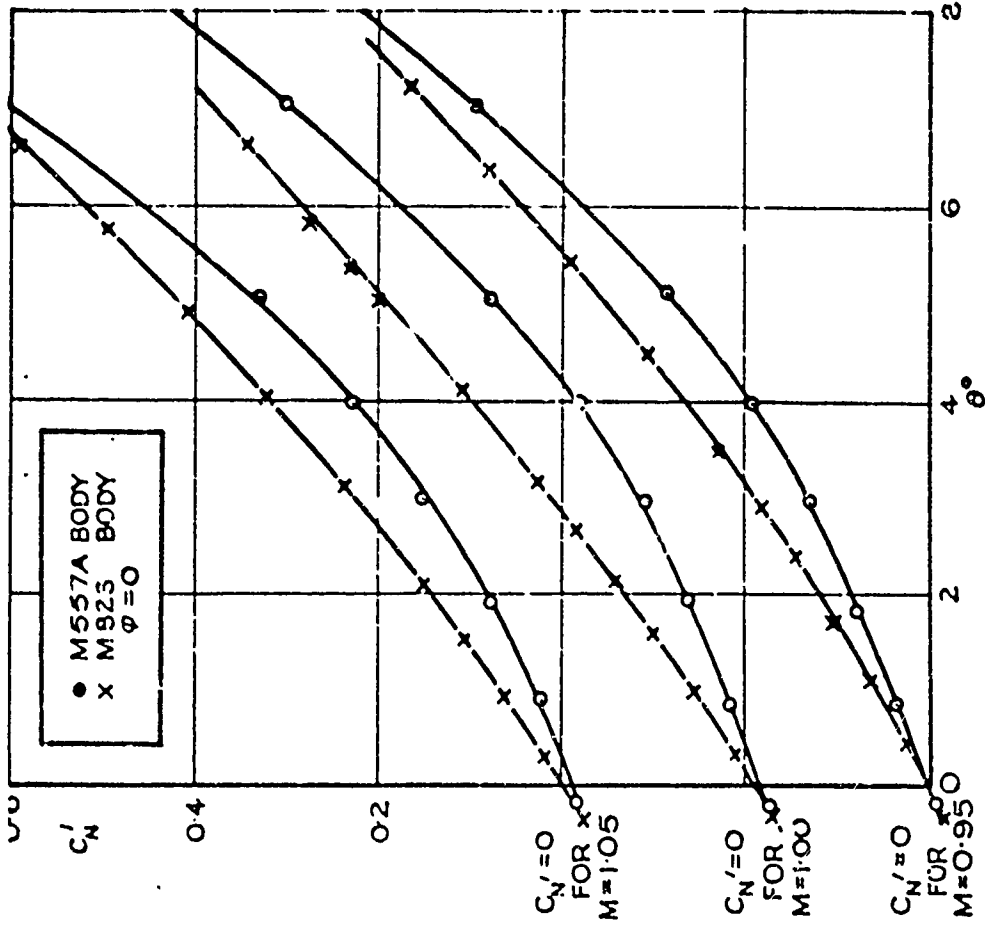
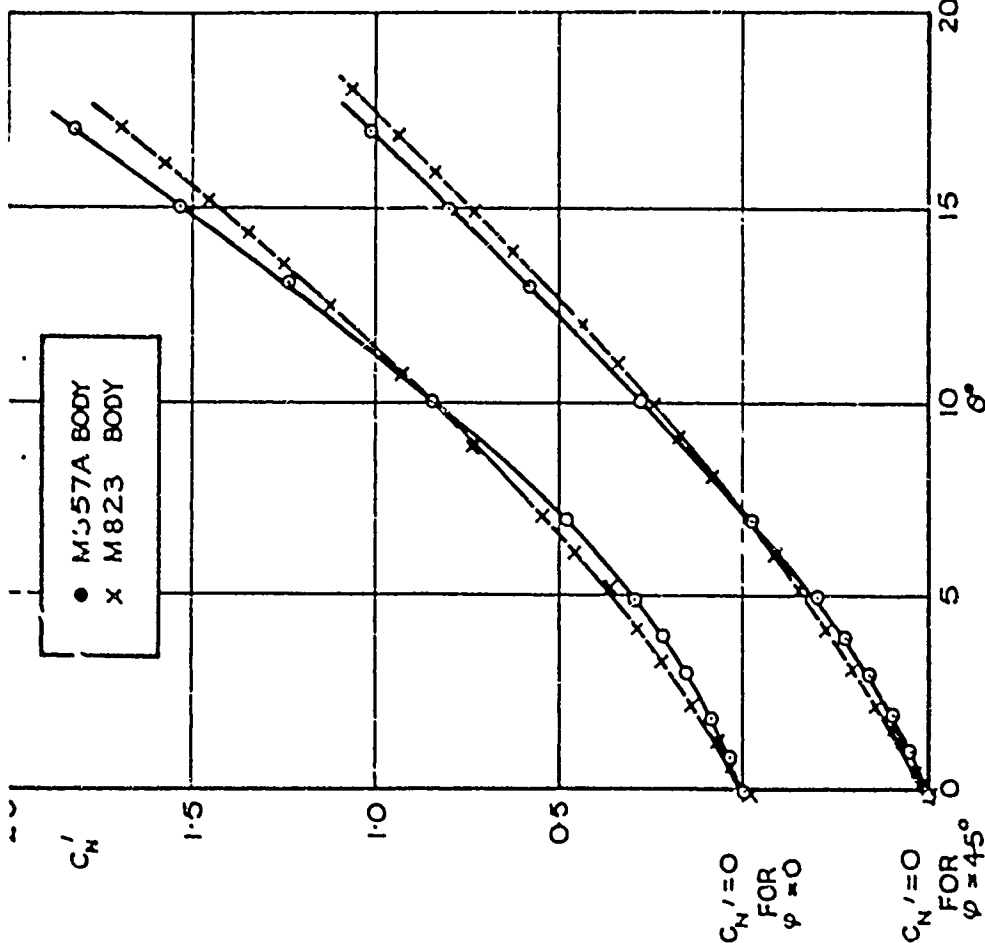


FIGURE 4. VARIATION OF NORMAL FORCE WITH ANGLE OF INCIDENCE, ROLL ATTITUDE AND MACH NUMBER FOR THE M557A LOW DRAG SHAPE

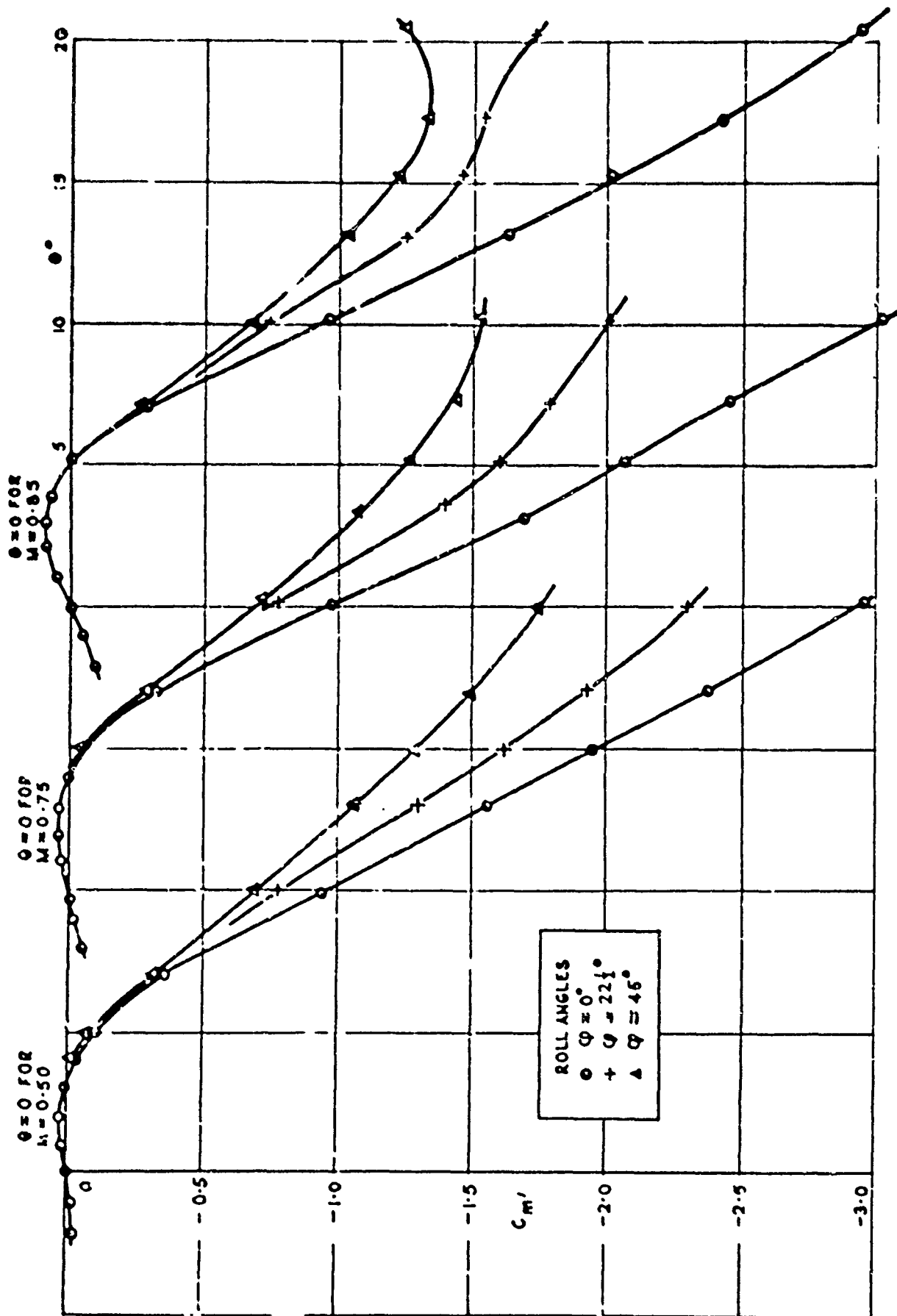


(a) Low Mach number changes ($M = 0.50$)



(b) Elimination of transonic non-linearities on M.823 body. Low incidence; region magnified.

FIGURE 5. CHANGES IN NORMAL FORCE CHARACTERISTICS WITH CHANGE FROM M557A TO M823 BODY SHAPE



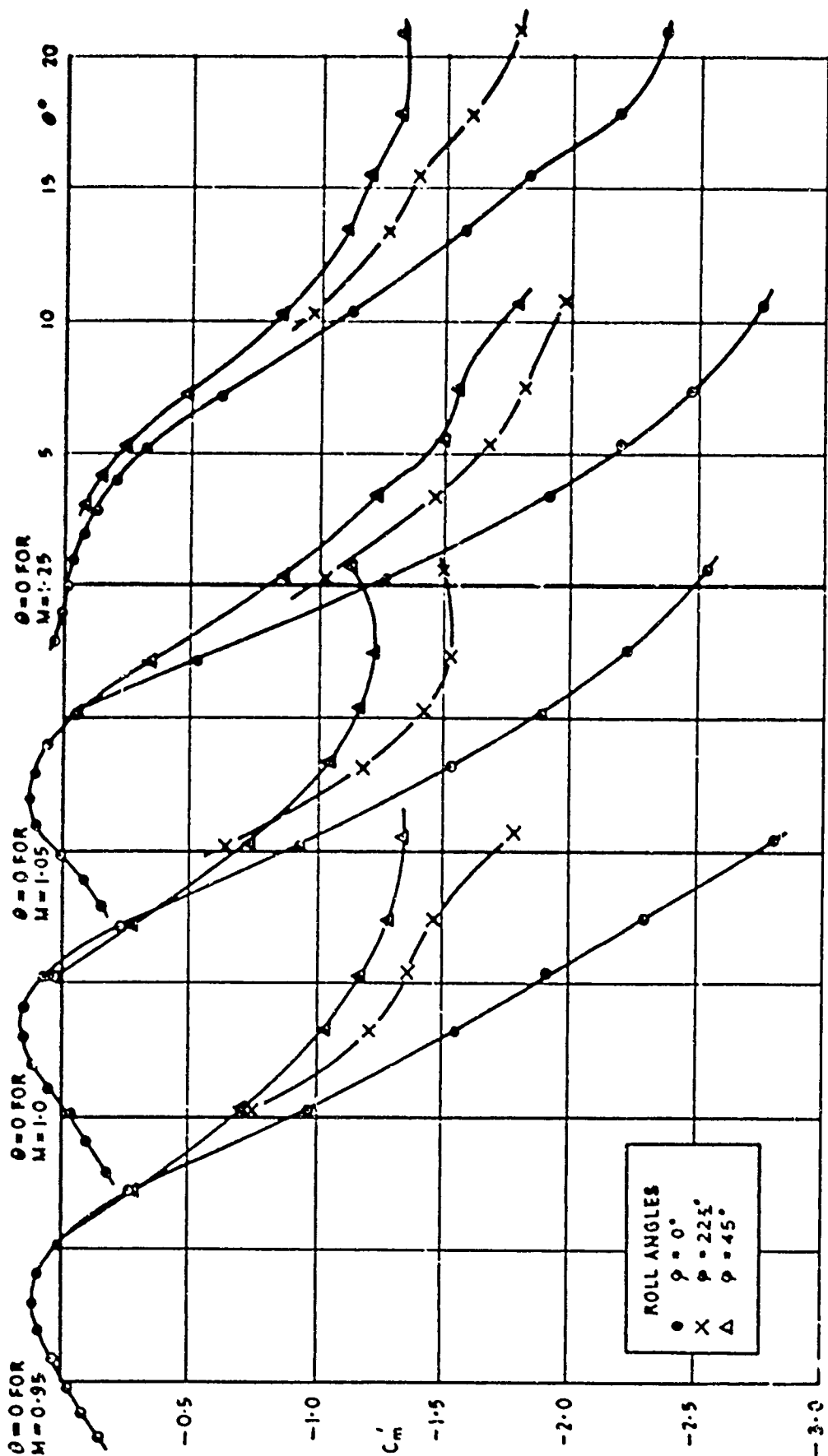


FIGURE 6(a) (Contd.). VARIATION OF RESTORING MOMENT WITH ANGLE OF INCIDENCE, ROLL ATTITUDE AND MACH NUMBER FOR THE M557A LOW DRAG SHAPE

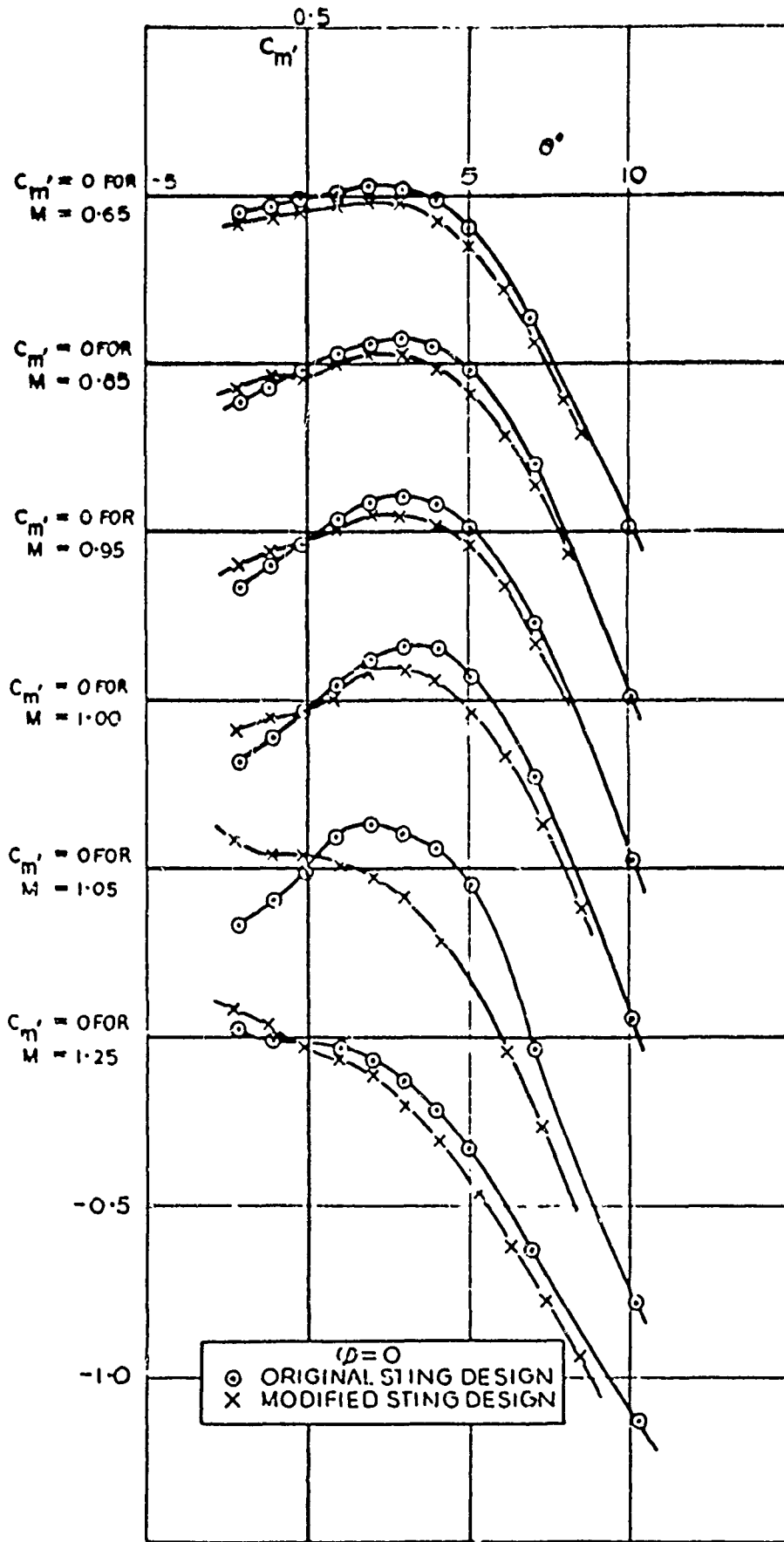
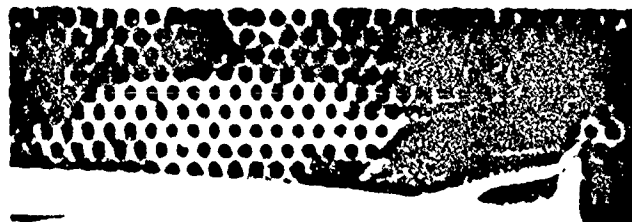
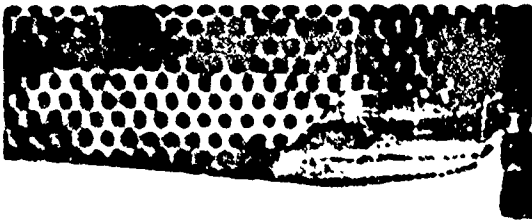
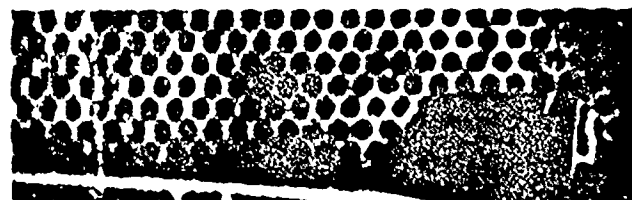
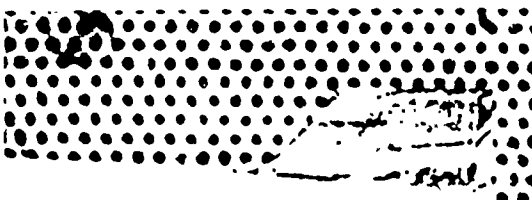


FIGURE 6(b). EFFECT OF DESIGN OF THE SUPPORTING STING BALANCE ON RESTORING MOMENT FOR THE M557A LOW DRAG SHAPE



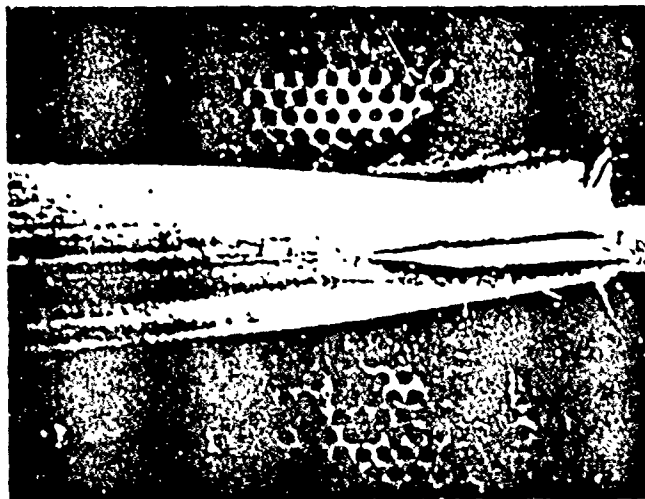
(a) $M = 0.95$ $\theta = 3^\circ$ Top view

(b) $M = 0.95$ $\theta = 6^\circ$ Top view



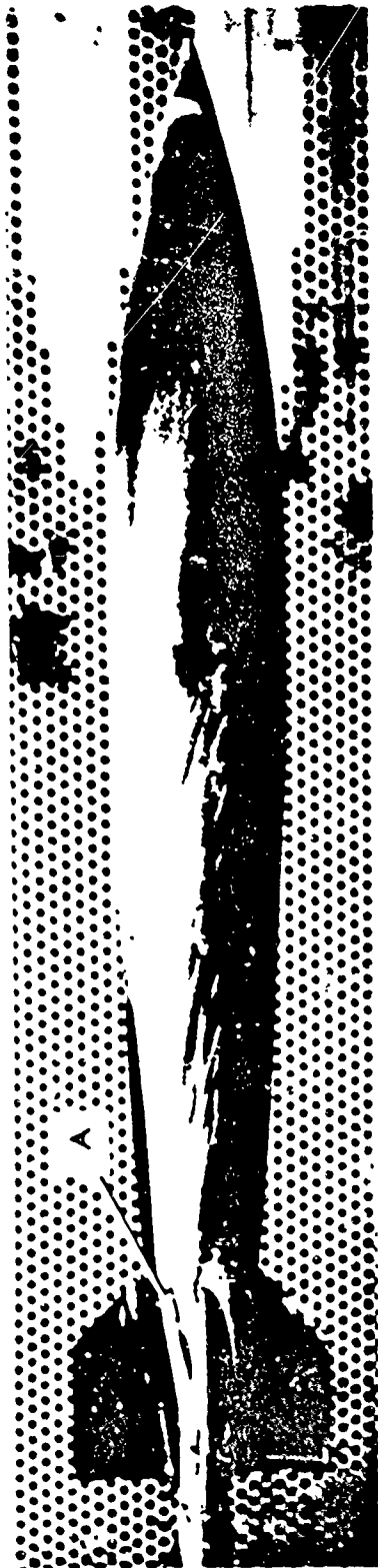
(c) $M = 0.95$ $\theta = 9^\circ$ Top view

(d) $M = 0.95$ $\theta = 3^\circ$ Bottom view

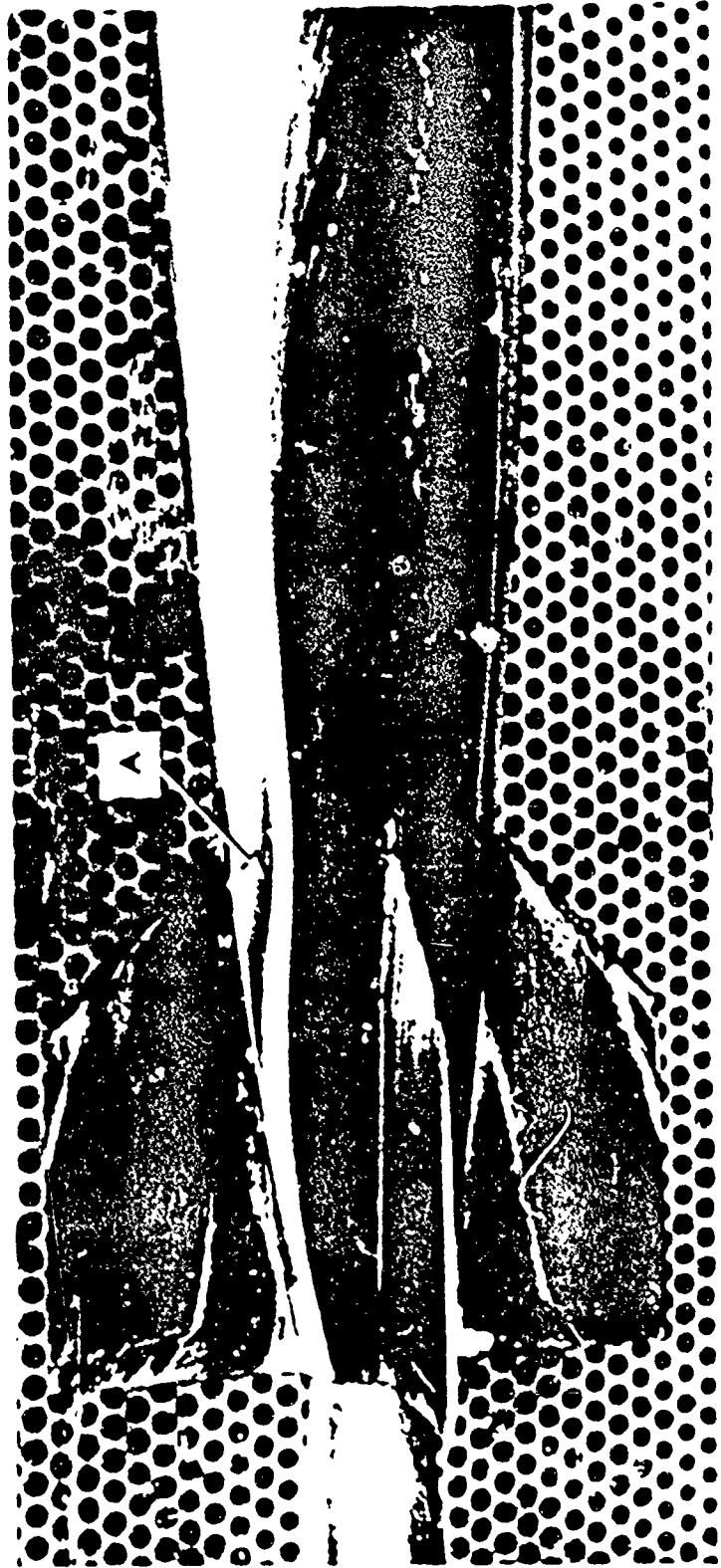


(e) $M = 1.25$ $\theta = 3^\circ$ Top view

FIGURE 7. FLOW VISUALISATION EXPERIMENTS ON THE LOW DRAG M557A SHAPE



(a) $M = 0.95$ $\theta = 9^\circ$ View from side



(b) $M = 0.95$ $\theta = 9^\circ$ Enlarged top view

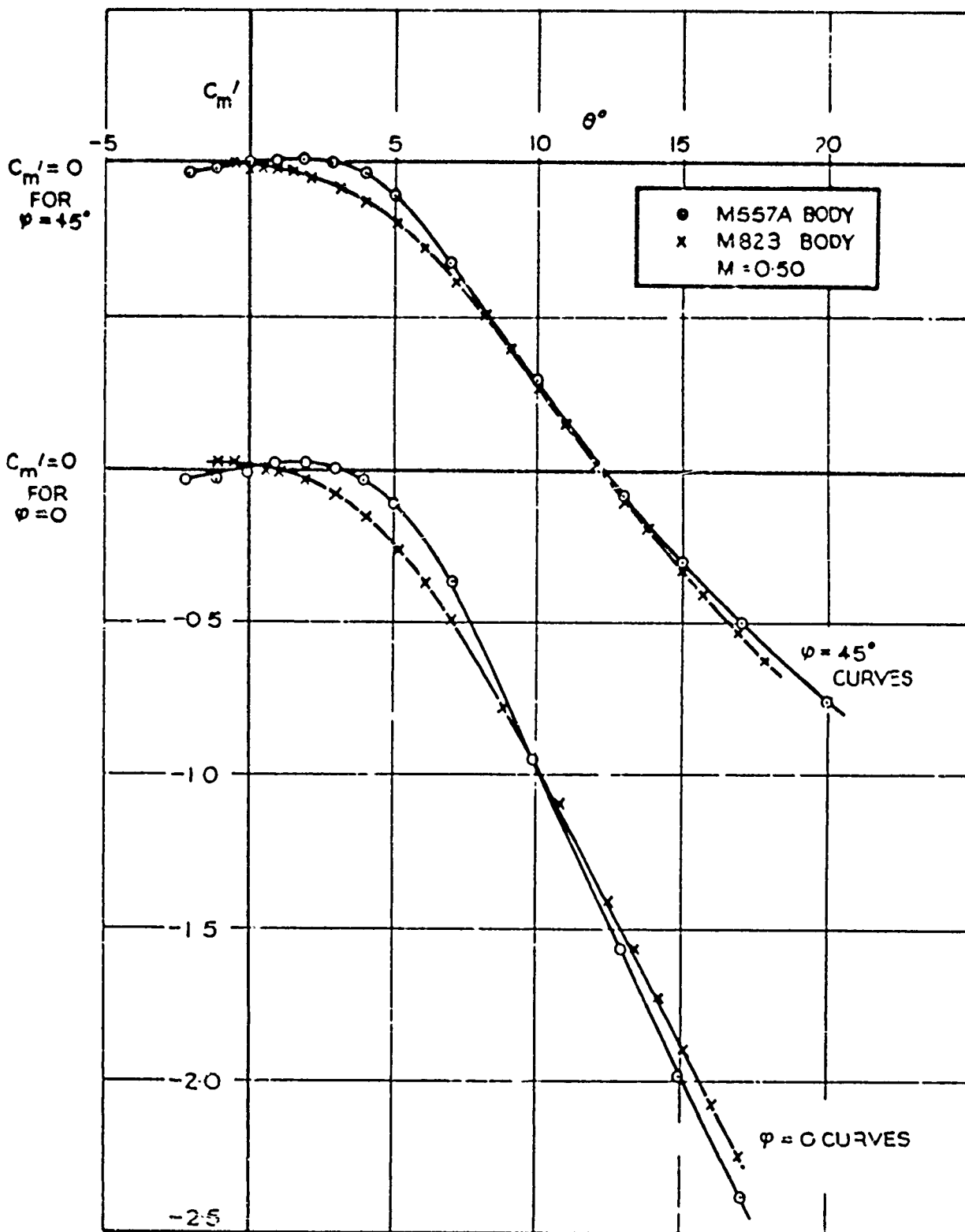


FIGURE 9. CHANGES IN LOW MACH NUMBER RESTORING MOMENT CHARACTERISTICS WITH CHANGE FROM M557A TO M823 BODY SHAPE

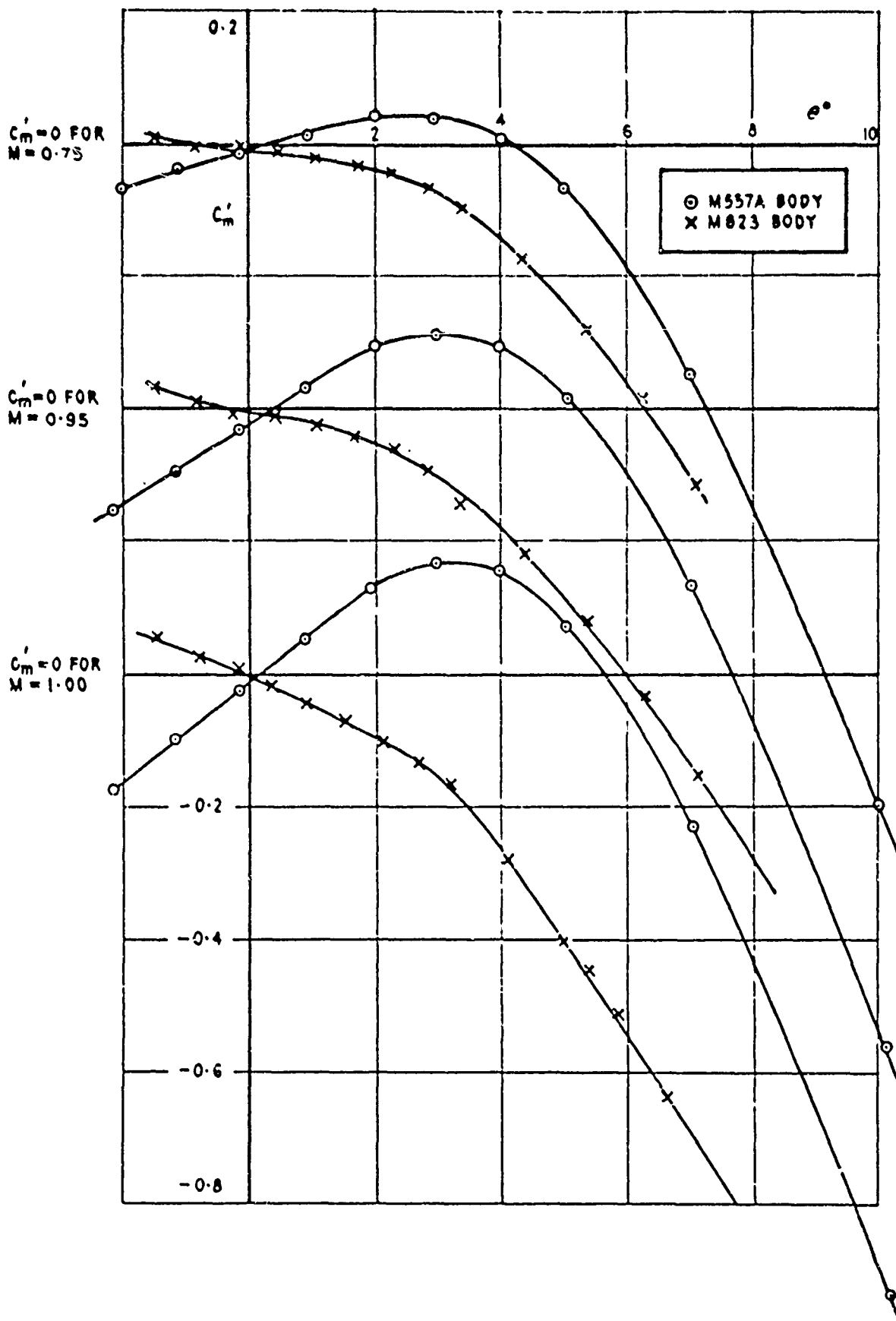


FIGURE 10. CHANGES IN RESTORING MOMENT CHARACTERISTICS WITH CHANGE FROM M557A TO M823 SHAPE. LOW INCIDENCE REGION AT ENLARGED SCALES

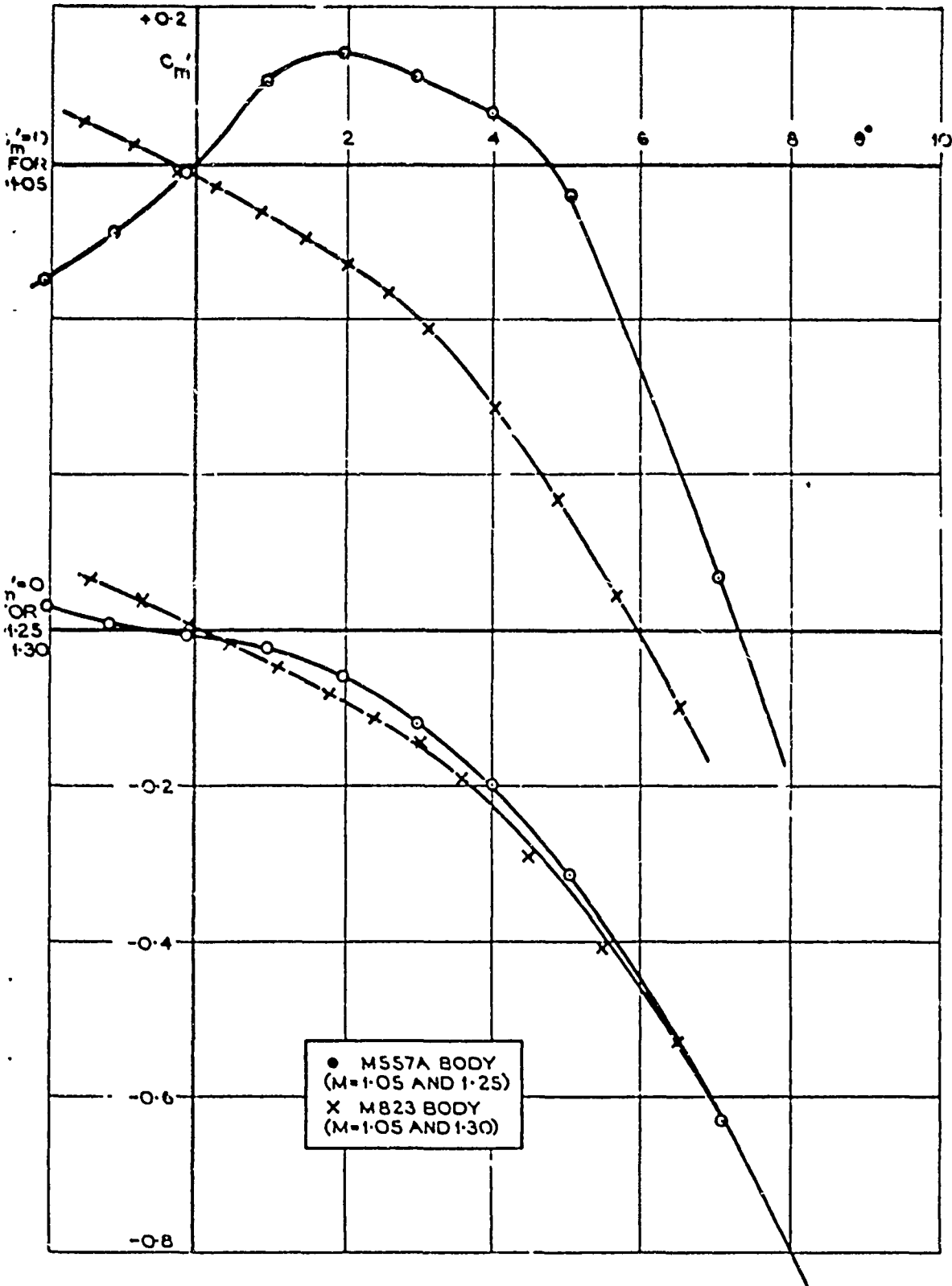


FIGURE 10 (Contd.). CHANGES IN RESTORING MOMENT CHARACTERISTICS WITH CHANGE FROM M557A TO M823 SHAPE. LOW INCIDENCE REGION AT ENLARGED SCALES.

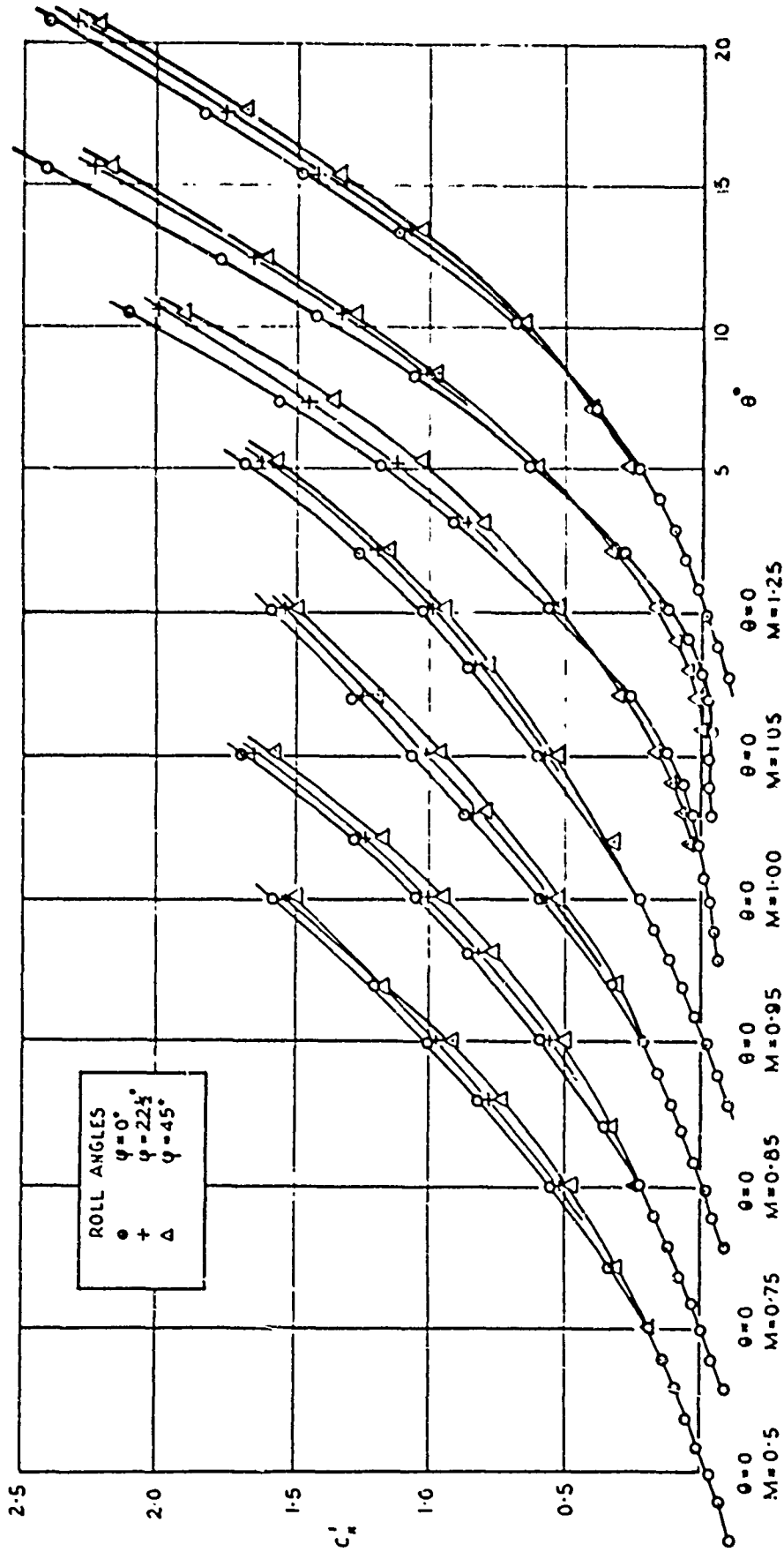


FIGURE 11. VARIATION OF NORMAL FORCE WITH ANGLE OF INCIDENCE, ROLL ATTITUDE AND MACH NUMBER FOR THE M557B BLUFF BODY SHAPE

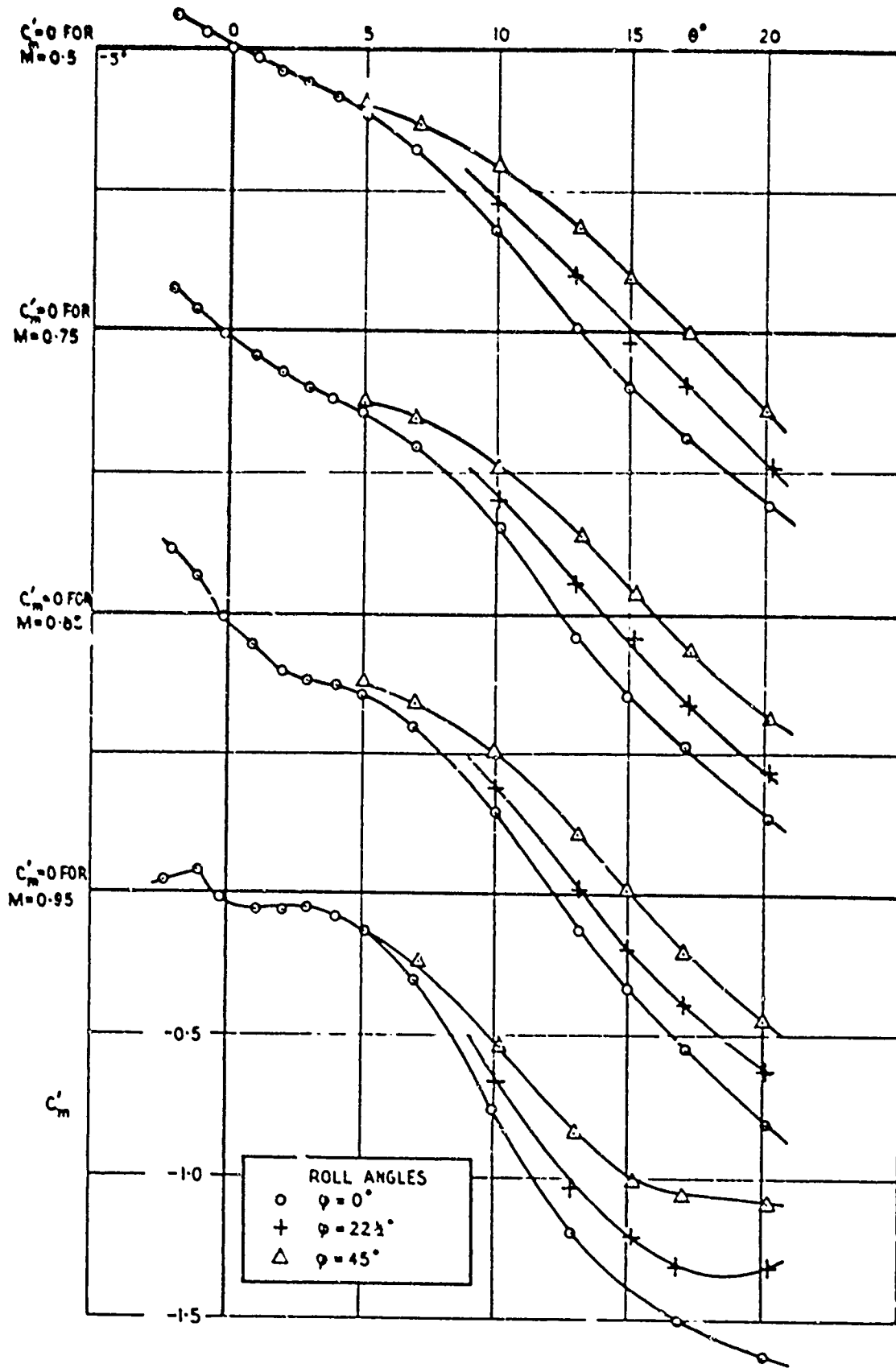


FIGURE 12. VARIATION OF RESTORING MOMENT WITH ANGLE OF INCIDENCE, ROLL ATTITUDE AND MACH NUMBER FOR THE M557B BLUFF BODY SHAPE

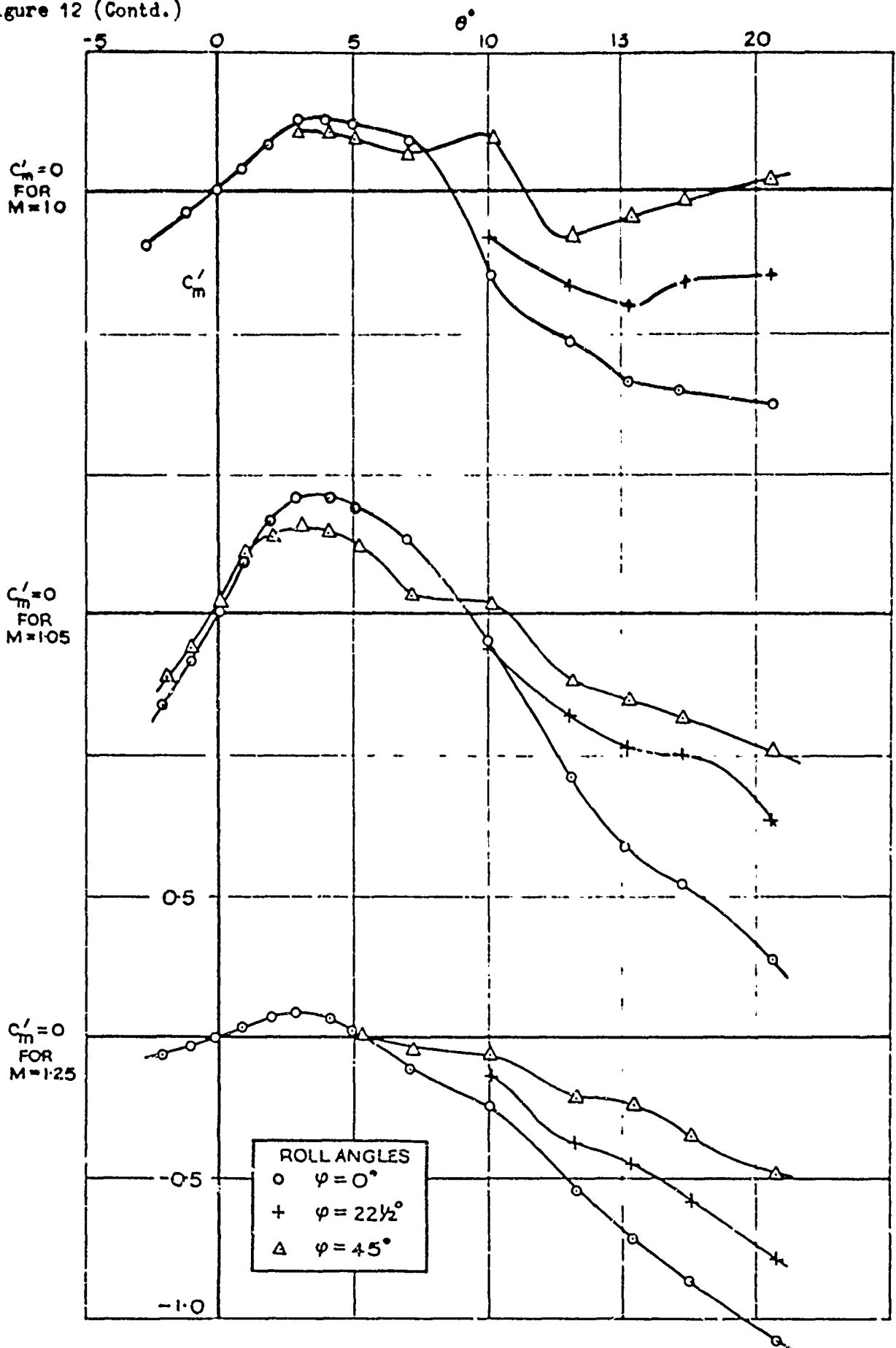


FIGURE 12 (Contd.). VARIATION OF RESTORING MOMENT WITH ANGLE OF INCIDENCE, RO: ATTITUDE AND MACH NUMBER FOR THE M557B BLUFF BODY SHAPE

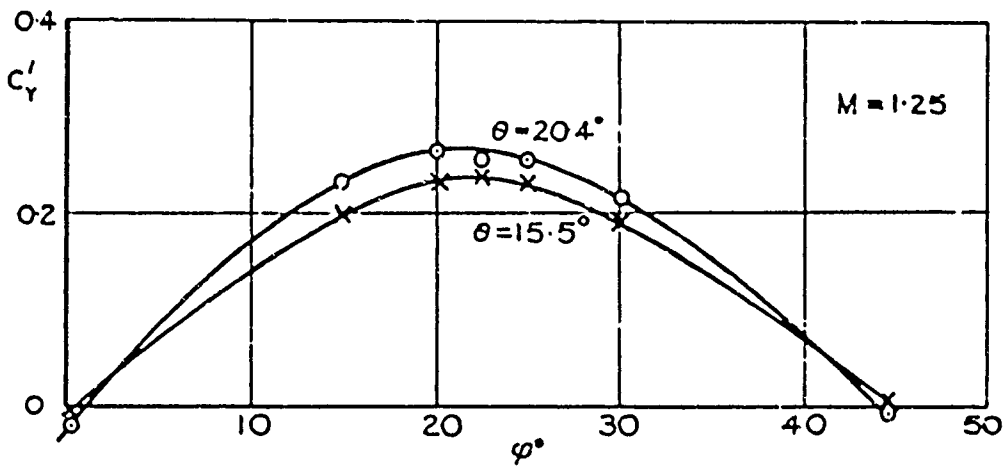
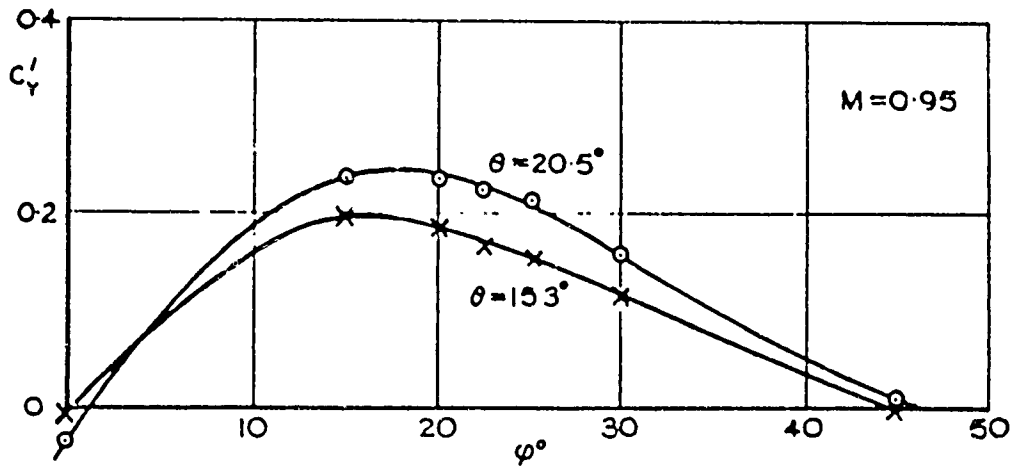
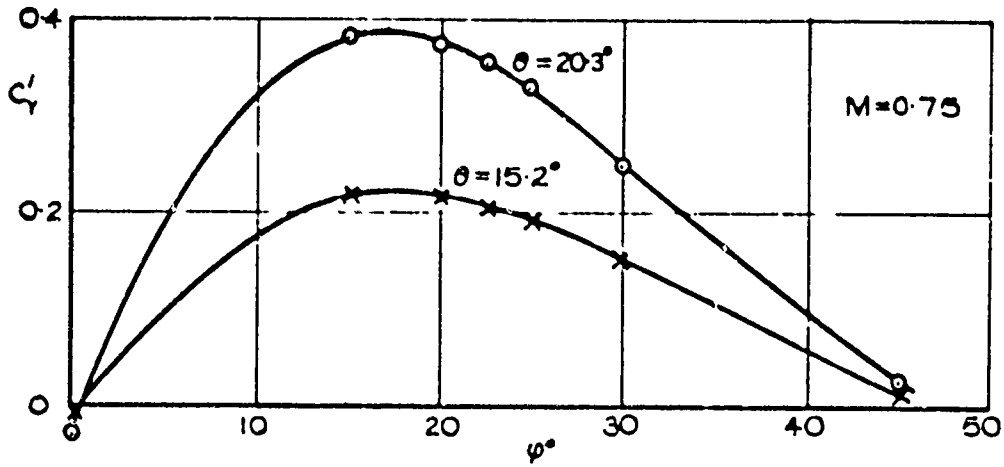


FIGURE 13. VARIATION OF INDUCED SIDE FORCE WITH ROLL ATTITUDE FOR THE M557A LOW DRAG SHAPES

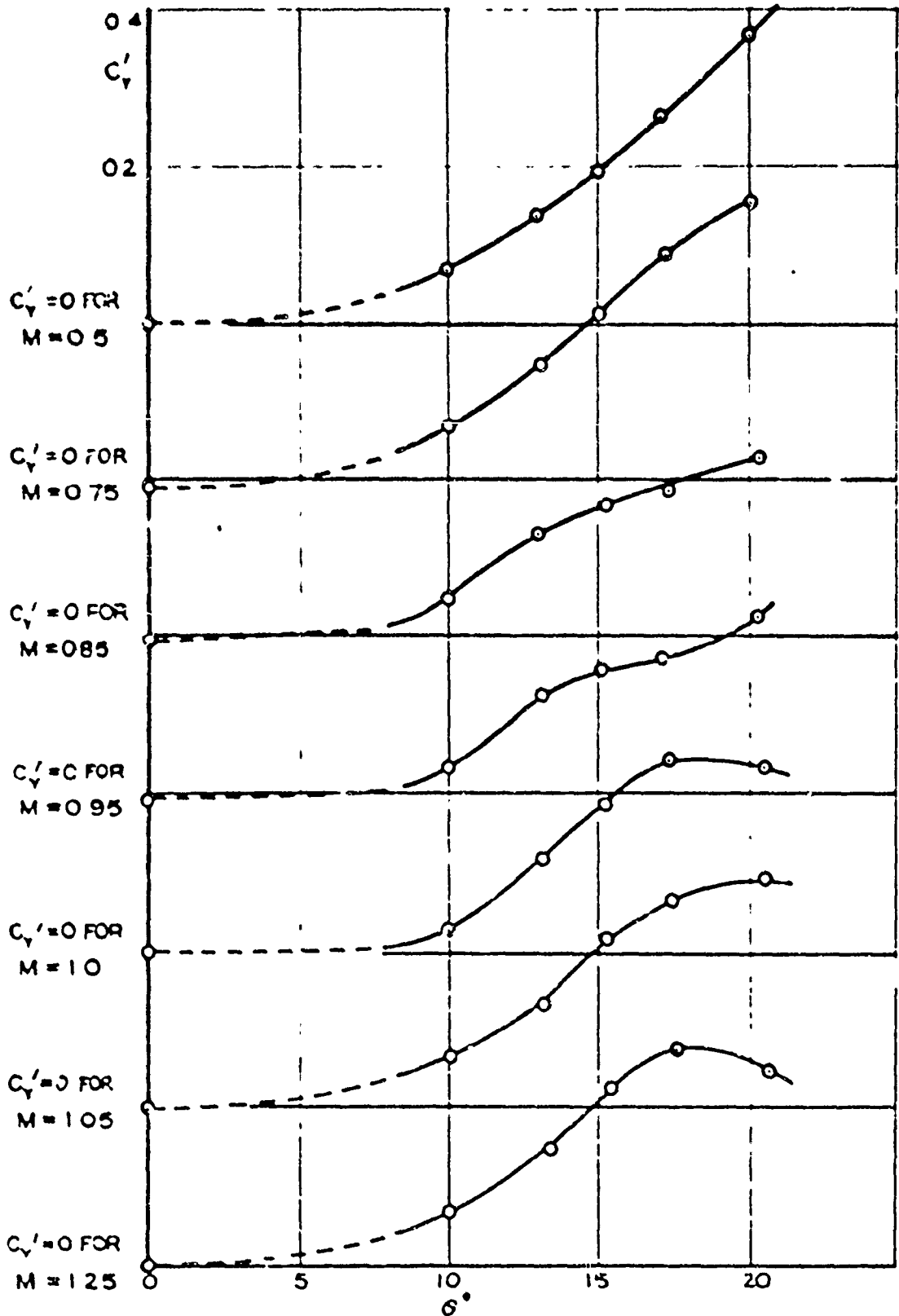


FIGURE 14. VARIATION OF PEAK INDUCED SIDE FORCE WITH ANGLE OF INCIDENCE FOR THE X557A LCW DRAG SHAPE ($\varphi = 22\frac{1}{2}^\circ$)

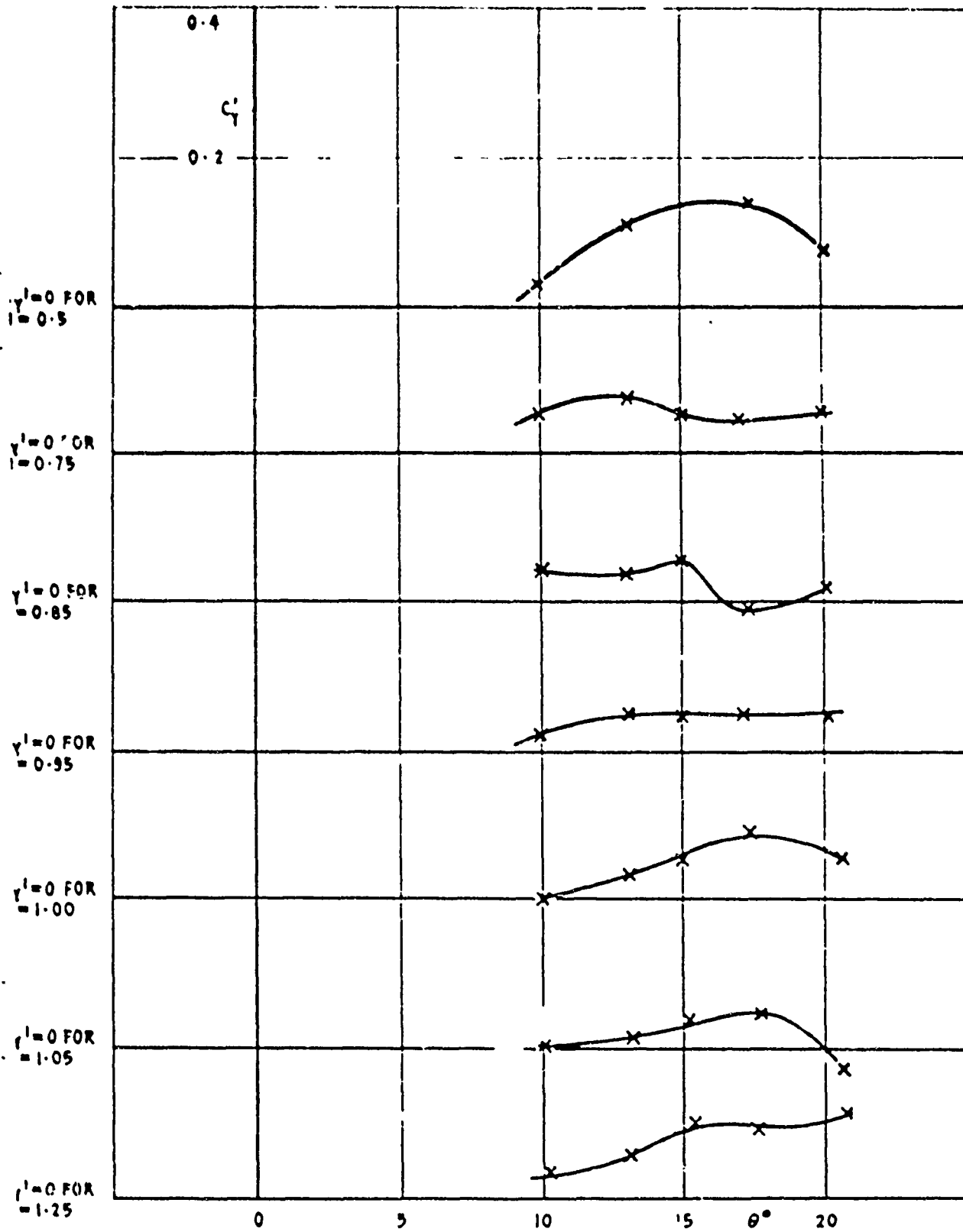


FIGURE 15. VARIATION OF PEAK INDUCED SIDE FORCE WITH ANGLE OF INCIDENCE FOR THE M557B BLUFF BODY SHAPE ($\psi = 22\frac{1}{2}^\circ$)

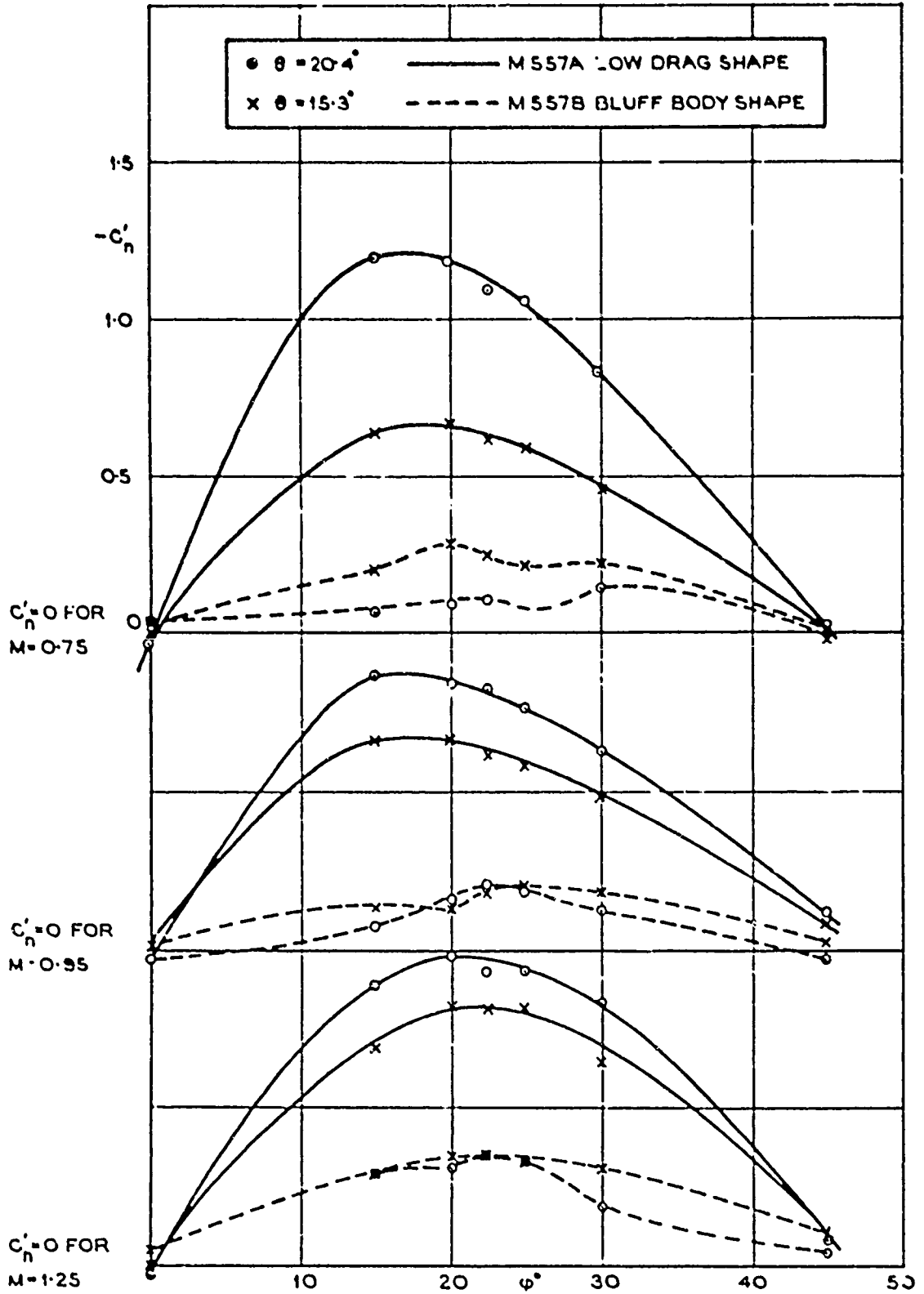


FIGURE 16. VARIATION OF INDUCED SIDE MOMENT WITH ROLL ATTITUDE FOR THE M557A LOW DRAG AND M557B BLUFF BODY SHAPES

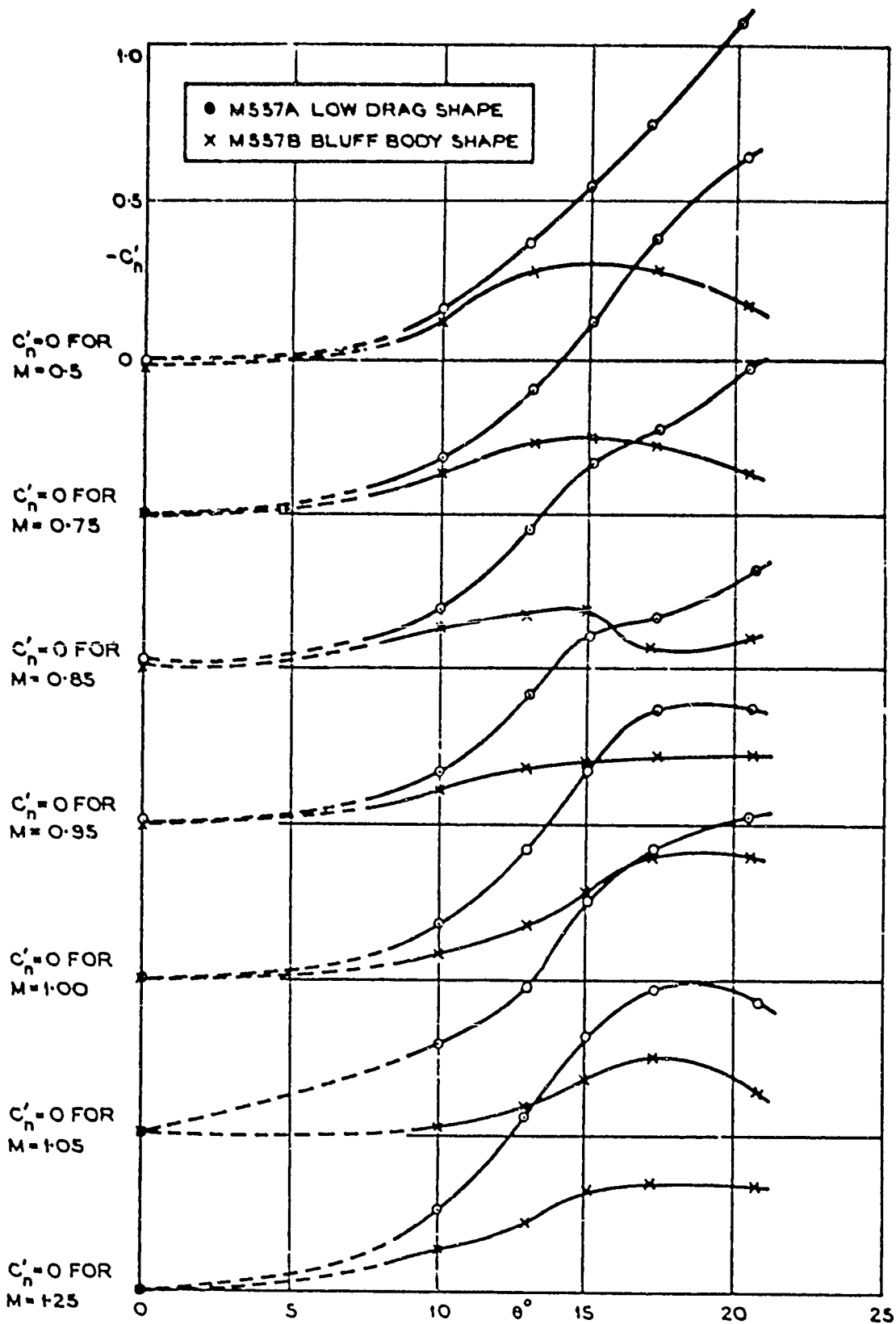


FIGURE 17. VARIATION OF PEAK INDUCED SIDE MOMENT WITH ANGLE OF INCIDENCE FOR THE M557A LOW DRAG AND M557B BLUFF BODY SHAPES ($\varphi = 22\frac{1}{2}^\circ$)

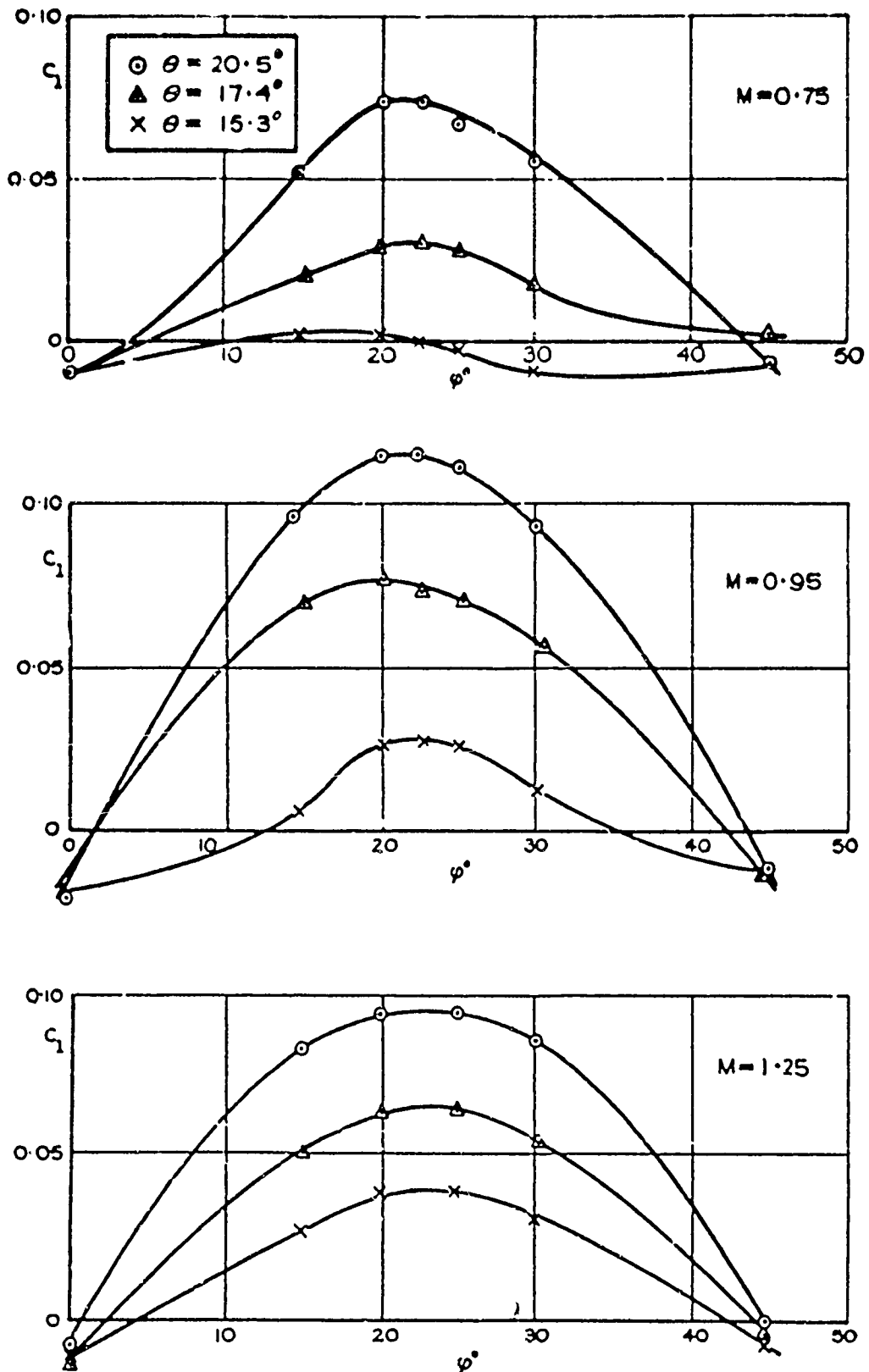


FIGURE 18. VARIATION OF INDUCED ROLLING MOMENT WITH ROLL ATTITUDE FOR THE M557A LOW DRAG SHAPE

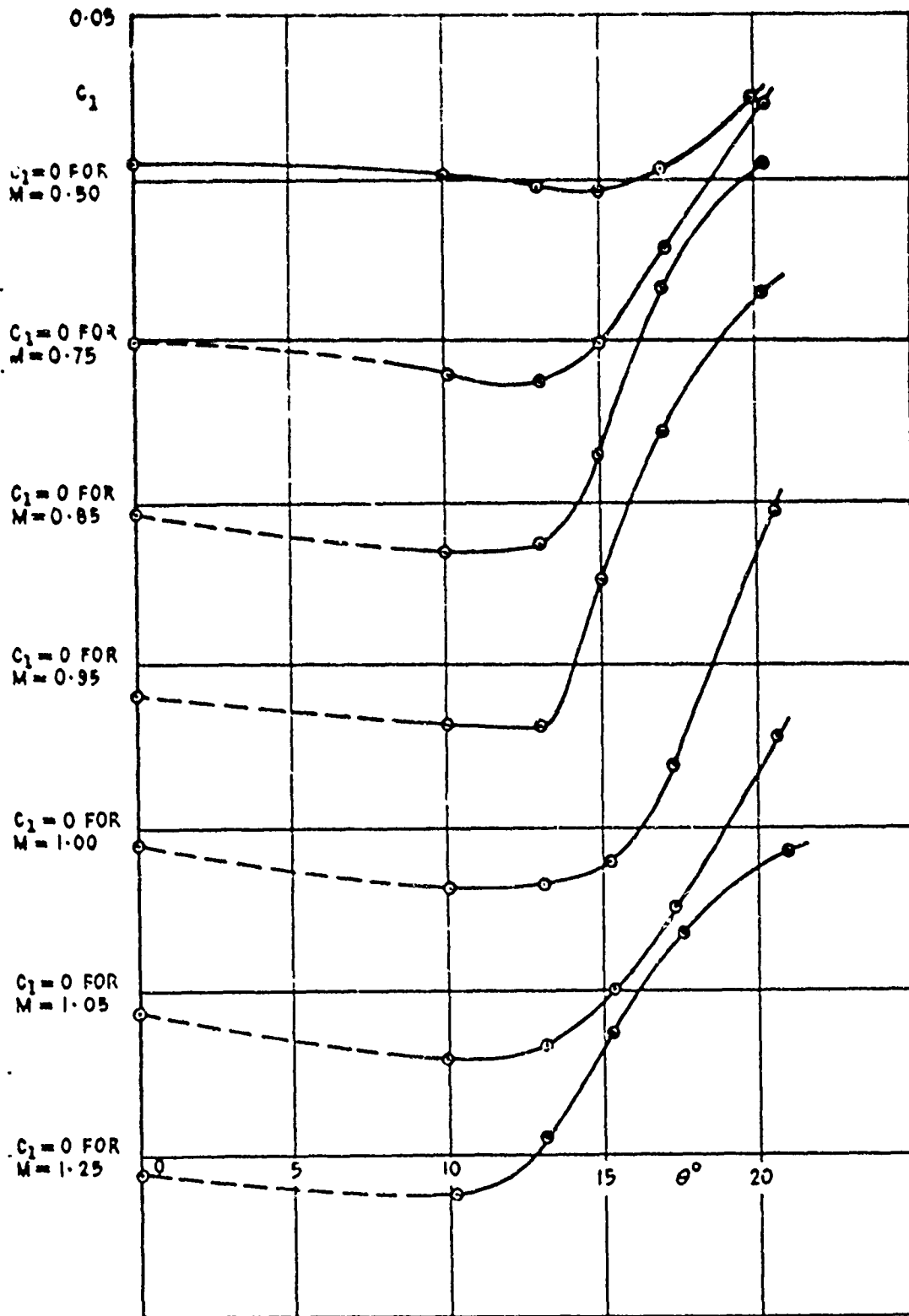


FIGURE 19. VARIATION OF PEAK INDUCED ROLLING MOMENT WITH ANGLE OF INCIDENCE FOR THE M557A LWJ DRAG SHAPE ($\varphi = 22\frac{1}{2}^\circ$)

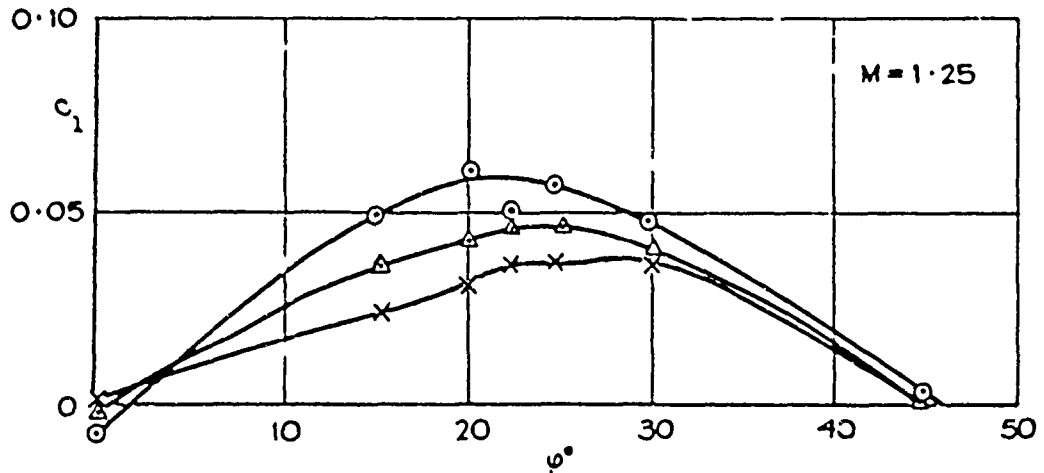
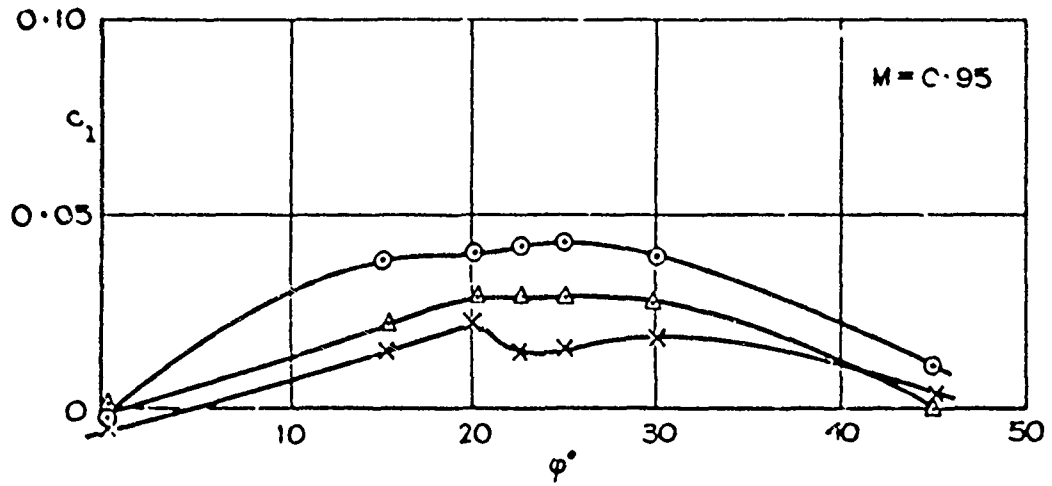
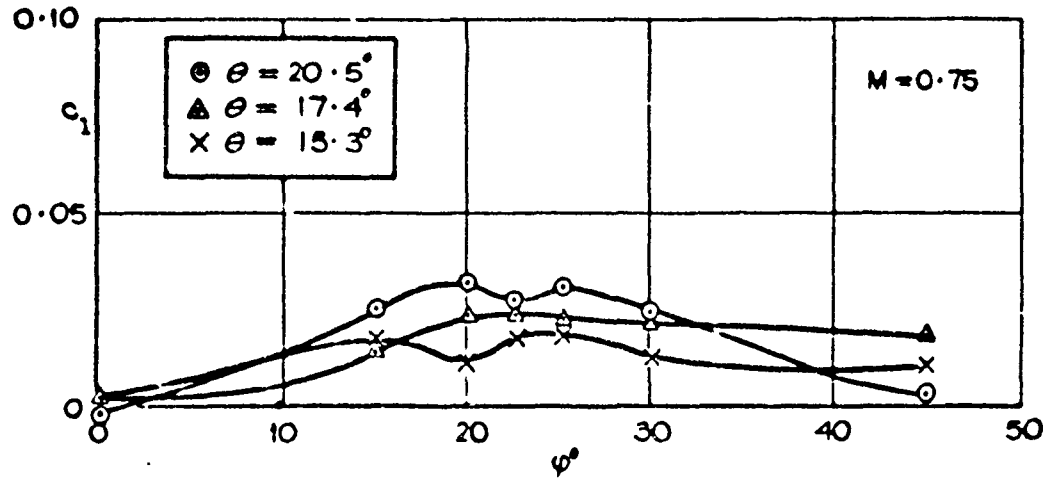


FIGURE 20. VARIATION OF INDUCED ROLLING MOMENT WITH ROLL ATTITUDE FOR THE M557B BLUFF BODY SHAPE

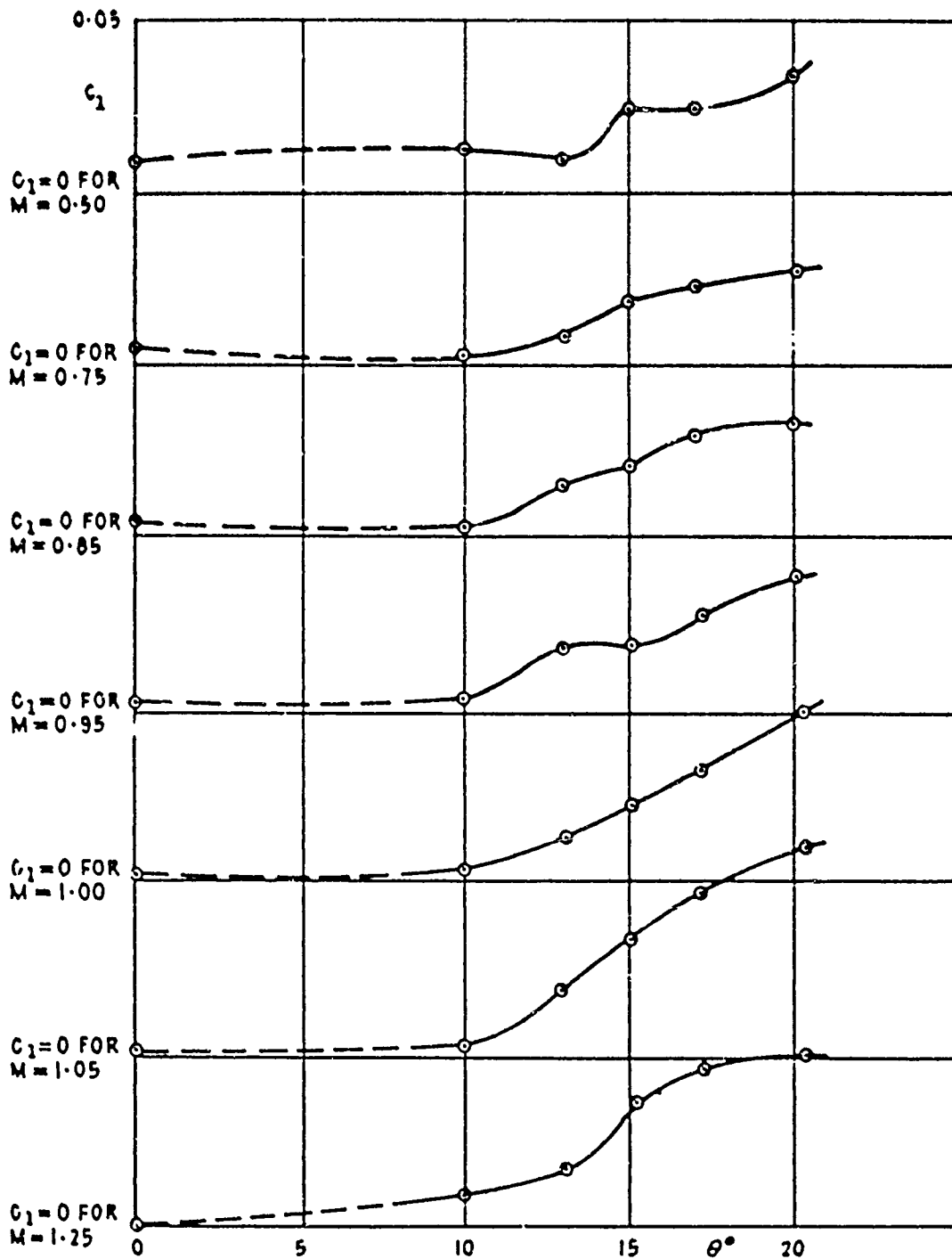
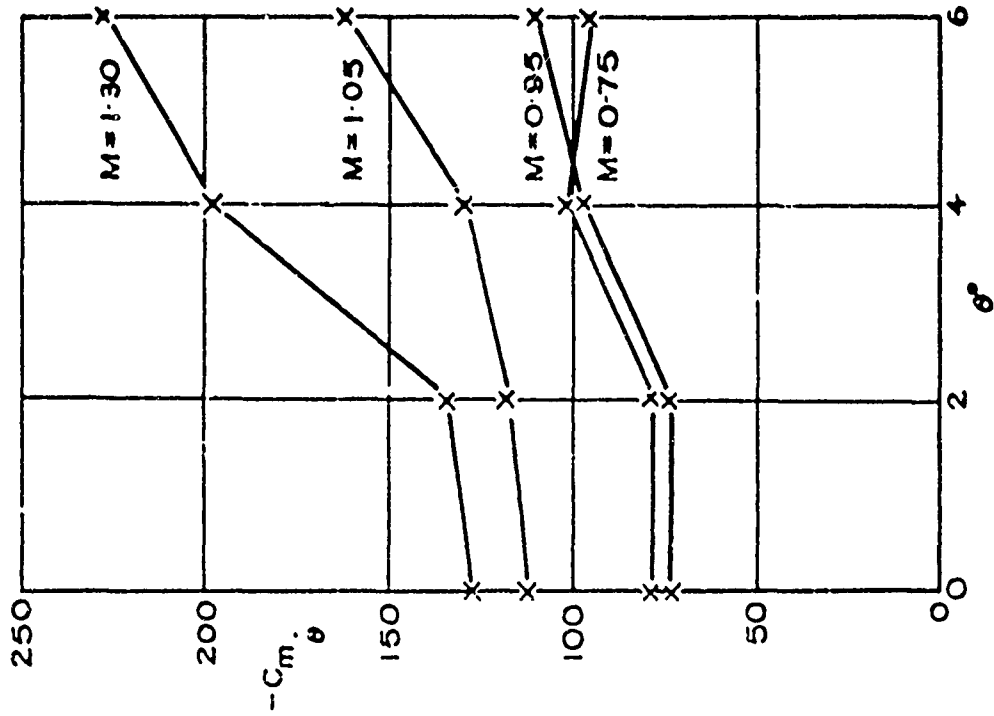
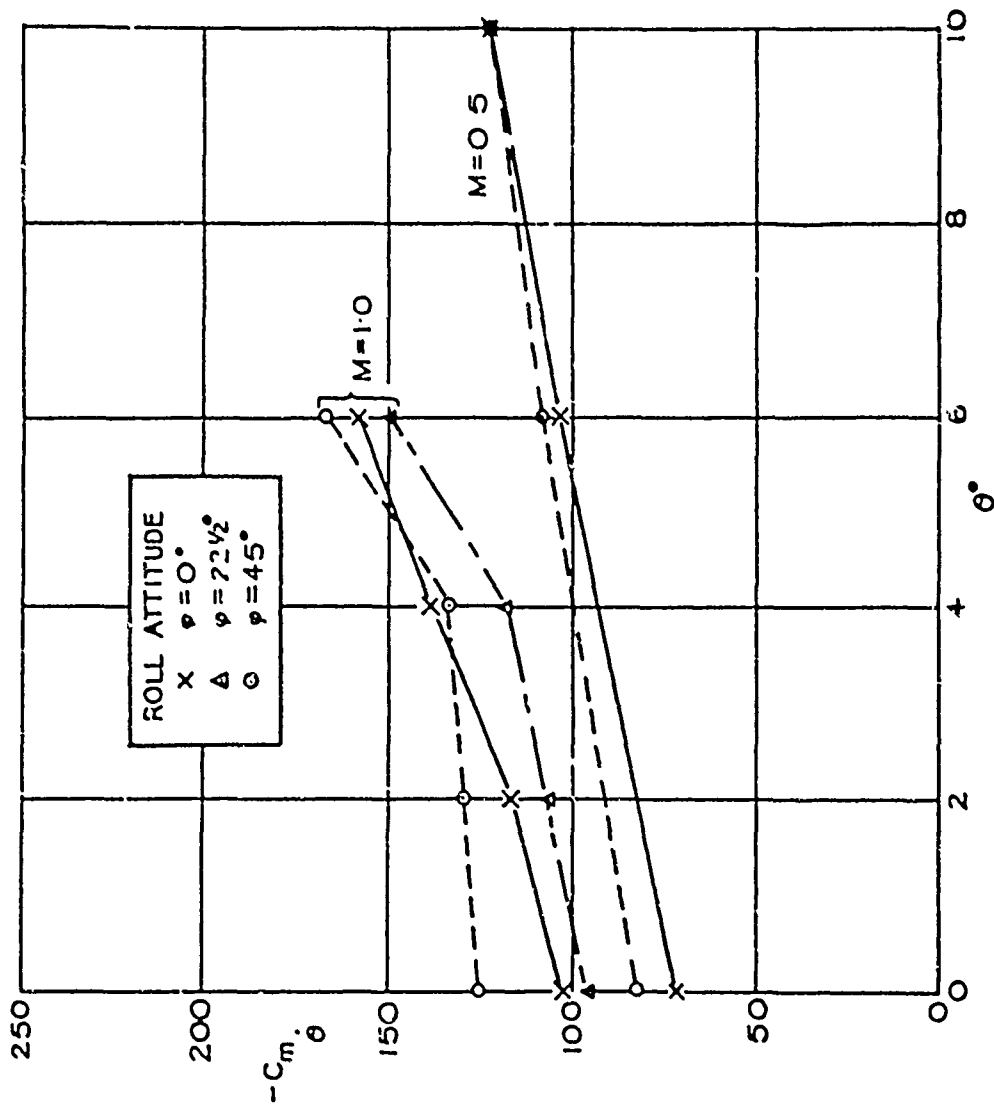


FIGURE 21. VARIATION OF PEAK INDUCED ROLLING MOMENT WITH ANGLE OF INCIDENCE FOR THE M557B BLUFF BODY SHAPE ($\varphi = 22\frac{1}{2}^\circ$)



(a) Effect of roll attitude and incidence



(b) Incidence angle effects at $\phi = 0$

FIGURE 22(a&b). VARIATION OF PITCH DAMPING WITH INCIDENCE, ROLL AND MACH NUMBER FOR THE M823 LOW DRAG SHAPE. TESTS IN THE A.R.A. WIND TUNNEL

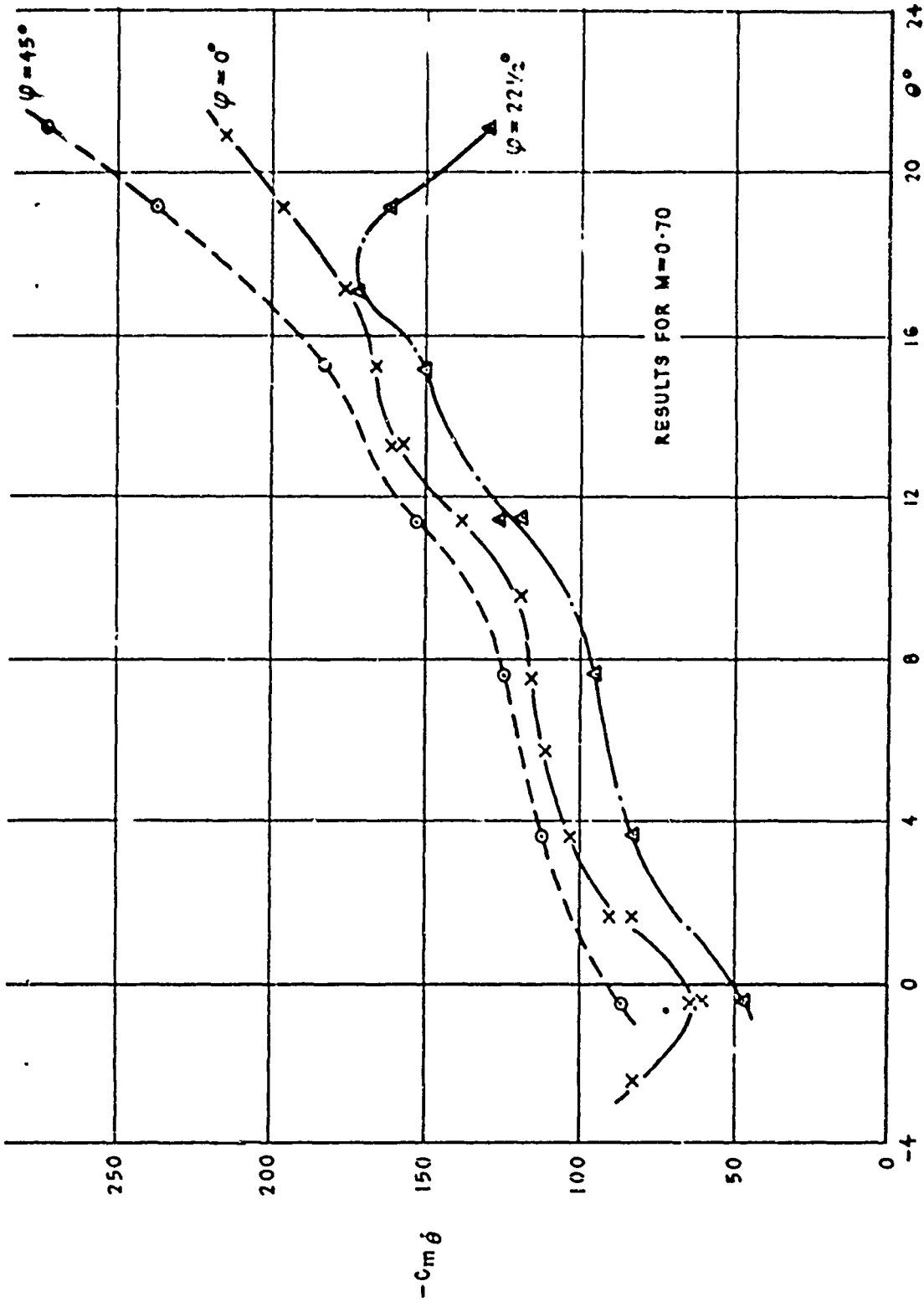


FIGURE 22(c). SUBSONIC VARIATION OF PITCH DAMPING WITH INCIDENCE AND ROLL FOR THE M623 LOW DRAG SHAPE. TESTS IN THE R.A.E. 8 FT S.S. WIND TUNNEL

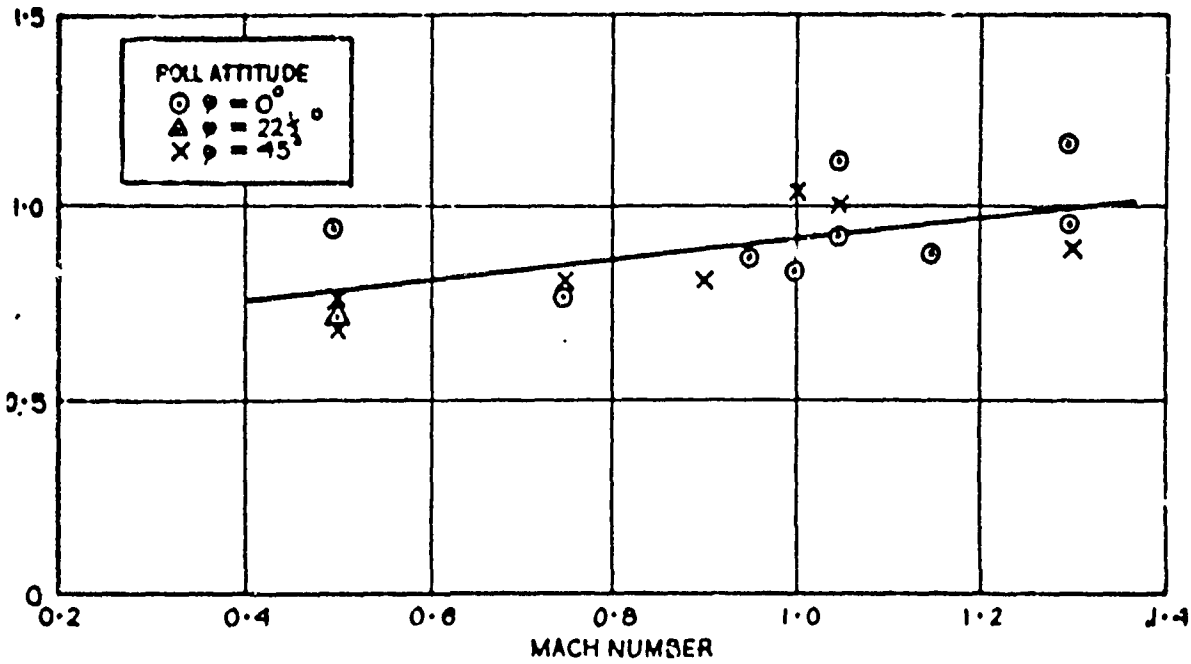


FIGURE 24. VARIATION OF ROLL DAMPING WITH MACH NUMBER

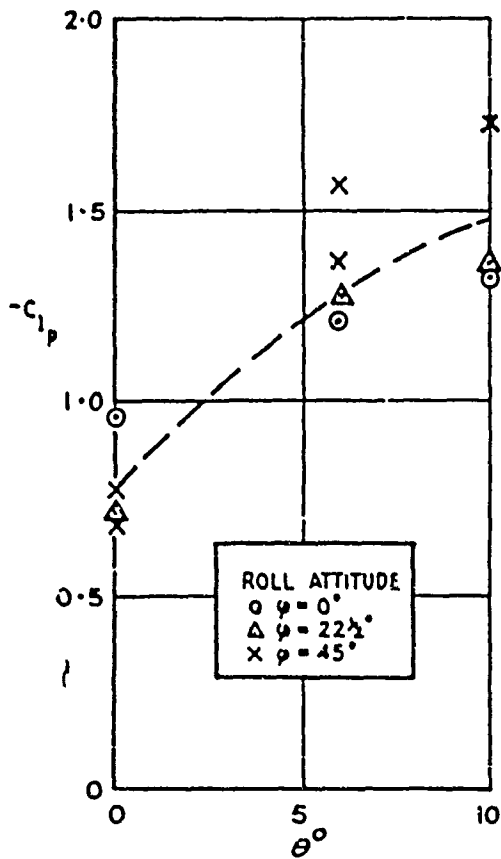


FIGURE 25. VARIATION OF ROLL DAMPING WITH INCIDENCE ANGLE AT LOW MACH NUMBER ($M = 0.5$)

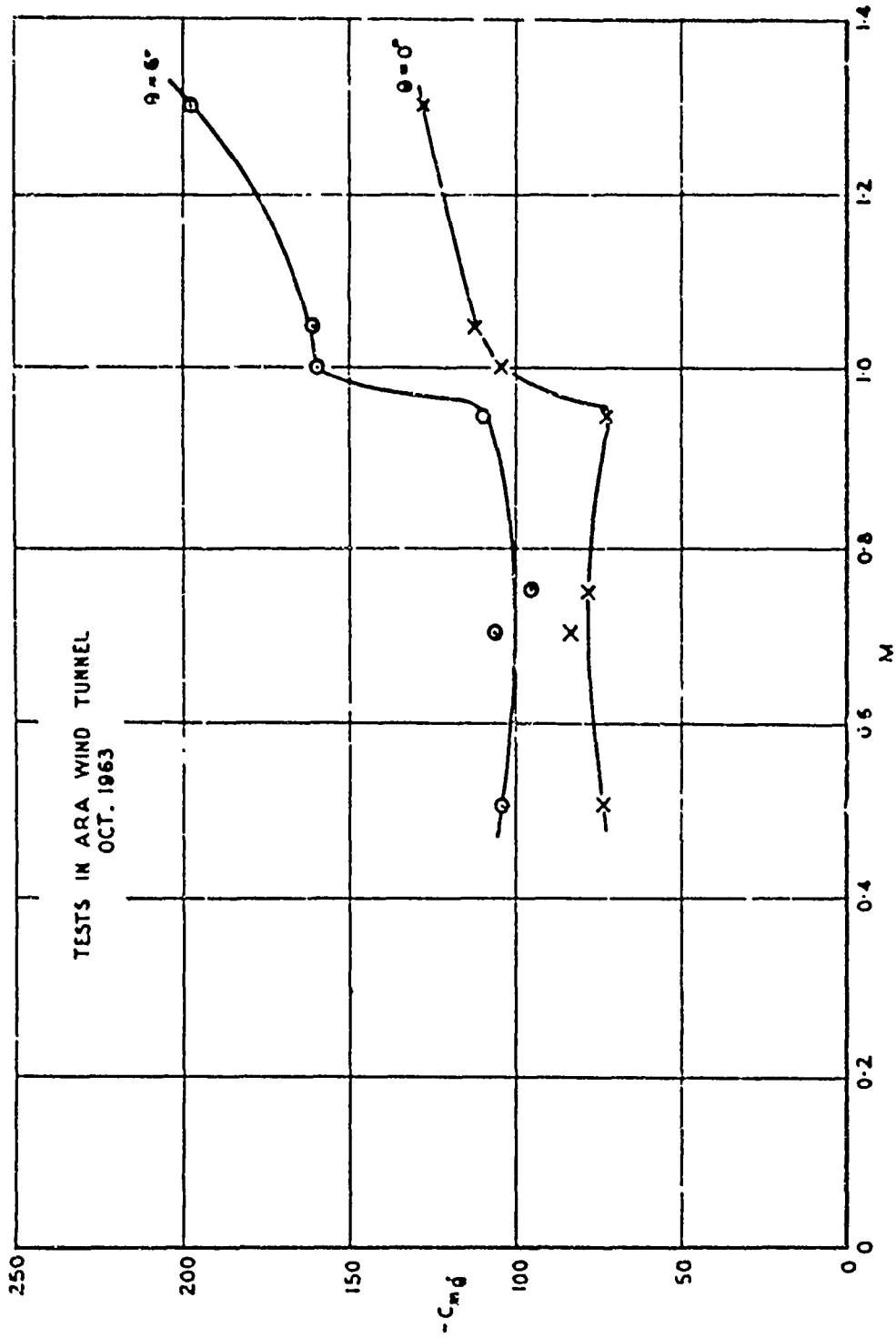


FIGURE 23. VARIATION OF PITCH DAMPING WITH MACH NUMBER FOR THE M823 LOW DRAG SHAPE ($\psi = 0$)

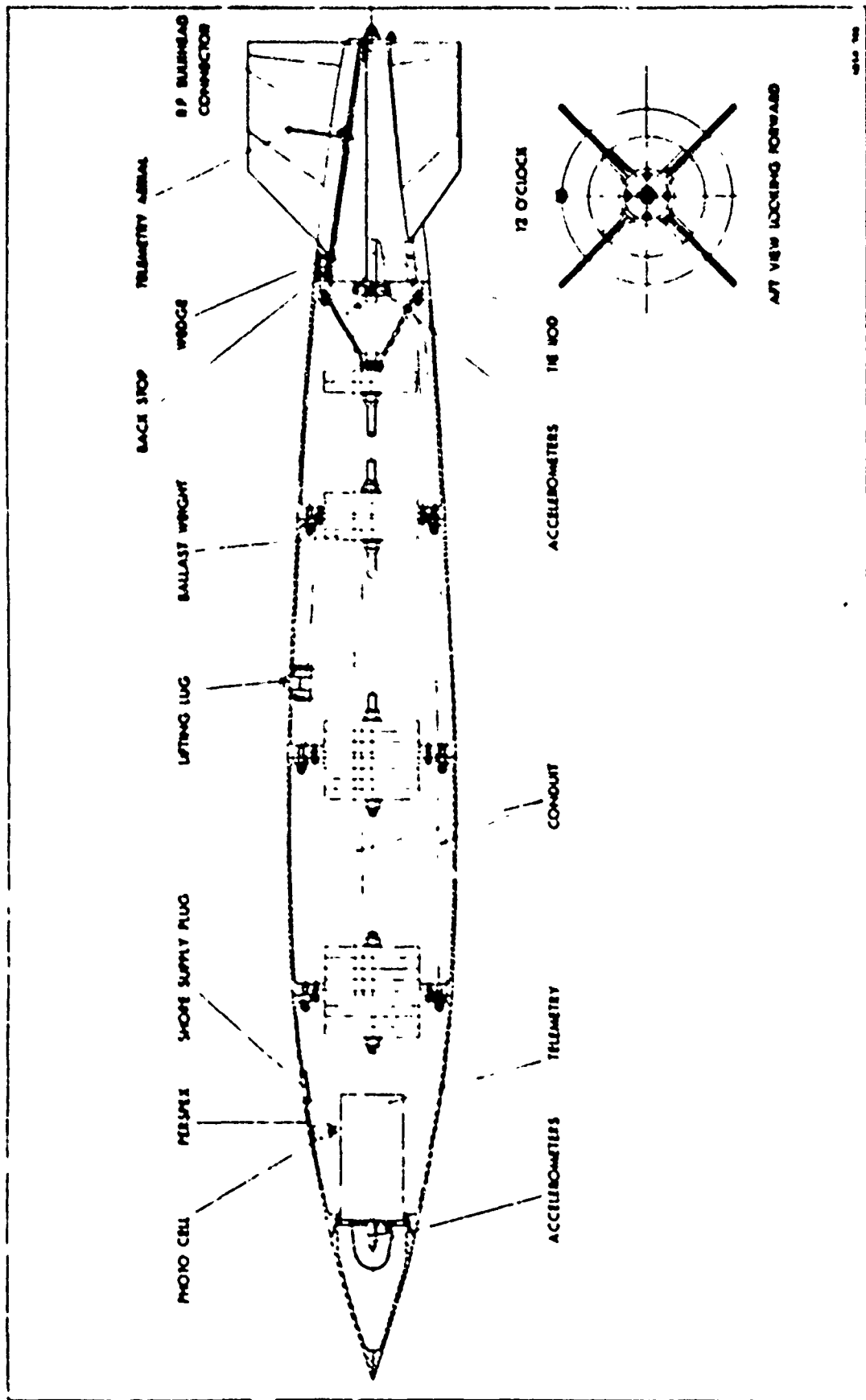


FIGURE 26. GENERAL ASSEMBLY OF THE M557A TEST VEHICLE

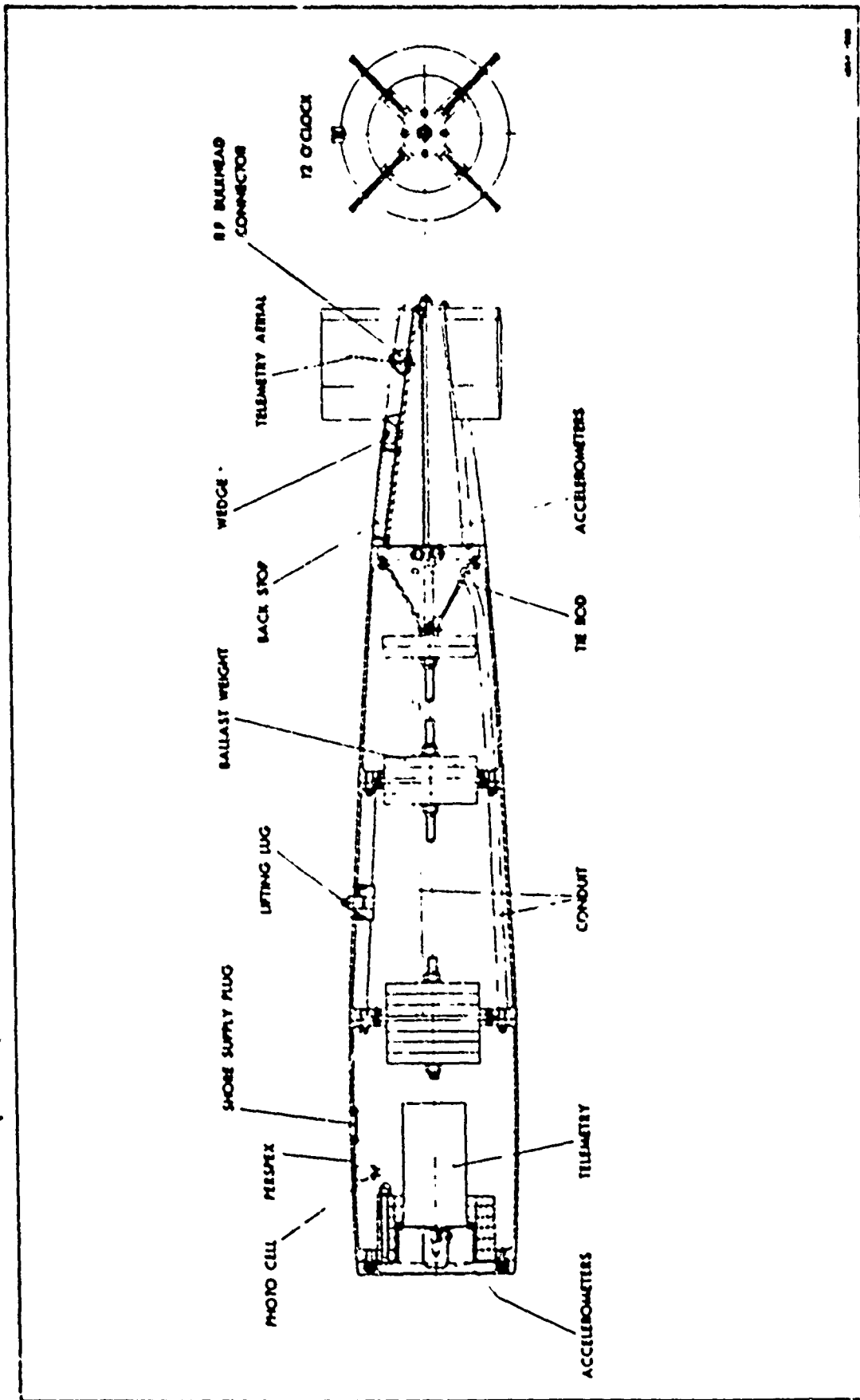


FIGURE 27. GENERAL ASSEMBLY OF THE M557B TEST VEHICLE

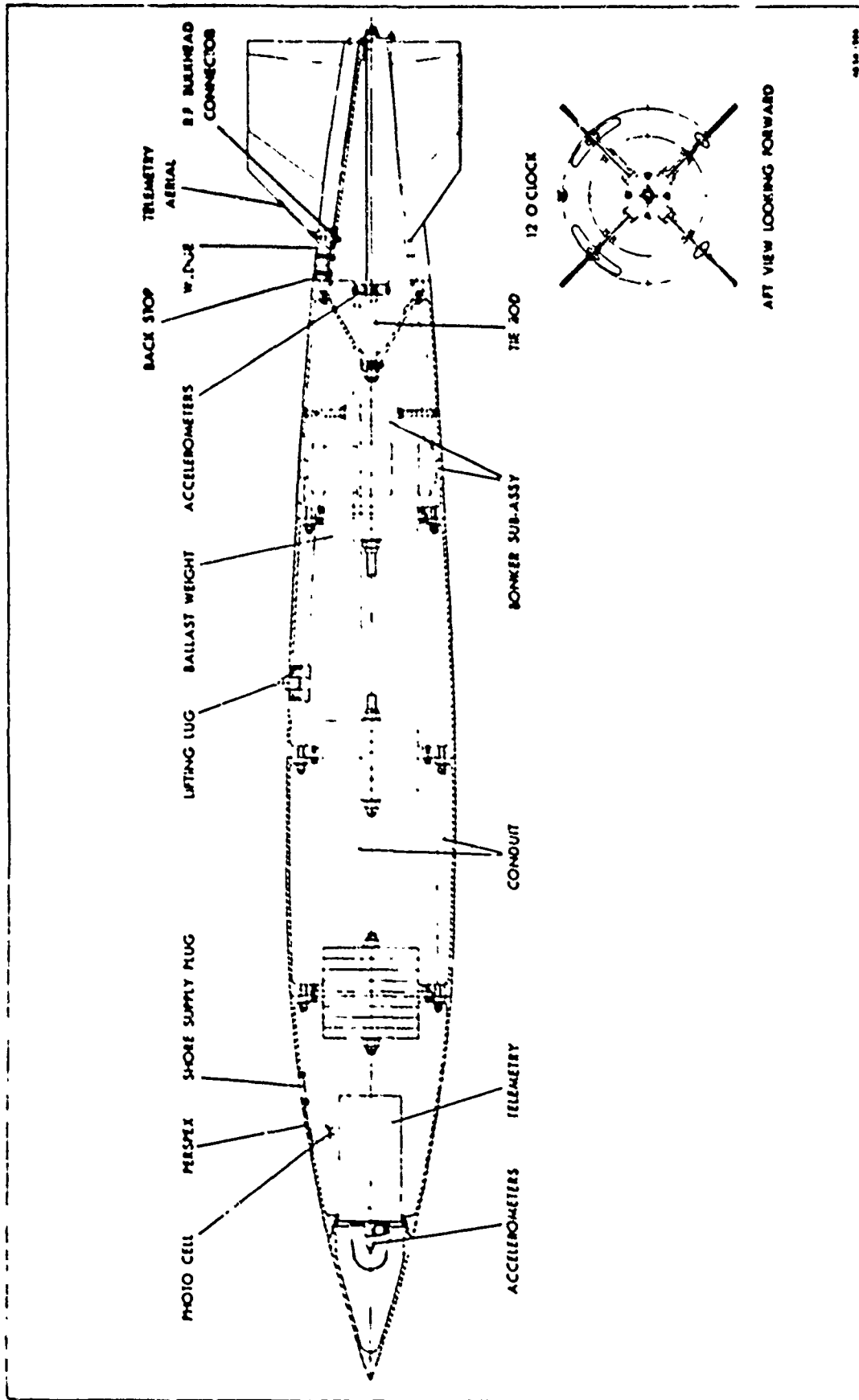


FIGURE 28. GENERAL ASSEMBLY OF THE M557A TEST VEHICLE FITTED WITH LATERAL PULSE ROCKETS

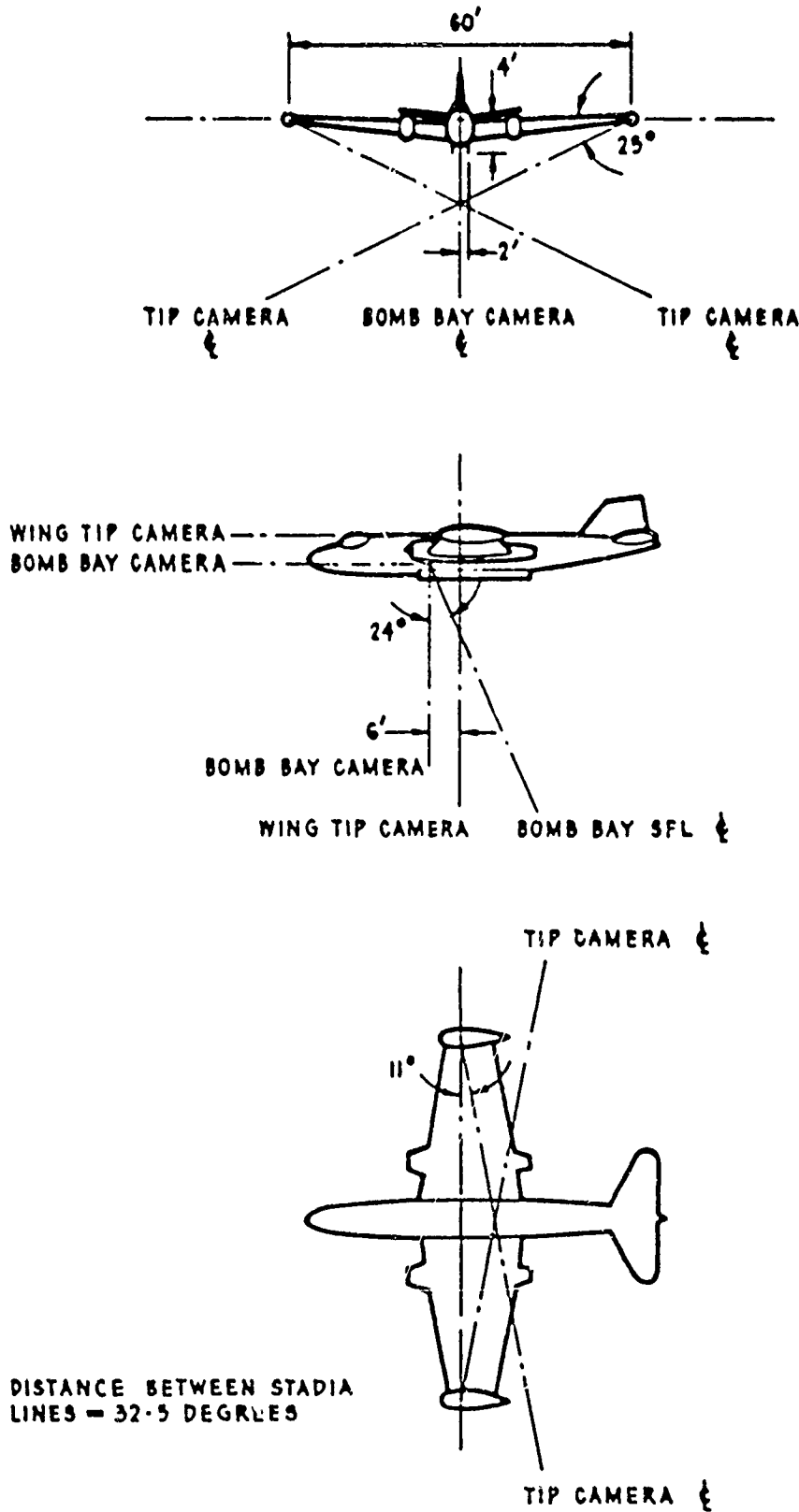
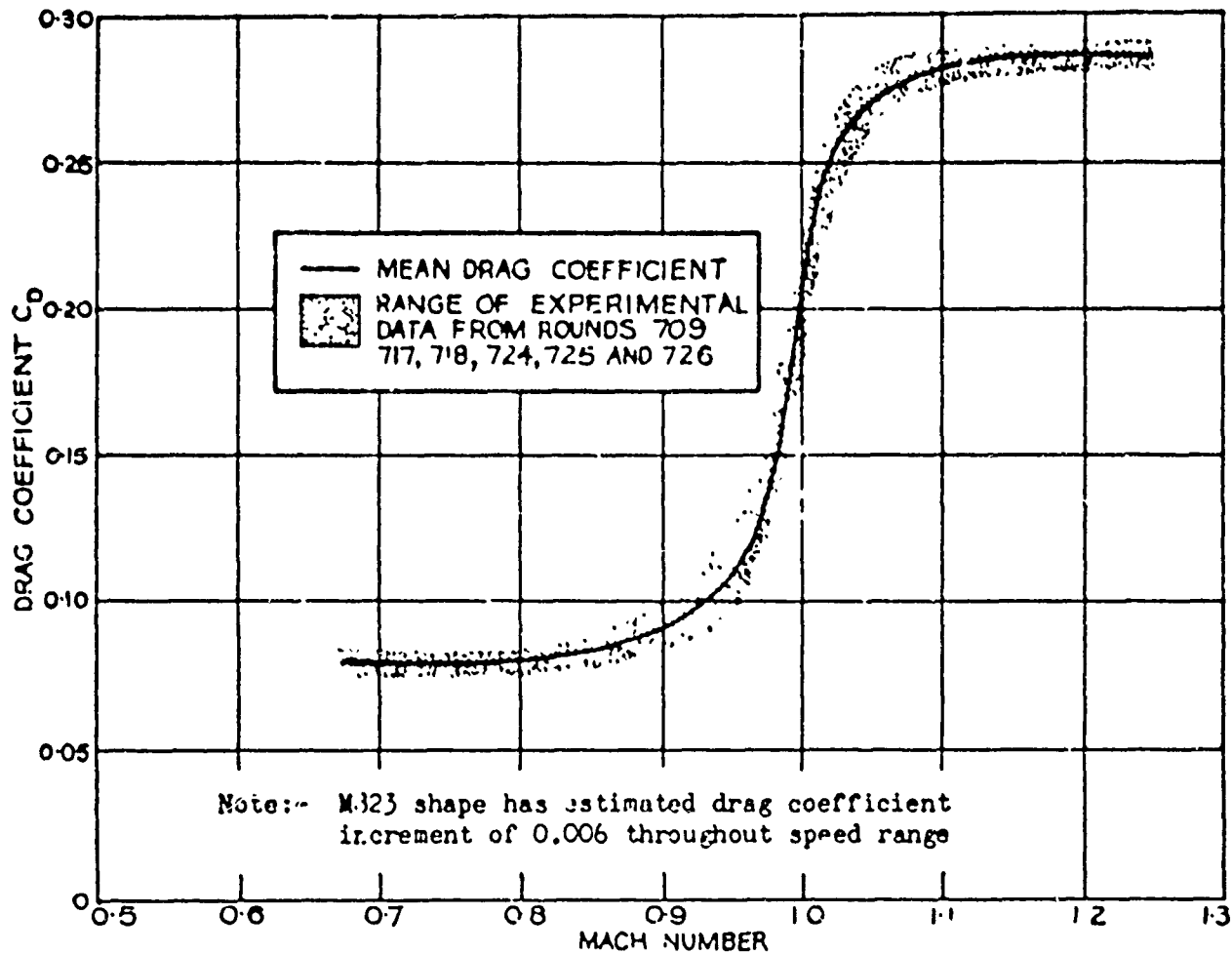
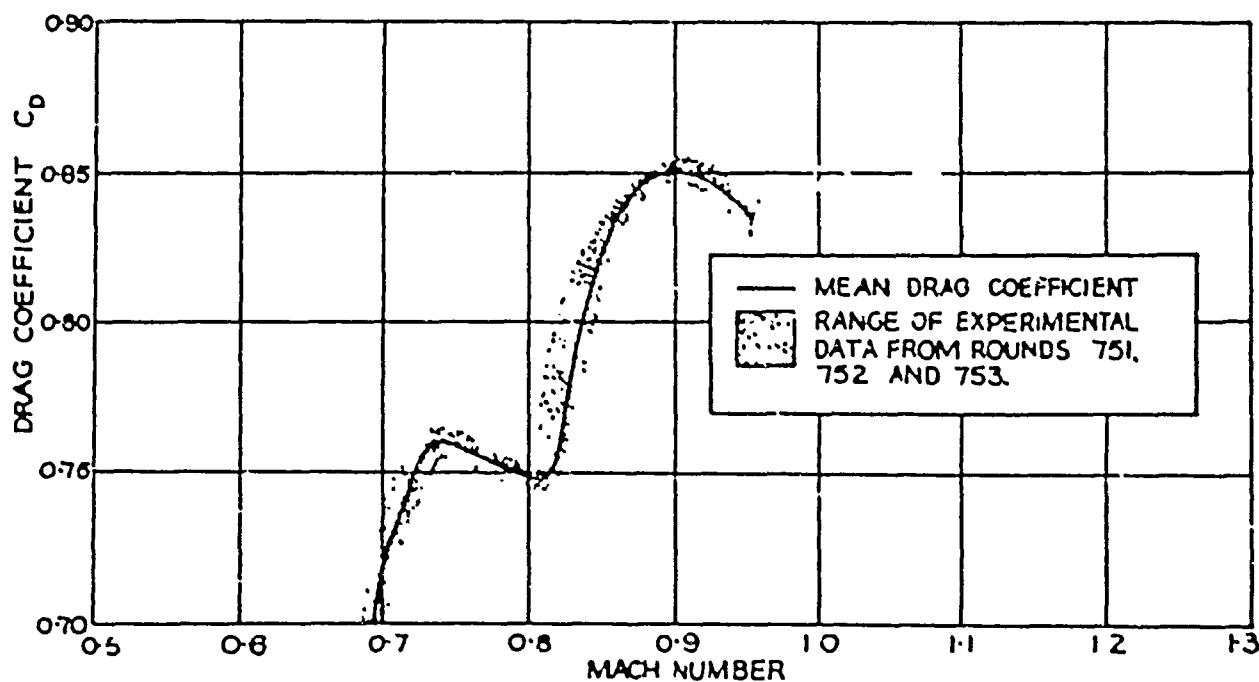


FIGURE 29. CANBERRA CAMERA INSTALLATION



(a) Streamlined body shape. M557A



(b) Bluff body shape. M557B

FIGURE 30. MEASURED VARIATION OF DRAG COEFFICIENT WITH MACH NUMBER FOR THE M557A AND M557B BODY SHAPES

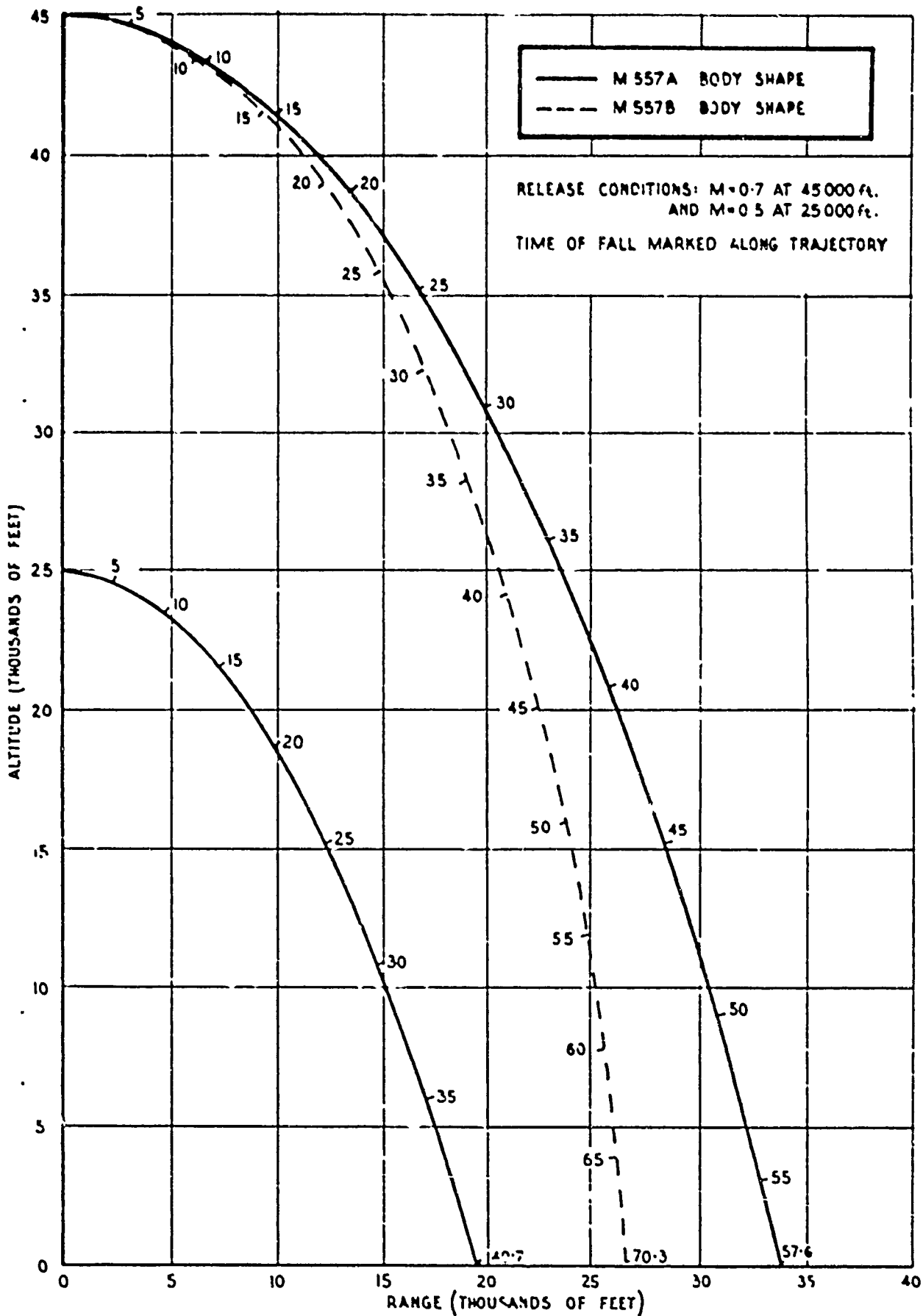
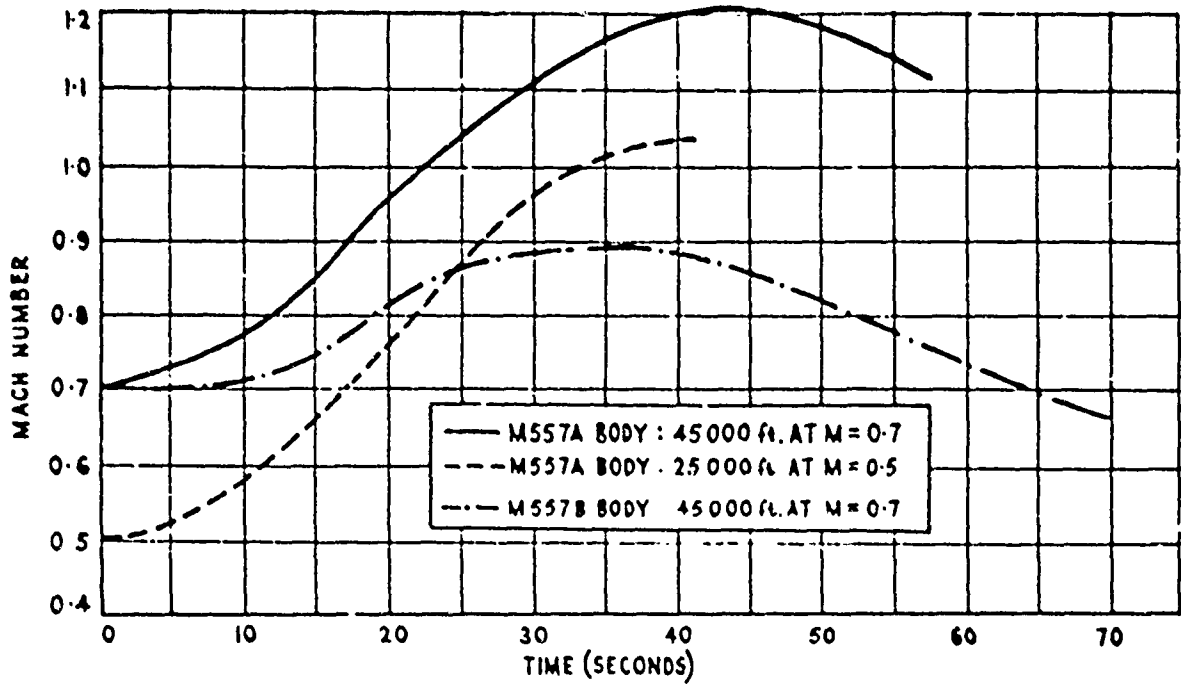
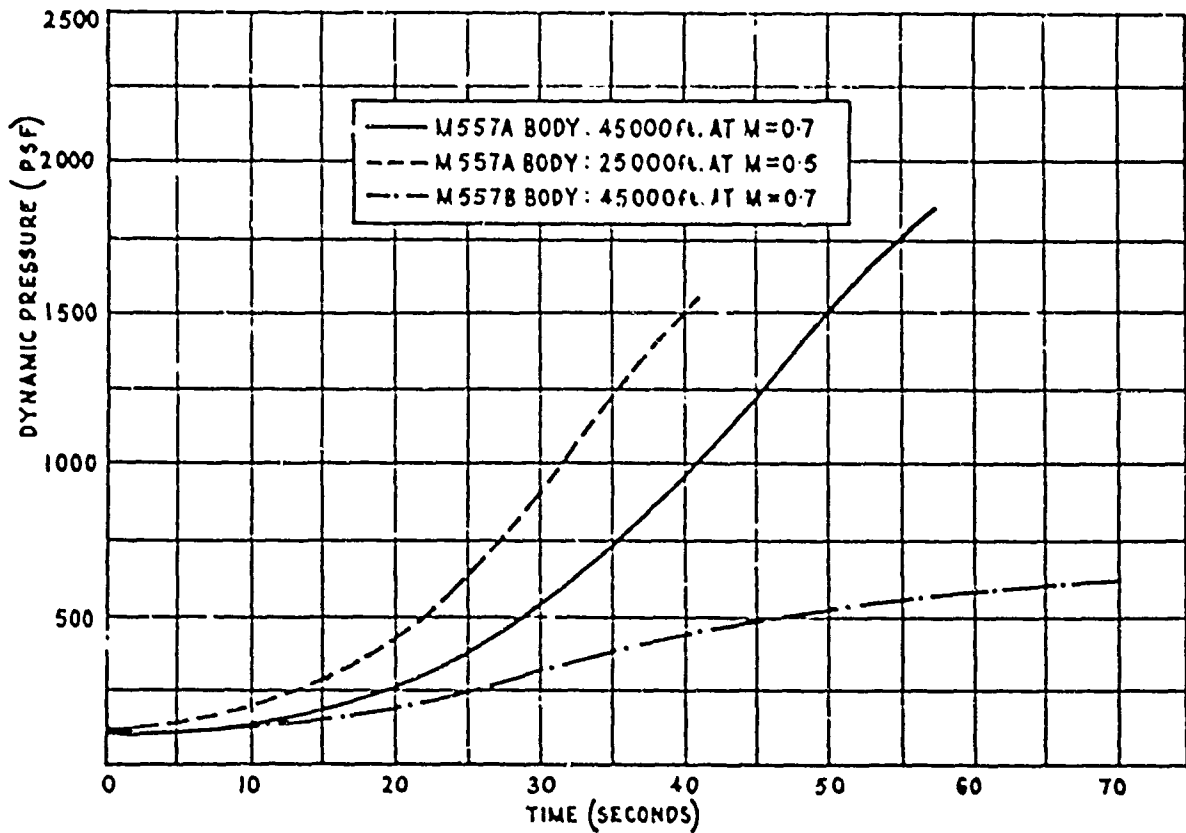


FIGURE 31. TYPICAL PARTICLE TRAJECTORIES OF THE M557A AND M557B BODY SHAPES (LEVEL RELEASES FROM 25000 FT AND 45000 FT ALTITUDE)

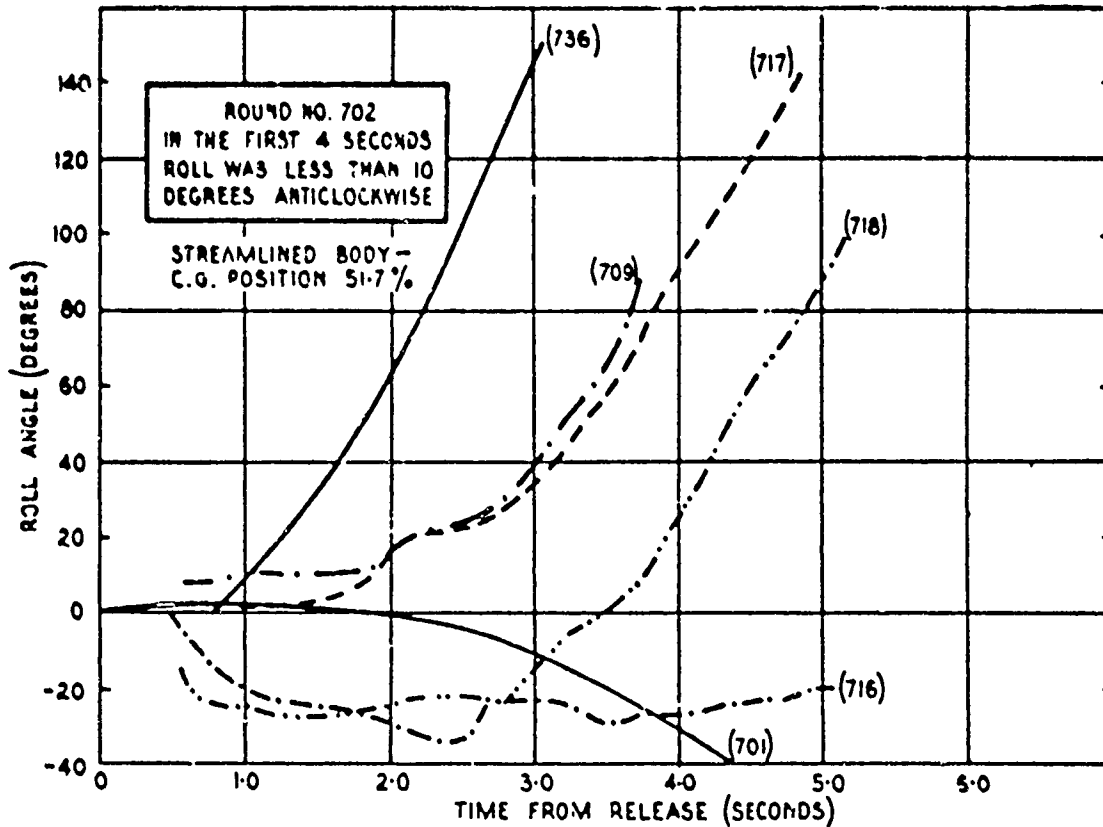


(a) Variation of Mach number with time

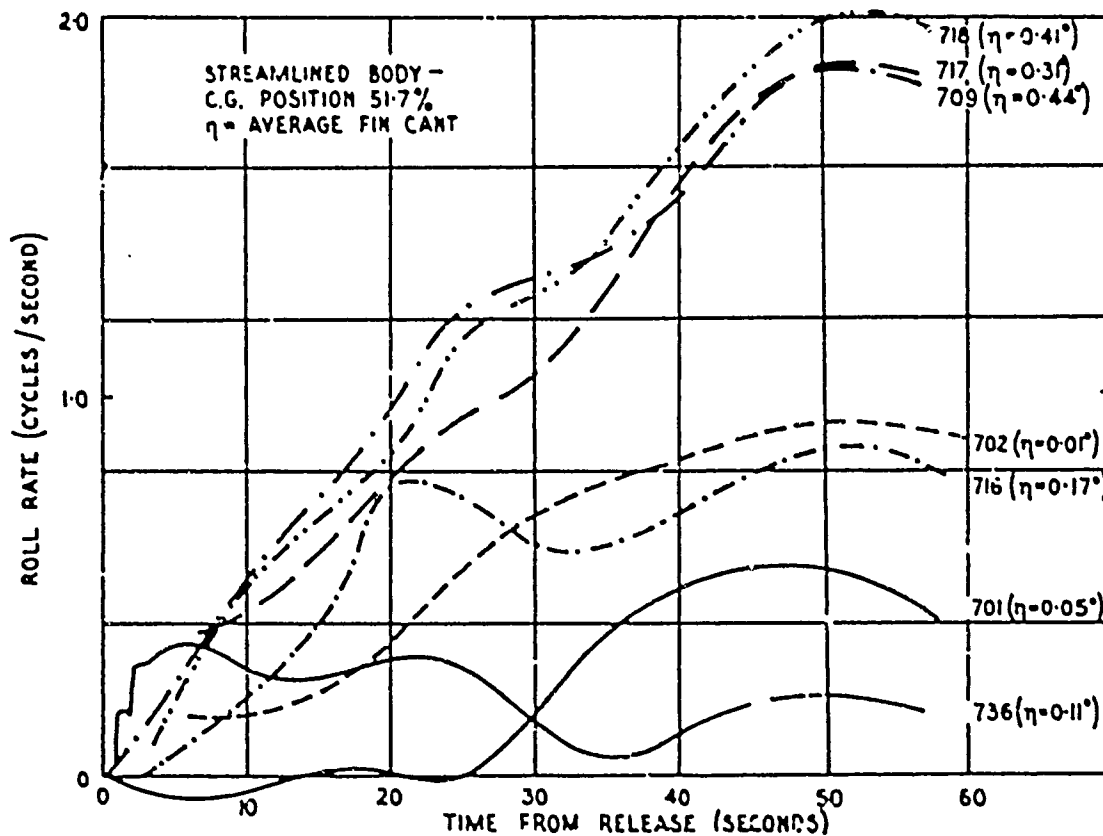


(b) Variation of dynamic pressure with time

FIGURE 32. TIME HISTORIES OF MACH NUMBER AND DYNAMIC PRESSURE FOR PARTICLE TRAJECTORIES OF THE M557A AND M557B BODY SHAPES (LEVEL RELEASES FROM 25 000 FT AND 45 000 FT ALTITUDE)

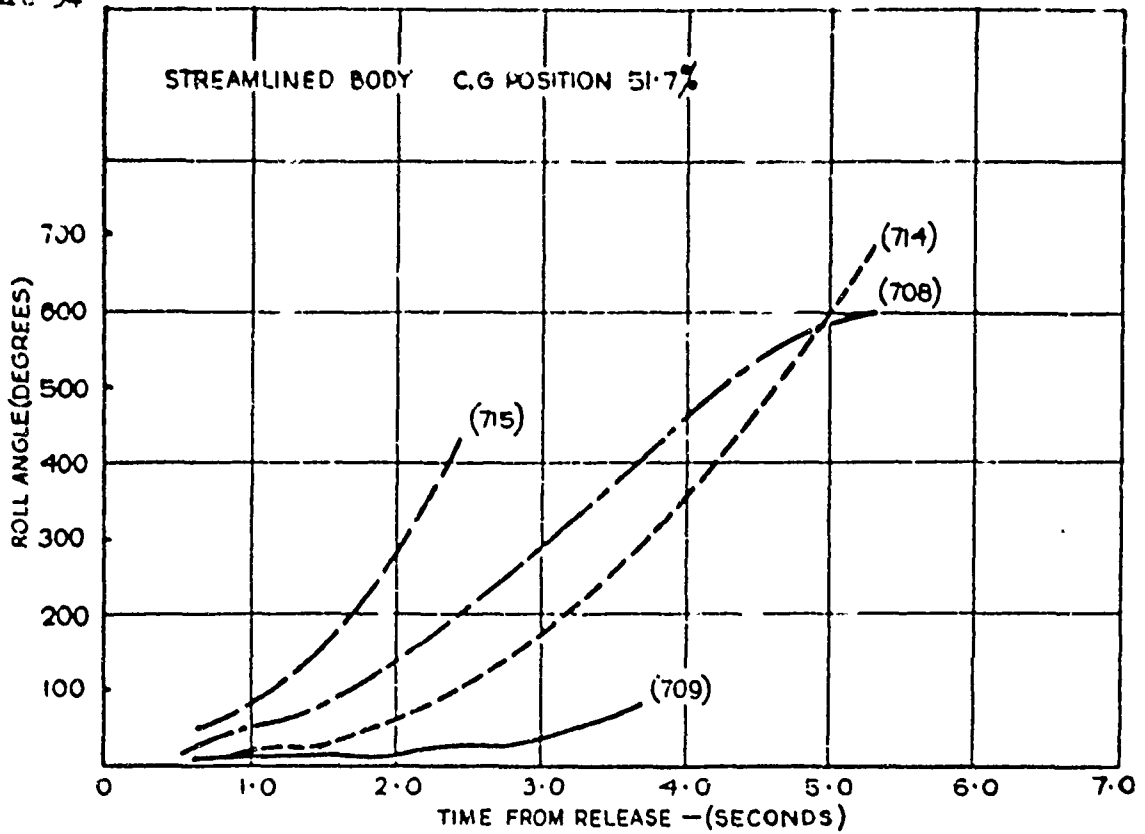


(a) Variation of roll angle with time from release

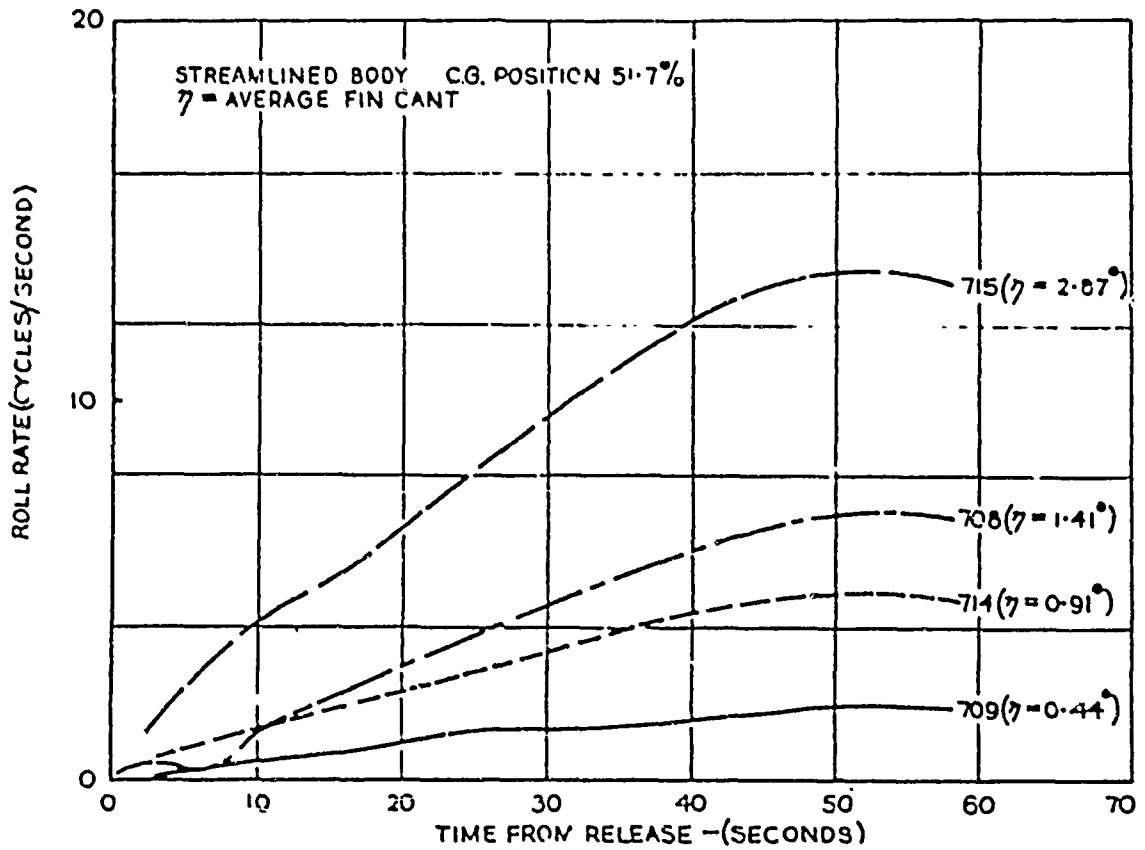


(b) Variation of roll rate with time from release

FIGURE 33. ROLL HISTORIES OF ROUND NUMBERS 701, 702, 709, 716, 717, 718 AND 736

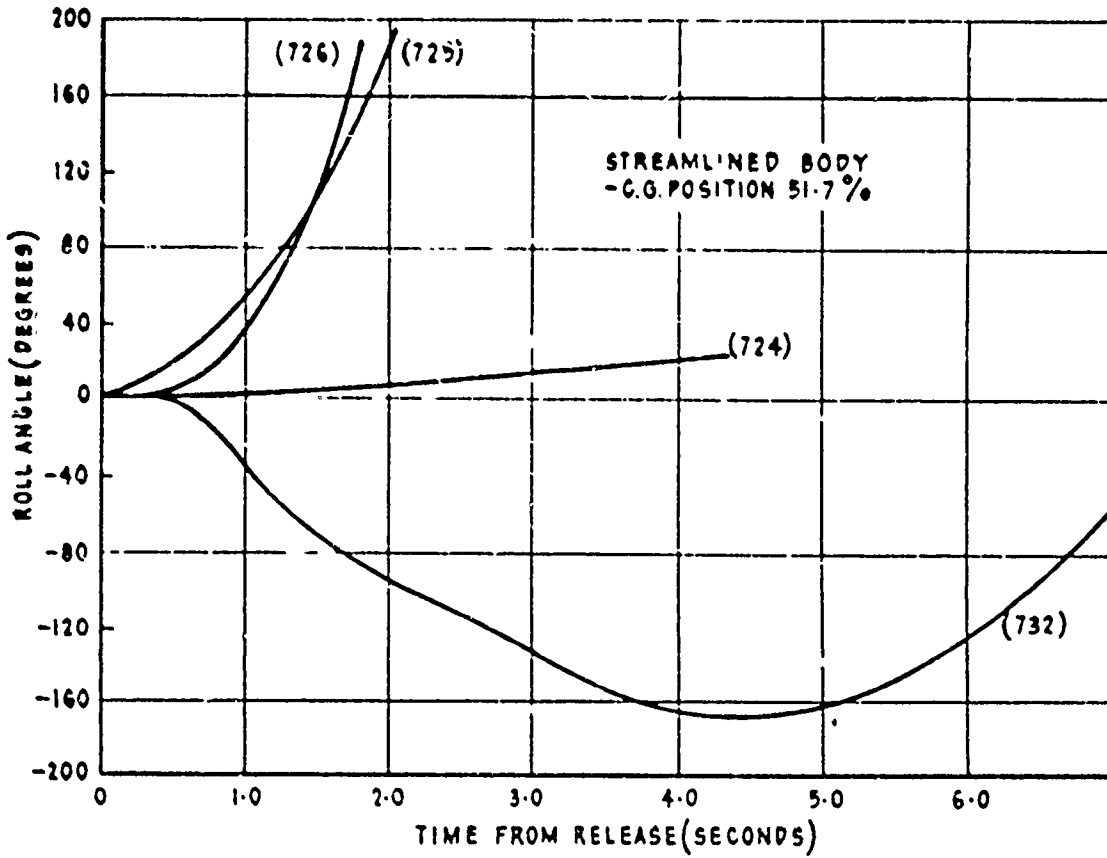


(a) Variation of roll angle with time from release

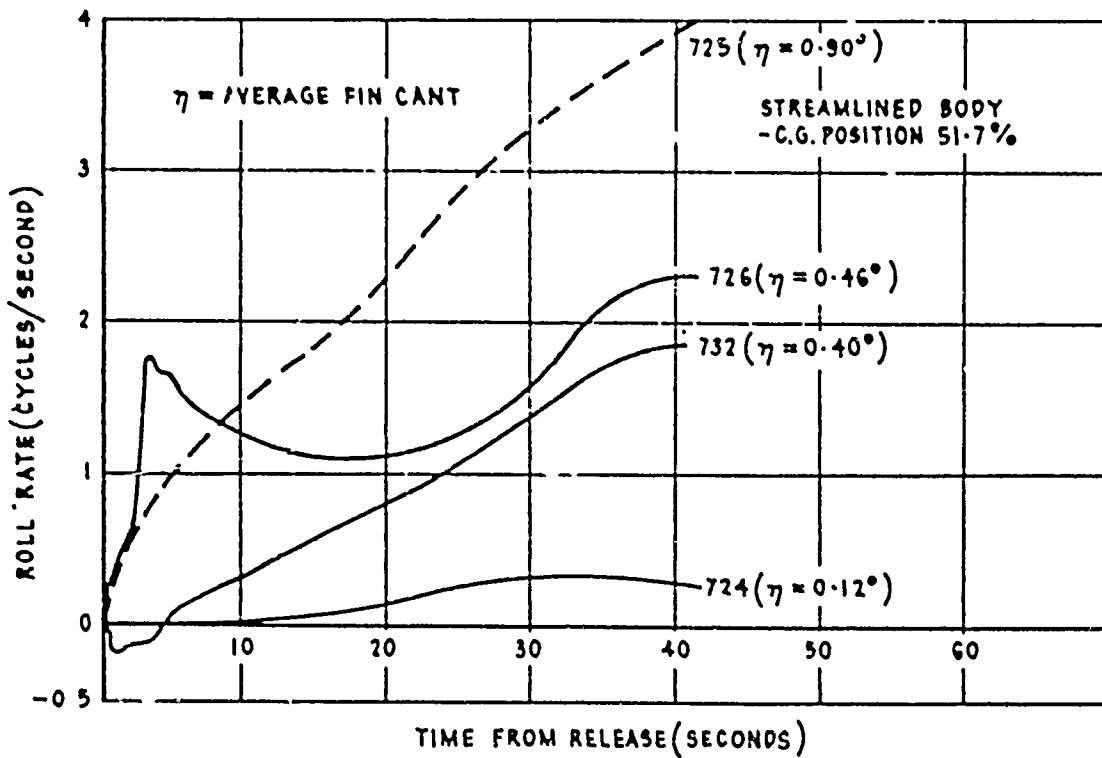


(b) Variation of roll rate with time from release

FIGURE 34. ROLL HISTORIES OF ROUND NUMBERS 708, 709, 714 AND 715

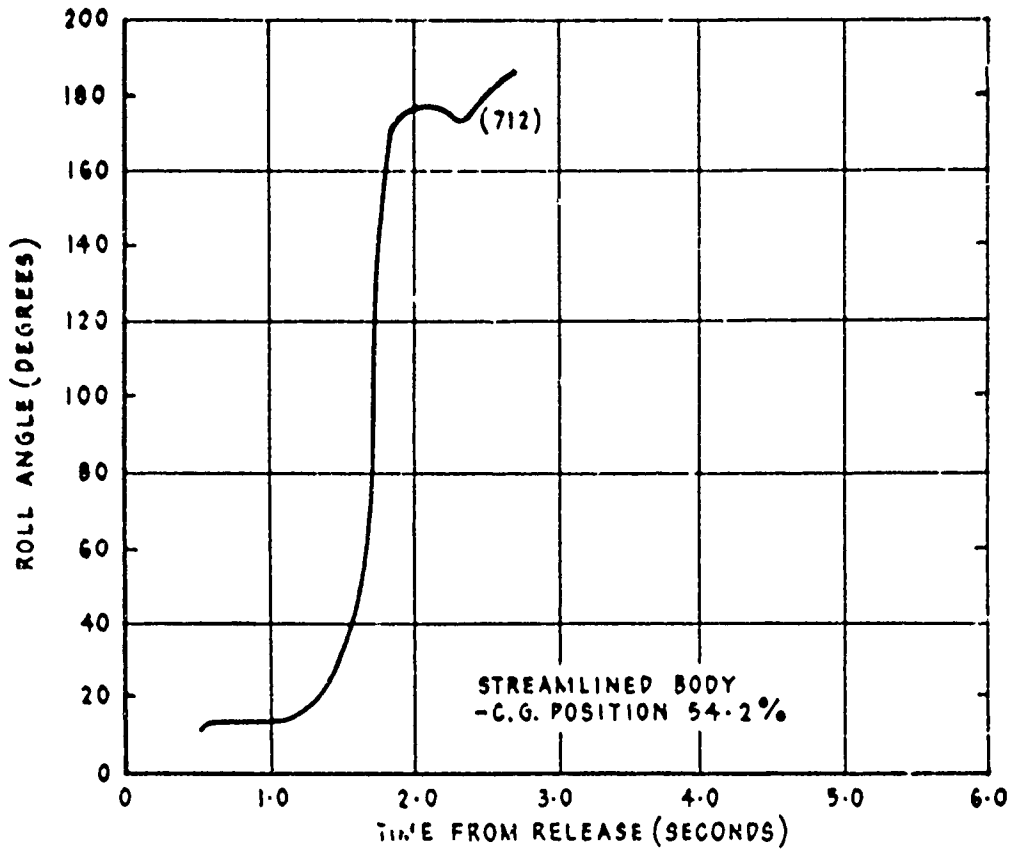


(a) Variation of roll angle with time from release

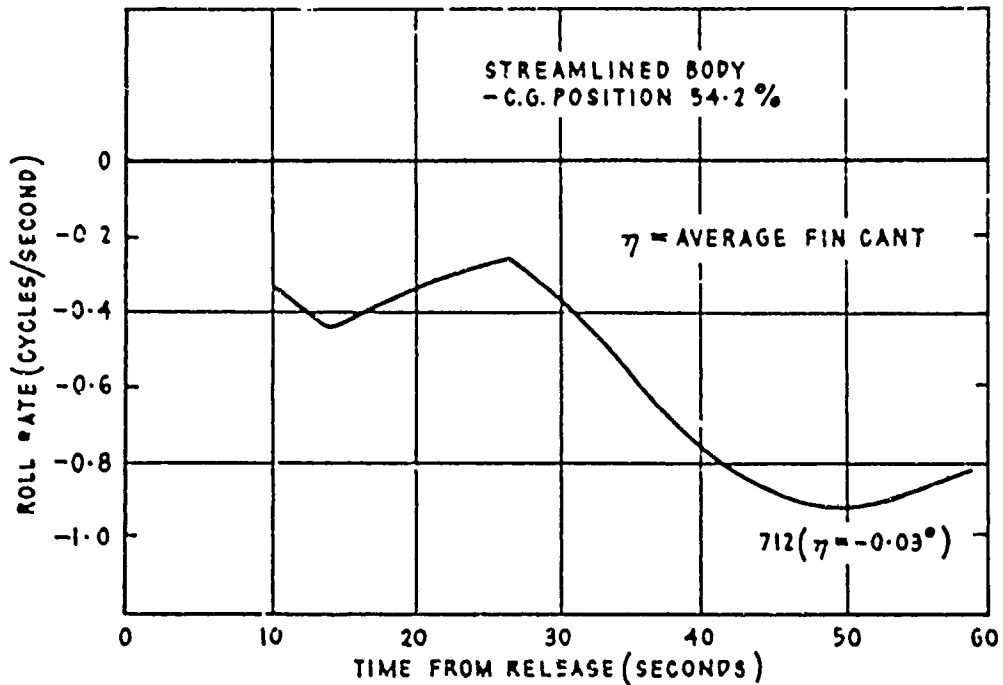


(b) Variation of roll rate with time from release

FIGURE 35. ROLL HISTORIES OF ROUND NUMBERS 724, 725, 726 AND 732

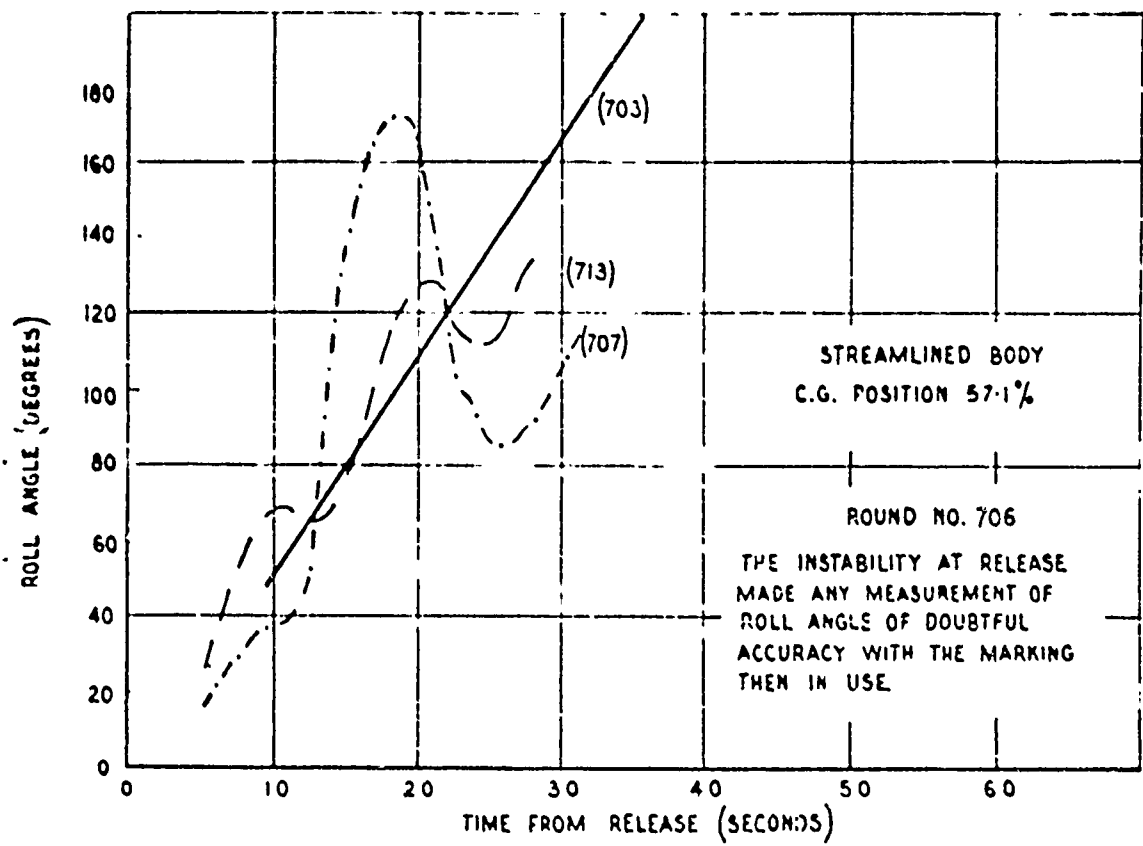


(a) Variation of roll angle with time from release

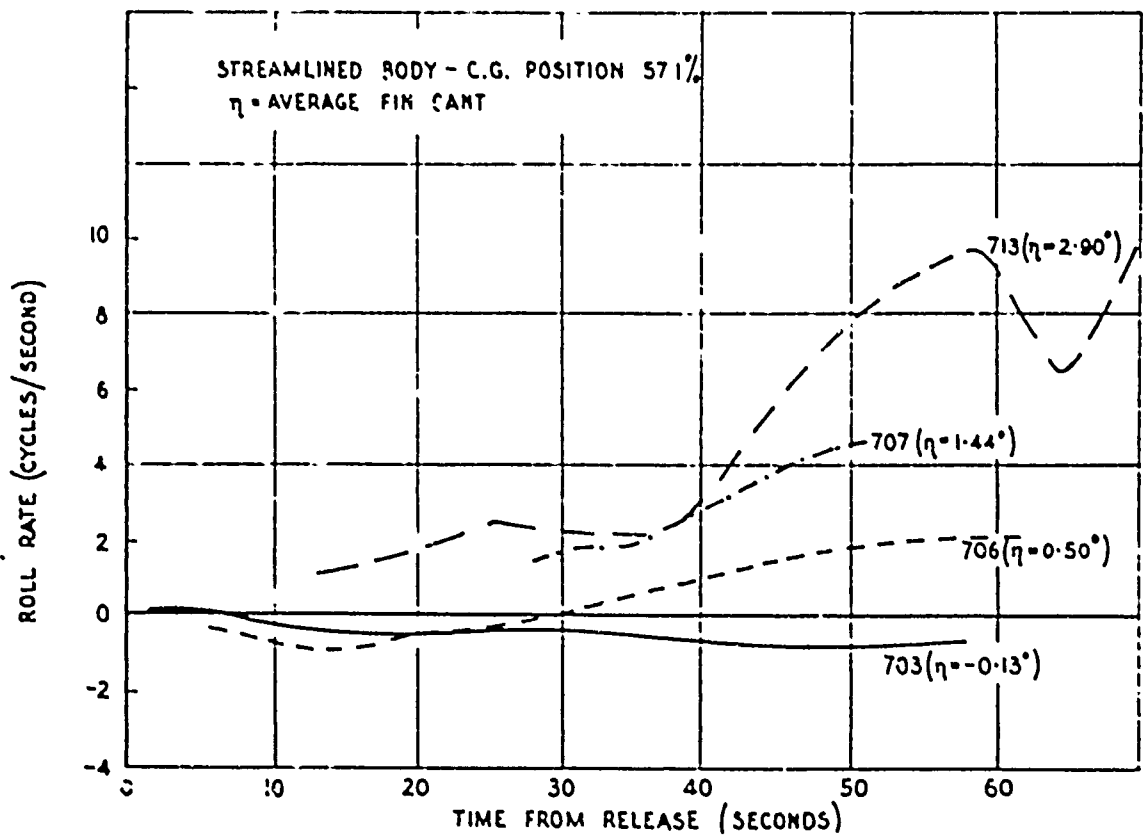


(b) Variation of roll rate with time from release

FIGURE 36. ROLL HISTORY OF ROUND NUMBER 712

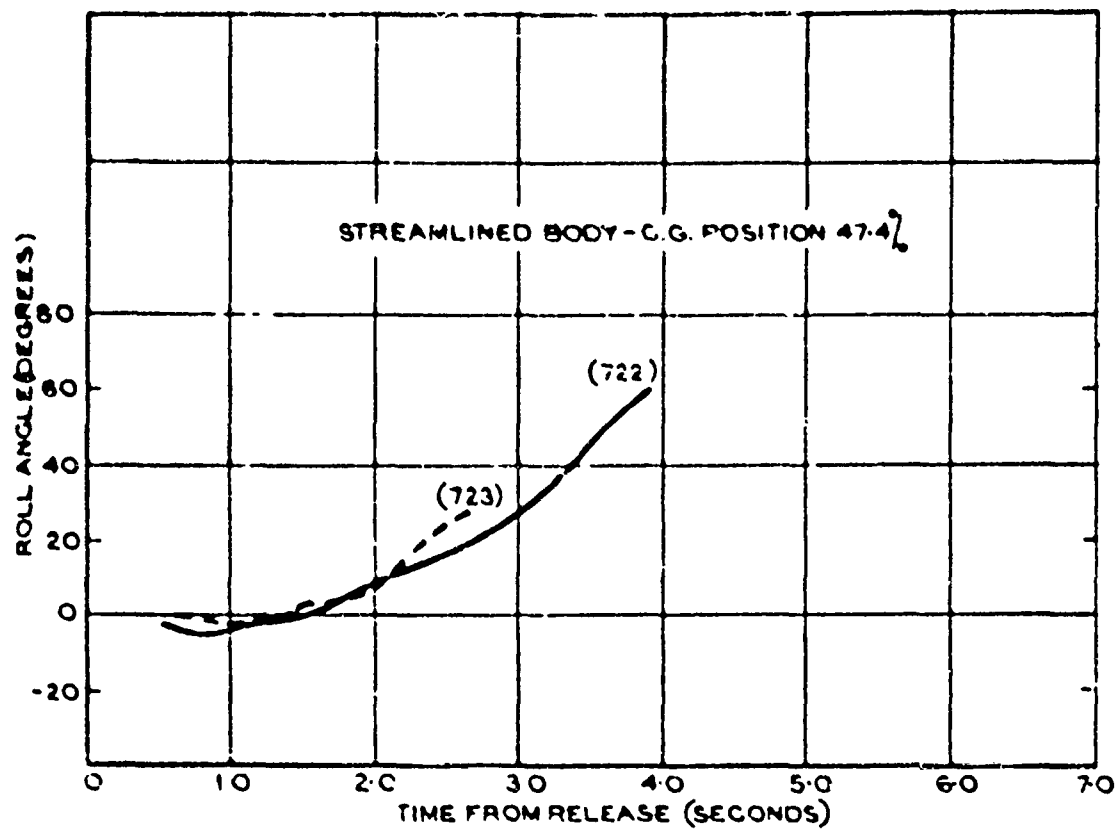


(a) Variation of roll angle with time from release

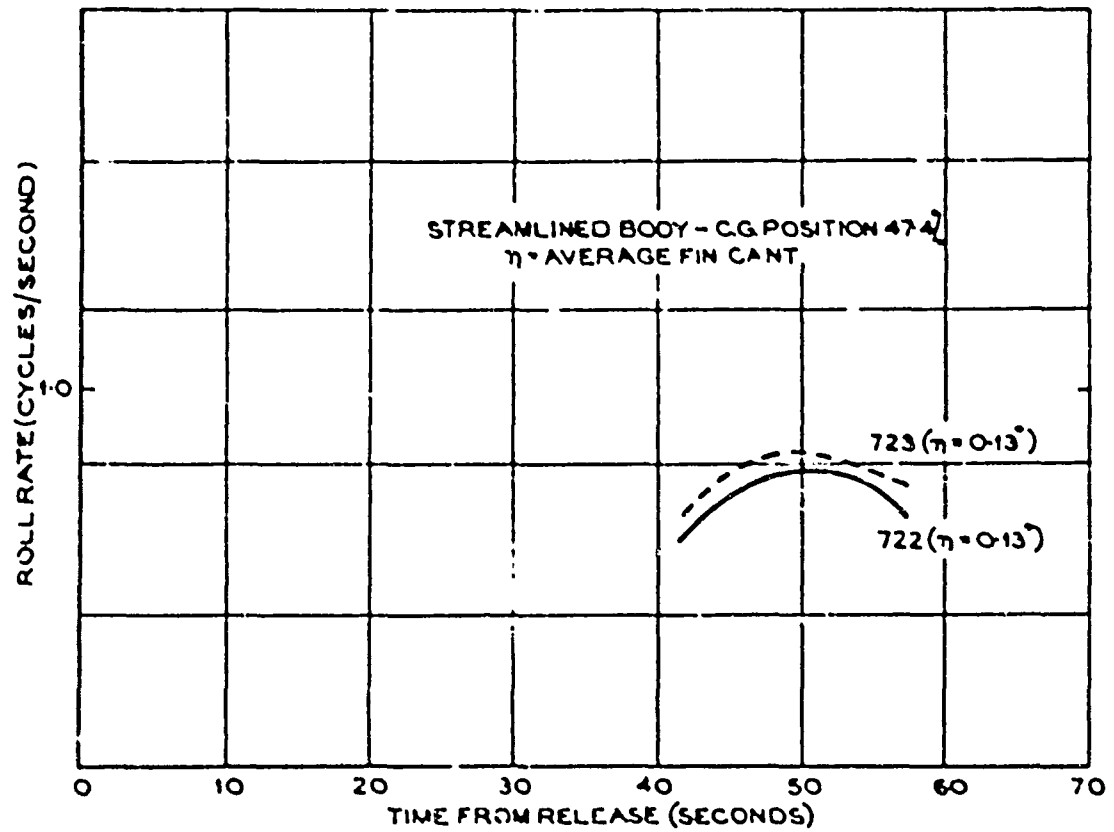


(b) Variation of roll rate with time from release

FIGURE 37. ROLL HISTORIES OF ROUND NUMBERS 703, 706, 707 AND 713

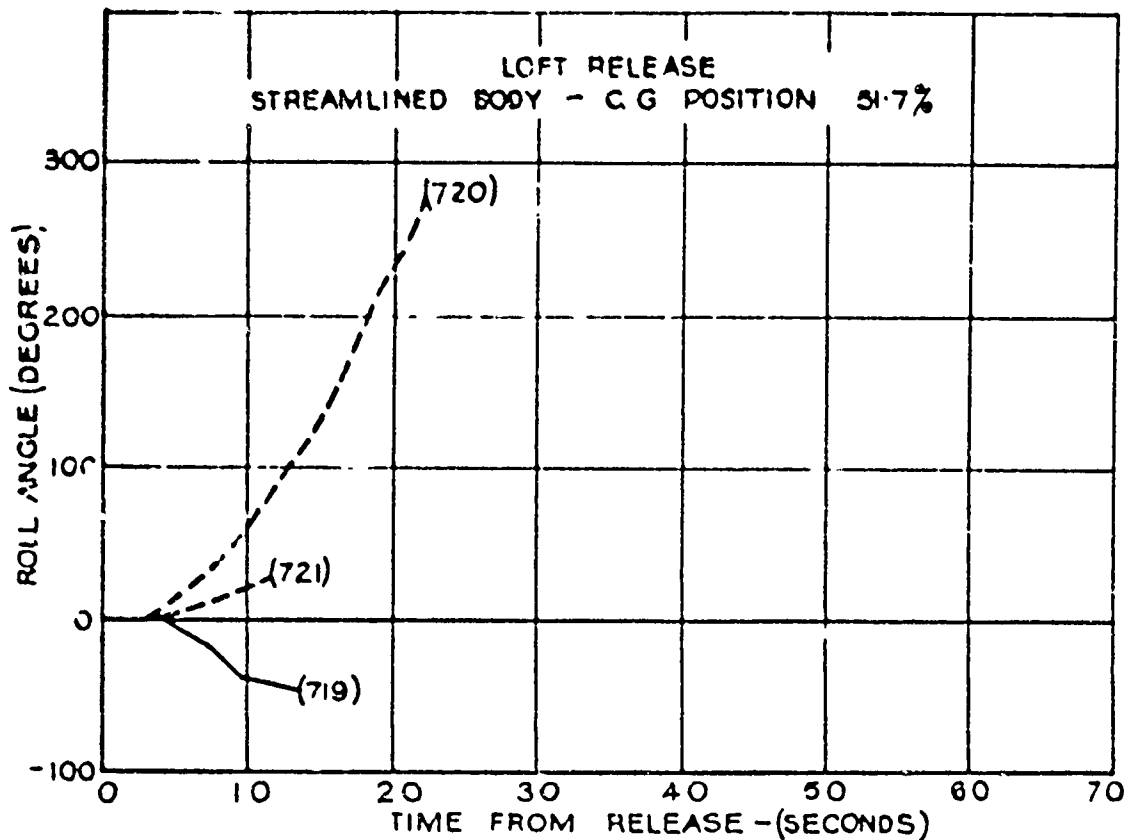


(a) Variation of roll angle with time from release

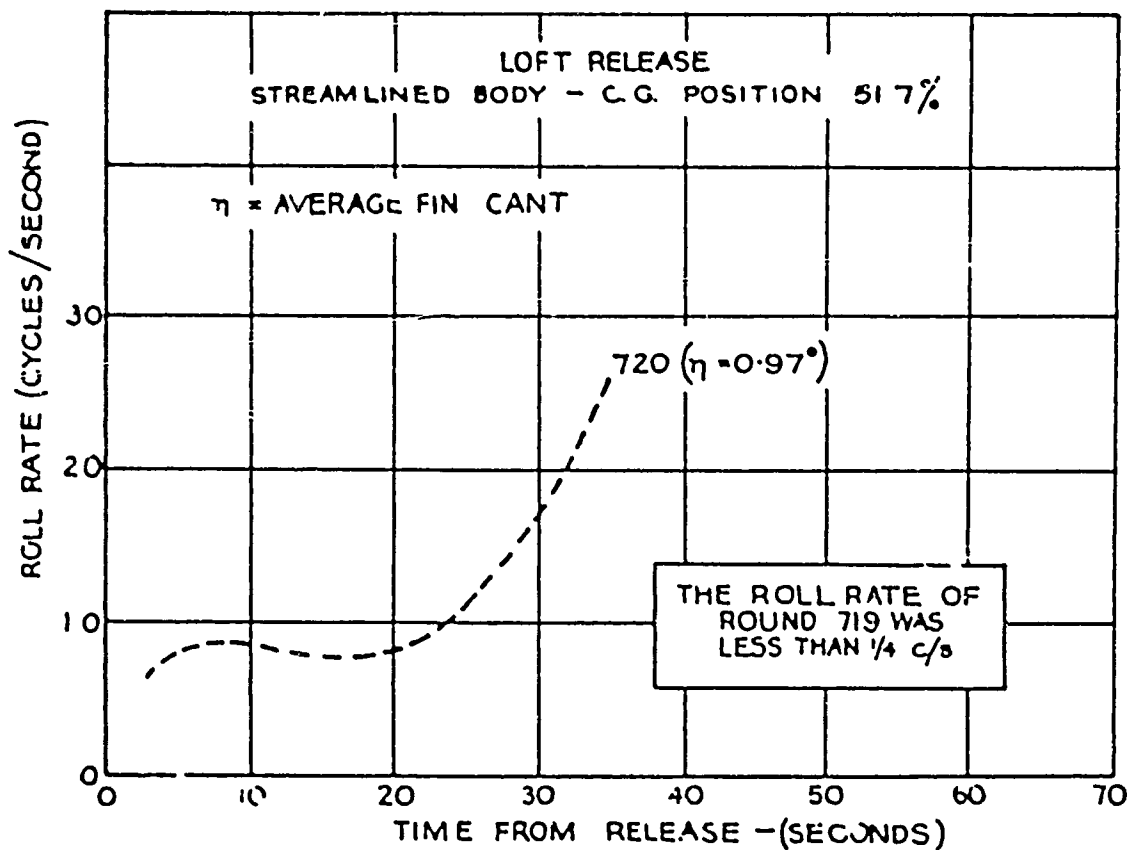


(b) Variation of roll rate with time from release

FIGURE 38. ROLL HISTORIES OF ROUND NUMBERS 722 AND 723



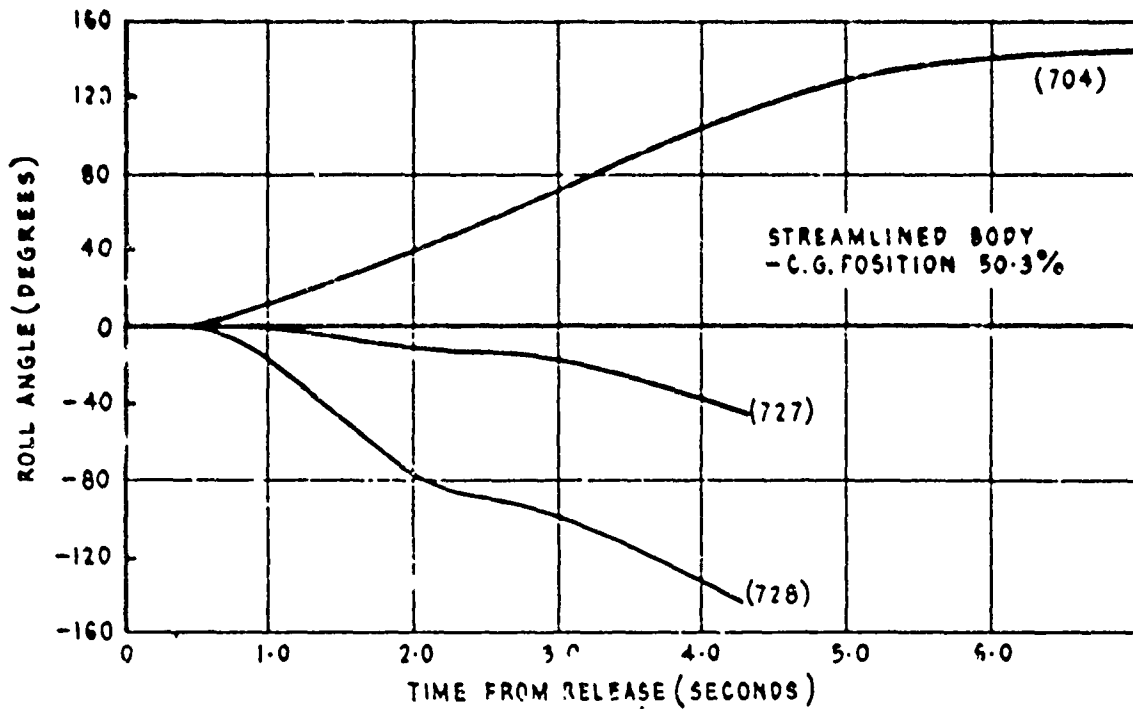
(a) Variation of roll angle with time from release



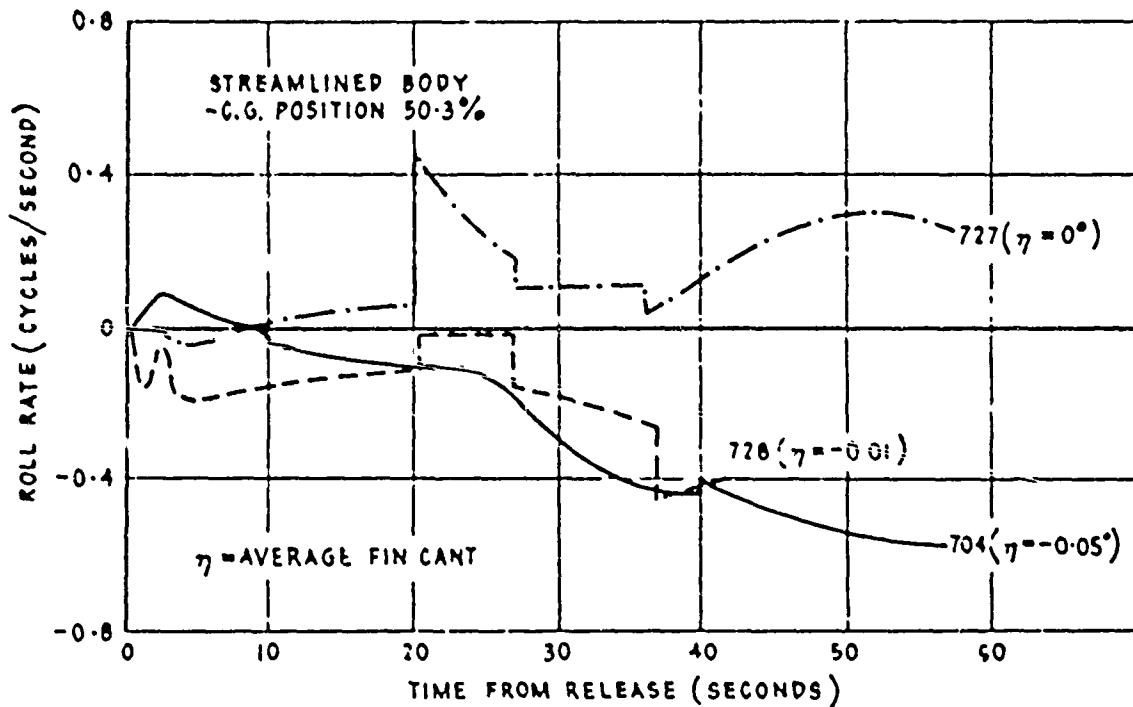
(b) Variation of roll rate with time from release

FIGURE 39. ROLL HISTORIES OF ROUND NUMBERS 719, 720 AND 721

Figure 40

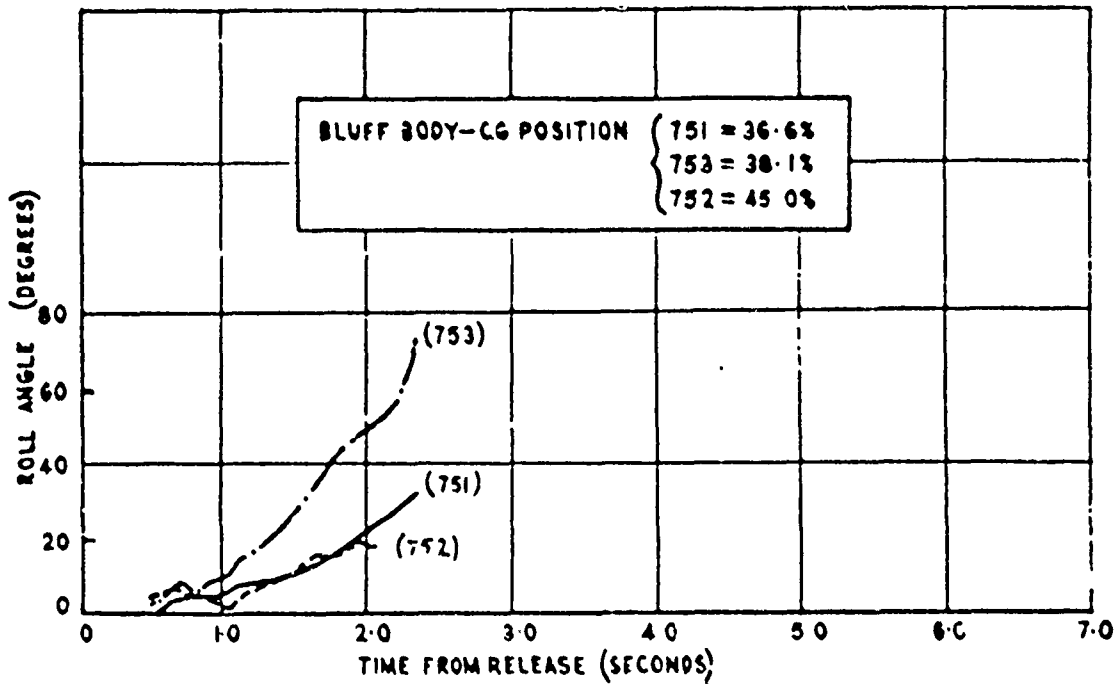


(a) Variation of roll angle with time from release

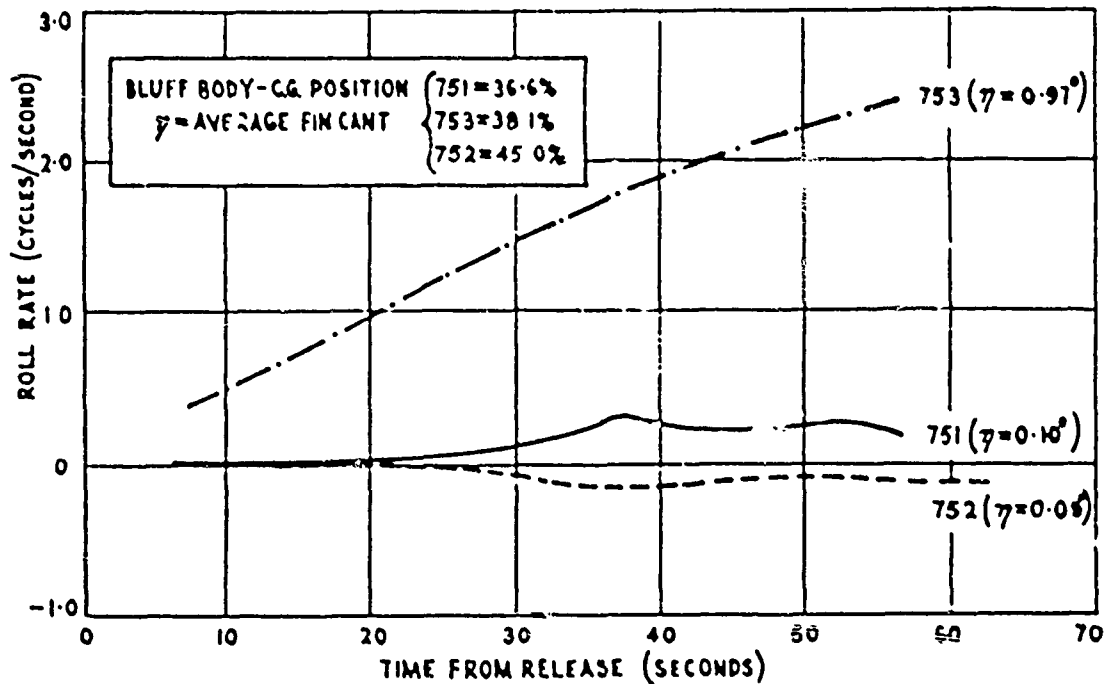


(b) Variation of roll rate with time from release

FIGURE 40. ROLL HISTORIES OF ROUND NUMBERS 704, 727 AND 728



(a) Variation of roll angle with time from release



(b) Variation of roll rate with time from release

FIGURE 41. ROLL HISTORIES OF ROUND NUMBERS 751, 752 AND 753

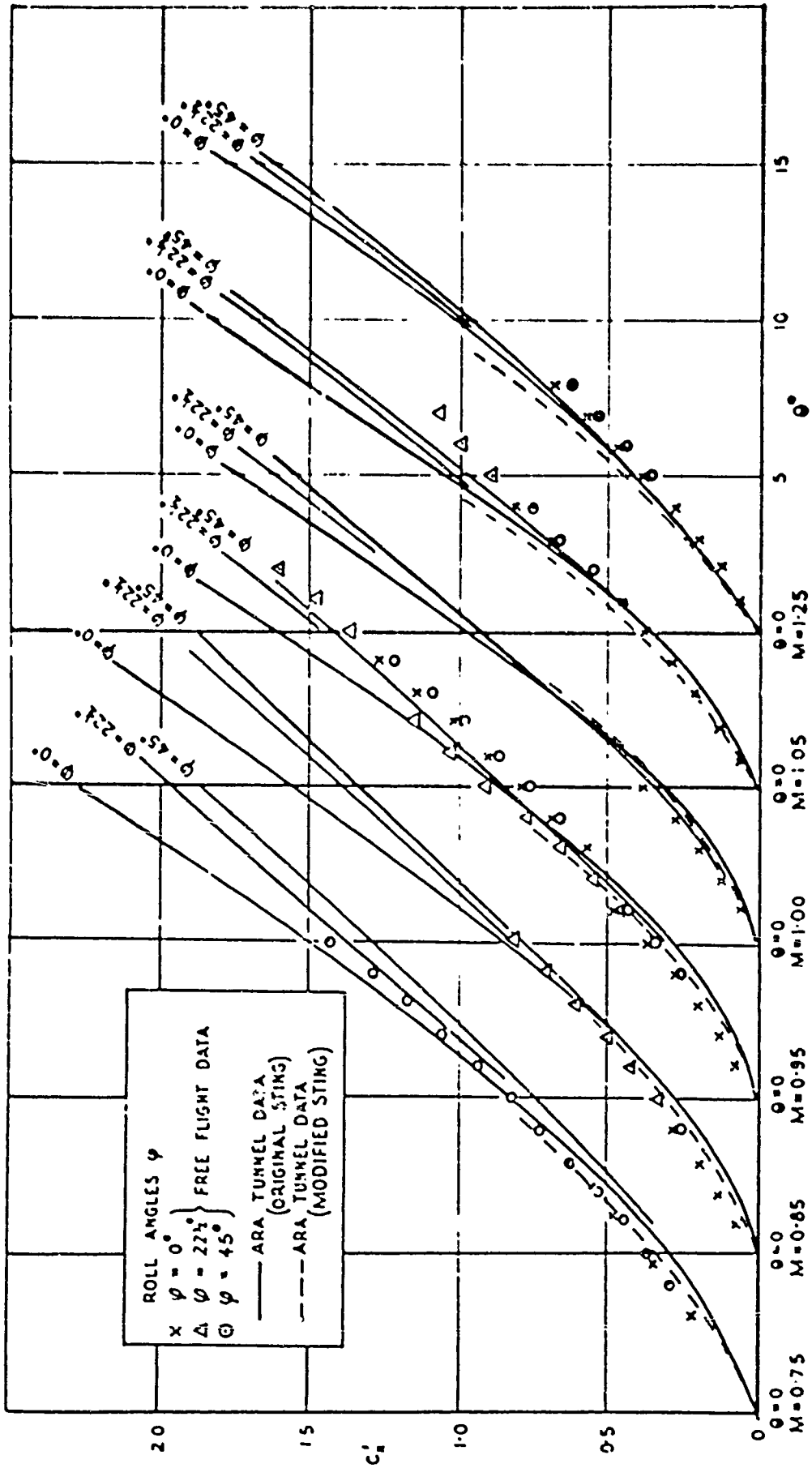


FIGURE 1.2. COMPARISON OF FREE FLIGHT AND WIND TUNNEL MEASUREMENTS; VARIATION OF NORMAL FORCE WITH INCIDENCE θ , ROLL ATTITUDE ϕ AND MACH NUMBER M FOR THE M557A BODY

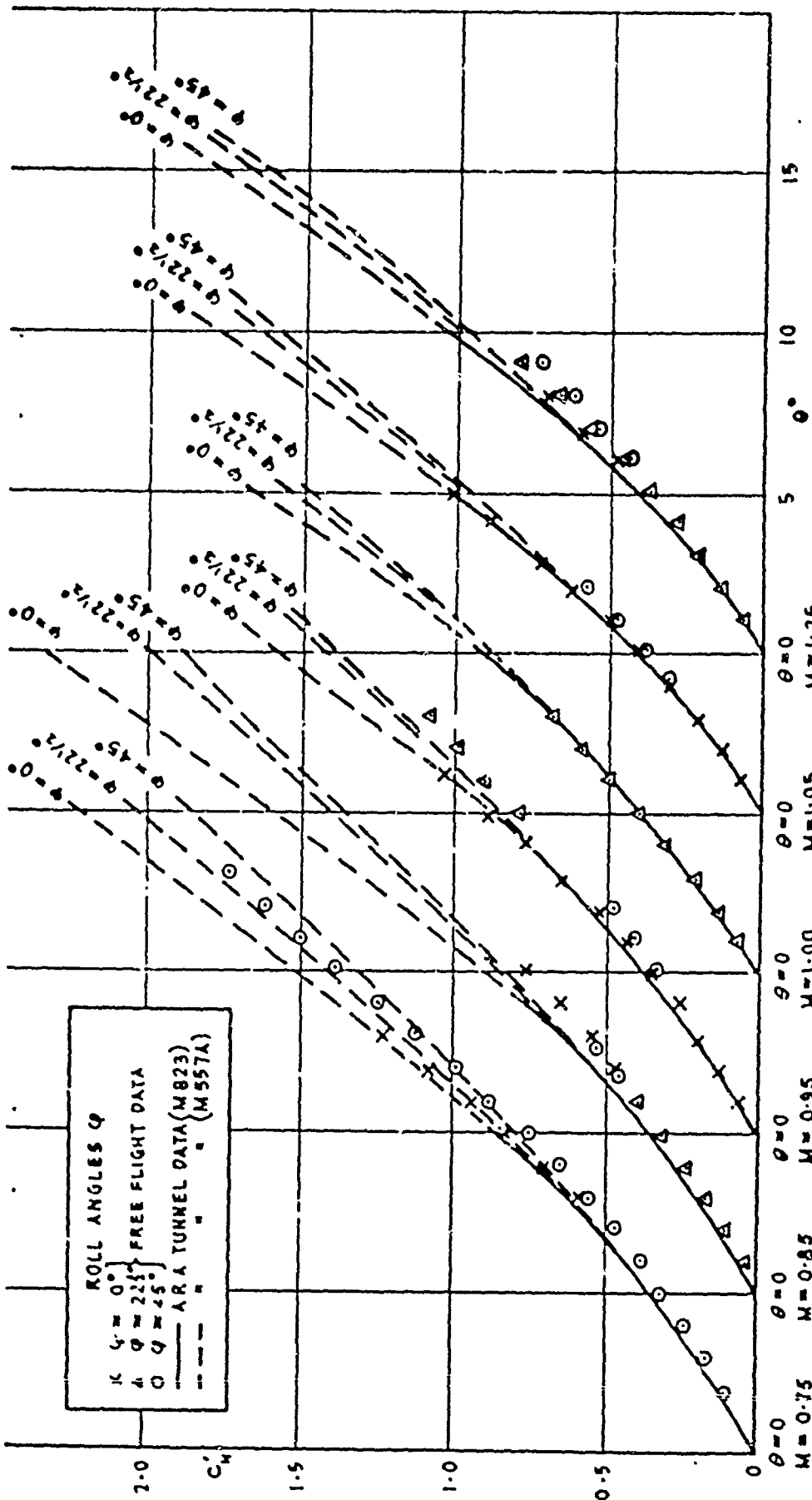


FIGURE 43. COMPARISON OF FREE FLIGHT AND WIND TUNNEL MEASUREMENTS: VARIATION OF NORMAL FORCE WITH INCIDENCE θ , ROLL ATTITUDE ϕ AND MACH NUMBER M FOR M823 BODY

Figure 44

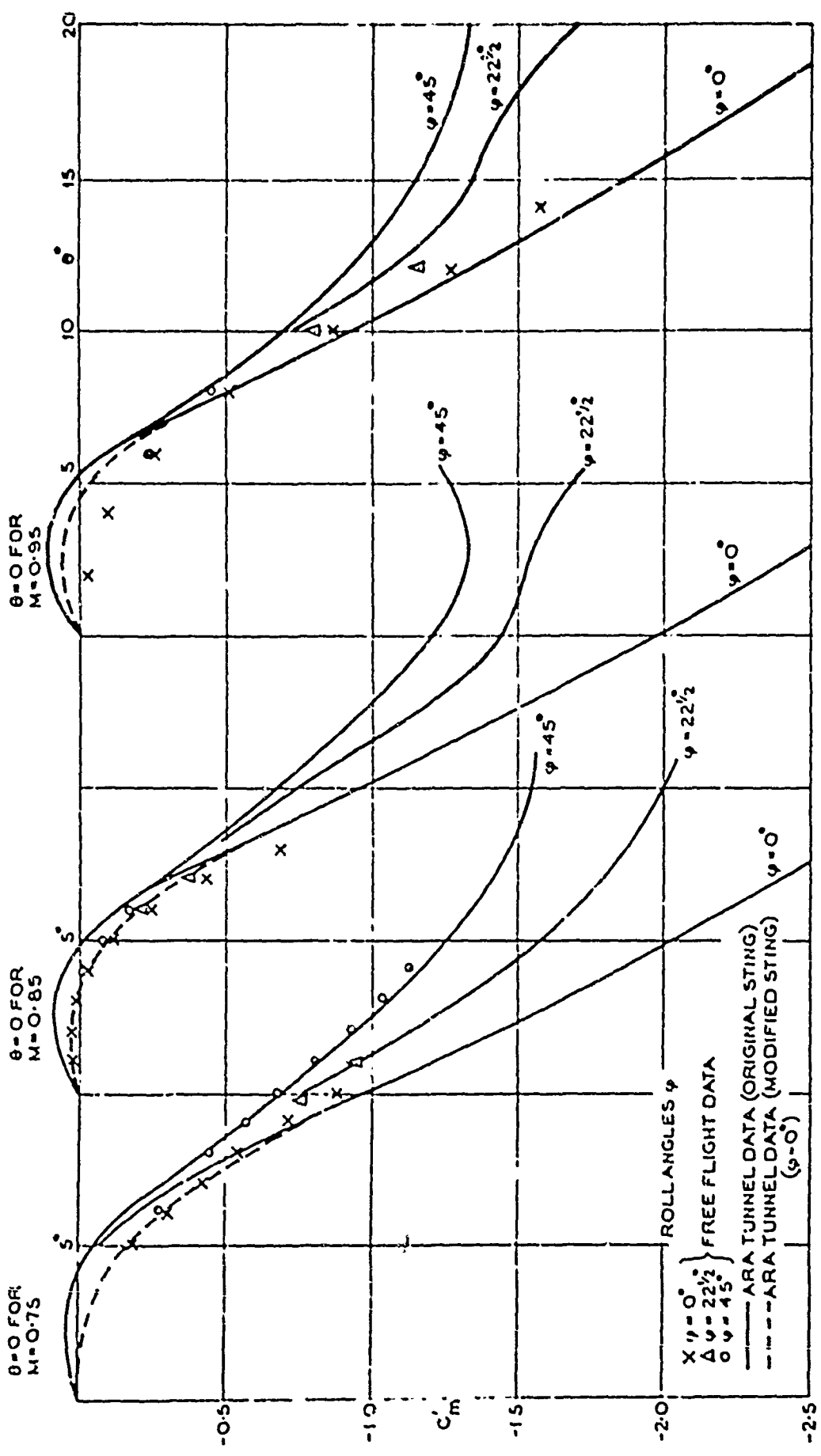


FIGURE 44. COMPARISON OF FREE FLIGHT AND WIND TUNNEL MEASUREMENTS: VARIATION OF RESTORING MOMENT WITH INCIDENCE θ , ROLL ATTITUDE ψ , AND MACH NUMBER M FOR THE V557A BODY

UNCLASSIFIED

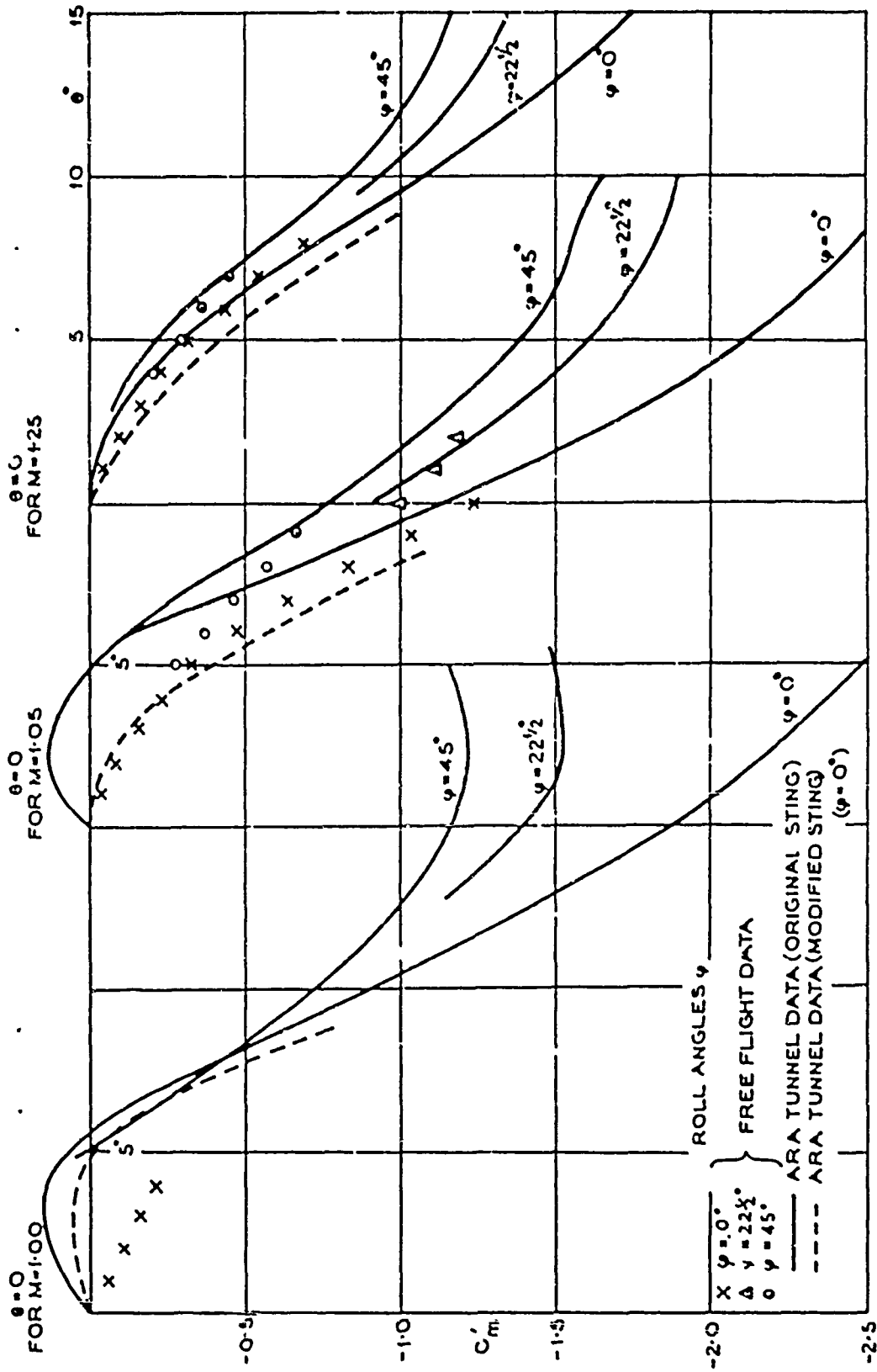


FIGURE 44 (Contd). COMPARISON OF FREE FLIGHT AND WIND TUNNEL MEASUREMENTS:
 VARIATION OF RESTORING MOMENT WITH INCIDENCE θ , ROLL ATTITUDE ϕ
 AND MACH NUMBER M FOR THE M557A BODY

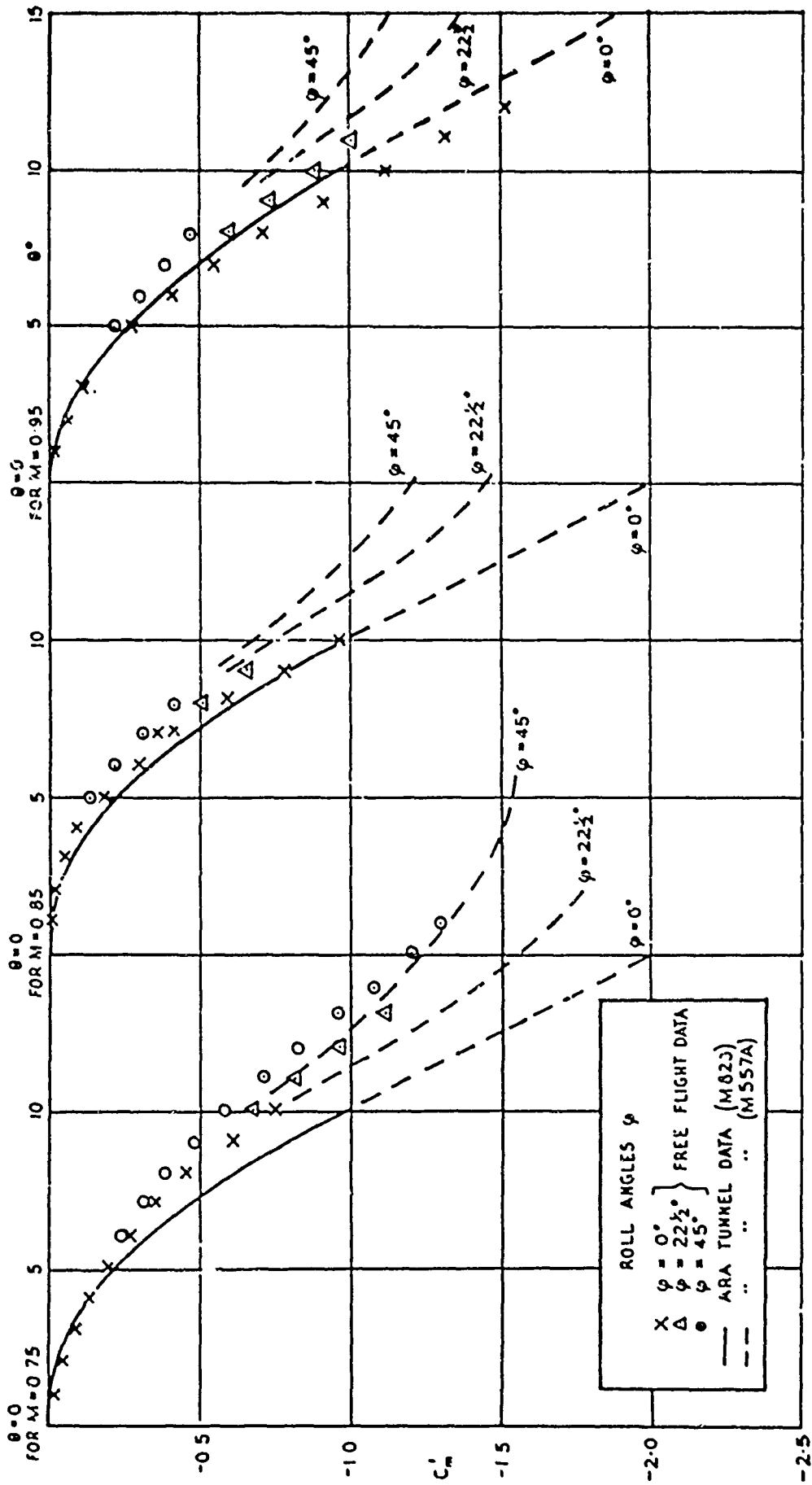


FIGURE 45. COMPARISON OF FREE FLIGHT AND WIND TUNNEL MEASUREMENTS: VARIATION OF RESTORING MOMENT WITH INCIDENCE θ , ROLL ATTITUDE ϕ AND MACH NUMBER M FOR THE M823 BODY

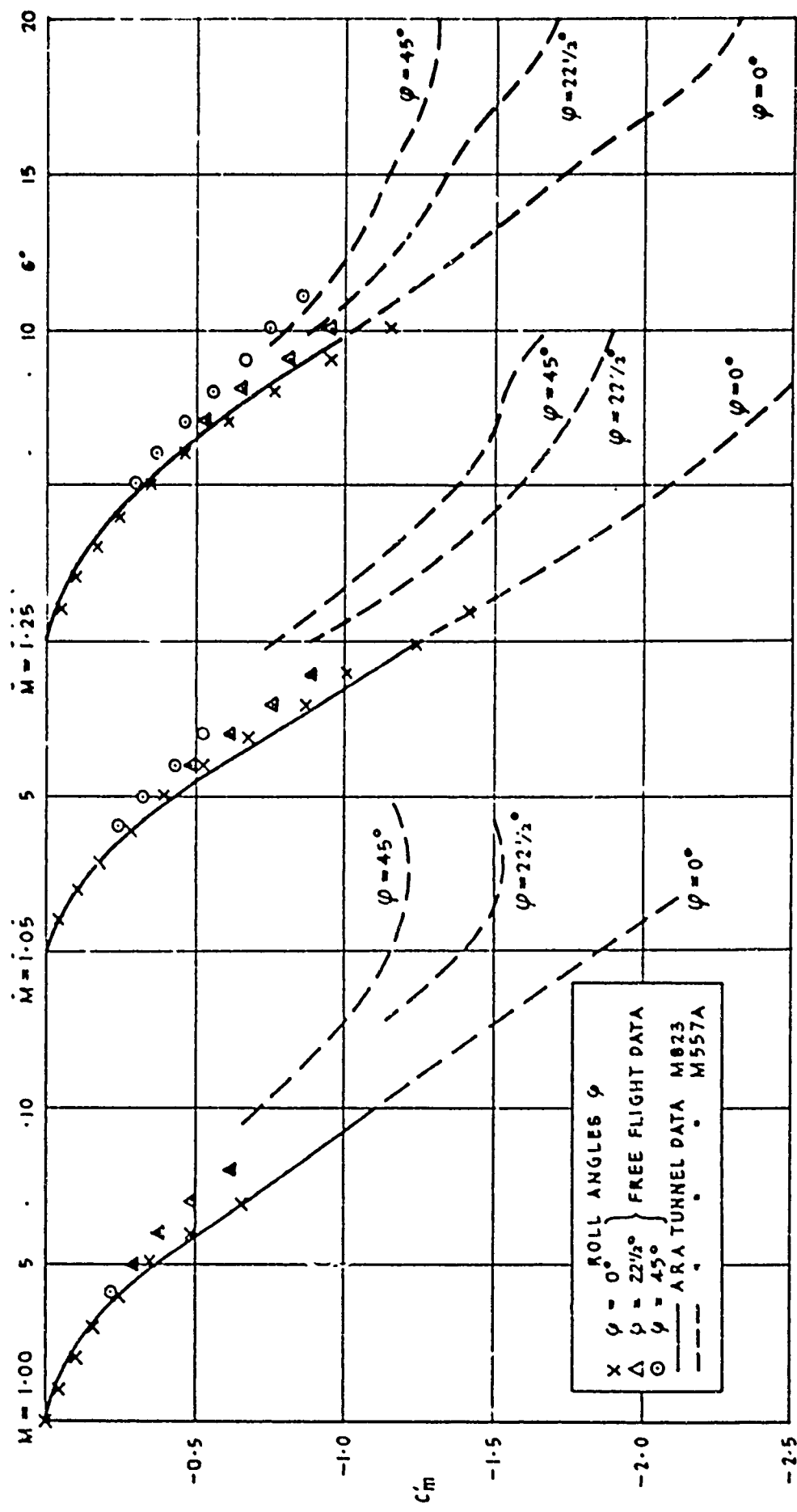


FIGURE 45 (Contd). COMPARISON OF FREE FLIGHT AND WIND TUNNEL MEASUREMENTS: VARIATION OF RESTORING MOMENT WITH INCIDENCE θ , ROLL ATTITUDE ϕ AND MACH NUMBER M FOR THE M823 BODY

Figure 46

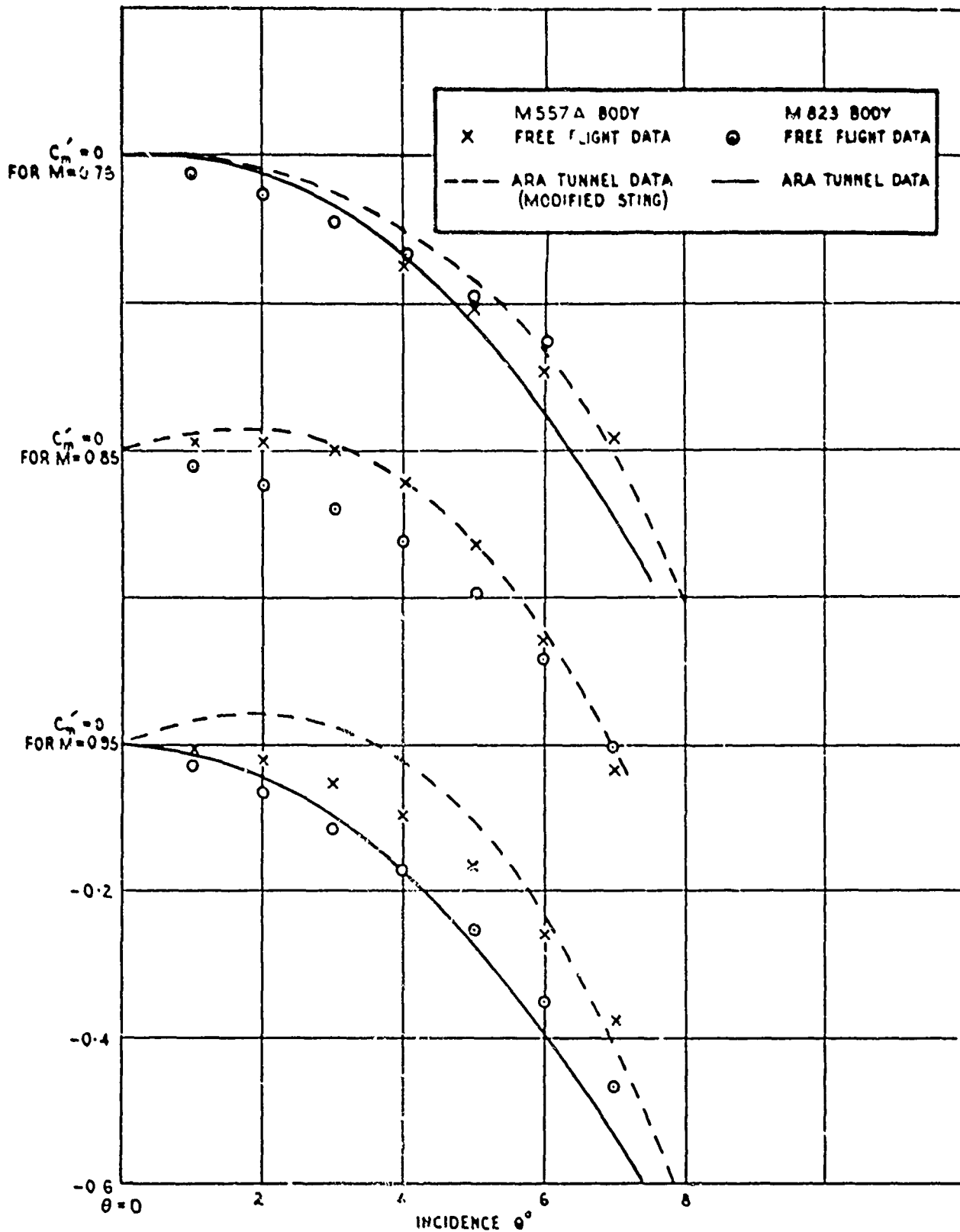


FIGURE 46. COMPARISON OF WIND TUNNEL AND FREE FLIGHT MEASUREMENTS: CHANGE IN RESTORING MOMENT WITH CHANGE OF BODY SHAPE AT LOW INCIDENCE FOR VARIOUS MACH NUMBERS ($\varphi = 0$)

UNCLASSIFIED

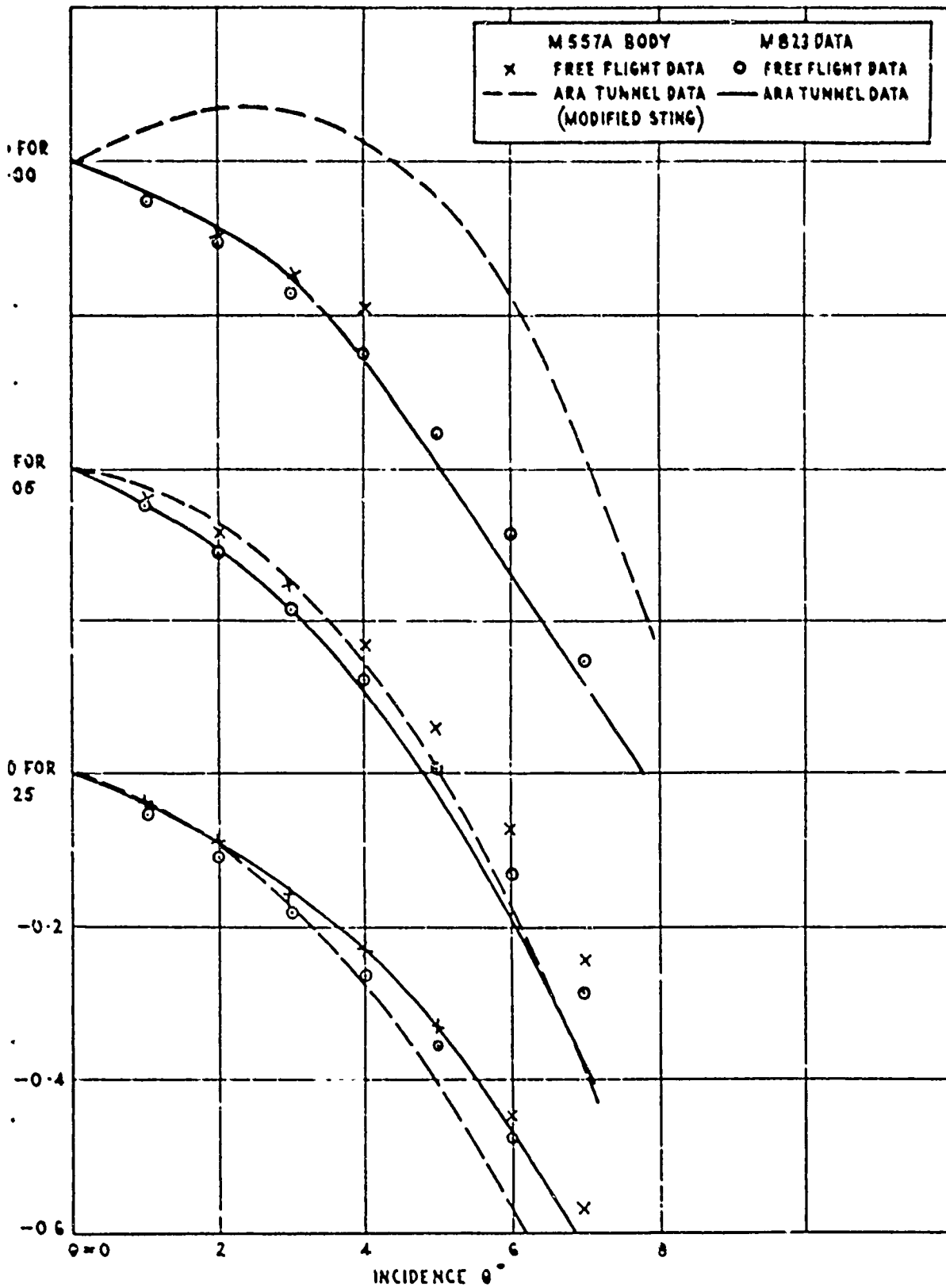


FIGURE 46 (Contd). COMPARISON OF WIND TUNNEL AND FREE FLIGHT MEASUREMENTS: CHANGE IN RESTORING MOMENT WITH CHANGE OF BODY SHAPE AT LOW INCIDENCE FOR VARIOUS MACH NUMBERS ($\phi = 0$)

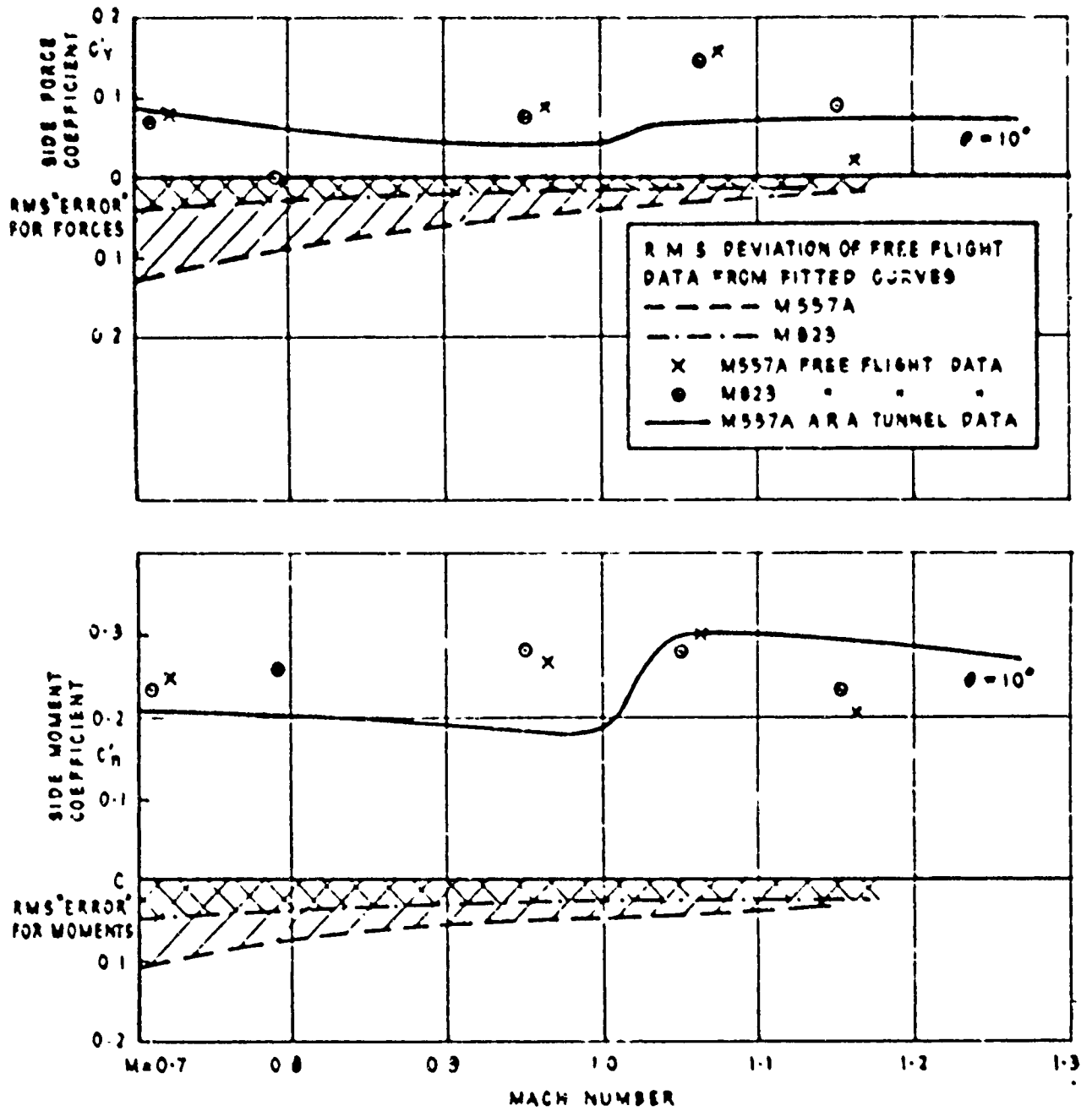


FIGURE 47. COMPARISON OF FREE FLIGHT AND WIND TUNNEL MEASUREMENTS: VARIATION OF INDUCED SIDE FORCE ($\theta = 10^\circ$) AND SIDE MOMENT ($\theta = 10^\circ$) WITH MACH NUMBER

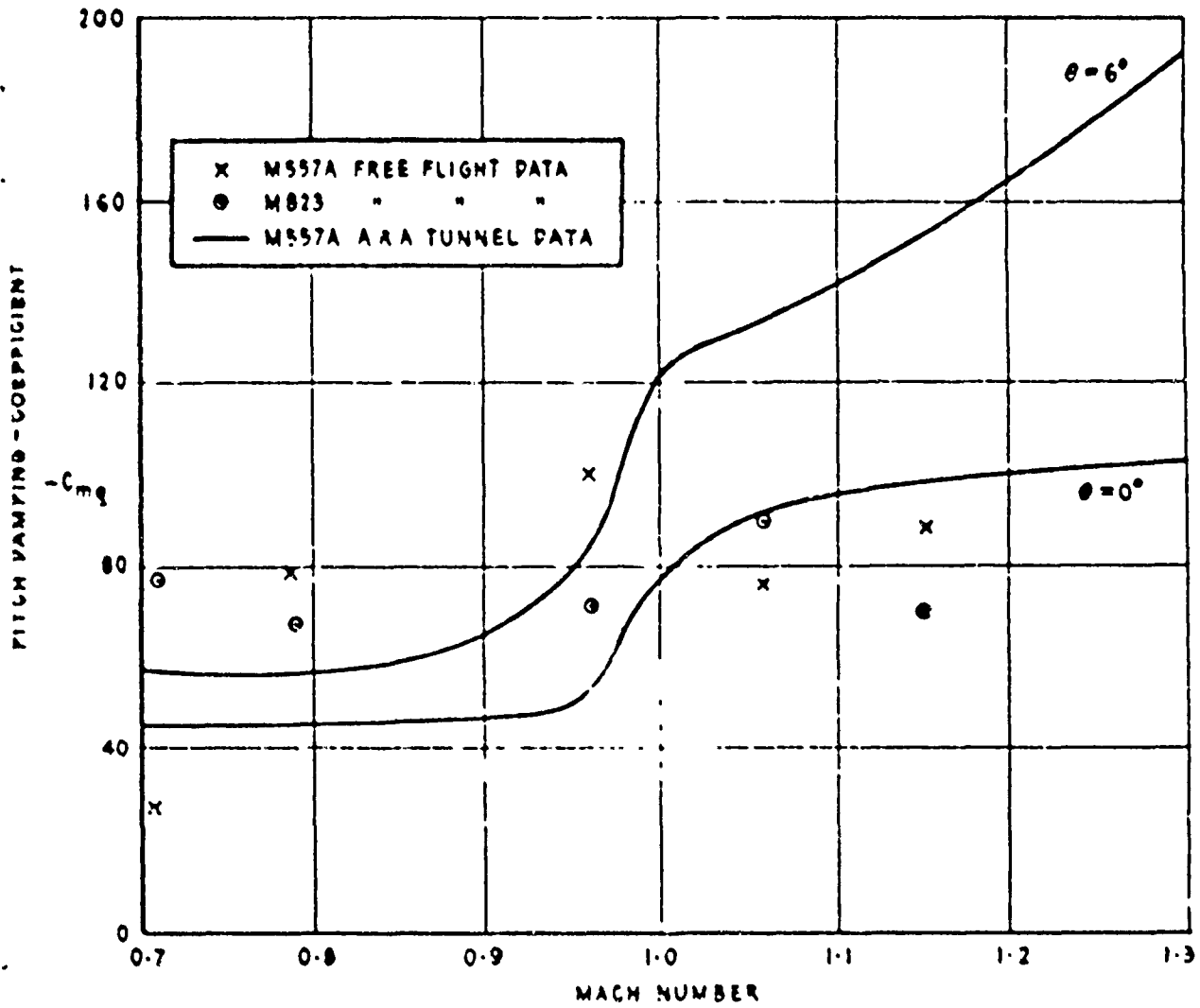


FIGURE 48. COMPARISON OF FREE FLIGHT AND WIND TUNNEL MEASUREMENTS: VARIATION OF PITCH DAMPING WITH MACH NUMBER

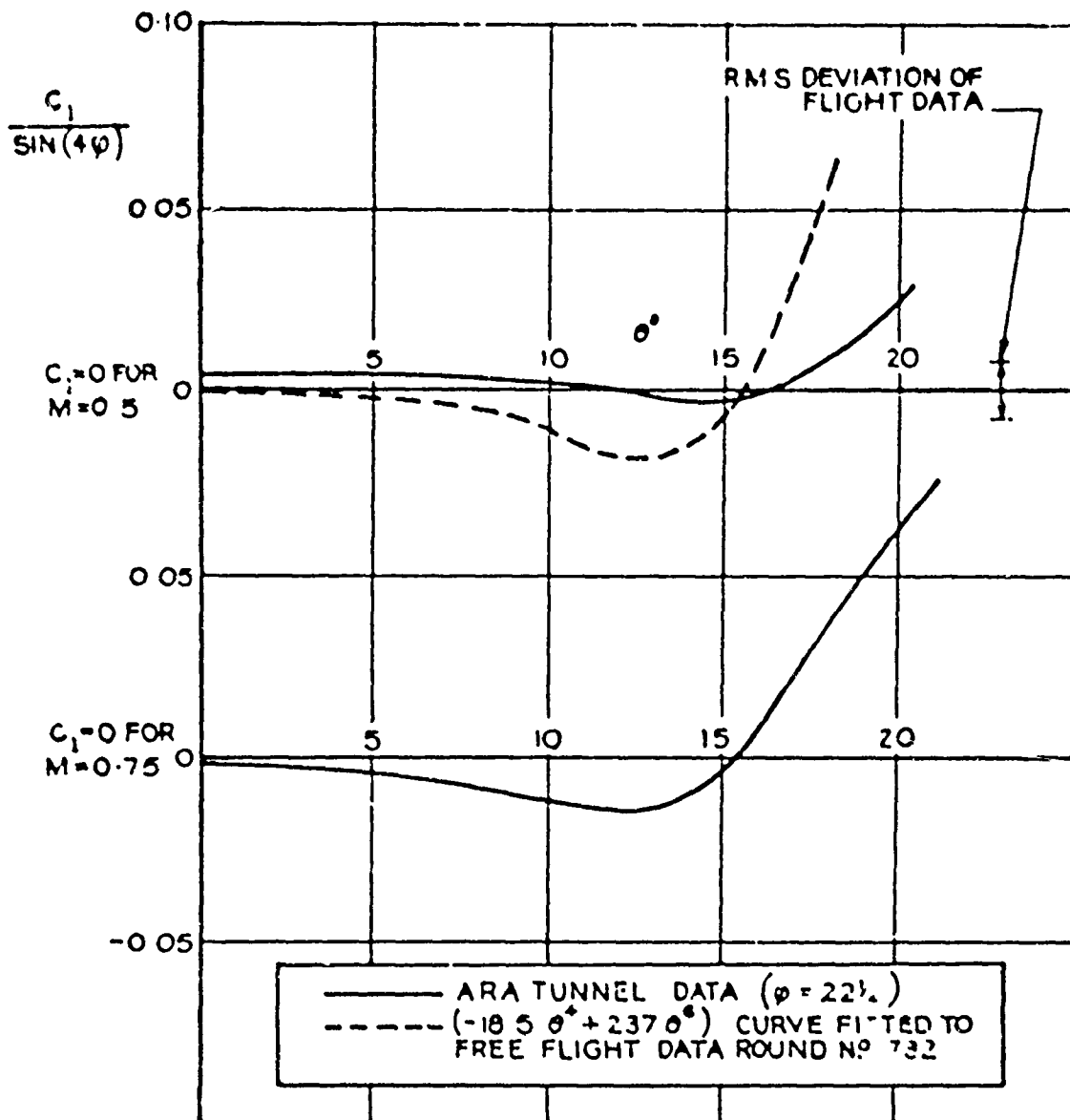


FIGURE 49. COMPARISON OF FREE FLIGHT AND WIND TUNNEL MEASUREMENTS: INDUCED ROLLING MOMENT AT $\phi = 22\frac{1}{2}^\circ$, $M = 0.5$ (M557A BODY)

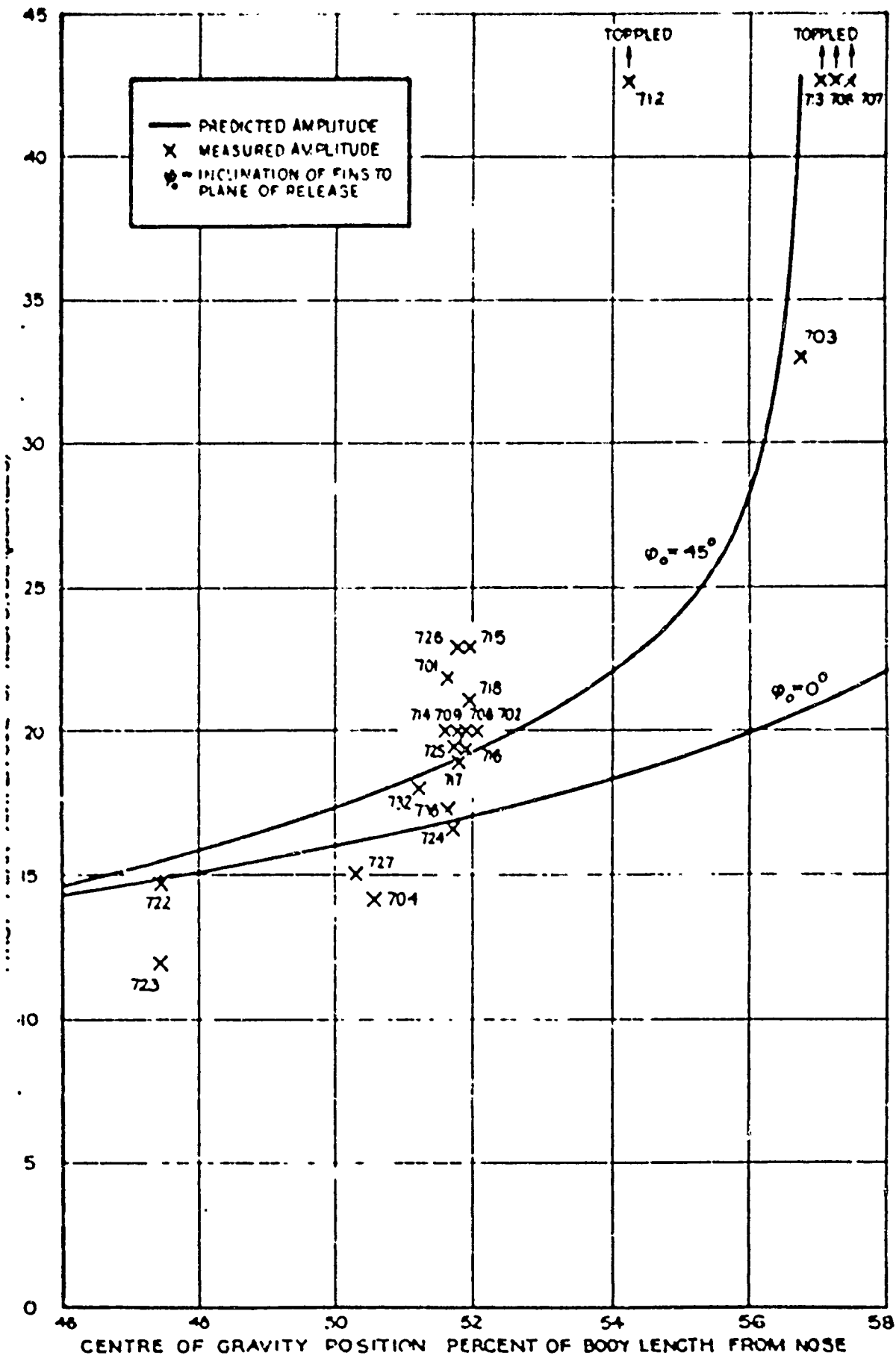


FIGURE 50. RELEASE DISTURBANCE FOR THE M557A BODY SHAPE: COMPARISON OF MEASURED AND PREDICTED FIRST PEAK AMPLITUDES

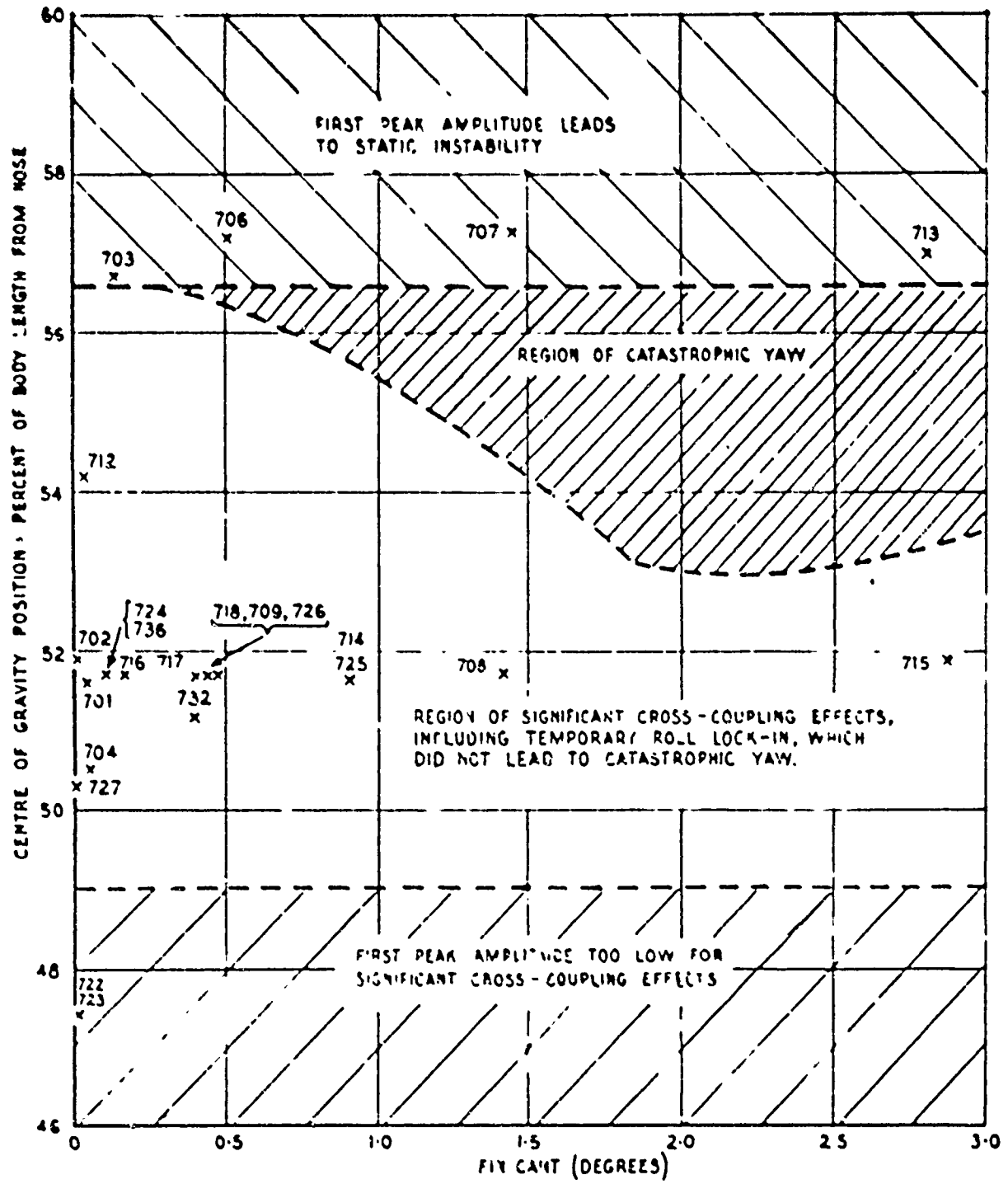


FIGURE 51. BOUNDARIES OF DYNAMIC BEHAVIOUR DURING RESPONSE TO RELEASE DISTURBANCE AS FUNCTIONS OF C.G. POSITION AND FIN CANT (M557A BODY SHAPE $\epsilon_0 = -5^\circ$)

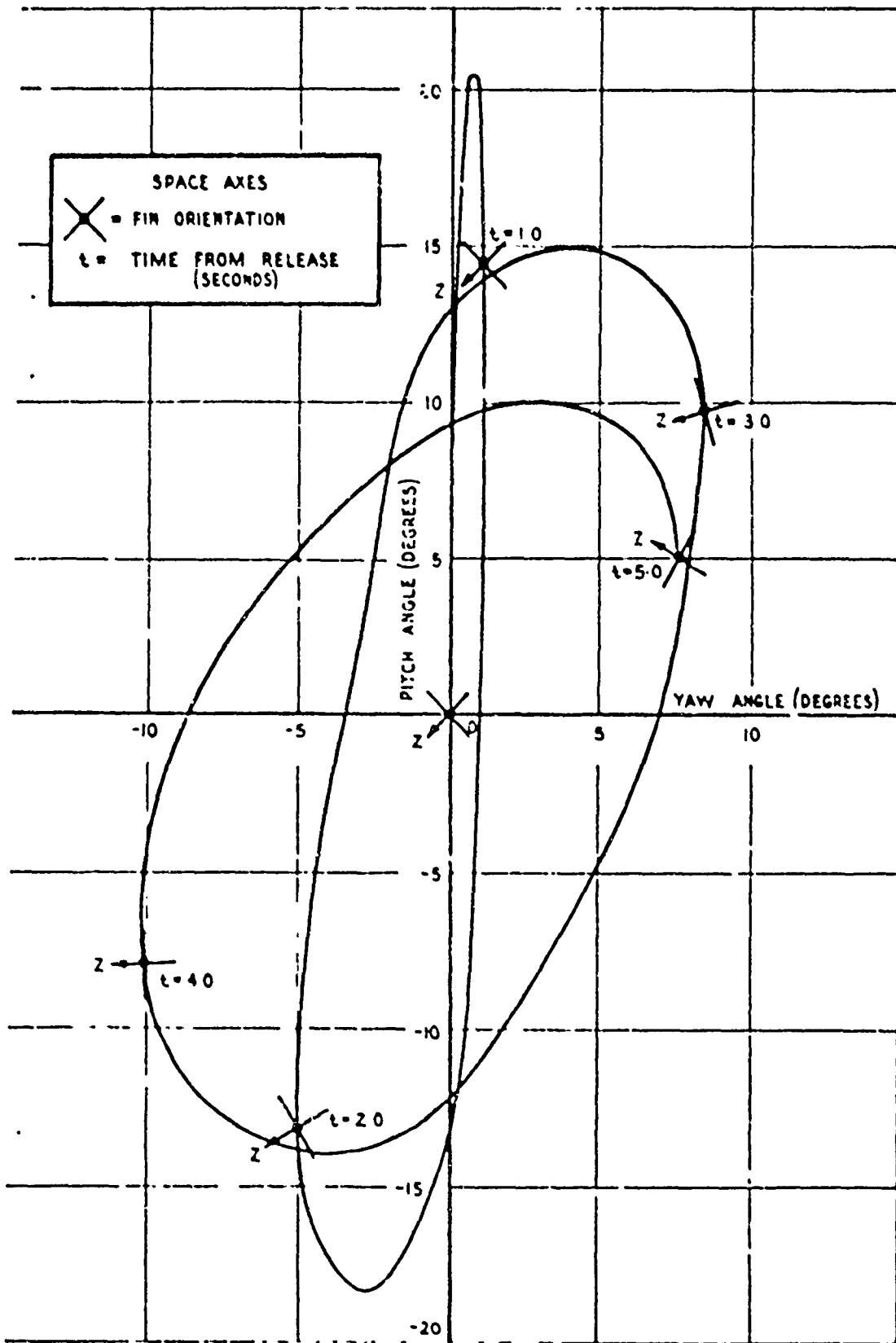


FIGURE 52(a). TYPICAL COMPUTED RESPONSE TO RELEASE DISTURBANCE: M557A BODY SHAPE WITH C.G. AT 51.7%, $\tau = 0.17^0$ AND $\tau_0 = 45^0$

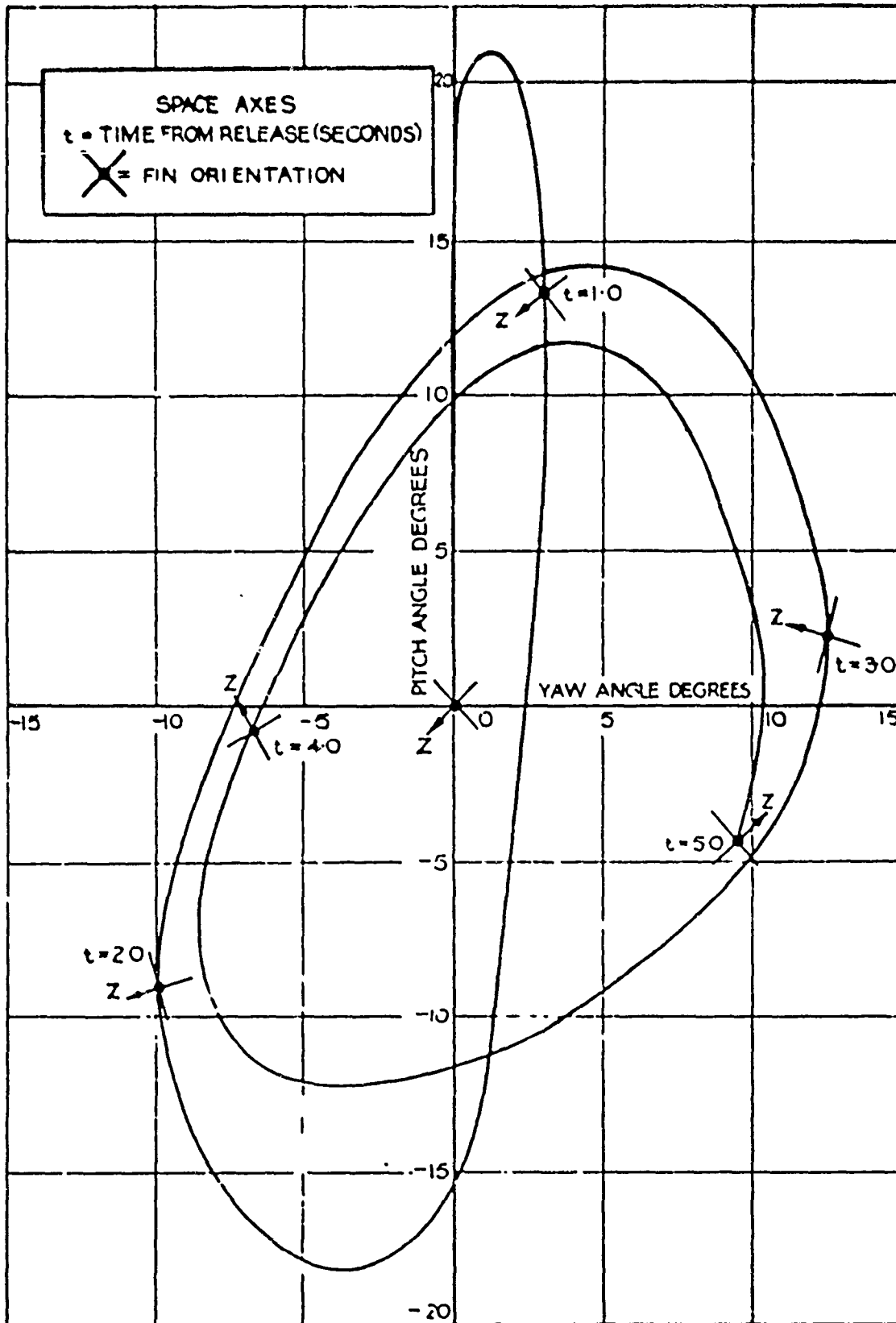
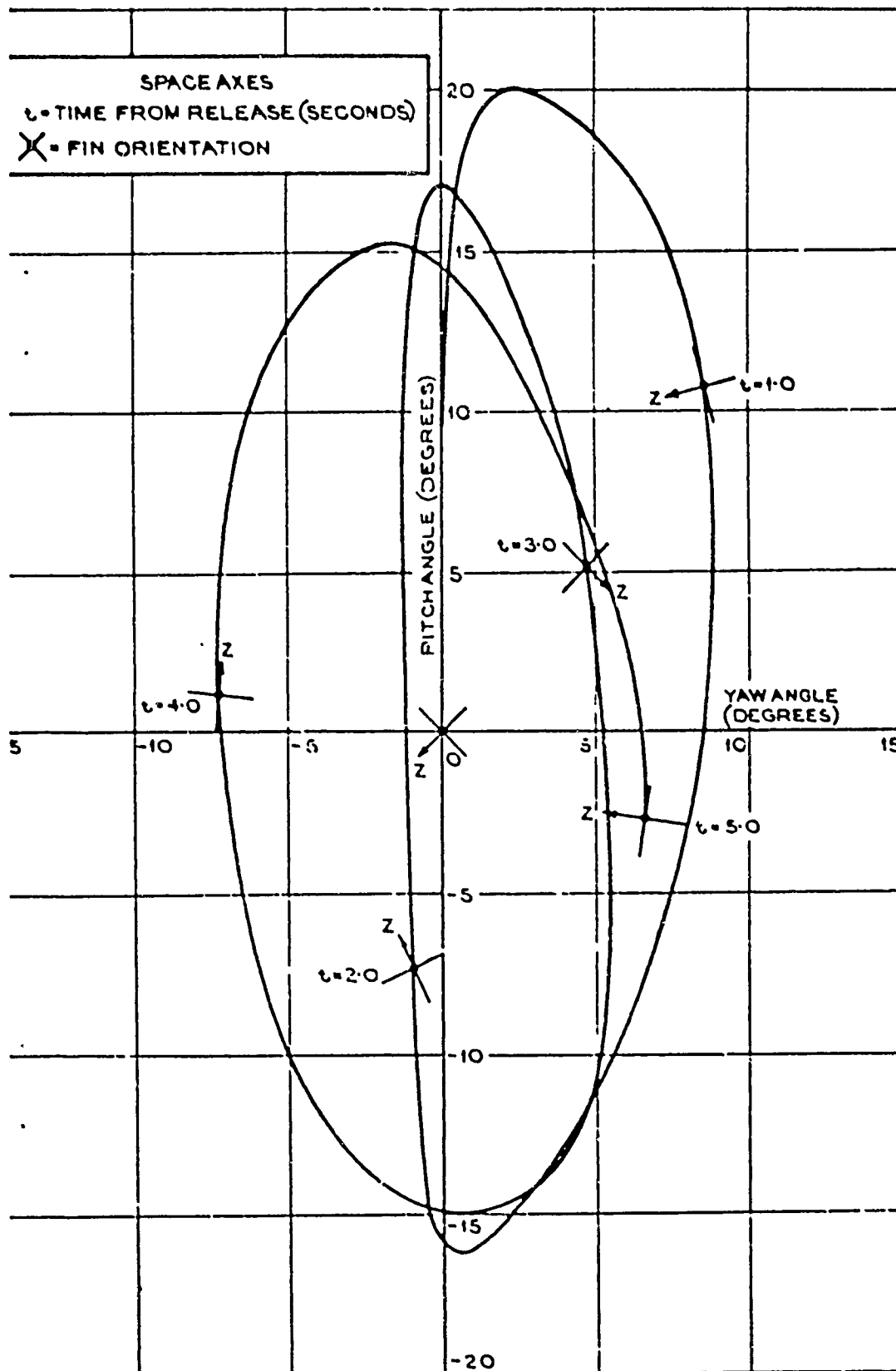


FIGURE 52(b). TYPICAL COMPUTED RESPONSE TO RELEASE DISTURBANCE: M557A BODY SHAPE WITH C.G. AT 51.1° , $\eta = 0.44$ AND $\phi_0 = 45^\circ$



RE 52(c). TYPICAL COMPUTED RESPONSE TO RELEASE DISTURBANCES: M557A PODY
 SHAPE WITH C.G. AT 51.7% , $\eta = 1.41^\circ$ AND $\varphi_0 = 45^\circ$

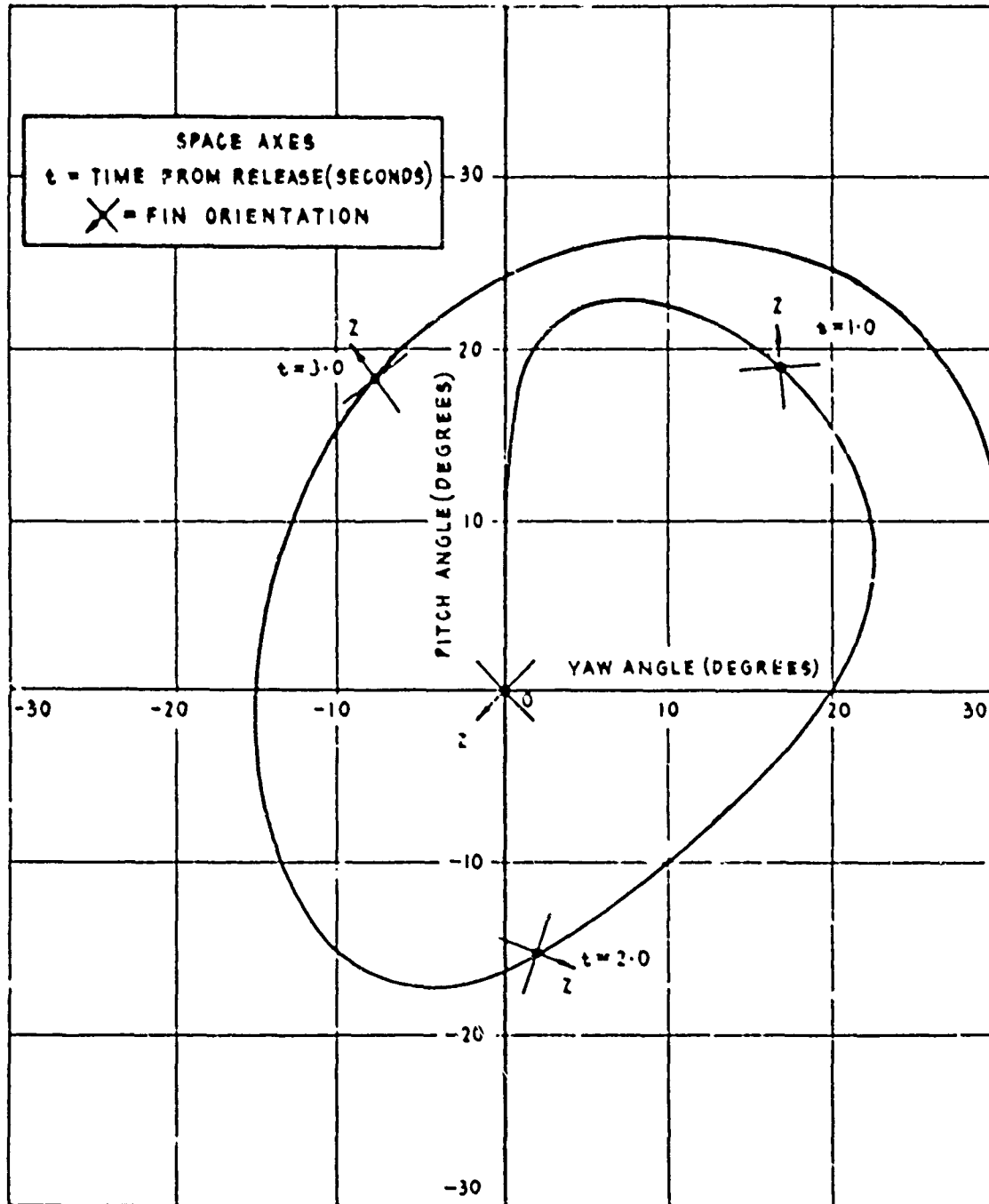


FIGURE 52(d). TYPICAL COMPUTED RESPONSE TO RELEASE DISTURBANCE: X557A BODY SHAPE WITH C.G. AT $55.5\bar{r}$, $\eta = 2.0^\circ$ AND $\varphi_0 = 45^\circ$

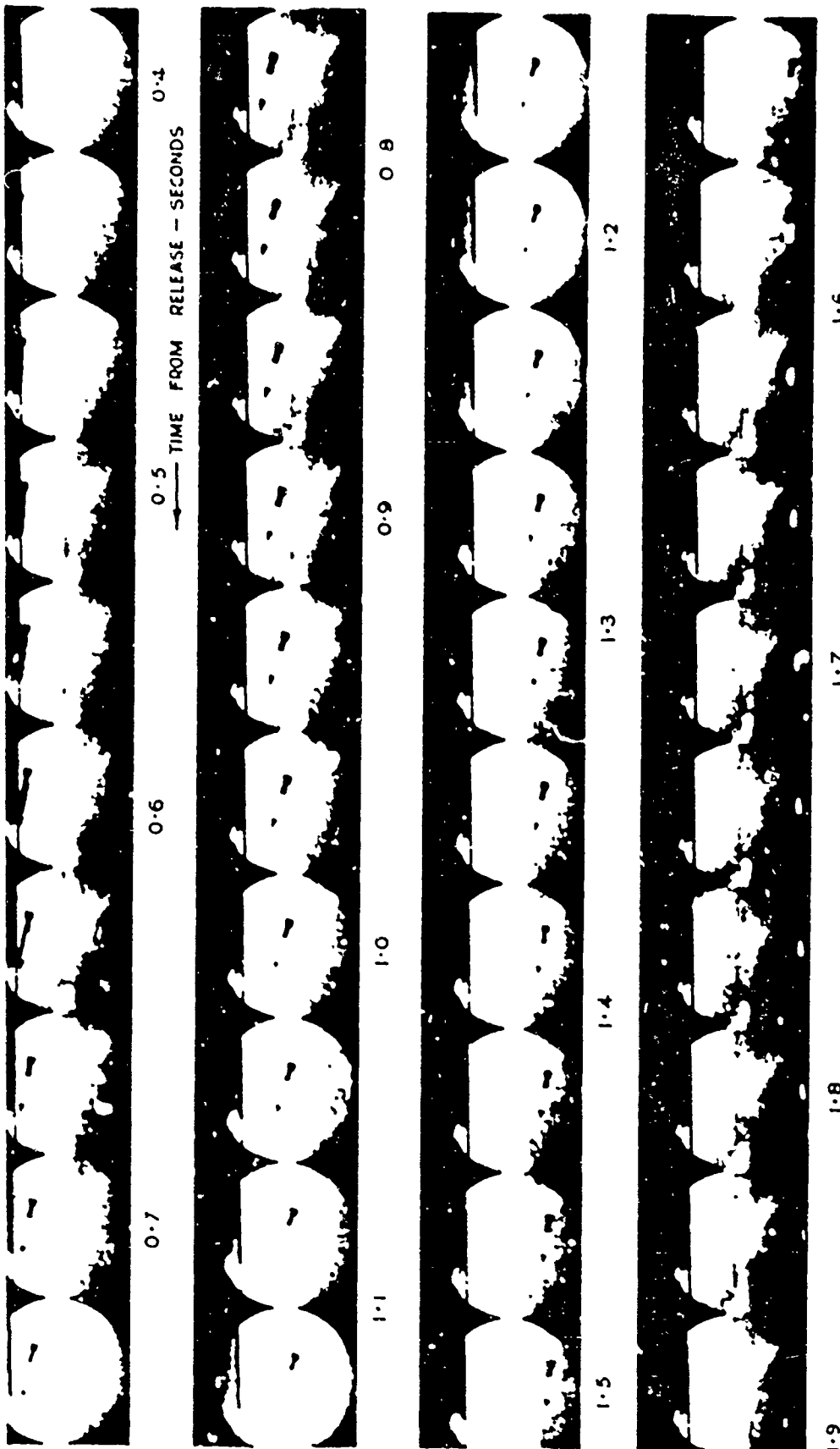


FIGURE 53(a). WING TIP CAMERA RECORD OF M57A BOMB - CLEAN RELEASE
(ROUND NO. 708 RELEASED FROM 46100 FT AT M = 0.69)

154

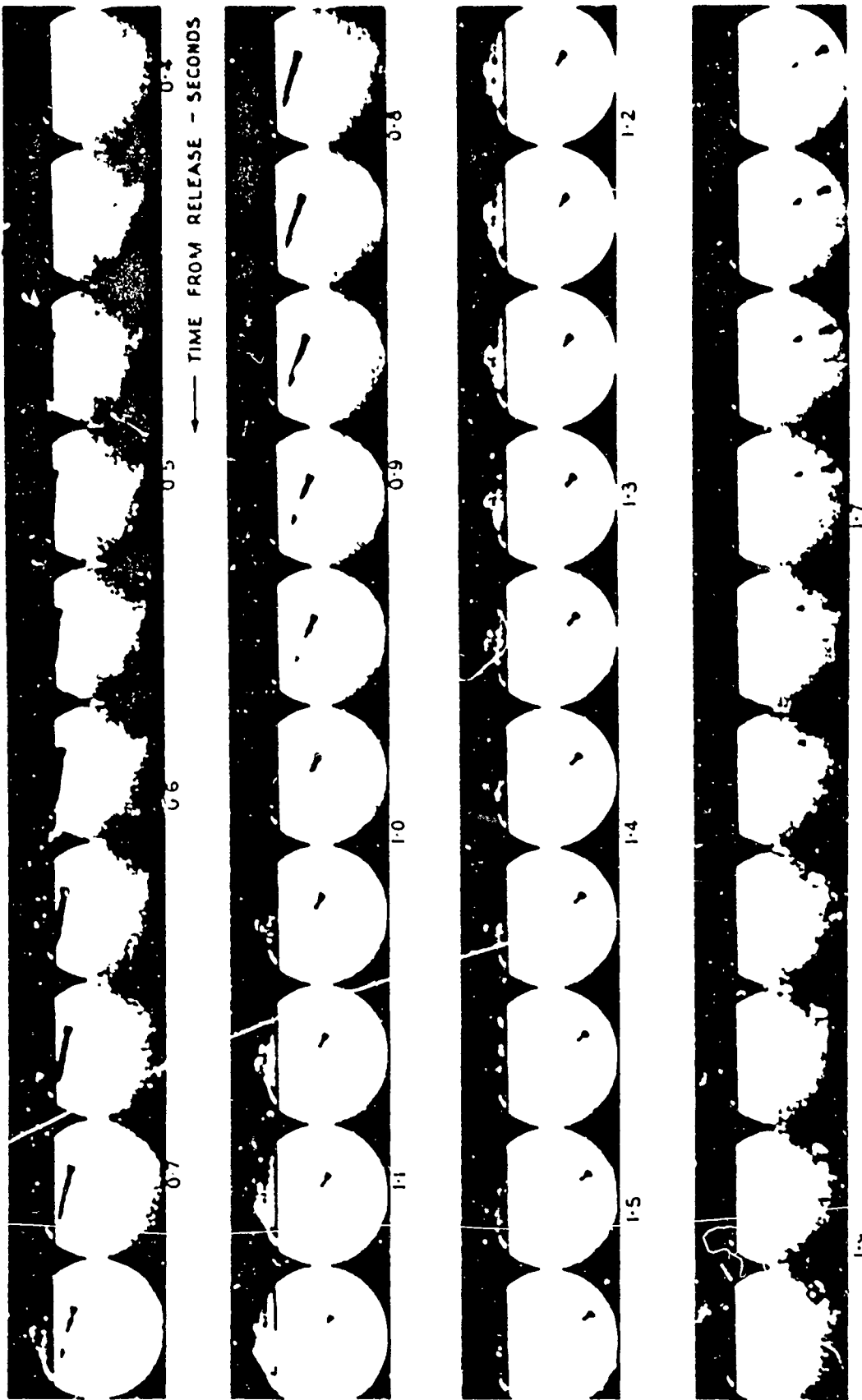


FIGURE 53(b). WING TIP CAMERA RECORD OF M557A BOMB - TOPPLE AT RELEASE
(ROUND NO. 707 RELEASED FROM 45400 FT AT M = 0.75)

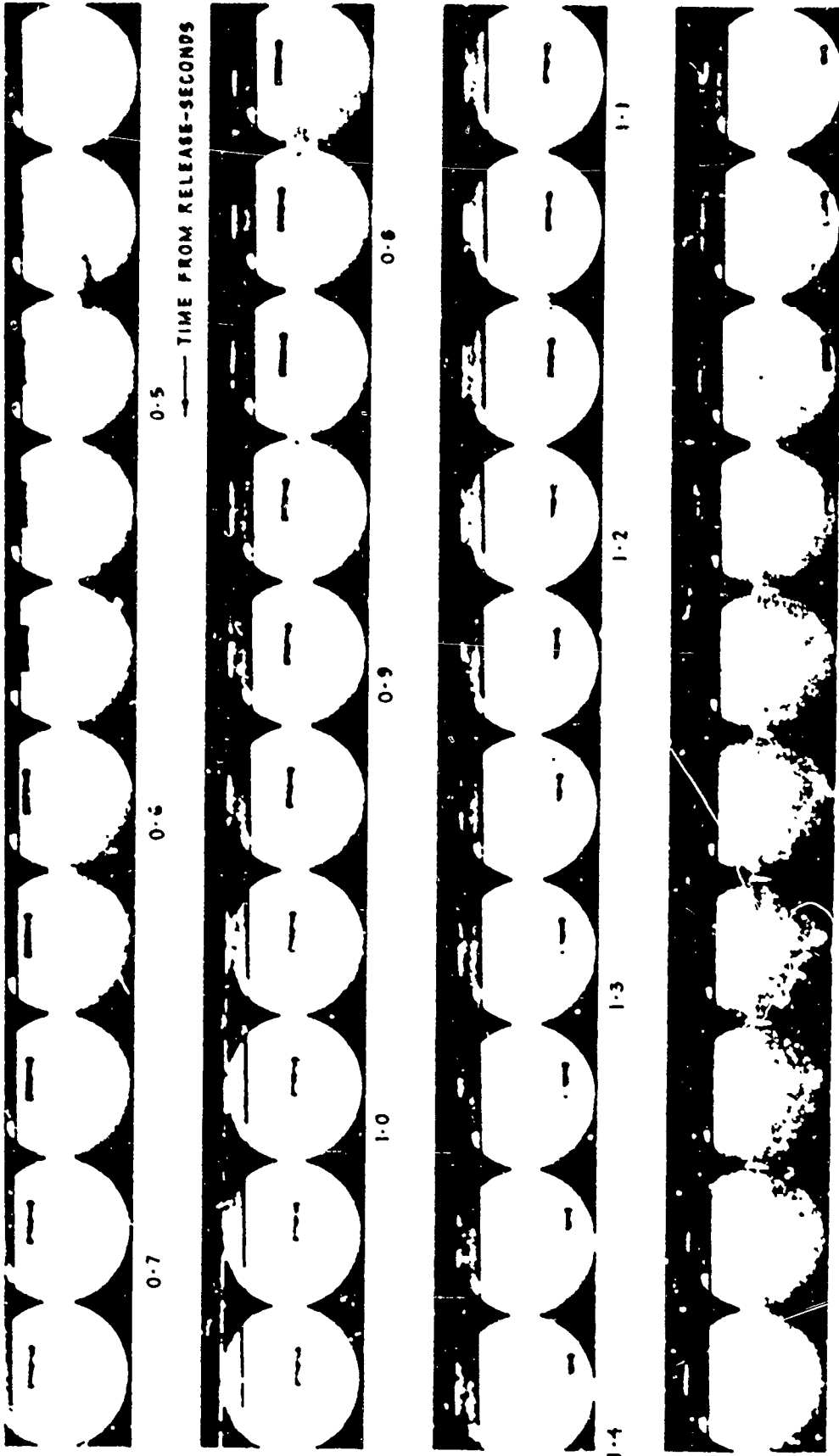


FIGURE 53(c). WING TIP CAMERA RECORD OF M557B BOMB - CLEAN RELEASE
(ROUND NO. 753 RELEASED FROM 45 600 FT AT $M = 0.70$)

	Copy No.
Officer of Scientific Research (U.S.A.P.)	57 - 62
U.S. Office of Technical Services	63
In Canada	
Canadian Defence Research Board	64
N.A.E. Ottawa	65
C.A.R.D.E., Valcartier	66
In Australia	
Chief Scientist	} 67
Controller, Research and Development	
Research and Development Division Library	68
Chief Superintendent, Aeronautical Research Laboratories	69
Superintendent, Aerodynamics Division	70
Library	71
Head of B.D.R.S.S. Melbourne	72 - 73
Head of B.D.R.S.S. Salisbury	74
Department of Air, Canberra	75 - 76
Internal	
Director	77
Deputy Director, Weapons Research and Development	78
Deputy Director, Trials Wing	79
Deputy Director, Space Physics Wing	80
Superintendent, Aerodynamics Division	81
Superintendent, Systems Assessment Division	82
Principal Officer, Free Flight Research Group	83
Principal Officer, Systems Studies (3) Group	84
Authors	85 - 86
W.R.E. Library	87
Aerodynamics Library	88 - 107

UNCLASSIFIED